

53469

75-8



National Library of Canada

Bibliothèque nationale du Canada

CANADIAN THESES ON MICROFICHE

THÈSES CANADIENNES SUR MICROFICHE

NAME OF AUTHOR/NOM DE L'AUTEUR Michael Raymond PIETRZYNSKI

TITLE OF THESIS/TITRE DE LA THÈSE P. Physiological Model For the Solution of Individual Muscle Forces During Normal Human Walking

UNIVERSITY/UNIVERSITÉ Simon Fraser University

DEGREE FOR WHICH THESIS WAS PRESENTED/ GRADE POUR LEQUEL CETTE THÈSE FUT PRÉSENTÉE Ph. D.

YEAR THIS DEGREE CONFERRED/ANNÉE D'OBTENTION DE CE GRADE 1982

NAME OF SUPERVISOR/NOM DU DIRECTEUR DE THÈSE Dr. James B. Morrison

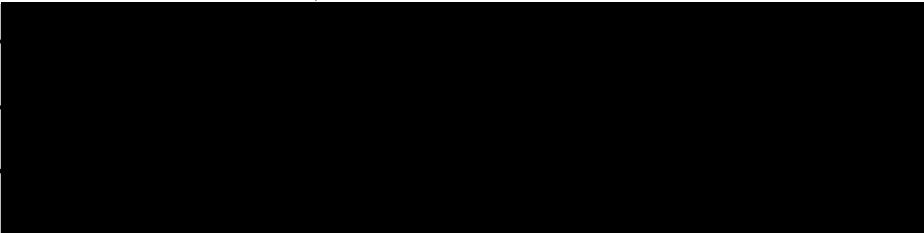
Permission is hereby granted to the NATIONAL LIBRARY OF CANADA to microfilm this thesis and to lend or sell copies of the film.

L'autorisation est, par la présente, accordée à la BIBLIOTHÈQUE NATIONALE DU CANADA de microfilmer cette thèse et de prêter ou de vendre des exemplaires du film.

The author reserves other publication rights, and neither the thesis nor extensive extracts from it may be printed or otherwise reproduced without the author's written permission.

L'auteur se réserve les autres droits de publication; ni la thèse ni de longs extraits de celle-ci ne doivent être imprimés ou autrement reproduits sans l'autorisation écrite de l'auteur.

DATED/DATÉ March 10, 1982 SIGNED/SIGNÉ

PERMANENT ADDRESS/RÉSIDENCE FIXÉE 



National Library of Canada  
Collections Development Branch

Canadian Theses on  
Microfiche Service

Bibliothèque nationale du Canada  
Direction du développement des collections

Service des thèses canadiennes  
sur microfiche

## NOTICE

The quality of this microfiche is heavily dependent upon the quality of the original thesis submitted for microfilming. Every effort has been made to ensure the highest quality of reproduction possible.

If pages are missing, contact the university which granted the degree.

Some pages may have indistinct print especially if the original pages were typed with a poor typewriter ribbon or if the university sent us a poor photocopy.

Previously copyrighted materials (journal articles, published tests, etc.) are not filmed.

Reproduction in full or in part of this film is governed by the Canadian Copyright Act, R.S.C. 1970, c. C-30. Please read the authorization forms which accompany this thesis.

**THIS DISSERTATION  
HAS BEEN MICROFILMED  
EXACTLY AS RECEIVED**

## AVIS

La qualité de cette microfiche dépend grandement de la qualité de la thèse soumise au microfilmage. Nous avons tout fait pour assurer une qualité supérieure de reproduction.

S'il manque des pages, veuillez communiquer avec l'université qui a conféré le grade.

La qualité d'impression de certaines pages peut laisser à désirer, surtout si les pages originales ont été dactylographiées à l'aide d'un ruban usé ou si l'université nous a fait parvenir une photocopie de mauvaise qualité.

Les documents qui font déjà l'objet d'un droit d'auteur (articles de revue, examens publiés, etc.) ne sont pas microfilmés.

La reproduction, même partielle, de ce microfilm est soumise à la Loi canadienne sur le droit d'auteur, SRC 1970, c. C-30. Veuillez prendre connaissance des formules d'autorisation qui accompagnent cette thèse.

**LA THÈSE A ÉTÉ  
MICROFILMÉE TELLE QUE  
NOUS L'AVONS REÇUE**

A PHYSIOLOGICAL MODEL FOR THE SOLUTION OF  
INDIVIDUAL MUSCLE FORCES DURING NORMAL HUMAN WALKING

by

Michael Raymond Pierrynowski  
B.Sc., University of Waterloo, 1976  
M.Sc., University of Waterloo, 1978

A THESIS SUBMITTED IN PARTIAL FULLFILLMENT OF  
THE REQUIREMENTS FOR THE DEGREE OF  
DOCTOR OF PHILOSOPHY

In the Department

of

Kinesiology

© Michael Raymond Pierrynowski 1982  
SIMON FRASER UNIVERSITY  
January, 1982.

All rights reserved. This thesis may not be reproduced  
in whole or in part by photocopy or other means without  
permission of the author.

PARTIAL COPYRIGHT LICENSE

I hereby grant to Simon Fraser University the right to lend my thesis, project or extended essay (the title of which is shown below) to users of the Simon Fraser University Library, and to make partial or single copies only for such users or in response to a request from the library of any other university, or other educational institution, on its own behalf or for one of its users. I further agree that permission for multiple copying of this work for scholarly purposes may be granted by me or the Dean of Graduate Studies. It is understood that copying or publication of this work for financial gain shall not be allowed without my written permission.

Title of Thesis/Project/Extended Essay

F. Physiological Model for the solution of individual muscle forces  
during normal human walking

Author:

(signature)

Michael R. Fierzynowski

(name)

MARCH 10, 1982

(date)

Approval

NAME: Michael Raymond Pierrynowski

DEGREE: Doctor of Philosophy

TITLE OF THESIS: A Physiological Model for the Solution  
of Individual Muscle Forces During Normal  
Human Walking

EXAMINING COMMITTEE:

Chairperson: Professor Margaret V. Savage

~~Dr. James B. Morrison~~  
Senior Supervisor

~~Dr. Arthur E. Chapman~~

~~Dr. Parveen N. Bawa~~

~~Dr. Thomas W. Calvert~~

~~Dr. Thomas K. Poiker~~  
Department of Geography  
and Computing Science  
Simon Fraser University

~~Dr. Roy D. Crowninshield~~  
External Examiner (in absentia)  
The University of Iowa  
Iowa City, Iowa

Date Approved:

March 17, 1982

## ABSTRACT

A major problem facing those trying to solve the forces within the human musculoskeletal system is deciding how to distribute the joint moments amongst muscular protagonists. In this thesis a hierarchical physiological model is developed which can resolve individual muscle forces. The lowest level is an anatomical model which consists of muscle geometry, fibre type and line of action. The data which is necessary to implement the model has been gleaned from various published sources. The middle level is a biomechanical description of a muscle unit which is used to estimate the force each muscle can exert at a certain stimulation given its previous activation and current kinematics. The data defining the mechanical properties of the muscle unit were obtained from the literature and include fibre types, force per unit cross-sectional area, the force-length and force-velocity relationships, activation, elastic and geometrical considerations. At the top of the hierarchy the control level provides a singular solution of the muscle forces which is based on a neurophysiological model of muscle recruitment. At this level muscle protagonists and antagonists are respectively facilitated or inhibited according to their ability to generate the required net muscle moments about those joint axes for which a large range of movement exists.

The model predicts the individual muscle force-time profiles strongly suggested by EMG data. This is in contrast to the reduction and optimization methods reported in the literature. The model also predicts peak muscle forces well within the imposed physiological constraints to generate the measured net muscle moments (peak muscle forces, normalized to isometric, of  $0.21 \pm 0.14$ ). Muscle recruitment was confined almost entirely to the slow twitch fibres during the walk and antagonistic muscle activity was demonstrated.

The results partially demonstrate that it is feasible to construct a hierarchical physiological model to evaluate individual muscle forces. This statement must be tempered somewhat knowing that better anatomical and neurophysiological data must be made available and that the model be rigorously validated to use it as a muscle force predictor.

### ACKNOWLEDGEMENTS

In appreciation the author would like to thank his senior supervisors Dr. James B. Morrison and Dr. Arthur E. Chapman for their kind assistance during the preparation of this work. Thanks are also extended to Drs. Parveen Bawa and Thomas Calvert for their help and guidance in the past three years. To Tom Poiker my gratitude for introducing me to the concept of homogeneous transformations. Special thanks are extended to Dr. D.G.E. Robertson and G. Caldwell for their help during the data collection and to the Department of Physical Education at the University of British Columbia for the use of their facilities. I am also indebted to my wife, Ruth, for her aid in the data collection and typing the final manuscript. G. Mackie's and D. Thomson's consent to act as subjects was also appreciated.

Financial assistance for this thesis was given by the Department of Kinesiology at Simon Fraser University, the School of Physical and Health Education at the University of Toronto, the British Columbia Arthritis Society, a grant from the British Columbia Health Care Research Foundation, and a scholarship from the Natural Sciences and Engineering Research Council (CANADA).



TABLE OF CONTENTS

ABSTRACT . . . . . iii  
ACKNOWLEDGEMENTS . . . . . v  
TABLE OF CONTENTS . . . . . vi  
LIST OF TABLES . . . . . ix  
LIST OF FIGURES . . . . . x  
NOMENCLATURE . . . . . xii

| Chapter  | page |
|--|------|
| I. INTRODUCTION . . . . .  | 1    |
| A. Statement of the Purpose . . . . .                            | 5    |
| B. Problems . . . . .  | 5    |
| C. Hypotheses . . . . .  | 5    |
| D. Scope of the Study . . . . .                                  | 6    |
| E. Rationale for the Study. . . . .                              | 6    |
| II. REVIEW OF RELATED LITERATURE. . . . .                        | 7    |
| A. Former Gait Investigations . . . . .                          | 7    |
| Kinematics . . . . .   | 8    |
| Joint Reaction Forces and Moments. . . . .                       | 10   |
| Muscle Force Analyses. . . . .                                   | 11   |
| B. Summary. . . . .  | 13   |
| III. MODEL FOR THE SOLUTION OF INDIVIDUAL MUSCLE FORCES. . . . . | 14   |
| A. Anatomical Model . . . . .                                    | 14   |
| System Definition. . . . .                                       | 14   |
| Muscle Line of Action and Moment Arms. . . . .                   | 20   |
| Ligament Line of Action and Moment Arms. . . . .                 | 25   |
| Muscle Geometry. . . . .   | 25   |
| Physical Properties of the Segments. . . . .                     | 33   |

|  |    |
|--|----|
| B. Muscle Model . . . . .                            | 34 |
| Terminology and the Mechanical Muscle Model. . . . . | 35 |
| Factors Modifying a Muscle's Force Output. . . . .   | 36 |
| a. Fibre composition. . . . .                        | 36 |
| b. Geometry . . . . .                                | 38 |
| c. Series elasticity. . . . .                        | 39 |
| d. Temporal phenomena . . . . .                      | 42 |
| e. Force-length relationship. . . . .                | 44 |
| f. Force-velocity relationship. . . . .              | 45 |
| Analysis . . . . .                                   | 49 |
| C. Control Model. . . . .                            | 50 |
| Neurophysiological Constraints . . . . .             | 50 |
| a. Fibre type recruitment . . . . .                  | 50 |
| b. Pattern generators . . . . .                      | 51 |
| Stimulation-Activation-Force Relationship. . . . .   | 55 |
| The Role of the Ligaments. . . . .                   | 57 |
| Analysis . . . . .                                   | 57 |
| D. Summary. . . . .                                  | 60 |
| IV. METHODS AND PROCEDURES. . . . .                  | 62 |
| A. Experimental Design. . . . .                      | 62 |
| B. Muscle Force Determination . . . . .              | 62 |
| Defining the Subject's Lower limb. . . . .           | 63 |
| a. Anatomical position. . . . .                      | 63 |
| b. During activity. . . . .                          | 66 |
| Net Muscle Moments . . . . .                         | 70 |
| a. Segment kinematics . . . . .                      | 70 |
| b. Ground reaction forces . . . . .                  | 72 |
| c. Analysis . . . . .                                | 73 |
| Model Implementation . . . . .                       | 75 |

|     |   |      |
|-----|---|------|
| V.  | RESULTS AND DISCUSSION. . . . .   | 79   |
| A.  | The Subject's Lower Limb . . . . .  | 79   |
|     | Anatomical Position. . . . .  | 79   |
|     | During Activity. . . . .  | 91   |
| B.  | Muscle Kinematics. . . . .  | 93   |
| C.  | Joint Moments. . . . .  | 106  |
| D.  | Model Results. . . . .  | 111  |
|     | Response of Some Muscles to Maximal Stimulation. . . . .                            | 112  |
|     | Muscle Forces During the Walk. . . . .  | 112  |
|     | Pattern Generator Outputs. . . . .  | 130  |
|     | Discussion and Implications of the Findings. . . . .                                | 141  |
| VI. | SUMMARY, CONCLUSIONS AND RECOMMENDATIONS. . . . .                                   | 145  |
| A.  | Summary. . . . .  | 145  |
| B.  | Conclusions. . . . .  | 146  |
| C.  | Recommendations for Future Work. . . . .  | 147  |
|     | Appendix . . . . .  | page |
| A.  | Homogeneous Transformation from one Three-dimensional<br>Space to Another . . . . . | 149  |
| B.  | Defining the Muscle Curvilinear Sections. . . . .                                   | 152  |
| C.  | Defining the Muscle and Ligament Moment Arms. . . . .                               | 153  |
| D.  | Three-Dimensional Filming Using the Direct Linear<br>Transformation . . . . .       | 154  |
| E.  | Data Smoothing Using the Fourier Transform. . . . .                                 | 159  |
| F.  | Changing Reference Systems. . . . .   | 161  |
|     | REFERENCES . . . . .  | 162  |

## LIST OF TABLES

| Table   | page |
|---|------|
| 1. Lower Extremity Muscles Included in the Model. . . . .   | 16   |
| 2. Lower Extremity Ligaments Included in the Model. . . . .                                       | 17   |
| 3. Points Defining the Skeletal Reference Systems<br>and the Centres of Mass. . . . .             | 20   |
| 4. Points Defining the Line of Action of the Muscles. . . . .                                     | 22   |
| 5. Location of the Muscles in the Transverse Plane at the<br>Hip, Knee and Ankle Joints . . . . . | 26   |
| 6. Points Defining the Line of Action of the Ligaments. . . . .                                   | 27   |
| 7. The 'Standard' Muscle Geometrical Data . . . . .   | 31   |
| 8. The Body Segment Parameters. . . . .   | 34   |
| 9. Hypothetical Moment Arms and Maximum Force of Five<br>Knee and Ankle Muscles . . . . .         | 59   |
| 10. Location of the Palpable Points. . . . .  | 64   |
| 11. Range of Motion of the Joints. . . . .  | 67   |
| 12. Location of the Markers. . . . .  | 69   |
| 13. Formulas Used to Calculate the Joint Reaction Forces<br>and Moments. . . . .                  | 75   |
| 14. Transformations Between the Skeleton and The Subject's<br>Palpable Points. . . . .            | 80   |
| 15. Subject's Skeletal Reference Systems and Centres<br>of Mass. . . . .                          | 81   |
| 16. Line of Action of the Muscles Within the Subject . . . . .                                    | 82   |
| 17. Line of Action of the Ligaments Within the Subject . . . . .                                  | 83   |
| 18. Moment Arms of the Muscles . . . . .  | 85   |
| 19. Moment Arms of the Ligaments . . . . .  | 86   |
| 20. The Subject's Muscle Geometrical Data. Part I. . . . .  | 88   |
| 21. The Subject's Muscle Geometrical Data. Part II . . . . .                                      | 89   |
| 22. Validation of of the Model's Estimation of the<br>Total Muscle Mass. . . . .                  | 91   |

LIST OF FIGURES

| Figure   | page |
|--|------|
| 1. The Skeletal Reference Systems . . . . .  | 18   |
| 2. The Three-Dimensional Anthropometer. . . . .  | 19   |
| 3. The Definition of a Quadricep Muscle . . . . .  | 24   |
| 4. Geometrical Characteristics of Parallel<br>and Pennate Muscles. . . . .                     | 29   |
| 5. Geometries of the Mechanical Models of Parallel<br>and Pennate Muscles. . . . .             | 37   |
| 6. The Normalized Force-Length Relationship of the<br>Fibre Series Elastic Component . . . . . | 41   |
| 7. The Normalized Force-Length Relationship of the<br>Tendon Series Elastic Component. . . . . | 42   |
| 8. The Activation-Time Relationship of the<br>Contractile Element. . . . .                     | 44   |
| 9. The Normalized Force-Length Relationship of the<br>Contractile Element. . . . .             | 46   |
| 10. The Force-Velocity Relationship of a Fast and Slow<br>Twitch Fibre Population. . . . .     | 47   |
| 11. Eleven Hypothetical Muscles Situated Around a Joint. . . . .                               | 54   |
| 12. Simplified Stimulation-Activation-Force Relationship<br>of a Hypothetical Muscle . . . . . | 56   |
| 13. A Simplified View of the <del>Knee and</del> Ankle Joints . . . . .                        | 58   |
| 14. The Normalized Power at each Harmonic Number . . . . .                                     | 71   |
| 15. A Free-Body Diagram of the Leg During Activity . . . . .                                   | 74   |
| 16. Block Diagram of the Computer Programmes . . . . .   | 78   |
| 17. The Muscle Lines of Action . . . . .   | 90   |
| 18. Kinematics of the Walk . . . . .   | 92   |
| 19. Muscle Lengths During the Walking Cycle. . . . .   | 94   |
| 20. Muscle Velocities During the Walking Cycle . . . . .                                       | 100  |

| Figure   | page |
|--|------|
| 21. Joint Forces in the Global Reference System. . . . .         | .107 |
| 22. Net Muscle Moments in the Global Reference System. . . . .   | .109 |
| 23. Net Muscle Moments in the Skeletal Reference System. . . . . | .113 |
| 24. Response of Some Muscles to Maximal Stimulation. . . . .     | .115 |
| 25. Muscle Forces During the Walk. . . . .                       | .118 |
| 26. Pattern Generator Outputs. . . . .                           | .131 |
| 27. Stimuli to the Muscles . . . . .                             | .134 |

## NOMENCLATURE

- $A^M$  - maximum physiological cross sectional area of a muscle
- $\bar{A}^M$  - mean physiological cross sectional area of a muscle
- $A^A$  - maximum anatomical cross sectional area of a muscle
- $\bar{A}^A$  - mean anatomical cross sectional area of a muscle
- $A^T$  - cross sectional area of a tendon
- $a$  - Hill's constant 'a'
- $b$  - Hill's constant 'b'
- $C_l$  - circumference of the lth segment
- $E$  - muscle shape factor ( $\bar{A}^M / \bar{A}^A$ )
- $f$  - maximum isometric muscle force per square centimeter of cross sectional area
- $F_j$  - the jth joint reaction force
- $F_p$  - the force exerted on the force plate
- $F^M$  - maximum isometric force a muscle can exert, in the direction of its tendon
- $F_{CE}^{\wedge}$  - the maximum possible force able to be developed by a CE, at a given length and velocity, in the direction of its tendon, at time t, given full stimulation from time t- $\Delta t$
- $F_{CE}^{\vee}$  - the minimum possible force able to be developed by a CE, at a given length and velocity, in the direction of its tendon, at time t, given full relaxation from time t- $\Delta t$
- $g$  - acceleration due to gravity ( $9.81 \text{ m s}^{-2}$ )
- $G_l$  - lean girth of the lth segment
- GRS - global reference system (absolute frame of reference)
- $I_l$  - moment of inertia of the lth segment
- $L_l$  - length of the lth segment
- $\%L^F$  - fibre length as a percentage of the anatomical muscle length
- $L^F$  - resting length of the muscle fibre
- $L^{SEC}$  - length of the SEC
- $L^M$  - muscle length
- $L^T$  - length of the tendon
- $\%L^T$  - tendon length as a percentage of the anatomical muscle length
- $L^{CE}$  - velocity of shortening of the CE

- m - muscle mass
- $M_j$  - the jth joint net muscle moment
- $MA_{j,k}$  - moment arm at the jth joint about the kth reference axis
- $M_l$  - mass of the lth segment
- O - centre of pressure on the foot during stance phase
- p - muscle density
- $P^m$  - maximum isometric force a muscle can exert, in the direction of its fibres
- $P^m$  - maximal force developed by a CE in eccentric contractions
- PRS - internal force plate reference system
- $\hat{q}_i$  - the maximum possible activation of fibre type i, at time t, given full stimulation from time t- $\Delta t$
- $\check{q}_i$  - the minimal possible activation of fibre type i, at time t, given full relaxation from time t- $\Delta t$
- $Q_l$  - the lth reference system by which the skeletal reference systems, muscle and palpable points were digitized
- R - the reference system by which the subjects palpable points and markers were digitized (anatomical position)
- s - distance the muscle belly has shortened from its initial length
- $\dot{s}$  - velocity of muscle belly shortening
- $SM_p$  - stimulation to a muscle from the pth pattern generator
- $SK_l$  - skinfold thickness of the lth segment
- $SRS_l$  - skeletal reference system for the lth segment
- $\hat{t}$  - time constant for the rise in activation
- $\check{t}$  - time constant for the fall in activation
- T - muscle thickness (pennate muscles only)
- $T_l$  - transformation between the lth skeletal segment and the subject in the anatomical position
- X, Y, Z - the coordinates of a point in the GRS
- $\ddot{X}, \ddot{Y}, \ddot{Z}$  - the acceleration of a point in the GRS
- $\alpha_l$  - angular acceleration of the lth segment
- $\alpha_m$  - angle of pennation of the mth muscle
- $\Delta t$  - time interval between sample periods



superscripts:

- B - muscle belly
- CE - contractile element
- F - muscle fibre
- M - total muscle
- SEC - series elastic component
- T - muscle tendon

superscribes:

- - first derivative with respect to time
- - second derivative with respect to time
- = - value when muscle is at its anatomical length
- ▷ - value when muscle is at its maximum length (also called the rest length)
- ◁ - value when muscle is at its minimum length
- - maximum isometric condition or arithmetic mean
- ~ - maximum eccentric condition or anatomical cross sectional area
- ^ - value reached undergoing full stimulation
- ∨ - value reached undergoing zero stimulation

subscripts:

fibre types

- i - index referring to the three fibre types
- SO - slow twitch, oxidative muscle fibres
- FO - fast twitch, oxidative muscle fibres
- FG - fast twitch, glycolytic muscle fibres

joints

- j - index referring to the jth joint
- PC - pubic crest
- H - hip
- K - knee
- A - tibiotarsal
- B - subtalar
- MTP - metatarsophalangeal

segments

- l - index referring to the lth segment
- Pe - pelvis
- T - thigh
- S - shank
- Ta - talus
- F - foot
- To - toes

## CHAPTER I

### INTRODUCTION

One of the most bewildering problems facing the biomechanics researcher is the mechanically redundant nature of the musculoskeletal system. Since there are often more muscles present than are required to produce any displacement pattern evident from kinematic data, the classical equations of kinetic analysis do not permit a unique solution of the muscular forces crossing the joints.

Two distinct procedures have been used to assign joint moments amongst muscular protagonists. Paul (1965) used what may be called the 'reduction' method to get a bounded or approximate solution thereby circumventing the redundancy problem at the hip during gait. This method was also used by Morrison (1968), together with EMG data, to assign the knee moments in dynamic situations. The goal of the reduction method is to reduce an initially indeterminate problem to one that is determinate. This method is useful in those instances where the objective is the joint force rather than muscle forces, and where the joint anatomy can be simplified by grouping muscles to eliminate the indeterminate forces.

The second procedure, the 'optimization' method, was introduced by Seireg and Arvikar (1973, 1975) but was limited to quasi-static gait. In this method it is assumed that the distribution process occurs in such a way as to optimize some physical property called the 'objective' function. The proper objective is not known a priori but must be theorized on the basis of biological significance.

Several optimization criteria have been suggested and examined in the literature. The most popular criterion concerns the principle of minimal total muscular force, which can be mathematically stated as minimizing the sum of the muscle forces.

Penrod et al. (1974) accepted this definition but Crowninshield et al. (1978a,b) adopted a slightly modified form. They divided the force in a muscle by its physiological cross-sectional area, in essence minimizing the stress in the muscle set. In a similar vein, Pedotti et al. (1978) examined four variations of the minimization of total muscular effort (the sum of forces in the muscles, the sum of forces squared, the sum of the ratios of actual force/maximal force, and the sum of squares of actual force/maximal force for all muscles). Their predicted results, compared to EMG data, indicated that the sum of squares of actual force/maximal force was the best criterion to use. However, one of the authors (Pedotti, 1974) investigating the same problem, reported that good results were obtained by minimizing the metabolic energy expenditure. As pointed out by Hatze (1979a) the most appropriate criterion remains unresolved.

Seireg and Arvikar (1973, 1975) examined the plausibility of minimizing the total muscular force while standing and during quasi-static gait. They rejected it in favour of a criterion which minimized the sum of all the muscle forces plus four times the sum of the moments at all the joints. This they determined by comparing the solutions of various objective functions with the muscle output as indicated by EMG. Seireg and Arvikar's work must be examined critically, however, since their objective function was selected examining a static posture, which may not hold up under dynamic situations. In addition, it is difficult to envisage the physiological justification of such a complex objective function.

The principle of minimal total muscle force has been challenged by Barbenel (1972) who studied the biomechanics of the temporomandibular joint and predicted that for minimal total muscular force, the only muscle acting during biting would be the masseter muscle. EMG evidence and palpation of the jaw muscles indicated many more muscles to be active. When studying the biomechanics of the elbow Yee (1976) concluded, as did Barbenel,

that the principle of minimal total muscular force is unlikely to be true. Hatze (1976) also disagreed with the principle stating that it is highly unlikely that all motions, especially time-optimal processes, obey the principle of minimal muscular effort. It should be noted that there seems to be an inherent assumption that time optimality is important. This may be true in a small subset of human activities but there is nothing to justify this assumption for human locomotion. In fact it suffers from the same criticisms as the above criteria.

The minimal force criterion tends to partition all of the force required into the single 'optimal' muscle, instead of distributing the load amongst synergists. Hardt (1978) suggests that it is important to consider muscles as more than just ideal unidirectional force actuators, since the central nervous system must surely consider their dynamic and static properties when devising a control strategy for their activation. Hardt and Mann (1979) developed a model relating the kinematics of a muscle to its metabolic cost. The minimization of the power requirement of the muscles was then used to solve for the muscular forces during human locomotion.

Although several investigators have hypothesized that the performance criterion governing the motion of an animal is the minimization of energy expended (Chow and Jacobsen, 1971; Hardt, 1978; Hatze, 1976; Nubar and Contini, 1961) this concept has not been proven at the level of selective activation. However, a variety of investigations suggest that it is followed globally. Saunders et al. (1953) have shown that the general motion of the body during walking is such that the movements of the centre of gravity of the body are minimized. Margaria (1976) has also demonstrated that normal walking speeds are usually chosen to require the least energy expenditure as measured by oxygen consumption per distance travelled.

The optimization of muscular power, as with force, tends to assign all of the activation to a single optimal muscle with

rapid power-switching amongst muscles (Hardt, 1978). This would lead to fatigue in those fibres activated. In addition, EMG evidence shows that muscles tend to act as a group synergistically (Paul, 1974; UCAL Berkeley, 1953). Since there is no known physiological evidence suggesting the direct monitoring and controlling of power in individual muscles, the 'optimization' method, in its present form, is not physiologically viable. This is supplemented by the recent work of Patriarco et al. (1981) who examined several optimization models to predict individual muscle forces. They concluded that "...the imposition of additional physiological-based constraints are essential to distinguishing (sic) the role of individual muscles."

In this thesis a departure from a mathematically optimal solution is presented. When one speculates on the evolution of two joint muscles (Elftman, 1939; Morrison, 1970) and the division of muscle into two major types (slow twitch which is both energy efficient at low shortening velocities and recruited first, and fast twitch which is more economical at higher shortening velocities and recruited second (Awan and Goldspink, 1972; Burke and Edgerton, 1975; Gibbs and Gibson, 1972; Wendt and Gibbs, 1973)), one is drawn to the conclusion that the minimization of metabolic cost is a goal of the neurological control system. This is not to say that an optimization procedure with the objective function chosen to minimize energy has to be performed. The concept of minimization of energy is not a criterion which the nervous system actively processes but one which is 'hard-wired' into the system through evolution. It is also likely that the criterion actually used to distribute force amongst the individual muscles is a compromise of competing objective functions such as endurance and speed.

## STATEMENT OF THE PURPOSE

The aim of this thesis was to formulate and implement a hierarchical physiological model, based on well-defined neurological, muscular and anatomical data, to solve for the individual muscle forces in the musculoskeletal system. The dynamic function of the lower limb during normal human locomotion was chosen to apply the model.

## PROBLEMS

These were 1) to define a standard lower limb which includes muscle geometries, muscle and ligament lines of action, segmental physical properties, and segmental reference axes, 2) to develop a method for scaling the standard lower limb to a subject, 3) to collect three-dimensional segmental kinematic and joint moment data during a normal gait pattern, 4) to calculate the muscle forces and 5) to compare the temporal sequence of the muscle forces with published EMG data.

## HYPOTHESES

On the basis of the literature concerned with the estimation of muscle forces during activity (Paul, 1965; Morrison, 1967; Seireg and Arvikar, 1973, 1975; Crowninshield *et al.*, 1978; Pedotti *et al.*, 1978; Hardt, 1978) it was hypothesized that accurate muscle force information can be estimated using the physiological model and data analyses presented in this thesis. Since direct verification of this hypothesis is impossible it was also hypothesized that the temporal sequence of the estimated muscle forces will compare favourably with published EMG data.

### SCOPE OF THE STUDY

The data-aquisition portion of this study was conducted in the Biomechanics facilities at the University of British Columbia and data-reduction was performed at Simon Fraser University. This study was restricted to one male student who had no known pathological or neurological disorder. The subject was required to undergo a lengthy anthropometric session so that a standard lower limb could be scaled to him. He was then required to perform a series of walking trials.

### RATIONALE FOR THE STUDY

Several investigators have attempted to estimate the magnitude of the muscle forces. All have resorted to using simplified systems (Paul, 1965; Morrison, 1967) or optimization methods (Crownshield *et al.*, 1978a,b; Hardt, 1978; Pedotti *et al.*, 1978; Seireg and Arvikar, 1975). One may argue that their muscle force values were generated using questionable models, but the rationale for undertaking such work is commendable. This thesis is an attempt to depart from a purely mathematical solution to solve for the individual muscle forces. It is clear that a complete kinetic description of human gait has many applications including the improvement of athletic performance and the clinical study of pathological gait arising from muscle activation abnormalities, tendon transplants or amputation. The model within this thesis could also be used as a research tool in which systematic alteration of the muscle properties would allow their true values to be estimated.

7

CHAPTER II

REVIEW OF RELATED LITERATURE

The application of scientific principles to the study of human motion began in the Renaissance period by such men as Leonardo da Vinci (1452-1519) in his "Notes on the Human Body" (O'Malley and Saunders, 1952) and Borelli (1609-1679) who studied human and animal muscle function (Norman and Winter, 1976). It was not until the latter half of the 19th and 20th centuries when reliable and accurate methods for the recording of movement were developed that the laws of mechanics were applied to the human body (Braune and Fisher, 1889; Elftman, 1938, 1939; Bresler and Frankel, 1950). In the past 20 years the history of computers has been instrumental in the growth of this branch of science now called biomechanics.

In this chapter a brief history of biomechanics as it relates to this thesis will be developed. Specifically, the state of knowledge regarding the mechanical aspects of human locomotion will be stressed. It will then become apparent how this study adds to the current body of knowledge.

The literature concerning the physiological model developed in this thesis (anatomical, muscle mechanics and neurophysiological considerations) are covered in the next chapter.

FORMER GAIT INVESTIGATIONS

The objective of most locomotion studies is to quantify the measurable components of gait. In these studies time is spent setting up a gait analysis laboratory to facilitate the reporting of kinematic or descriptive data. This is an important function and has led to considerable instrumentation development. However, some investigators apply the kinematic data to models of the lower limb to estimate the joint reaction forces and moments. A small subset of this biomechanics literature defines models



representing the anatomical structure in order to partition the joint moments amongst the muscles. This thesis falls into the latter group.

### Kinematics

Locomotion as a function of time and space has been the focus of most gait investigations. Regardless of the complexity of the analyses, the human limb is modelled as a series of stick-like rigid linkages (Chaffin, 1969; Dempster, 1955; Plagenhoef, 1971; Thurnaur, 1967). Appropriate anthropometric measures are defined (i.e. mass, location of the centre of mass, moment of inertia) such that the model behaves realistically (Dempster, 1955; Drillis and Contini, 1966; Page, 1969a,b, 1970a,b; Hatze, 1975b). The description of the displacement history for each link in the model is the most elementary form of kinematic analysis (Blacharski et al., 1975; Grieve and Gear, 1966; Kettlekamp, 1970; Lamoreux, 1972; Saito et al., 1974). Other measurements are the calculation of the segment and total body centres of mass, velocities and accelerations (Plaja et al., 1975; Winter et al., 1975). The normal range of the kinetic variables of the lower limb has been the subject of several studies (Lamoreux, 1972; Levens et al., 1948; Murray et al., 1964; Saunders et al., 1953) and these have been compared with atypical populations (Bartholomew, 1952; van Faassen et al., 1969; Finlay and Karpovich, 1964; Soderberg et al., 1975).

The major problem with the kinematic studies is that they offer descriptive parameters but little explanation of the underlying causes of movement. These studies are important, however, as they have been responsible for the development of rapid measurement systems. Two techniques which have received much interest are cinematography and electrogoniometry. Both measurement systems have the same purpose, to yield a complete kinematic description of gait, but they achieve this goal from two different approaches.

The photographic measurement of movement, begun by Marey (1873) in France and Muybridge (1955) in America, is the most widely used data acquisition system (Sutherland, 1972). Cinefilm has the advantage that it can be rerun to get a qualitative assessment of the movement, and with stop motion capability there is considerable benefit in both athletic and clinical settings. The prolonged development time and the manual labour required to extract the quantitative data, even with semi-automated film analysers, can be restrictive and render such systems impractical for routine clinical use (Smith, 1976; Winter, 1976). There are also calibration problems when three-dimensional data is required (Cavanagh, 1979; van Gheluwe, 1974; Woltring, 1975, 1976). Newer, more automated, electro-optical systems (eg SELSPOT by SELCOM AB of Sweden) are available but the error in point location and costs may be excessive depending upon the application (Antonsson, 1979; Arcan et al.; 1979; Oberg, 1974).

Electrogoniometers give a direct electrical measure of the joint angles and are relatively inexpensive. However, they must be correctly aligned with the adjacent limb segments to give reproducible values (Winter, 1976). A variety of custom made devices have appeared and the more recent ones do not have to be aligned. One such electrogoniometer is that developed by a team at the Canadian Arthritis Research Society in conjunction with engineers at the University of British Columbia. This device measures three mutually orthogonal rotations at the hip, knee and ankle joints, bilaterally (Hannah, 1980). As with all electrogoniometers, although direct readout is available, calibration procedures must be performed to relate the electrical signals to relative joint angles. For kinematic measurements of gait this calibration is sufficient (Lamoreux, 1972). However, if gait dynamics are desired, the location of the subject in space (absolute frame of reference) is necessary (Winter, 1979). This requires knowing the absolute location of an end segment and then using the joint angles to fix the other segments in space. To this authors knowledge no such system is available to perform these analyses.

Cinematographic and electrogoniometric data acquisition systems generate displacement-time or angle-time histories of the segments being studied. For those investigations which estimate the joint and muscle forces (see below) the determination of the derivatives of the displacement data are necessary. Until recently problems existed due to the amplification of noise in the raw data by differentiation (Felkel, 1951; Pezzack et al., 1977). To minimize the noise many methods have been developed such as polynomial fittings (Kuo, 1965; Plagenhoef, 1968), cubic splines (Wold, 1974; Zerniche et al., 1976), digital filtering (Pezzack et al., 1977) and Fourier series (Cappozzo et al., 1975; Hatze, 1977b; McGhee, 1976). All of these methods essentially low-pass filter the data before any differentiation is attempted. If the displacement function is periodic the Fourier technique is attractive since the filter cutoff frequency is determined by the number of harmonics included in the reconstruction (Hardt, 1978). However, the cubic spline and digital filtering are the two most widely used techniques since the displacement function is generally non-periodic (Miller, 1980).

#### Joint Reaction Forces and Moments

Analyses of human locomotion have led many researchers to investigate the magnitude of the joint reaction forces and moments. In all of these studies there is the inherent assumption that the reactions are provided by forces and pure moment generators. Since the true joint forces (called the articular or bone-on-bone forces) are a result of the external, gravitational, inertial and the muscle and ligament forces acting through moment arms, the reaction forces can significantly underestimate the loading on the joints.

To determine the joint reaction forces and moments, the limb kinematics and the magnitude and location of the external forces acting on the system are used in conjunction with an appropriate model. The Inverse Dynamics Problem (so called because conventional dynamics predict displacements from forces) has only

recently been applied to the human body. Elftman's (1939) work was an early attempt at these calculations but was limited to two-dimensions. It is the paper by Bresler and Frankel (1950) that stands out as the classic dynamic work in the biomechanics literature of gait. They present three-dimensional reaction force and moment curves for the hip, knee and ankle joints during level walking. More recent investigators present similar curves for normal (Cappozzo et al., 1975; Cavanagh and Gregor, 1975; Chow and Jacobsen, 1971; McGhee et al., 1976; Oberg, 1974), pathological (Marks and Hirschberg, 1958) and athletic activities (Mann and Sprague, 1980; Zdziorsky and Aleshinsky, 1975).

The estimation of joint reaction forces and moments is based on accurately knowing the kinematics and anthropometry of an appropriate model. A large part of current biomechanics research is concerned with the estimation of these parameters with minimal error. It has been suggested that current techniques yield values of reaction forces and moments within an acceptable 10 percent error (Cappozzo et al., 1975; Cavanagh, 1979; Norman and Winter, 1976).

### Muscle Force Analyses

The next step in the understanding of locomotion is the inclusion of internal modelling so that muscle and articular forces may be calculated. However, the human musculoskeletal system is mechanically redundant and the classical equations of kinetic analysis permit an infinite number of solutions to satisfy the joint moment equations. In work where it has been necessary to resolve this dilemma, investigators have generally used one of two methods.

Fenrod et al. (1974) best describes the first method, the 'reduction' technique, by stating that the number of active muscles or muscle groups will be no greater than the number of rotational degrees of freedom at any given joint. Both Paul (1965) and Morrison (1967) applied this technique to get an approximate solution of the muscle forces about the hip and knee,

respectively. Paul's work is interesting in that several muscle groups were known to have complimentary functions at the hip. To resolve this, Paul attributed all of the force action to each group in turn instead of defining a single equivalent muscle. Knowing that the force must be shared by the two groups, the true solution must lie within the two singular solutions obtained. A refinement of the 'reduction' technique is the division of force amongst muscles in a group depending upon their respective cross-sectional areas (Alexander and Vernon, 1975). In summary, the goal of the reduction method is to reduce an initially indeterminate solution to one that is amenable to solution.

The 'optimization' method is the alternative procedure for solving muscle forces. Since its introduction by Seireg and Arvikar (1973) and Penrod et al. (1974) it has been applied to gait by several investigators (Crowninshield et al., 1978a,b; Hardt, 1978; Pedotti et al., 1978; Seireg and Arvikar, 1975). In this method it is assumed that the muscle forces are partitioned in such a way as to optimize some objective. Several optimization criteria have been examined. Examples include the minimization of 1) the sum of the muscle forces (Crowninshield et al., 1978b; Penrod et al., 1974), 2) the sum of the squares of actual muscle force/maximal muscle force (Pedotti et al., 1978), 3) the sum of the muscle forces plus four times the sum of the moments at all the joints (Seireg and Arvikar, 1973, 1975) and 4) the muscular power (Hardt, 1978).

The appropriateness of these two techniques to estimate the muscle forces was not known a priori and had to be established indirectly on the basis of experimental or published data. The correlation between the temporal sequence of the predicted muscle forces with EMG is generally used since non-invasive methods to determine the actual muscle forces are not available. Both the 'reduction' and 'optimization' techniques reveal serious doubts to their acceptability. When the temporal sequence of muscle force were compared with EMG, good agreements were found for some

muscles and total disagreement in others. One also gets the impression that both methods are mechanical and mathematical solutions, respectively, and that the body of physiological and neurological data has not been adequately examined to define additional relationships.

#### SUMMARY

In this chapter a brief overview of the biomechanics of human gait was presented. It was suggested that current techniques can estimate the joint reaction forces and moments to a high degree of accuracy. However, no model has yet been published which adequately partitions the joint moments amongst the muscles. This thesis was therefore initiated to develop a technique to estimate the muscle forces during human locomotion.

CHAPTER III

MODEL FOR THE SOLUTION OF INDIVIDUAL MUSCLE FORCES

The approach developed to estimate the muscular forces in the lower limb is a hierarchical model. The lowest level, the anatomical model, concerns itself with the data necessary to define the musculoskeletal system. These include the muscle's moment arms, lengths and velocities. Data describing the muscle anatomy and bone structure are also included. The middle section, the muscle model, defines the force-length-velocity-activation relationship of a single muscle unit. These data, with those from the anatomical model, are used to estimate the maximum and minimum force a muscle can exert given its previous force history, current kinematics and previous stimulation. The stimulation to generate any intermediate muscle force is also defined. At the top of the hierarchy the control model provides a singular solution of the muscle forces, within the constraints defined in the muscle model, to satisfy the net muscle moments about those joint axes for which large range of movement exist.

ANATOMICAL MODEL

The human right lower limb was selected for mathematical analysis. The skeleton with attached muscles, ligaments and imbedded reference systems were included. Data defining the muscle geometries were also gathered to estimate their mechanical properties.

System Definition

The right human locomotor system was modelled as six segments, the pelvis, thigh, shank, talus, foot and toes. These segments were articulated at the hip, knee, ankle and metatarsophangeal (MTP) joints with three, one, two and one degrees of freedom, respectively. The two degrees of freedom at the ankle joint were the tibiotarsal (TT) and subtalar (ST) axes separated by the

talus segment. It should be noted that the MTP joint was included to estimate the maximum and minimum lengths of the muscles crossing it; moments were not solved about this joint.

An examination of the muscular system of the lower limb revealed 38 muscles of major importance. Several muscles were partitioned into two or more distinct structures due to functional considerations (Grant, 1972). In all, 47 'muscles' were deemed significant and are listed in Table 1. Muscles omitted include articularis genus, because of its small size and specialized function, and seven muscles intrinsic to the foot.

Twenty-five ligaments were defined crossing the hip, knee and ankle joints. These are listed in Table 2. Note that two ligaments, the posterior capsular and the deltoid, were subdivided into several distinct functional sections. It must be noted that forces were not assigned to the ligaments in this thesis. The ligaments were included in the anatomical model for future analytical consideration.

To establish a mathematical model, skeletal reference systems (SRS) were defined for the pelvis, thigh, shank, talus, foot and toe segments. The primary SRS were located at the pubic crest, hip, knee, tibiotalar, subtalar and MTP joint centres, respectively, as shown in Figure 1. Secondary SRS were defined by translating the primary SRS to the distal end of the segment (eg. primary pelvis at the pubic crest to secondary pelvis at the hip joint centre).

Coordinates defining the SRS were measured from a disarticulated dried male Caucasian skeleton using separate reference systems ( $Q_i$ ) for the  $i$ th segment. The talus and toes were included with the foot for these measurements. A special coordinate measuring device was built to collect these data and it defined the reference system  $Q$  (see Figure 2). The resolution of this three-dimensional anthropometer was approximately 1 mm throughout its working volume of 0.4 x 1.2 x 0.5 m. Cartesian



Table 1 The Lower Extremity Muscles Included in the Model.

| Muscle |                           | Joint Involvement |      |       |     |
|--------|---------------------------|-------------------|------|-------|-----|
| Index  | Name                      | Hip               | Knee | Ankle | MTP |
| 1      | Psoas major               | X                 |      |       |     |
| 2      | Iliacus                   | X                 |      |       |     |
| 3      | Gemellus superior         | X                 |      |       |     |
| 4      | Gemellus inferior         | X                 |      |       |     |
| 5      | Obturator externus        | X                 |      |       |     |
| 6      | Obturator internus        | X                 |      |       |     |
| 7      | Piriformis                | X                 |      |       |     |
| 8      | Quadratus femoris         | X                 |      |       |     |
| 9      | Pectineus                 | X                 |      |       |     |
| 10     | Adductor longus           | X                 |      |       |     |
| 11     | Adductor magnus (ant)     | X                 |      |       |     |
| 12     | Adductor magnus (mid)     | X                 |      |       |     |
| 13     | Adductor magnus (post)    | X                 |      |       |     |
| 14     | Adductor brevis           | X                 |      |       |     |
| 15     | Gluteus minimus (ant)     | X                 |      |       |     |
| 16     | Gluteus minimus (mid)     | X                 |      |       |     |
| 17     | Gluteus minimus (post)    | X                 |      |       |     |
| 18     | Gluteus medius (ant)      | X                 |      |       |     |
| 19     | Gluteus medius (mid)      | X                 |      |       |     |
| 20     | Gluteus medius (post)     | X                 |      |       |     |
| 21     | Gluteus maximus (deep)    | X                 |      |       |     |
| 22     | Gluteus maximus (sup)     | X                 |      |       |     |
| 23     | Tensor fascia latae       | X                 | X    |       |     |
| 24     | Semimembranosus           | X                 | X    |       |     |
| 25     | Semitendinosus            | X                 | X    |       |     |
| 26     | Gracilis                  | X                 | X    |       |     |
| 27     | Sartorius                 | X                 | X    |       |     |
| 28     | Rectus femoris            | X                 | X    |       |     |
| 29     | Biceps femoris (long)     | X                 | X    |       |     |
| 30     | Biceps femoris (short)    | X                 | X    |       |     |
| 31     | Vastus lateralis          |                   | X    |       |     |
| 32     | Vastus intermedius        |                   | X    |       |     |
| 33     | Vastus medialis           |                   | X    |       |     |
| 34     | Popliteus                 |                   | X    |       |     |
| 35     | Gastrocnemius (lateral)   |                   | X    | X     |     |
| 36     | Gastrocnemius (medial)    |                   | X    | X     |     |
| 37     | Plantaris                 |                   | X    |       |     |
| 38     | Soleus                    |                   |      | X     |     |
| 39     | Tibialis anterior         |                   |      | X     |     |
| 40     | Tibialis posterior        |                   |      | X     |     |
| 41     | Peroneus longus           |                   |      | X     |     |
| 42     | Peroneus brevis           |                   |      | X     |     |
| 43     | Peroneus tertius          |                   |      | X     |     |
| 44     | Extensor digitorum longus |                   |      | X     | X   |
| 45     | Extensor hallucis longus  |                   |      | X     | X   |
| 46     | Flexor digitorum longus   |                   |      | X     | X   |
| 47     | Flexor hallucis longus    |                   |      | X     | X   |

Table 2 The Lower Extremity Ligaments Included in the Model.

| Ligament |                          | Joint Involvement |      |     |    |
|----------|--------------------------|-------------------|------|-----|----|
| Index    | Name                     | Hip               | Knee | TT. | ST |
| 1        | Superior iliofemoral     | X                 |      |     |    |
| 2        | Inferior iliofemoral     | X                 |      |     |    |
| 3        | Pubofemoral              | X                 |      |     |    |
| 4        | Ishiofemoral             | X                 |      |     |    |
| 5        | Medial collateral        |                   | X    |     |    |
| 6        | Lateral collateral       |                   | X    |     |    |
| 7        | Med. posterior capsular  |                   | X    |     |    |
| 8        | Mid. posterior capsular  |                   | X    |     |    |
| 9        | Lat. posterior capsular  |                   | X    |     |    |
| 10       | Anterior cruciate        |                   | X    |     |    |
| 11       | Posterior cruciate       |                   | X    |     |    |
| 12       | Oblique popliteal        |                   | X    |     |    |
| 13       | Anterior talofibular     |                   |      | X   |    |
| 14       | Posterior talofibular    |                   |      | X   |    |
| 15       | Anterior talotibial      |                   |      | X   |    |
| 16       | Posterior talotibial     |                   |      | X   |    |
| 17       | Calcaneofibular          |                   |      | X   | X  |
| 18       | Tibionavicular           |                   |      | X   | X  |
| 19       | Middle deltoid           |                   |      | X   | X  |
| 20       | Posterior deltoid        |                   |      | X   | X  |
| 21       | Talcnavicular            |                   |      |     | X  |
| 22       | Ant. Int. talocalcaneal  |                   |      |     | X  |
| 23       | Post. Int. talocalcaneal |                   |      |     | X  |
| 24       | Lateral talocalcaneal    |                   |      |     | X  |
| 25       | Posterior talocalcaneal  |                   |      |     | X  |

coordinates of the origin and a point 50 mm along the positive X, Y, and Z axes for each of the primary SRS, and the origin of the secondary SRS were measured and are given in Table 3.

Lew and Lewis (1977) examined a variety of scaling techniques and demonstrated the superiority of the homogeneous deformation over other scaling schemes. In the present model an analogous scaling technique was used which employs the homogeneous coordinate representation of a point and a completely generalized 4x4 transformation matrix to transform one three-dimensional space to another (Pierrynowski, 1980). Knowing the location of several points of prominence on a skeletal segment, and the corresponding location of these same points measured in vivo on a subject, a transformation matrix can be calculated which transforms the data from a disarticulated skeletal segment into

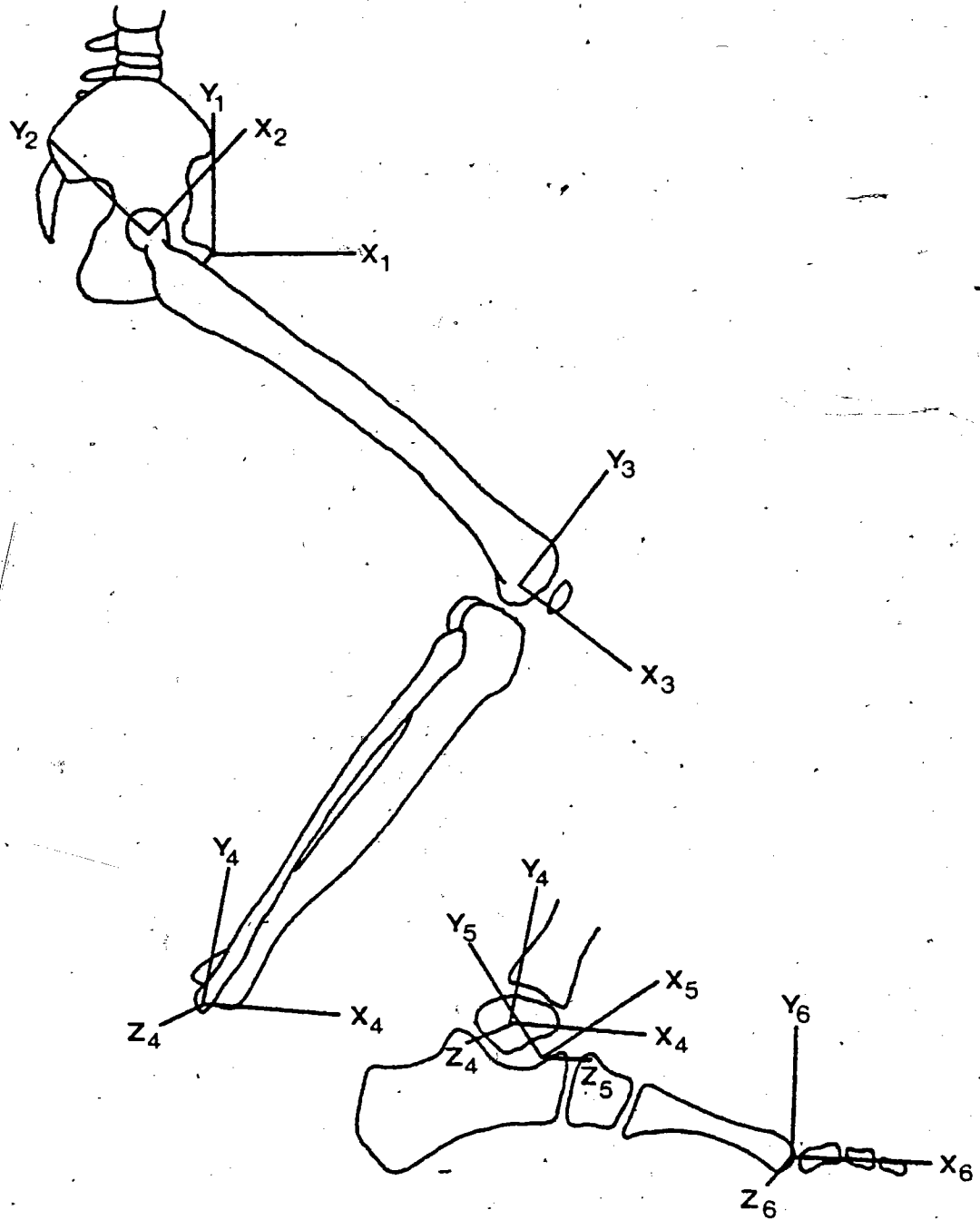
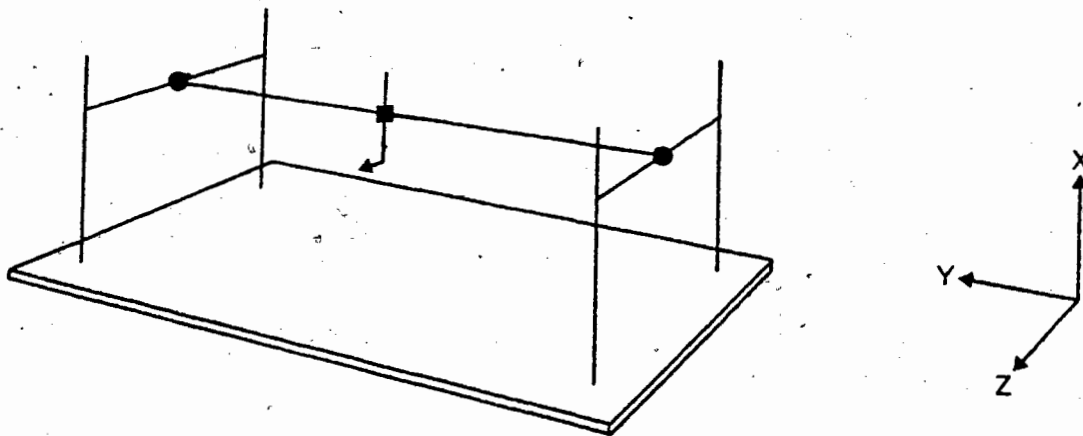


Figure 1

The skeletal reference systems (SRS) for the human lower extremity: 1 - pelvis at the Pubic Crest; 2 - Thigh at the Hip Joint; 3 - Shank at the Knee Joint; 4 - Talus at the Tibiotalarsal Joint; 5 - Foot at the Subtalar Joint; 6 - Toes at the MTP Joint. Note that the Z-axis for SRS 1, 2 and 3 are perpendicular to the paper and towards the reader.



- - slides along the Z axis
- - slides along the X and Y axes

Figure 2 The three dimensional anthropometer.

that segment of the subject. When applied with a group of at least four points on a body segment a rigid body translation and rotation is performed along with a homogeneous deformation of the initial segment (skeleton) into the final segment (subject). These transformations were used to locate the SRS within the subject. Specifics regarding the method of implementing the transformational scaling is found in Chapter IV. The theory underlying the transformation is found in Appendix A.

Table 3 The Points Defining the Primary and Secondary Skeletal Reference Systems (SRS) and the Centres of Mass for each Skeletal Segment. All values in mm.

| Reference System  | Origin                                    | +X          | +Y          | +Z          |
|---|---|-------------|-------------|-------------|
| Seg/ <sup>1</sup> <sub>2</sub> <sup>2</sup> <sub>3</sub> <sup>3</sup> |   |             |             |             |
| Pelvis/ <sup>1</sup> PC<br>/ <sup>2</sup> H<br>/ <sup>3</sup> CM      | 268 246 241<br>225 248 314                | 318 246 241 | 268 296 241 | 268 246 291 |
| Thigh / <sup>1</sup> H<br>/ <sup>2</sup> K<br>/ <sup>3</sup> CM       | 144 561 106<br>115 170 138<br>132 393 118 | 194 556 106 | 148 611 102 | 144 565 156 |
| Shank / <sup>1</sup> K<br>/ <sup>2</sup> TT<br>/ <sup>3</sup> CM      | 173 644 143<br>191 255 143<br>180 485 143 | 123 646 143 | 171 694 143 | 173 644 193 |
| Talus / <sup>1</sup> TT<br>/ <sup>2</sup> ST<br>/ <sup>3</sup> CM     | 191 255 143<br>182 245 144<br>191 255 143 | 239 252 157 | 191 294 152 | 177 256 190 |
| Foot / <sup>1</sup> ST<br>/ <sup>2</sup> MTP<br>/ <sup>3</sup> CM     | 182 245 144<br>296 222 174<br>232 226 143 | 222 273 132 | 155 286 152 | 196 245 192 |
| Toes / <sup>1</sup> MTP   | 296 222 174                               | 336 222 203 | 290 271 182 | 289 215 223 |

- 1 location of the primary reference system  
 2 location of the secondary reference system  
 3 location of the centre of mass

### Muscle Line of Action and Moment Arms

The lines of action of the locomotor muscles have been modelled as straight lines joining origin to insertion (Hardt, 1978; Dostal and Andrews, 1981). However, many muscles are deflected over the skeletal framework or pass through tendon sheaths which are constrained. Seireg and Arvikar (1973) represented many of the muscles crossing the ankle in two parts to account for their large change in direction. However, their method of collection of data from an anatomical atlas, with a resolution of 3mm (Arvikar, 1971), must be suspect. Frigo and Pedotti (1977)

improved upon the one or two straight line representation of the muscles by using lines and arcs of circles to model the course of 11 major locomotor muscles, but they did not scale the muscle paths for different subjects. The work of Jensen and co-workers (1975a,b) strongly suggests that the centroid line of the muscle should be used; they present data on three of the muscles crossing the hip to support their case. Although their technique is one of the most accurate methods of defining the course of a muscle, a balance between accuracy and simplicity must be kept in mind.

In this thesis the same skeleton used to define the SRS was used to define the line of action of a muscle. Each muscle was represented by an elastic thread which connected from the centroid of its area of origin to the centroid of its area of insertion. Between these two end points, up to four additional points were defined from anatomical considerations, through which the muscle was constrained to pass. The coordinates of these points are presented in Table 4 relative to the appropriate skeletal segment (reference system  $Q_1$ ). Using the transformation described above the locations of the points which define the muscles can be relocated within any subject.

A muscle's line of action within a subject was obtained by joining its defined points with a combination of straight and curvilinear sections. Straight lines were used whenever a muscle ran freely from point to point, and a curve was fitted when a muscle was forced to alter its course by either bony prominences (eg. condyles) or other constraints (eg. ligaments at the ankle).

For most muscles an even number of points were defined through which the muscle was constrained to pass. For these muscles each pair of points (point 1 to 2, point 3 to 4, point 5 to 6) were joined by a straight line and its length calculated. For those non-linear sections between these straight lines (point 2 to 3, point 4 to 5) a parametric cubic polynomial was fitted, the theory of which is found in Appendix B.

| Muscle | Segment number | 1   | 2   | 3   | 4   | 5   | 6   |
|--------|----------------|-----|-----|-----|-----|-----|-----|
| 1      | 1              | 228 | 251 | 125 | 250 | 235 | 125 |
| 2      | 1              | 198 | 232 | 164 | 220 | 214 | 180 |
| 3      | 1              | 220 | 240 | 174 | 248 | 223 | 172 |
| 4      | 1              | 245 | 252 | 166 | 296 | 231 | 143 |
| 5      | 1              | 253 | 252 | 132 | 293 | 231 | 161 |
| 6      | 1              | 190 | 251 | 135 | 239 | 211 | 141 |
| 7      | 1              | 217 | 251 | 120 | 242 | 226 | 129 |
| 8      | 1              | 189 | 232 | 174 | 204 | 219 | 164 |
| 9      | 1              | 198 | 234 | 166 | 220 | 214 | 180 |
| 10     | 1              | 220 | 240 | 174 | 248 | 223 | 172 |
| 11     | 1              | 245 | 252 | 166 | 296 | 231 | 143 |
| 12     | 1              | 253 | 252 | 132 | 293 | 231 | 161 |
| 13     | 1              | 190 | 251 | 135 | 239 | 211 | 141 |
| 14     | 1              | 217 | 251 | 120 | 242 | 226 | 129 |
| 15     | 1              | 189 | 232 | 174 | 204 | 219 | 164 |
| 16     | 1              | 198 | 234 | 166 | 220 | 214 | 180 |
| 17     | 1              | 220 | 240 | 174 | 248 | 223 | 172 |
| 18     | 1              | 245 | 252 | 166 | 296 | 231 | 143 |
| 19     | 1              | 253 | 252 | 132 | 293 | 231 | 161 |
| 20     | 1              | 190 | 251 | 135 | 239 | 211 | 141 |
| 21     | 1              | 217 | 251 | 120 | 242 | 226 | 129 |
| 22     | 1              | 189 | 232 | 174 | 204 | 219 | 164 |
| 23     | 1              | 198 | 234 | 166 | 220 | 214 | 180 |
| 24     | 1              | 220 | 240 | 174 | 248 | 223 | 172 |
| 25     | 1              | 245 | 252 | 166 | 296 | 231 | 143 |
| 26     | 1              | 253 | 252 | 132 | 293 | 231 | 161 |
| 27     | 1              | 190 | 251 | 135 | 239 | 211 | 141 |
| 28     | 1              | 217 | 251 | 120 | 242 | 226 | 129 |
| 29     | 1              | 189 | 232 | 174 | 204 | 219 | 164 |
| 30     | 1              | 198 | 234 | 166 | 220 | 214 | 180 |
| 31     | 1              | 220 | 240 | 174 | 248 | 223 | 172 |
| 32     | 1              | 245 | 252 | 166 | 296 | 231 | 143 |
| 33     | 1              | 253 | 252 | 132 | 293 | 231 | 161 |
| 34     | 1              | 190 | 251 | 135 | 239 | 211 | 141 |
| 35     | 1              | 217 | 251 | 120 | 242 | 226 | 129 |
| 36     | 1              | 189 | 232 | 174 | 204 | 219 | 164 |
| 37     | 1              | 198 | 234 | 166 | 220 | 214 | 180 |
| 38     | 1              | 220 | 240 | 174 | 248 | 223 | 172 |
| 39     | 1              | 245 | 252 | 166 | 296 | 231 | 143 |
| 40     | 1              | 253 | 252 | 132 | 293 | 231 | 161 |
| 41     | 1              | 190 | 251 | 135 | 239 | 211 | 141 |
| 42     | 1              | 217 | 251 | 120 | 242 | 226 | 129 |
| 43     | 1              | 189 | 232 | 174 | 204 | 219 | 164 |
| 44     | 1              | 198 | 234 | 166 | 220 | 214 | 180 |
| 45     | 1              | 220 | 240 | 174 | 248 | 223 | 172 |
| 46     | 1              | 245 | 252 | 166 | 296 | 231 | 143 |
| 47     | 1              | 253 | 252 | 132 | 293 | 231 | 161 |
| 48     | 1              | 190 | 251 | 135 | 239 | 211 | 141 |
| 49     | 1              | 217 | 251 | 120 | 242 | 226 | 129 |
| 50     | 1              | 189 | 232 | 174 | 204 | 219 | 164 |
| 51     | 1              | 198 | 234 | 166 | 220 | 214 | 180 |
| 52     | 1              | 220 | 240 | 174 | 248 | 223 | 172 |
| 53     | 1              | 245 | 252 | 166 | 296 | 231 | 143 |
| 54     | 1              | 253 | 252 | 132 | 293 | 231 | 161 |
| 55     | 1              | 190 | 251 | 135 | 239 | 211 | 141 |
| 56     | 1              | 217 | 251 | 120 | 242 | 226 | 129 |
| 57     | 1              | 189 | 232 | 174 | 204 | 219 | 164 |
| 58     | 1              | 198 | 234 | 166 | 220 | 214 | 180 |
| 59     | 1              | 220 | 240 | 174 | 248 | 223 | 172 |
| 60     | 1              | 245 | 252 | 166 | 296 | 231 | 143 |
| 61     | 1              | 253 | 252 | 132 | 293 | 231 | 161 |
| 62     | 1              | 190 | 251 | 135 | 239 | 211 | 141 |
| 63     | 1              | 217 | 251 | 120 | 242 | 226 | 129 |
| 64     | 1              | 189 | 232 | 174 | 204 | 219 | 164 |
| 65     | 1              | 198 | 234 | 166 | 220 | 214 | 180 |
| 66     | 1              | 220 | 240 | 174 | 248 | 223 | 172 |
| 67     | 1              | 245 | 252 | 166 | 296 | 231 | 143 |
| 68     | 1              | 253 | 252 | 132 | 293 | 231 | 161 |
| 69     | 1              | 190 | 251 | 135 | 239 | 211 | 141 |
| 70     | 1              | 217 | 251 | 120 | 242 | 226 | 129 |
| 71     | 1              | 189 | 232 | 174 | 204 | 219 | 164 |
| 72     | 1              | 198 | 234 | 166 | 220 | 214 | 180 |
| 73     | 1              | 220 | 240 | 174 | 248 | 223 | 172 |
| 74     | 1              | 245 | 252 | 166 | 296 | 231 | 143 |
| 75     | 1              | 253 | 252 | 132 | 293 | 231 | 161 |
| 76     | 1              | 190 | 251 | 135 | 239 | 211 | 141 |
| 77     | 1              | 217 | 251 | 120 | 242 | 226 | 129 |
| 78     | 1              | 189 | 232 | 174 | 204 | 219 | 164 |
| 79     | 1              | 198 | 234 | 166 | 220 | 214 | 180 |
| 80     | 1              | 220 | 240 | 174 | 248 | 223 | 172 |
| 81     | 1              | 245 | 252 | 166 | 296 | 231 | 143 |
| 82     | 1              | 253 | 252 | 132 | 293 | 231 | 161 |
| 83     | 1              | 190 | 251 | 135 | 239 | 211 | 141 |
| 84     | 1              | 217 | 251 | 120 | 242 | 226 | 129 |
| 85     | 1              | 189 | 232 | 174 | 204 | 219 | 164 |
| 86     | 1              | 198 | 234 | 166 | 220 | 214 | 180 |
| 87     | 1              | 220 | 240 | 174 | 248 | 223 | 172 |
| 88     | 1              | 245 | 252 | 166 | 296 | 231 | 143 |
| 89     | 1              | 253 | 252 | 132 | 293 | 231 | 161 |
| 90     | 1              | 190 | 251 | 135 | 239 | 211 | 141 |
| 91     | 1              | 217 | 251 | 120 | 242 | 226 | 129 |
| 92     | 1              | 189 | 232 | 174 | 204 | 219 | 164 |
| 93     | 1              | 198 | 234 | 166 | 220 | 214 | 180 |
| 94     | 1              | 220 | 240 | 174 | 248 | 223 | 172 |
| 95     | 1              | 245 | 252 | 166 | 296 | 231 | 143 |
| 96     | 1              | 253 | 252 | 132 | 293 | 231 | 161 |
| 97     | 1              | 190 | 251 | 135 | 239 | 211 | 141 |
| 98     | 1              | 217 | 251 | 120 | 242 | 226 | 129 |
| 99     | 1              | 189 | 232 | 174 | 204 | 219 | 164 |
| 100    | 1              | 198 | 234 | 166 | 220 | 214 | 180 |
| 101    | 1              | 220 | 240 | 174 | 248 | 223 | 172 |
| 102    | 1              | 245 | 252 | 166 | 296 | 231 | 143 |
| 103    | 1              | 253 | 252 | 132 | 293 | 231 | 161 |
| 104    | 1              | 190 | 251 | 135 | 239 | 211 | 141 |
| 105    | 1              | 217 | 251 | 120 | 242 | 226 | 129 |
| 106    | 1              | 189 | 232 | 174 | 204 | 219 | 164 |
| 107    | 1              | 198 | 234 | 166 | 220 | 214 | 180 |
| 108    | 1              | 220 | 240 | 174 | 248 | 223 | 172 |
| 109    | 1              | 245 | 252 | 166 | 296 | 231 | 143 |
| 110    | 1              | 253 | 252 | 132 | 293 | 231 | 161 |
| 111    | 1              | 190 | 251 | 135 | 239 | 211 | 141 |
| 112    | 1              | 217 | 251 | 120 | 242 | 226 | 129 |
| 113    | 1              | 189 | 232 | 174 | 204 | 219 | 164 |
| 114    | 1              | 198 | 234 | 166 | 220 | 214 | 180 |
| 115    | 1              | 220 | 240 | 174 | 248 | 223 | 172 |
| 116    | 1              | 245 | 252 | 166 | 296 | 231 | 143 |
| 117    | 1              | 253 | 252 | 132 | 293 | 231 | 161 |
| 118    | 1              | 190 | 251 | 135 | 239 | 211 | 141 |
| 119    | 1              | 217 | 251 | 120 | 242 | 226 | 129 |
| 120    | 1              | 189 | 232 | 174 | 204 | 219 | 164 |
| 121    | 1              | 198 | 234 | 166 | 220 | 214 | 180 |
| 122    | 1              | 220 | 240 | 174 | 248 | 223 | 172 |
| 123    | 1              | 245 | 252 | 166 | 296 | 231 | 143 |
| 124    | 1              | 253 | 252 | 132 | 293 | 231 | 161 |
| 125    | 1              | 190 | 251 | 135 | 239 | 211 | 141 |
| 126    | 1              | 217 | 251 | 120 | 242 | 226 | 129 |
| 127    | 1              | 189 | 232 | 174 | 204 | 219 | 164 |
| 128    | 1              | 198 | 234 | 166 | 220 | 214 | 180 |
| 129    | 1              | 220 | 240 | 174 | 248 | 223 | 172 |
| 130    | 1              | 245 | 252 | 166 | 296 | 231 | 143 |
| 131    | 1              | 253 | 252 | 132 | 293 | 231 | 161 |
| 132    | 1              | 190 | 251 | 135 | 239 | 211 | 141 |
| 133    | 1              | 217 | 251 | 120 | 242 | 226 | 129 |
| 134    | 1              | 189 | 232 | 174 | 204 | 219 | 164 |
| 135    | 1              | 198 | 234 | 166 | 220 | 214 | 180 |
| 136    | 1              | 220 | 240 | 174 | 248 | 223 | 172 |
| 137    | 1              | 245 | 252 | 166 | 296 | 231 | 143 |
| 138    | 1              | 253 | 252 | 132 | 293 | 231 | 161 |
| 139    | 1              | 190 | 251 | 135 | 239 | 211 | 141 |
| 140    | 1              | 217 | 251 | 120 | 242 | 226 | 129 |
| 141    | 1              | 189 | 232 | 174 | 204 | 219 | 164 |
| 142    | 1              | 198 | 234 | 166 | 220 | 214 | 180 |
| 143    | 1              | 220 | 240 | 174 | 248 | 223 | 172 |
| 144    | 1              | 245 | 252 | 166 | 296 | 231 | 143 |
| 145    | 1              | 253 | 252 | 132 | 293 | 231 | 161 |
| 146    | 1              | 190 | 251 | 135 | 239 | 211 | 141 |
| 147    | 1              | 217 | 251 | 120 | 242 | 226 | 129 |
| 148    | 1              | 189 | 232 | 174 | 204 | 219 | 164 |
| 149    | 1              | 198 | 234 | 166 | 220 | 214 | 180 |
| 150    | 1              | 220 | 240 | 174 | 248 | 223 | 172 |
| 151    | 1              | 245 | 252 | 166 | 296 | 231 | 143 |
| 152    | 1              | 253 | 252 | 132 | 293 | 231 | 161 |
| 153    | 1              | 190 | 251 | 135 | 239 | 211 | 141 |
| 154    | 1              | 217 | 251 | 120 | 242 | 226 | 129 |
| 155    | 1              | 189 | 232 | 174 | 204 | 219 | 164 |
| 156    | 1              | 198 | 234 | 166 | 220 | 214 | 180 |
| 157    | 1              | 220 | 240 | 174 | 248 | 223 | 172 |
| 158    | 1              | 245 | 252 | 166 | 296 | 231 | 143 |
| 159    | 1              | 253 | 252 | 132 | 293 | 231 | 161 |
| 160    | 1              | 190 | 251 | 135 | 239 | 211 | 141 |
| 161    | 1              | 217 | 251 | 120 | 242 | 226 |     |

For those muscles with an odd number of points (muscles 1, 2, 22, 23, 25, 27, and 34) simple straight line segments were used to join the points and to calculate the muscle lengths. For all muscles, summing along the length of all of the sections comprising it, albeit straight or curved, gave its length ( $L^m$ ).

Since the patella was not included in the model additional constraints were necessary to define the location of the quadriceps (muscles 28, 31, 32, 33) at the knee. Each of these muscles was assumed to arise from its respective origin (point 1), converge and meet at a point 6mm anterior to the most anterior and superior aspect of the femoral patellar surface (point 2), curve to a third point (point 3), and then insert into the tibial tuberosity (point 4). These points are shown in Figure 3 relative to the thigh and shank segments.

To define the line of action of a quadricep, the line through the 3rd and 4th points was constrained to intersect the long axis of the tibia, in the plane of the hip, knee and ankle joints, with an angle ( $A$ ) in degrees given by:

$$A = 15 + 0.317\theta - 0.0084\theta^2 + 0.000031\theta^3 \quad (1)$$

where  $\theta$  is the angle of the thigh relative to the shank (full extension is zero degrees). This equation was calculated from data collected from in vivo sagittal plane X-ray photographs of a male knee joint (Morrison, 1967). By defining the distance between point 3 and point 4 to be a constant value (eg. 2 mm), the location of the third point was calculated. Fitting a curve from point 2 to 3 (see Appendix B) completely described the location of each quadricep muscle.

Knowing the line of action of the muscles in the neighbourhood of the joint centres, the moment arms were calculated. Details are found in Appendix C. It should be noted that this analysis technique does not take into account the influence of one muscle



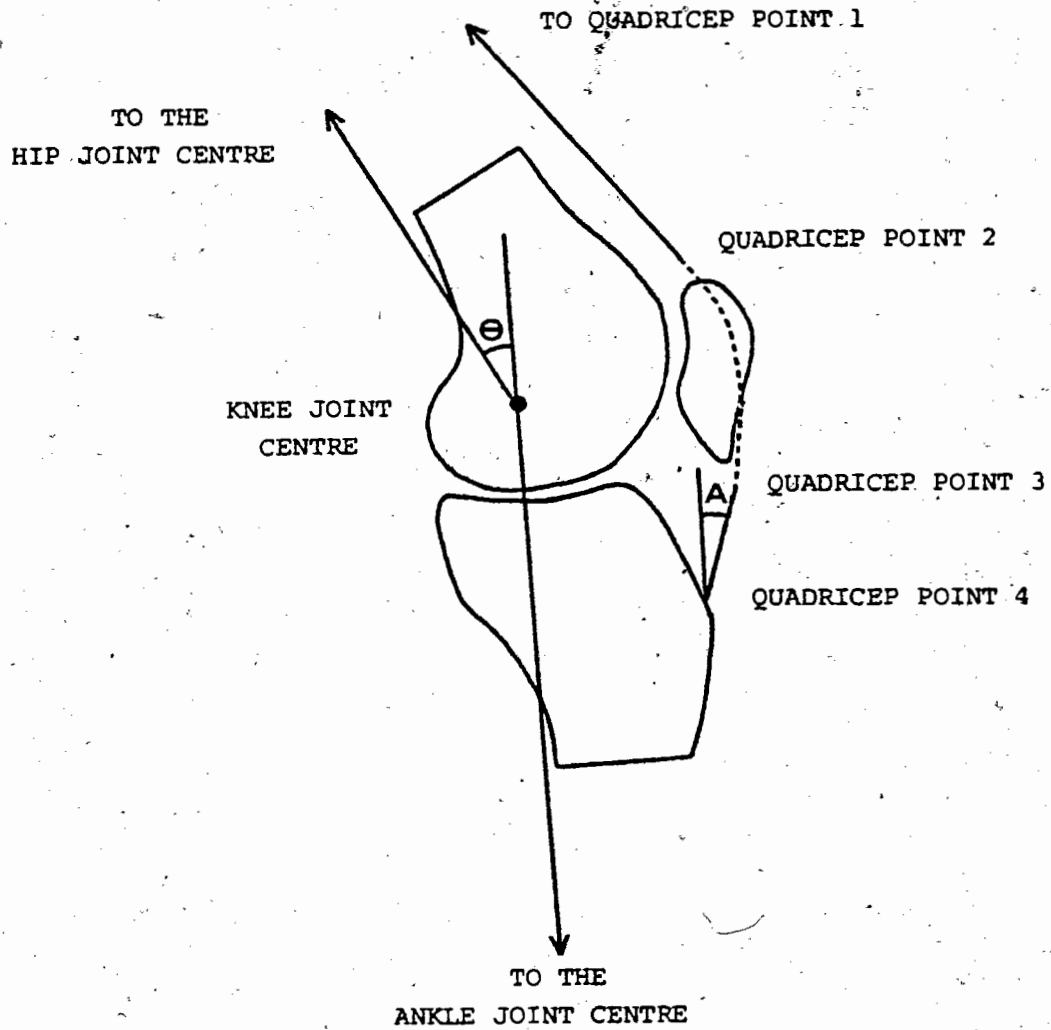


Figure 3 The definition of a quadriceps muscle in the neighbourhood of the knee joint. A sagittal plane view is shown.

overlying another. Since this tends to increase the distance the superficial muscles lie from the joint centres the calculated muscle moment arms are underestimated. To correct these underestimations Eycleshymer and Schoemakers (1970) atlas of cross-section anatomy was used to define the location of the muscles as they passed through the transverse plane centred at the hip, knee and ankle joints. These data are found in Table 5 scaled to the skeleton. Those muscles with zero values were not modified.

#### Ligament Line of Action and Moment Arms

The line of action of the ligaments were defined in the same manner as the muscles. Each ligament was represented by an elastic thread which connected from the centroid of its area of origin to the centroid of its area of insertion. However, unlike the muscles all ligaments were defined as one straight line section. The coordinates of these points are given in Table 6 relative to the appropriate skeletal segment (reference system  $Q_1$ ). These points were transformed to the subject and the length of each ligament calculated. The ligament's moment arms, relative to the joint centres, were calculated in a similar manner as the muscles.

#### Muscle Geometry

The geometry of the human ambulatory muscles is available in the form of qualitative information, but there is a definite lack of reliable quantitative data. Alexander and Vernon (1975) present complete sets of geometrical data on 17 of the muscles crossing the knee and ankle, but their work can be criticized on the grounds of low sample size ( $n=1$ ) and exclusion of tendons. Pedotti *et al.* (1978) present the mean lengths, fibre lengths and cross-sectional areas on 11 major locomotor muscles but no indication of their data source is given. Schumacher and Wolff (1966a,b) report the dry mass and physiological cross-sectional area of many of the lower limb muscles, but because of the advanced age of their 21 cadavers (mean age 72.5 years), and

Table 5 Location of the Muscles in the Transverse Plane at the Hip, Knee and Ankle Joints. All values in mm.

| Muscle | Hip |    | Knee |   | Ankle |   |
|--------|-----|----|------|---|-------|---|
|        | X   | Z  | X    | Z | X     | Z |
| 1      | 16  | 8  |      |   |       |   |
| 2      | 14  | 24 |      |   |       |   |
| 3      | 0   | 0  |      |   |       |   |
| 4      | 0   | 0  |      |   |       |   |
| 5      | 0   | 0  |      |   |       |   |
| 6      | 0   | 0  |      |   |       |   |
| 7      | 0   | 0  |      |   |       |   |
| 8      | 0   | 0  |      |   |       |   |
| 9      | 0   | 0  |      |   |       |   |
| 10     | 0   | 0  |      |   |       |   |
| 11     | 0   | 0  |      |   |       |   |
| 12     | 0   | 0  |      |   |       |   |
| 13     | 0   | 0  |      |   |       |   |
| 14     | 0   | 0  |      |   |       |   |
| 15     | 0   | 0  |      |   |       |   |
| 16     | 0   | 0  |      |   |       |   |
| 17     | 0   | 0  |      |   |       |   |
| 18     | 0   | 0  |      |   |       |   |
| 19     | 0   | 0  |      |   |       |   |
| 20     | 0   | 0  |      |   |       |   |
| 21     | 0   | 0  |      |   |       |   |
| 22     | 0   | 0  |      |   |       |   |
| 23     | 0   | 0  |      |   |       |   |
| 24     | 0   | 0  |      |   |       |   |
| 25     | 0   | 0  |      |   |       |   |
| 26     | 0   | 0  |      |   |       |   |
| 27     | 0   | 0  |      |   |       |   |
| 28     | 0   | 0  |      |   |       |   |
| 29     | 0   | 0  |      |   |       |   |
| 30     | 0   | 0  |      |   |       |   |
| 31     | 0   | 0  |      |   |       |   |
| 32     | 0   | 0  |      |   |       |   |
| 33     | 0   | 0  |      |   |       |   |
| 34     | 0   | 0  |      |   |       |   |
| 35     | 0   | 0  |      |   |       |   |
| 36     | 0   | 0  |      |   |       |   |
| 37     | 0   | 0  |      |   |       |   |
| 38     | 0   | 0  |      |   |       |   |
| 39     | 0   | 0  |      |   |       |   |
| 40     | 0   | 0  |      |   |       |   |
| 41     | 0   | 0  |      |   |       |   |
| 42     | 0   | 0  |      |   |       |   |
| 43     | 0   | 0  |      |   |       |   |
| 44     | 0   | 0  |      |   |       |   |
| 45     | 0   | 0  |      |   |       |   |
| 46     | 0   | 0  |      |   |       |   |
| 47     | 0   | 0  |      |   |       |   |

Note: With the skeleton in the anatomical position +X is anterior and +Z is lateral.

Table 6 The Points Defining the Line of Action of the Ligaments within the Skeleton. All values in mm.

| Ligament | on<br>segment<br>number         | point |     |     |     |     |     |
|----------|---------------------------------|-------|-----|-----|-----|-----|-----|
|          |                                 | 1.    |     |     | 2   |     |     |
| 1        | 1 2                             | 249   | 273 | 310 | 148 | 543 | 147 |
| 2        | 1 1 2 2 2                       | 249   | 273 | 310 | 147 | 519 | 137 |
| 3        | 1 1 2 2 2 2                     | 254   | 248 | 283 | 140 | 515 | 125 |
| 4        | 1 1 2 2 2 2 2                   | 191   | 241 | 303 | 128 | 554 | 142 |
| 5        | 1 1 2 2 2 2 2 2                 | 115   | 167 | 103 | 187 | 547 | 131 |
| 6        | 2 2 2 2 2 2 2 2 2               | 115   | 173 | 174 | 183 | 597 | 183 |
| 7        | 2 2 2 2 2 2 2 2 2 2             | 106   | 182 | 122 | 150 | 606 | 131 |
| 8        | 2 2 2 2 2 2 2 2 2 2 2           | 102   | 184 | 144 | 159 | 606 | 153 |
| 9        | 2 2 2 2 2 2 2 2 2 2 2 2         | 106   | 187 | 164 | 166 | 608 | 170 |
| 10       | 2 2 2 2 2 2 2 2 2 2 2 2 2       | 102   | 172 | 150 | 183 | 628 | 139 |
| 11       | 2 2 2 2 2 2 2 2 2 2 2 2 2 2     | 118   | 160 | 131 | 159 | 608 | 151 |
| 12       | 2 2 2 2 2 2 2 2 2 2 2 2 2 2 2   | 105   | 182 | 124 | 153 | 604 | 128 |
| 13       | 3 3 3 3 3 3 3 3 3 3 3 3 3 3 3 3 | 194   | 259 | 169 | 197 | 256 | 157 |
| 14       | 3 3 3 3 3 3 3 3 3 3 3 3 3 3 3 3 | 181   | 268 | 156 | 172 | 258 | 148 |
| 15       | 3 3 3 3 3 3 3 3 3 3 3 3 3 3 3 3 | 202   | 272 | 121 | 213 | 254 | 128 |
| 16       | 3 3 3 3 3 3 3 3 3 3 3 3 3 3 3 3 | 186   | 163 | 120 | 176 | 259 | 129 |
| 17       | 3 3 3 3 3 3 3 3 3 3 3 3 3 3 3 3 | 180   | 250 | 172 | 168 | 237 | 162 |
| 18       | 3 3 3 3 3 3 3 3 3 3 3 3 3 3 3 3 | 205   | 278 | 126 | 223 | 252 | 130 |
| 19       | 3 3 3 3 3 3 3 3 3 3 3 3 3 3 3 3 | 202   | 273 | 121 | 211 | 250 | 125 |
| 20       | 3 3 3 3 3 3 3 3 3 3 3 3 3 3 3 3 | 198   | 268 | 122 | 202 | 252 | 121 |
| 21       | 4 4 4 4 4 4 4 4 4 4 4 4 4 4 4 4 | 216   | 253 | 141 | 222 | 255 | 139 |
| 22       | 4 4 4 4 4 4 4 4 4 4 4 4 4 4 4 4 | 207   | 253 | 146 | 202 | 250 | 151 |
| 23       | 4 4 4 4 4 4 4 4 4 4 4 4 4 4 4 4 | 196   | 244 | 151 | 200 | 250 | 151 |
| 24       | 4 4 4 4 4 4 4 4 4 4 4 4 4 4 4 4 | 188   | 242 | 160 | 170 | 228 | 163 |
| 25       | 4 4 4 4 4 4 4 4 4 4 4 4 4 4 4 4 | 164   | 252 | 144 | 157 | 243 | 147 |

possible atrophy of the muscles, one must be cautious when extrapolating these data to a younger population. All of the above studies are limited in their application in that there is minimal information provided with which to scale the tabulated values to other individuals.

Skeletal muscles comprise two fibre orientations, parallel and pennate, and their fibres may attach into the skeletal framework directly or via tendons. Various characteristics of these structures can be defined as shown in Figure 4. Six values which were deemed important are the tendon and fibre lengths as a percentage of the total muscle length ( $\%L^T$ ,  $\%L^F$ ), a muscle shape factor (E) which is the maximum anatomical cross-sectional area ( $\bar{A}^m$ ) divided by its mean anatomical cross-sectional area ( $\bar{A}$ ),

cross-sectional area of the tendon ( $A^T$ ), fibre angle of pennation ( $\alpha$ ) and the muscle mass ( $m$ ). If a muscle had two tendons the effective cross-sectional area was calculated, to give a correct value of composite compliance.

Eycleshymer and Schoemaker's atlas of cross-section anatomy (1970) was used to define a 'standard' set of representative muscles and tendons. In this work the body of a black American male, fixed in the anatomical position, was serially sliced and meticulously reproduced. Since the location of the 'slices' were depicted with appropriate scaling information, the anatomical cross-sectional areas, length and volume of most of the desired muscles and tendons could be determined. Areas were measured by planimetry and volume obtained by summing the products of the area and 'slice' thickness. The muscle mass was estimated by multiplying the volume by the density of muscle ( $1050 \text{ kg m}^{-3}$ ). Additional information were also available for scaling purposes.

Muscle geometries were also acquired from four other major and many minor sources. A reference able to supply more than 30 of the desired items of information was defined as a major source. These were the works of Voss (1956), Schumacher and Wolff (1966a,b), Alexander and Vernon (1975) and Pedotti *et al.* (1978), which respectively supplied 34, 94, 68 and 33 items of information. It should be noted that Schumacher and Wolff's raw data was collected by several students who each examined a few muscles in detail. These original studies were referred to for more detailed information (Bub, 1963; Iadrick, 1963; G. Muller, 1966; K. Muller, 1967; Neumann, 1963; Rohmann, 1963). As noted in the introductory paragraph to this section, this author was skeptical of these data because of low sample sizes and non-typical subjects. The minor sources typically present detailed geometrical data on one or two muscles, although some offered a variety of information. Published data used include the works of Arnold and Worthman (1974), Barret (1962), Benninghoff and Rollhauser (1952), Blanton and ~~Biggs~~ Biggs (1970), Chhibber and

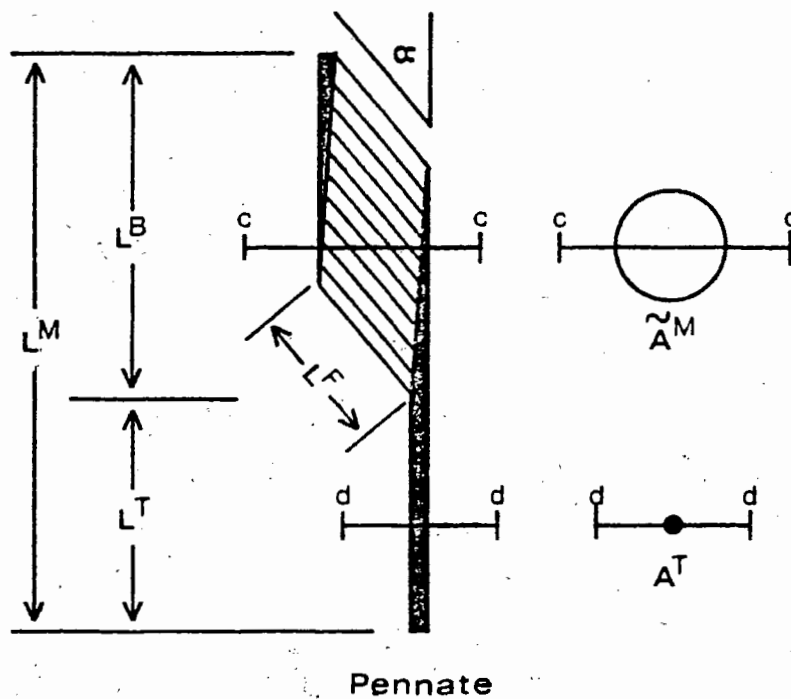
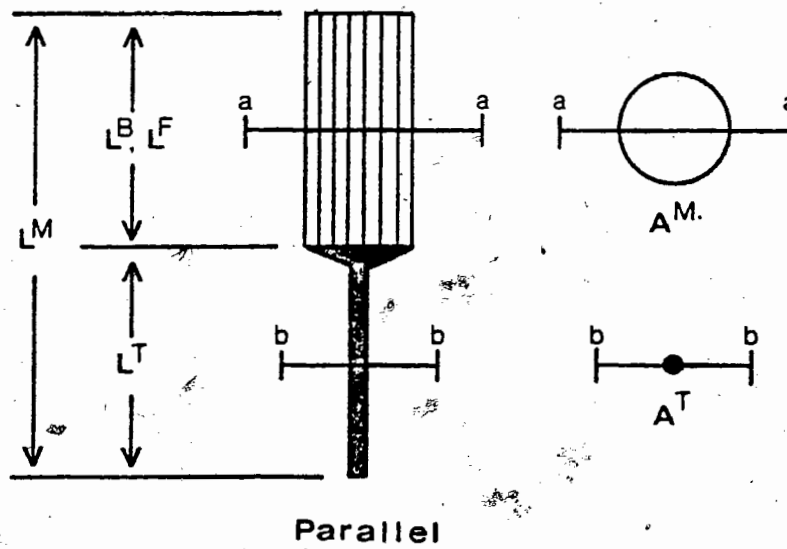


Figure 4 Geometrical characteristics of parallel and pennate muscles. Symbols are explained in the text.

Singh (1970), Fisher (1906), Haggmark et al. (1978), Haxton (1944), Jensen and Metcalf (1975a,b), Kann (1957), Kapanji (1970), Khan and Khan (1976), Kolb (1937), Reys (1915), Schwarzacher (1959), Sokolowska-Pituchowa et al. (1974), Trzenschik and Loetzke (1969), and Walker et al. (1964).

The data from the major and minor sources were compared to Eycleshymer and Schoemaker's work to determine their suitability and to complete the table. The resulting muscle and tendon geometries, measured at the anatomical length, are presented in Table 7. Note that the glutei minimus and medius were split into three equal sections. It was also assumed that 25 percent of the gluteus maximus fibres insert into the ilio-tibial tract. Entries enclosed in brackets are those for which the author was unable to locate sufficient information to be confident of the result.

In addition to the muscle geometries the area representation of the three fibre types (SO, FO, FG) within a given muscle were also required. Few data exist in the literature and many values had to be estimated, especially for the subdivision of the fast twitch fibres into the oxidative and glycolytic groups. It should be noted that for those muscles partitioned into two or more distinct structures, due to functional considerations, they were considered identical in fibre type distribution.

Two papers supplied most of the human fibre typing data and deserve special mention. Johnson et al. (1973) examined the distribution of fibre types in 36 muscles from six young male subjects (mean age 22 years). Fourteen of the muscles were obtained from the lower limb. This paper is limited in that they only subdivided the fibre populations into fast and slow twitch groupings. Nevertheless, this reference supplied the SO distribution for muscles 1, 2, 11, 12, 13, 21, 22, 27, 28, 29, 30, 33, 39 and 41. The second paper (Edgerton et al., 1975) examined four leg muscles in 32 humans (mean age 59 years) but report the distribution of the three fibre types. This paper supplied the SO, FO, FG distribution for vastus lateralis and

Table 7 The 'Standard' Muscle Geometrical Data.

| Muscle | %L <sup>F</sup> | %L <sup>T</sup> | $\alpha$<br>(°) | E | A <sup>T</sup><br>(mm <sup>2</sup> ) | mass<br>(g) | %SO | %FO | %FG |
|--------|-----------------|-----------------|-----------------|---|--------------------------------------|-------------|-----|-----|-----|
| 1      | .8              | .2              | 0               | 2 | 32                                   | 102         | 0   | 0   | 0   |
| 2      | 1               | .0              | 0               | 2 | 14                                   | 114         | 0   | 0   | 0   |
| 3      | .9              | .1              | 0               | 1 | 15                                   | 4           | 0   | 0   | 0   |
| 4      | .9              | .1              | 0               | 1 | 15                                   | 6           | 0   | 0   | 0   |
| 5      | .6              | .3              | 0               | 2 | 15                                   | 27          | 0   | 0   | 0   |
| 6      | .5              | .5              | 0               | 1 | 15                                   | 23          | 0   | 0   | 0   |
| 7      | .7              | .2              | 0               | 1 | 15                                   | 24          | 0   | 0   | 0   |
| 8      | .0              | .0              | 0               | 1 | 1                                    | 11          | 0   | 0   | 0   |
| 9      | .0              | .0              | 0               | 2 | 1                                    | 11          | 0   | 0   | 0   |
| 10     | .0              | .0              | 0               | 2 | 1                                    | 11          | 0   | 0   | 0   |
| 11     | .0              | .0              | 0               | 2 | 1                                    | 11          | 0   | 0   | 0   |
| 12     | .0              | .0              | 0               | 2 | 1                                    | 11          | 0   | 0   | 0   |
| 13     | .7              | .2              | 0               | 2 | 15                                   | 80          | 0   | 0   | 0   |
| 14     | .5              | .5              | 0               | 2 | 15                                   | 48          | 0   | 0   | 0   |
| 15     | .8              | .2              | 0               | 1 | 19                                   | 57          | 0   | 0   | 0   |
| 16     | .8              | .2              | 0               | 1 | 19                                   | 17          | 0   | 0   | 0   |
| 17     | .8              | .2              | 0               | 1 | 19                                   | 17          | 0   | 0   | 0   |
| 18     | .5              | .5              | 0               | 1 | 13                                   | 47          | 0   | 0   | 0   |
| 19     | .8              | .1              | 0               | 1 | 13                                   | 47          | 0   | 0   | 0   |
| 20     | .5              | .5              | 0               | 1 | 13                                   | 47          | 0   | 0   | 0   |
| 21     | .8              | .1              | 0               | 1 | 13                                   | 47          | 0   | 0   | 0   |
| 22     | .3              | .7              | 0               | 1 | 6                                    | 26          | 0   | 0   | 0   |
| 23     | .1              | .8              | 0               | 1 | 7                                    | 23          | 0   | 0   | 0   |
| 24     | .0              | .9              | 0               | 1 | 5                                    | 23          | 0   | 0   | 0   |
| 25     | .6              | .3              | 0               | 1 | 6                                    | 17          | 0   | 0   | 0   |
| 26     | .6              | .4              | 0               | 1 | 9                                    | 10          | 0   | 0   | 0   |
| 27     | .8              | .2              | 0               | 1 | 4                                    | 6           | 0   | 0   | 0   |
| 28     | .1              | .4              | 15              | 1 | 7                                    | 10          | 0   | 0   | 0   |
| 29     | .4              | .4              | 15              | 1 | 9                                    | 11          | 0   | 0   | 0   |
| 30     | .4              | .5              | 20              | 1 | 9                                    | 8           | 0   | 0   | 0   |
| 31     | .1              | .8              | 20              | 1 | 7                                    | 5           | 0   | 0   | 0   |
| 32     | .1              | .8              | 10              | 1 | 7                                    | 5           | 0   | 0   | 0   |
| 33     | .1              | .8              | 25              | 1 | 8                                    | 3           | 0   | 0   | 0   |
| 34     | .1              | .8              | 10              | 1 | 7                                    | 1           | 0   | 0   | 0   |
| 35     | .8              | .2              | 10              | 1 | 7                                    | 12          | 0   | 0   | 0   |
| 36     | .1              | .8              | 15              | 1 | 7                                    | 20          | 0   | 0   | 0   |
| 37     | .2              | .8              | 5               | 2 | 4                                    | 6           | 0   | 0   | 0   |
| 38     | .1              | .8              | 15              | 1 | 9                                    | 15          | 0   | 0   | 0   |
| 39     | .2              | .8              | 10              | 2 | 2                                    | 20          | 0   | 0   | 0   |
| 40     | .0              | .8              | 20              | 2 | 0                                    | 17          | 0   | 0   | 0   |
| 41     | .8              | .0              | 10              | 2 | 7                                    | 21          | 0   | 0   | 0   |
| 42     | .2              | .8              | 10              | 2 | 7                                    | 11          | 0   | 0   | 0   |
| 43     | .5              | .5              | 10              | 1 | 4                                    | 10          | 0   | 0   | 0   |
| 44     | .1              | .8              | 15              | 1 | 9                                    | 13          | 0   | 0   | 0   |
| 45     | .1              | .8              | 10              | 2 | 5                                    | 13          | 0   | 0   | 0   |
| 46     | .8              | .0              | 20              | 2 | 0                                    | 12          | 0   | 0   | 0   |
| 47     | .5              | .5              | 20              | 1 | 8                                    | 15          | 0   | 0   | 0   |



intermedius, gastrocnemius and soleus. Additional references used for isolated fibre type data include Anderson (1975), Buchthal (1970), Costill (1976), Elder (1980), Prince (1976, 1977) and Viitasalo (1978).

Ariano (1973) presented data on the tripartite fibre composition of the locomotor muscles of cat, rat and guinea pig. A transformation between the vastus lateralis and intermedius, gastrocnemius and soleus fibre composition of man (Edgerton et al., 1975) and mammals (Ariano, 1973) was defined. This transformation was used to estimate the fibre composition of muscle 11, 12, 13, 27, 28, 29, 30, 33, 39 and 41. Since the predicted values were relatively close to those reported by Johnson et al. (1973), this author was confident of the suitability of using mammalian fibre type data, suitably transformed. Nevertheless, the known SO distributions were used and the predicted error divided amongst the FO and FG fibres. The fibre composition of muscles 9, 10, 14, 23, 24, 25, 26, 34, 37, 40, 42, 43, 44, 46 and 47 were defined by the transformation technique exclusively.

No data were available for several muscles and these were subdivided into the ratios 50:20:30 for the SO:FO:FG fibre types. These muscles were numbered 3 to 8, 15 to 20 and 45. For muscles 1, 2, 21 and 22 the SO distribution was known (Johnson et al., 1973) and the remainder was split between the FO and FG fibres in the ratio 2:3.

The tripartite fibre type distributions for each of the muscles included in the model are given in Table 7. It is important to note that the fibre type populations are only approximately correct. The vastus lateralis muscle has been extensively biopsied and the distribution of fibre types within it varies with sex (Komi et al., 1977) and athletic ability (Costill et al., 1976; Gollnick et al., 1972; Thorstensson et al., 1976). Ideally a series of muscle biopsies on the subject would give more confident results but most subjects would object

to such a procedure. However, unless several biopsies were analyzed from at least the largest muscles, the biopsies would not be of much use because of variability (Elder, 1977; Green, 1979).

### Physical Properties of the Segments

To calculate the joint moments and forces in an individual it is necessary to determine a set of numerical input values which characterized that subject. These values consist of the mass, the location of the centre of mass and the three principal moments of inertia for each segment of interest.

Several researchers (Braune and Fisher, 1889; Dempster, 1955; Drillis and Contini, 1966) present cadaver data on body segment parameters. Predictive equations have also been developed (Fisher, 1906; Clauser et al., 1969; Hanavan, 1964; Hatze, 1980a; Jensen, 1975; Drillis and Contini, 1966), using simple anthropometric measures. These equations are superior to cadaver data because the age and physical characteristics of the cadavers may not correlate with the subject pool. The best method of estimating these parameters, however, is to measure them directly. Bresler and Frankel (1950) using a quick release technique, and Hatze (1975b) and Allum and Young (1976), applying the relaxed oscillation method, determined the moment of inertia of several segments. The application of these two techniques are simple, do not require much instrumentation and are very reproduceable. However, these techniques must be applied to end segments and only in those planes where the segment is allowed to rotate.

Data from the papers cited above were used to estimate the mass, mass centroid and the three principal moments of inertia for the thigh, shank and foot segments (the toe and talus segments were included within the foot). These are presented in Table 8. The mass values are given as a percentage of the subject's total body mass. The three radii of gyration, relative to the SRS imbedded at the centre of mass for each segment, are

Table 8 The Body Segment Parameters.

| Segment            | Mass <sup>2</sup> | X    | $K_c^1$<br>Y | Z    |
|--------------------|-------------------|------|--------------|------|
| Thigh <sup>3</sup> | .110              | .290 | .132         | .292 |
| Shank <sup>4</sup> | .047              | .278 | .081*        | .278 |
| Foot <sup>5</sup>  | .015              | .214 | .484         | .472 |

<sup>1</sup> radius of gyration of the segment about the centre of mass as a fraction of the segment length

<sup>2</sup> mass as a fraction of the total body mass

<sup>3</sup> hip to the knee joint

<sup>4</sup> knee to the TT joint

<sup>5</sup> TT to the MTP joint

given as a percentage of the subject's segment length. The moment of inertia is calculated using:

$$I_1 = (K_1 * L_1)^2 * M_1 \quad (2)$$

where  $I_1$  - moment of inertia of the lth segment about its centre of mass,  $K_1$  - the radius of gyration as a fraction of the segment length,  $L_1$  - the segment length and  $M_1$  - the mass of the segment.

The location of each segment's centre of mass are given in coordinates relative to the reference system by which the SRS, muscle, ligament and palpable points were digitized ( $Q_i$ ). These data are found in Table 3.

### MUSCLE MODEL

In locomotion only one force, that produced by muscle, can be voluntarily modulated to produce varying movement patterns. The capacity of a muscle to produce force is dependent upon its fibre composition, substrate availability, geometry and instantaneous length and velocity. Recent evidence suggests that the activation history of a muscle also affects its force output.

### Terminology and the Mechanical Model of Muscle

In this section a transition from the real anatomical structure of muscle to a mechanical model is presented. Since this modelling takes place within the framework imposed by the muscle this in turn suggests that the mechanical elements must correspond to structural elements.

If an unactivated muscle is stretched, tension will be observed which is due to a passive parallel elastic component (PEC). In the human body the passive tension-length curves of the muscles vary greatly depending upon the percentage of connective tissue (Carlson and Wilkie, 1974). Several studies have measured the extension of a muscle to various applied loads (Chapman, 1975; Engin, 1979; Herman *et al.*, 1966; Otahal, 1971; Tardieu *et al.*, 1976) and all report negligible passive forces in the muscles crossing the joints, within the normal range of movement. For this reason, the PEC was omitted from the present analyses.

When a muscle is activated it produces tension which is transferred via elastic structures to the skeleton. Termed the series elastic components (SEC) they exist within the contractile machinery (Huxley and Simmons, 1971; Jewell and Wilkie, 1958) and the tendons. In the model the fibre and tendon elastic components were treated separately.

A muscle, freed of all its elastic elements, can now be regarded as a pure contractile element (CE). The CE is the only active component in the mechanical model and its force output depends on its length, velocity and temporal phenomena. Muscle fibres also fall into three types, slow-oxidative (SO), fast-oxidative (FO) and fast-glycolytic (FG) which are intimately associated with the force output of the CE.

The elements included in the mechanical muscle model were assembled as shown in Figure 5. Two configurations were defined to account for the parallel and pennate fibre geometries. In

Figure 5 the superscripts M, B, F, T, CE and SEC denote the total muscle, muscle belly, muscle fibre, tendon, contractile element and the series elastic component. The subscripts i, SO, FO, FG represent the three fibre type designations. Additional symbols are geometrical, indicating lengths (L,T) and angles ( $\alpha$ ). The superscripts  $\dot{\phantom{L}}$ ,  $\hat{\phantom{L}}$ ,  $\hat{\phantom{L}}^{\text{max}}$ , and  $\hat{\phantom{L}}^{\text{min}}$  are used above  $L^F$  and  $L^M$  to indicate the first derivative with respect to time, and the anatomical, maximum and minimum lengths, respectively. The resting lengths of the SEC and CE were defined as being one-half the fibre length when the muscle is at its maximum *in vivo* length ( $\hat{L}^F$ ) (Bahler *et al.*, 1968; Joyce *et al.*, 1969). It is at this length that a muscle can exert its greatest isometric force.

### Factors Modifying A Muscle's Force Output

Fibre Composition It is well-established that mammalian skeletal muscle fibres can be classified into three fibre types on the basis of their metabolic and electrophysiological characteristics (Burke, 1975; Close, 1972; Eberstein and Goodgold, 1968; Goslow *et al.*, 1977a,b; Schumalbruch and Kamieniacka, 1974). Slow contracting fibres (SO) form a homogeneous group which show considerable resistance to fatigue. The faster fibres are less uniform than the slow group, developing a wide range of fatigue resistance. However, they can be divided into two groups, one which is fatigue resistant (FO) while the other consists of highly fatiguable fibres (FG).

Available evidence indicates that the force developed by a given amount of contractile material is approximately the same in fast and slow muscle (Alexander and Goldspink, 1977; Fenn and Marsh, 1935; Hellander and Thulin, 1962; Sexton and Gerston, 1967; Wells, 1965). Excised muscles from a wide variety of vertebrates have been found to attain maximum isometric stresses in the range of 20-35 N cm<sup>-2</sup> (Alexander and Vernon, 1975).

Many experiments have been performed to measure the maximum forces which can be exerted by groups of human muscles. In many cases the force has been divided by the anatomical

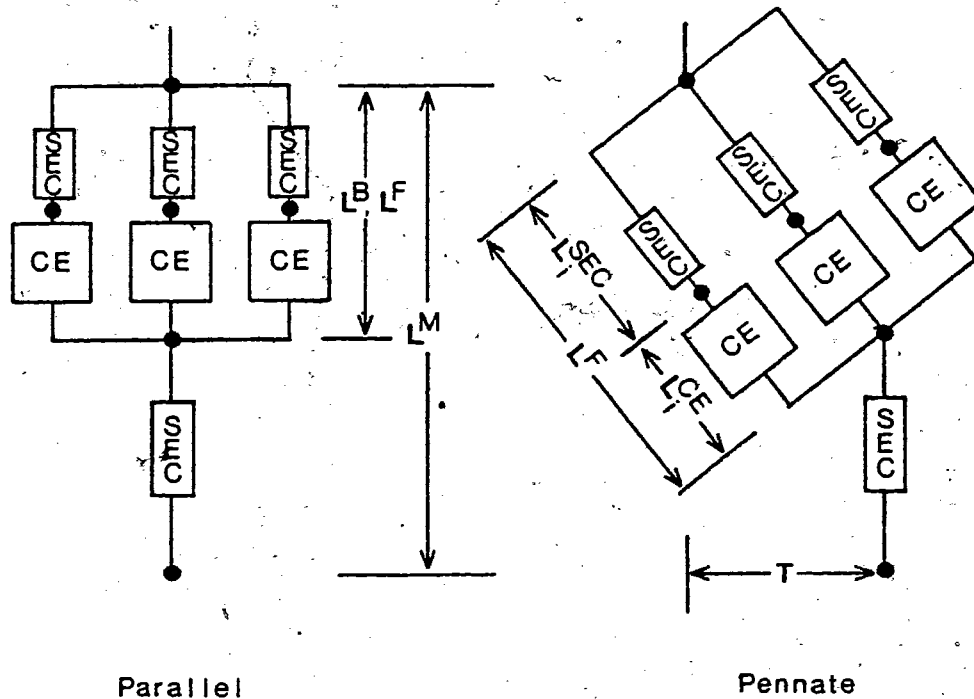


Figure 5 Geometries of the mechanical models of parallel and pennate muscles. Symbols are explained in the text.

cross-sectional area of the muscle, giving values up to  $100 \text{ N cm}^{-2}$  (Ikai and Fukunga, 1970). Values obtained in this way are not the stresses acting in the muscle fibres, if the muscles are pennate. Haxton (1944) devised the correct method for relating force to stress in pennate muscle (outlined below) and found that the ankle extensors can exert stresses up to  $38 \text{ N cm}^{-2}$ . In the muscle model a value of  $40 \text{ N cm}^{-2}$  was assigned to the maximum isometric force per unit of physiological cross-sectional area ( $f$ ). It should be noted that the physiological cross-sectional area of a muscle was measured at its anatomical length ( $\bar{L}^m$ ) and the maximum force occurs at the maximum in vivo fibre length ( $\hat{L}^m$ ).

Geometry To estimate the maximum isometric force exerted by a muscle in the direction of its tendon ( $\bar{F}^M$ ), it was necessary to know certain characteristics of that muscle such as the anatomical length of the muscle fibres ( $\bar{l}^F$ ), mass ( $m$ ), density ( $\rho$ ) and the arrangement of fibres within it. The density of muscle has been reported to be  $1050 \text{ kg m}^{-3}$  (Alexander and Vernon, 1975). If a muscle is pennate, it was also necessary to know its angle of pennation ( $\alpha$ ). When  $\alpha$  and  $\bar{l}^F$  are measured at the muscle's anatomical length, they are denoted with a '=' superscribe.

The physiological cross-sectional area of a muscle was given by:

$$A^M = m / (\rho \bar{l}^F) * E \quad (3)$$

where  $m$  and  $\bar{l}^F$  are obtained from the standard geometrical data scaled to the subject and  $E$ , the muscle shape factor, from Table 7. The shape factor was necessary to estimate the muscle's maximum cross-sectional area from the mean area.

The maximum isometric force a muscle can exert in the direction of its fibres was simply force per unit area multiplied by its physiological cross-sectional area:

$$\bar{P}^M = f * A \quad (4)$$

The maximum isometric force a muscle can exert in the direction of its tendon was given by:

$$\bar{F}^M = \bar{P}^M * \cos \alpha \quad (5)$$

Note that the angle of pennation for a parallel fibred muscle is zero degrees, that  $A^M$  was constant at all fibre lengths, and that  $\bar{F}^M$  occurred at  $\hat{l}^M$ .

In the next section we wish to extend from the maximum isometric force exerted by a muscle to all conditions of length and velocity. First, let us examine the length and velocity of shortening (or lengthening) of the muscle fibres in relation to the muscle belly length ( $L^b$ ). The solution of the fibre length and velocity in a parallel-fibred muscle is trivial. If  $L^b$  decreases by a distance  $s$  ( $s$  is positive for a shortening muscle), at the velocity  $\dot{s}$ , the muscle fibres are doing the same.

Considering the pennate muscle the assumption was made that the angle of pennation varies but the muscle thickness ( $T$ ) does not. Calow and Alexander (1973) reported this finding after examining the contraction of frog hind leg muscles. Letting the belly shorten a distance  $s$ , the angle of pennation at any length was:

$$\alpha = \tan^{-1}(\bar{L}^f \sin \bar{\alpha} / (\bar{L}^f \cos \bar{\alpha} - s)) \quad (6)$$

It was now possible to determine that a decrease in the belly length ( $L^b$ ) results in the fibre length to change to:

$$L^f = \bar{L}^f \sin \bar{\alpha} / \sin \alpha \quad (7)$$

Knowing the lengths of the fibres in time, the velocity of fibre shortening was calculated by differentiation. The instantaneous fibre lengths and velocities were used to modify the maximum force output of a muscle.

Series Elasticity When a muscle is activated its tension is transferred via the series elastic components (SEC) to the skeleton. In the model this elasticity was divided into two parts, that of the fibre and the tendon. The SEC cannot change the magnitude of the force being transmitted through them but they alter the instantaneous length and velocity of the CE which modifies the force output.



Comparing published data, a normalized force-length relationship for the fibre SEC was estimated. Only those results obtained from mammalian muscles were used (Close, 1972). No differences in the properties of the SEC between different fibre types have been indicated (Close, 1964).

The maximum extension of the fibre SEC at  $\bar{P}^m$  is approximately  $0.07 \hat{L}^f$  and its normalized compliance  $(L^f / \hat{L}^f) / (P^m / \bar{P}^m)$  typically varies from  $1.25 \cdot 10^{-2}$  at  $P$  to  $13.15 \cdot 10^{-2}$  at  $0.2 \bar{P}^m$  (Bahler, 1967, 1968; Bahler et al., 1968; McCrorey et al., 1966; Parmley et al., 1970). These data were fitted by a third order polynomial equation to estimate the length of the fibre SEC knowing the force in the corresponding CE:

$$L_{SEC}^f = \hat{L}_{SEC}^f + \hat{L}^f (Ax + Bx^2 + Cx^3) \quad (8)$$

where A, B, C and x are 0.21188, -0.22625, 0.08438 and  $P_{CE}^m / \bar{P}_{CE}^m$ , respectively. The normalized length-tension curve for the fibre series elasticity is shown in Figure 6.

For many muscles the tendinous elasticity dominates the SEC. Unfortunately, most investigations examine the effects of age, internal structure and embalming techniques on the ultimate strength of tendon (Blanton and Biggs, 1970; Cronkite, 1936; Yamada, 1970). Since tendon ruptures at approximately 7 per cent strain these data were of little use in estimating the stress-strain characteristics of tendon up to 2 percent strain, thought to be the normal physiological range (Gratz, 1931; Harris et al., 1964). However, Benedict et al. (1968) do present data within this range on the flexor and extensor muscles of the human toes. An average stress-strain relationship was estimated from their results. Up to 4 per cent strain the modulus of elasticity is constant and approximately equals 200,000 psi ( $1400 \text{ N mm}^{-2}$ ). Knowing a tendons cross-sectional area in mm ( $A^T$ ) and its anatomical length ( $\bar{L}^T$ ) we can estimate the length of the tendon at any force  $F^m$  from the following equation:

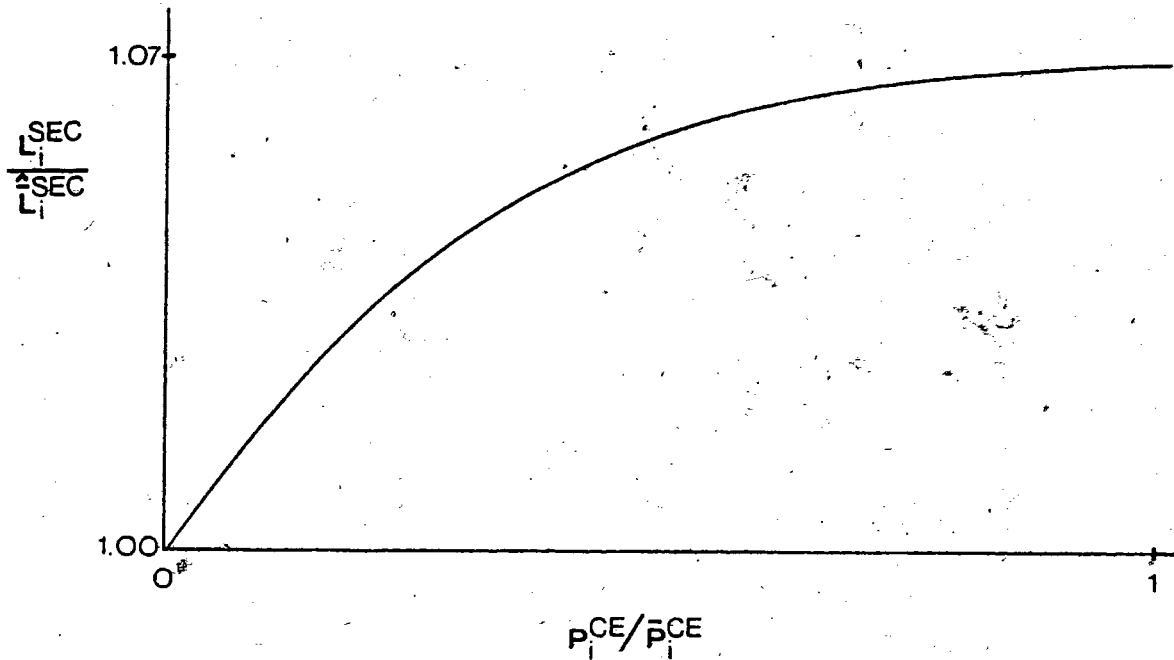


Figure 6 The normalized Force-Length relationship of the fibre series elastic component.

$$L^T = \bar{L}^T * (1.0 + F^M / (1400 * A^T)) \quad (9)$$

The normalized length-tension curve for the tendon series elasticity is shown in Figure 7.

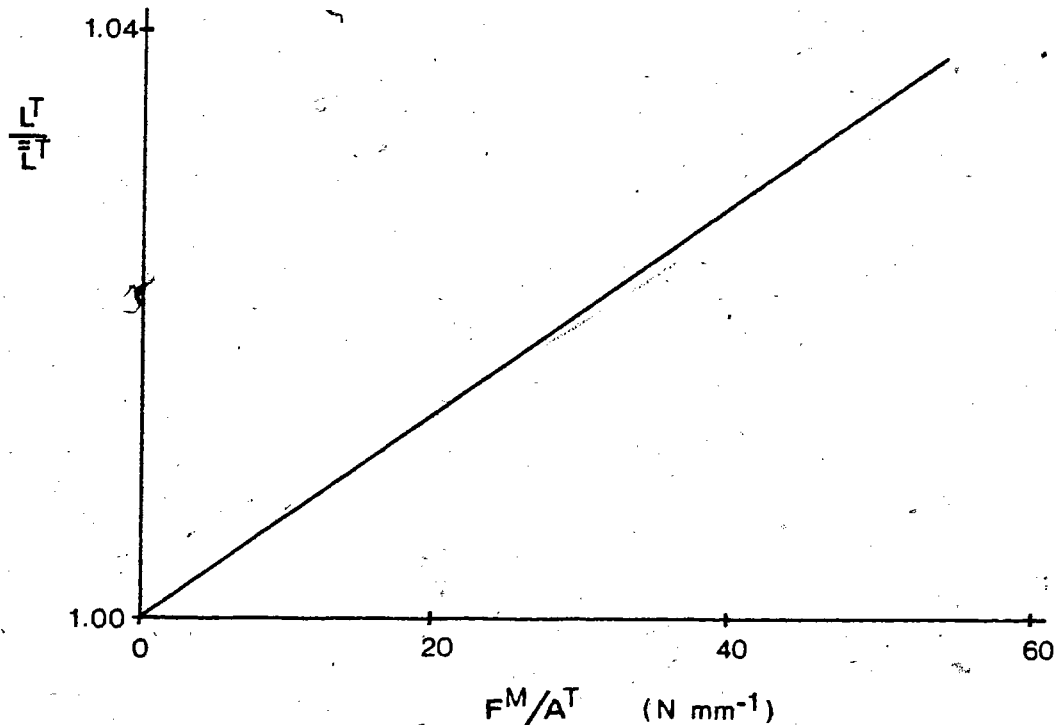


Figure 7 The normalized Force-Length relationship of the tendon series elastic component.

---

Temporal Phenomena It is well known that a muscle cannot be activated or relaxed instantaneously (Stein and Wong, 1974). This is partially due to the force-velocity relationship but the time course of a muscle's activation is also responsible. Defining the active state ( $q$ ) to be the relative amount of calcium bound to the troponin molecule (Esbashi and Endo, 1968), the contractile element produces no force when  $q=0$  and maximum at  $q=1$ . Note that active state is linearly related to a mixture of the amount of contractile material recruited, and frequency of firing, but does not specify their relative contributions unlike Hatze's (1977a, 1980b) model.

The rise and fall of activation were modelled by exponential equations with suitable time constants,  $\hat{t}$  and  $\check{t}$ , respectively. Knowing the previous activation  $g$ , at time  $t-\Delta t$  (where  $1/\Delta t$  is the sampling frequency), the boundary activations at time  $t$  were estimated. For maximal stimulation ( $S=1$ ) the upper boundary activation is:

$$\hat{g} = g + (2S - 1) * (1 - \exp(-\Delta t/\hat{t})) * (1-g) \quad (10)$$

and for full relaxation ( $S=0$ ) the lower boundary activation is:

$$\check{g} = g + (2s - 1) * (1 - \exp(-\Delta t/\check{t})) * g \quad (11)$$

Note that when the stimulation equals 0.5 the activation does not change.

The values of the time constants for the three fibre types were estimated from published curves (Bahler et al., 1967; Burke et al., 1973a). The time constants for the rise in activation for the three fibre types were estimated at 0.003 s. The time constants for the fall in activation for the SO, FO and FG fibres were 0.073, 0.034 and 0.034 s, respectively. The active states ( $g$ ) for a fast and slow twitch fibre population are plotted against time in Figure 8. Both fibre groups received maximum stimulation from 0.0 to 0.02s; stimulation ceased at 0.02s.

It should be noted that differences in the rise of tension are predominantly due to the fibre force-velocity relationships, not activation. Also the above relations are only approximate at best. Stein and Wong (1974) and Wells (1965) remark that the decay of activation is only approximately exponential. Of more importance, Edman and co-workers (1971, 1978) and van Atteveldt and Crowe (1980) report of transient enhancing and depressing effects on contractile force by previous stretch and shortening of the muscle fibres. These mechanical effects probably modify the concentration of calcium bound to the contractile filaments.

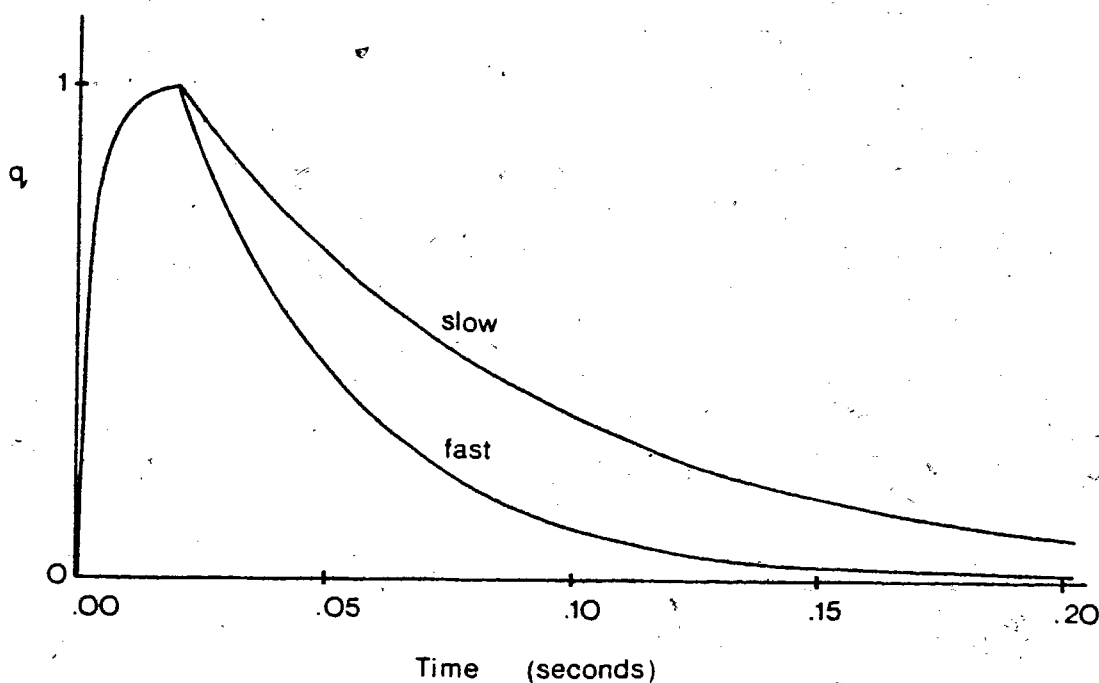


Figure 8 The Activation-Time relationship of a fast and slow twitch fibre population.

Future refinements of the model should incorporate these findings.

The Force - Length Relationship - One of the earliest predictions from the sliding filament theory of contraction was that as a muscle is lengthened, the area of overlap of the actin and myosin filaments should diminish, and therefore, the tension developed should also decrease (Hanson and Huxley, 1953). Previously published work by Ramsey and Street (1940), duplicated by Gordon et al. (1966) confirmed this theoretical prediction.

Several authors have described the force-length relationship mathematically. Bahler (1968), using experimental data from 28 rat gracilis anticus muscles, fitted a parabolic equation to the force-length data from 0.7 to 1.2  $\hat{L}^F$ . As pointed out by Hatze (1975a), his equation was accurate for the range indicated but muscles frequently exceed these limits. Hatze, modelled the relationship from 0.58 to 1.8  $\hat{L}^F$ . It should be noted that neither of the above equations have any physiological significance besides describing the relationship.

In the present investigation the force-length relationship was described using Hatze's (1977a) equation:

$$P_i^{ca} / \bar{P}_i^{ca} = 0.32 + 0.71 \exp(-1.112 (L^F / \hat{L}^F - 1.0)) \\ * \sin(3.722 (L^F / \hat{L}^F - 0.656)) \quad (12)$$

where all of the symbols have been previously defined. The normalized length-tension relationship for the CF is shown in Figure 9. Although equation (12) follows the force-length relationship of a muscle fibre and not that of a whole muscle it was thought the best available in the literature. Also, since the equation defines the force-length relationship beyond the maximum in vivo length defined in this thesis ( $1.0\hat{L}^F$ ) alternative rest lengths can be easily defined and incorporated into the model when more definitive rest length data becomes available.

The Force - Velocity Relationship In 1938 Hill determined that the previously well known inverse relationship between muscle force and the speed of contraction, near optimal length, for  $\dot{L}^{ca} \geq 0$  (Fenn and Marsh, 1935; Hill, 1922; Levin and Wymar, 1927; Wilkie, 1950), could be represented by

$$P^{ca} = ((\bar{P}^{ca} + a)b / (\dot{L}^{ca} + b)) - a \quad (13)$$

where 'a' and 'b' are physiological constants proportional to the cross-sectional area of the muscle and its fibre length.

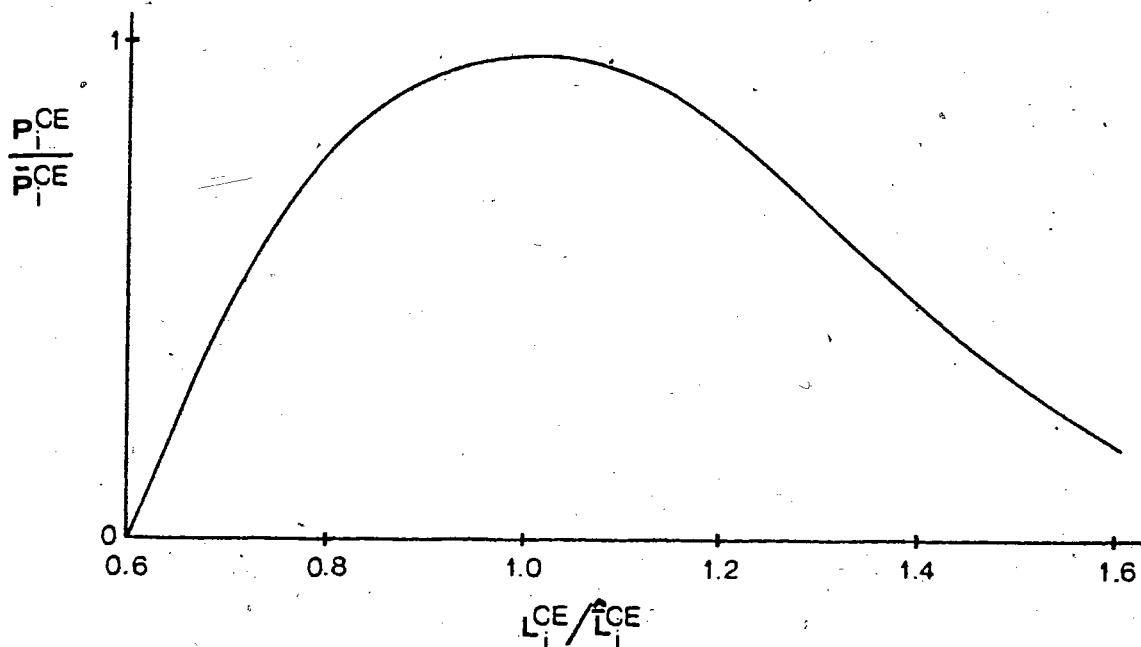


Figure 9 The normalized Force-Length relationship of the contractile element.

Hill's constant 'a' has the units of force and is higher for fast than slow muscles. In the model 'a' was assigned  $0.20, 0.35$  and  $0.35 \bar{P}^{ce}$  for the SO, FO, and FG fibre types, respectively. The constant 'b' has the units of velocity and is approximately six times greater for a fast than a slow muscle. For each muscle in the model 'b' was assigned  $0.40 \hat{L}^F, 2.25 \hat{L}^F$  and  $2.25 \hat{L}^F$  for the SO, FO and FG fiber types, respectively (Close, 1964; Wells, 1965). The force-velocity relationship of a fast and slow twitch fibre population are shown in Figure 10. For both fibre groups  $\bar{P}^{ce} = 1000\text{N}, \hat{L}^F = 0.05\text{m}, L^F = 0.05\text{m}$  and  $q = 1.0$ .

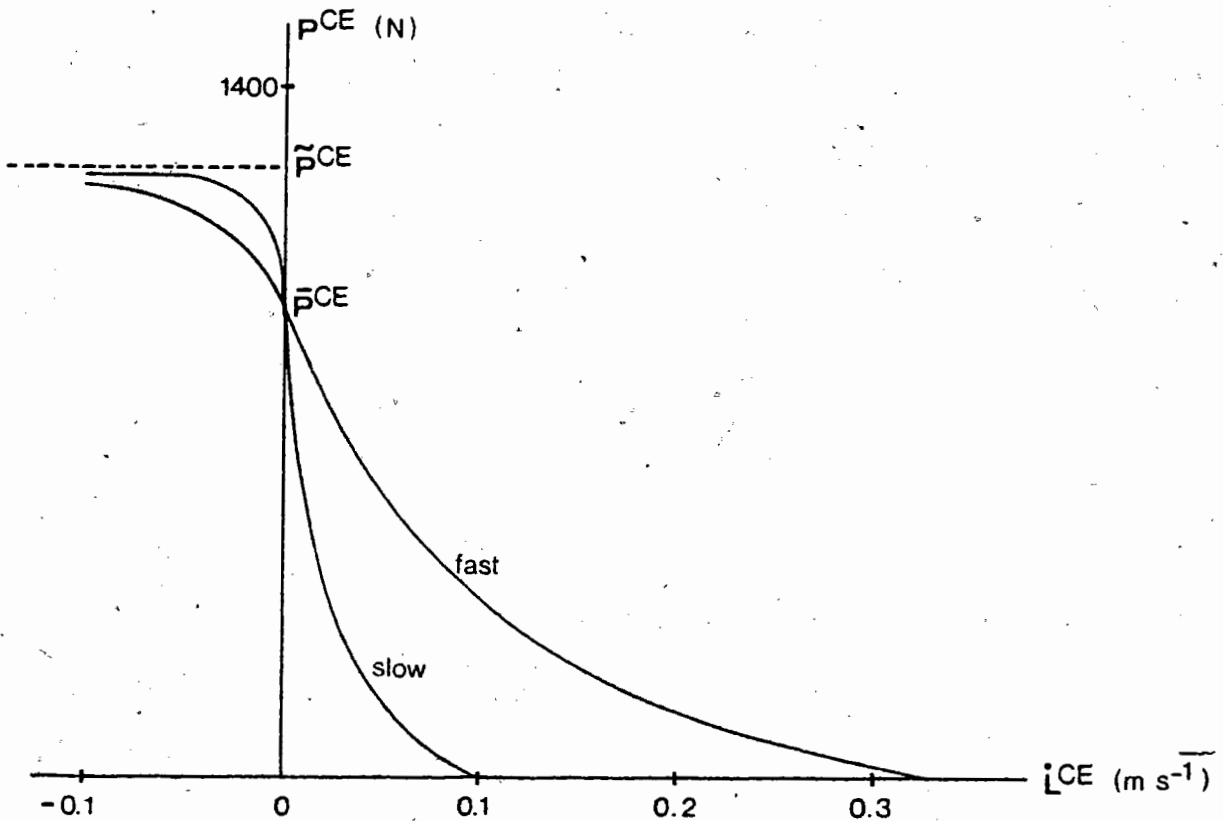


Figure 10 The Force-Velocity relationship of a fast and slow twitch fibre population.

In the model, no mechanical differences were assumed to exist between the two fast twitch fibre types. However, the distribution of force amongst muscles according to fibre type would be quantitatively different if they were not subdivided. Also future refinements to the model could include the decay of force with fatigue (Burke *et al.*, 1973a).



Hill's equation suffers from a number of deficiencies, the major one being that it is confined to concentric contractions even though a large proportion of muscle activity is eccentric (Abbott et al., 1952). However, little is known about the maximum force output of a muscle undergoing an eccentric contraction. Sugi (1972) studied the force changes during these contractions and has clearly demonstrated that as stretching velocities increase the force rises above isometric ( $\bar{P}^{ce}$ ) to a plateau. This is shown in Figure 10. It can be seen that Hill's equation provides a good description of the relationship between force and velocity only for muscle shortening. Once muscle is lengthened, a different relationship is followed. The maximum force developed by a muscle in eccentric contractions was defined to be  $1.25 \bar{P}^{ce} = \tilde{P}^{ce}$  (Joyce et al., 1969; Katz, 1939) and the relationship between force and lengthening velocity follows a hyperbolic relationship, albeit, one different than the shortening condition.

The equation used to describe the eccentric half of the force-velocity relationship ( $\dot{L}^{ce} < 0$ ) was rewritten from Fitzhugh (1977) and follows:

$$P_i^{ce} = \tilde{P}_i^{ce} - D(\tilde{P}_i^{ce} - \bar{P}_i^{ce}) / (D - \dot{L}_i^{ce})$$

where  $D = b(\tilde{P}_i^{ce} - \bar{P}_i^{ce}) / (\bar{P}_i^{ce} + a)$  (14)

The second shortcoming of Hill's equation is that the parameters  $\tilde{P}^{ce}$  and 'a' are not constant but functions of the length of the CE and activation. Nevertheless, Hill's equation has been extensively reported on in the literature and the parameters 'a' and 'b' are related to the energy production of a muscle (Hatze and Buys, 1977; Hill, 1938). To adjust equations (13) and (14) both  $\tilde{P}^{ce}$  and 'a' were scaled by the force-length relationship, given in equation (12) (Abbott and Wilkie, 1953; Bornhorst and Minardi, 1970; Matsumoto, 1967), and the activation  $q$ , given in equations (10) and (11) (Bigland and Lippold, 1954; Miyashita et al., 1969).

### Analysis

In this section the technique used to estimate the force a muscle can exert at time  $t$ , given its force and activation at time  $t-\Delta t$ , and its current kinematics will be outlined. For demonstration purposes the maximum (full stimulation,  $S=1$ ) and minimum (no stimulation,  $S=0$ ) force a muscle can exert is discussed. At some intermediate stimulation the actual muscle force would lie between these values. The force-stimulation pair for each muscle are input to the control model which calculates the actual stimulation (and therefore muscle force) required to balance the joint moments.

To solve for the maximum and minimum muscle forces an iterative procedure was used. Since the equations are identical for both the rise and fall in activation conditions, these are discussed together below. The time interval between frames ( $\Delta t$ ) was divided into  $k$  equal increments each of time  $dt$ . This was necessary since a finite difference method was used to estimate structure velocities. If  $dt$  is small a much better estimate can be made.

To begin, the length and velocity of the muscle ( $L^m, \dot{L}^m$ ) were determined at each iteration. Since these values were known at each frame, two linear equations were used to solve for  $L^m$  and  $\dot{L}^m$  at each  $dt$ .

The following values were known at time  $t-\Delta t$ :

- 1 the force ( $P_i^{ce}$ ) and activation ( $q_i$ ) of the contractile elements, calculated in the control model,
- 2 the lengths of the SEC ( $L_i^{sc}$ ) and tendon ( $L^T$ ), derived from  $P_i^{ce}$  and  $F^m$  using equations (8) and (9),
- 3 the length ( $L^m$ ) and velocity ( $\dot{L}^m$ ) of the muscle from the limb kinematics and

4. the velocities of the SEC's ( $L_i^{SEC}$ ) and tendon ( $L_i^T$ ). How these were derived is discussed below.
5. Knowing the lengths and velocities of the muscle, SEC and tendon, the lengths and velocities of the CE's ( $L_i^{CE}$ ,  $\dot{L}_i^{CE}$ ) were calculated from geometrical relationships.

The boundary activation levels of the three CE's at time  $t-\Delta t+dt$  were calculated using equations (10) and (11). Knowing the lengths and velocities at time  $t-\Delta t$ , and the activation level of the three CE's at time  $t-\Delta t+dt$ , these were used to estimate the forces in the CE's at time  $t-\Delta t+dt$  using equations (13) and (14). Knowing the forces  $P_i^{CE}$ , the corresponding lengths of the SEC and tendons at time  $t-\Delta t+dt$  were derived. Since we now know  $L_i^{SEC}$  and  $L_i^T$  at times  $t-\Delta t$  and  $t-\Delta t+dt$ , the velocities of these structures were estimated from their change in length times the reciprocal of  $dt$ .

Sufficient information now existed to calculate the lengths and velocities of the CE's at time  $t-\Delta t+dt$ . It can be seen that the above steps were performed  $k$  times, to estimate the muscle force and activation at time  $t$ .

### CONTROL MODEL

In the last section the force a muscle exerts when experiencing a particular stimulation was developed. The control model selects the muscle stimuli based on a neurophysiological model of muscle recruitment to generate the net muscle moments. This model is discussed below.

#### Neurophysiological Constraints

Fibre Type Recruitment It is well known that most mammalian muscles are composed of different fibre types, which can be conveniently lumped into the three categories SO, FO and FG. In terms of function, the FG units are for short-term powerful, phasic activity, and the FO fibres are better adapted for repetitive phasic activity. On the other hand, the SO fibres are

low-speed economical contractile units, suitable for sustained tonic activity. It is thought that during voluntary muscle contractions, muscle units are recruited in order of diminishing fatigue resistance. This pattern has been experimentally shown in both cat (Binder *et al.*, 1978; Goslow *et al.*, 1977b; Henneman and Olson, 1965; Walmsley *et al.*, 1978) and human studies (Desmedt and Godaux, 1977a,b; Gollnick *et al.*, 1974; Henneman *et al.*, 1965; Milner-Brown *et al.*, 1973). It has also been reported that when higher level muscle fibres are recruited, those previously recruited are not deactivated (Desmedt and Godaux, 1977a; Gollnick *et al.*, 1974). Defining the recruitment pattern of fibre types as fixed we can write:

$$SO \text{ ----> } SO + FO \text{ ----> } SO + FO + FG \quad (15)$$

There is still some debate about this recruitment order, concerning whether all fibres in a lower level must be recruited before the next level is entered. The best evidence comes from glycogen depletion studies (Burke and Tsairis, 1973; Essen and Henriksson, 1974; Garnett *et al.*, 1978; Gollnick *et al.*, 1974) which indicate the homogeneous loss of substrate from all fibres of a similar type, indicating that all fibres were in use. However, some researchers have hypothesized the movement of substrate from one fibre to another (Essen and Haggmark, 1975) casting doubt on the above evidence. Nevertheless, the present model incorporates an immutable recruitment order of muscle fibres given by relation (15).

Pattern Generators Three major components of the neural control system for locomotion have been identified and include 1) a relatively autonomous generator, residing in the interneurons of the lumbar spinal cord, which can provide for rhythmic stepping, 2) a spinal system receiving activating signals from supraspinal sources, and 3) a segmental afferent input which interacts with the spinal programme either by direct feedback or channelling through ascending neural pathways.

That the lumbar spinal cord could support stepping movements in the limbs of animals without higher level input has been known a long time (Graham Brown, 1916; Grillner, 1973; Shurrager and Dykman, 1951). Further, the afferent input, if surgically removed, was also found to be non-essential to rhythmic activity (Grillner and Zangger, 1974; Taub and Berman, 1968). This evidence suggests that one or more pattern generators can produce relatively effective movement patterns. Such a scheme is demonstrated by much experimental evidence, at least in the cat (Grillner, 1975; Perret and Cabelguen, 1980; Shik and Orlovsky, 1976).

In the present model those factors deemed necessary were as follows:

- 1 Up to three pattern generators (neural signal outputs) exist at each joint, corresponding to the number of degrees of freedom that joint provides. For example, the foot was constrained to move about the uni-axial tibiotarsal and subtalar joints, relative to the shank. Two generators were assumed to control the muscle moments about these two axes. The output level of a generator varies in order to match the moment requirements at each joint, and it was controlled by supraspinal and segmental signals.
- 2 For each pattern generator its protagonists and antagonists were respectively facilitated and inhibited by the same signal. This presupposes that there was no afferent input modifying the signal to a selected muscle. In other words, a feed forward system was modelled. It is known that the feedback signals are not essential for producing the basic movement patterns. The signals from the muscle, joint and skin receptors are used as a fine control and to modify the output to correct for unforeseen disturbance (i.e. fatigue or stepping on a pebble). Since these afferent signals are non-essential to rhythmic activity (Grillner, 1975) they were

excluded from the model for simplicity at this stage. Future refinements to the model could add such afferent feedback.

Two simple examples are given to illustrate the control model. Consider eleven muscles situated around a hypothetical joint that has two degrees of freedom, flexion-extension and adduction-abduction (see Figure 11). All of the muscles have the moment arms shown. If equal flexion and adduction moments are desired muscles 4 and 10 are stimulated 1.42 ( $0.71 + 0.71$ ) times and muscles 9 and 11 1.30 ( $0.38 + 0.92$ ) times as strongly as muscles 3 and 5; muscles 2 and 6 receive a net stimulus signal of zero, and the remaining three muscles are inhibited by the control model. This is an example of a group of muscles being preferentially recruited because they satisfy two moments at a single joint. Note that muscles 4, 9, 10 and 11 do not receive all of the stimulation from the flexion-extension and the abduction-adduction pattern generators since they are not pure flexors or adductors. They receive inputs calculated trigonometrically based on their position (see Figure 11).

The second example concerns itself with the ability of a single muscle to satisfy the net muscle moments at two different joints. If a muscle can generate part of the required net muscle moment at more than one joint it will be preferentially selected by virtue of receiving positive stimuli from two or more generators.

The control model recruits groups of muscles in accordance to their ability to generate a required net muscle moment. Individual muscles within a specific group may receive different activating signals, depending upon their ability to satisfy one or more net muscle moments. Since there is little neurophysiological evidence to substantiate the number of independent stimuli and how they are assigned to the locomotor muscles the actual neural control of individual muscle recruitment must be largely theorized. Until better spatial and temporal neurophysiological data is obtained, considering all

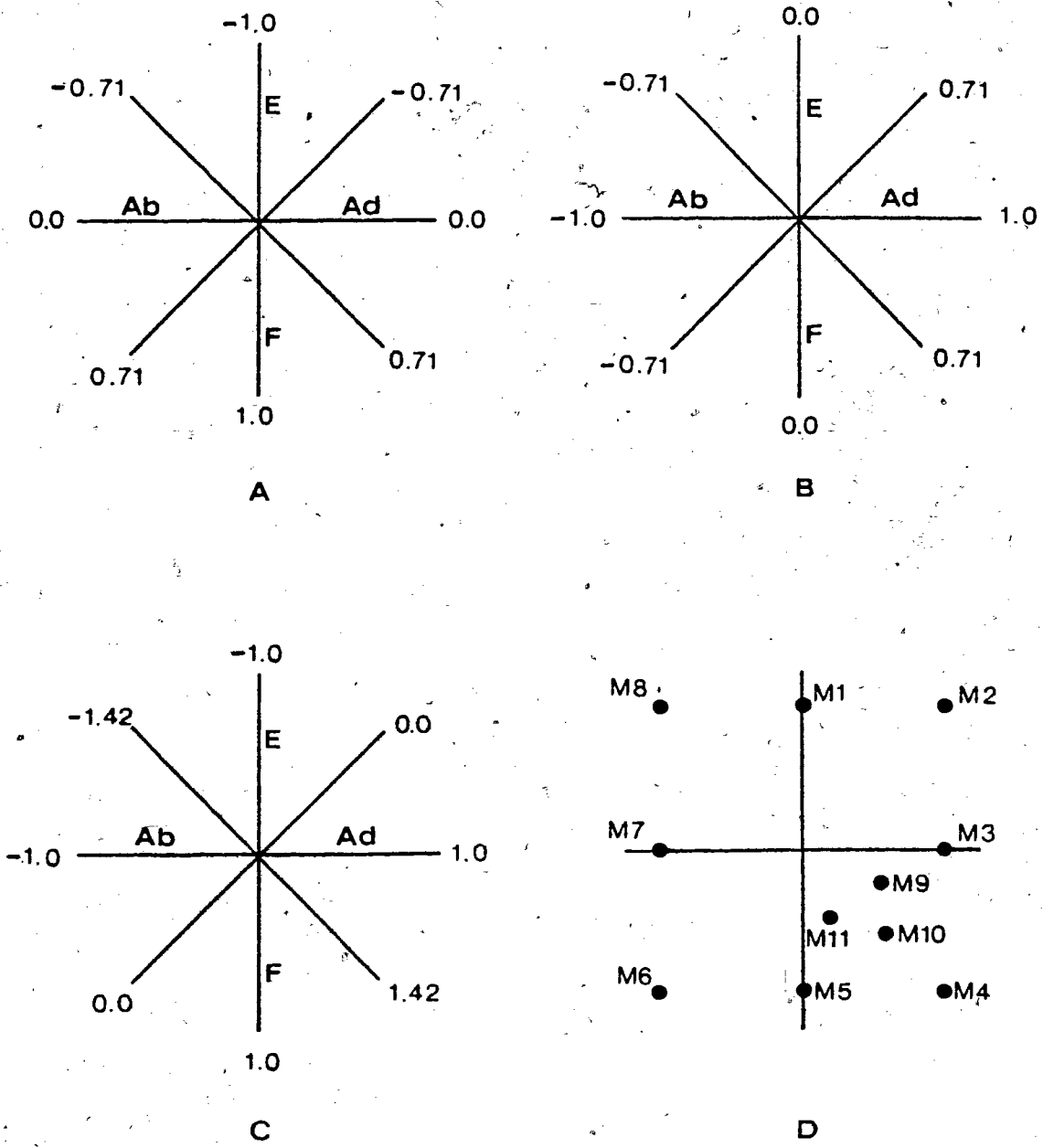


Figure 11 Eleven hypothetical muscles situated around a joint where both flexion (F) and adduction (Ad) muscle moments are required. A) The normalized stimulation from the flexion/extension pattern generator, B) the normalized stimulation from the abduction/adduction pattern generator, C) the stimulation map at the joint, and D) the location of the eleven muscles.

degrees of freedom in the locomotor system and the influence of peripheral inflow, the control model will be scientifically unsupported.

#### Stimulation-Activation-Muscle Force Relationship

The ability of a signal from a pattern generator (SM) to produce a muscle force depends upon the factors modifying the muscle's force output. These were discussed extensively in the muscle model section in which the boundary maximum and minimum force outputs of a muscle were calculated. These are available as the maximum ( $\hat{F}_t^{ca}$ ) and minimum ( $\check{F}_t^{ca}$ ) muscle forces and the maximum ( $\hat{q}_t$ ) and minimum ( $\check{q}_t$ ) activations at time  $t$ . The stimulation to generate any intermediate muscle force is also defined.

One example is presented. In Figure 12 the relationship between a CE's activation, stimulation and force output is diagrammed. In the example  $\check{F}_t^{ca}$ ,  $\hat{F}_t^{ca}$ ,  $\check{q}_t$ ,  $q_t$  and  $\hat{q}_t$  are 61 N, 100 N, 0.60, 0.80 and 1.00 for the SO fibres, 33 N, 150 N, 0.22, 0.40 and 1.00 for the FO fibres, and 0 N, 199 N, 0.00, 0.00 and 1.00 for the FG fibres when  $t$  is 0.02 s. Since the FO fibres are activated after the SO fibres, and the FG after the FO, these curves are shifted to the right to fall between 1 and 2, and 2 to 3 SM, respectively. Note that since the level of activation ( $\check{q}_t$  and  $\hat{q}_t$ ) remains constant at stimulations below 0, and above 1 (see Equations 10 and 11) the force generated by the SO fibre remains constant at stimulations below 0 and above 1. Similar relationships hold for the FO and FG fibres. It should also be noted that a linear relationship was assumed between the activation and the fibre forces for this example only. In general the relationship is nonlinear and depends upon the muscle's geometry, kinematics and previous activation.



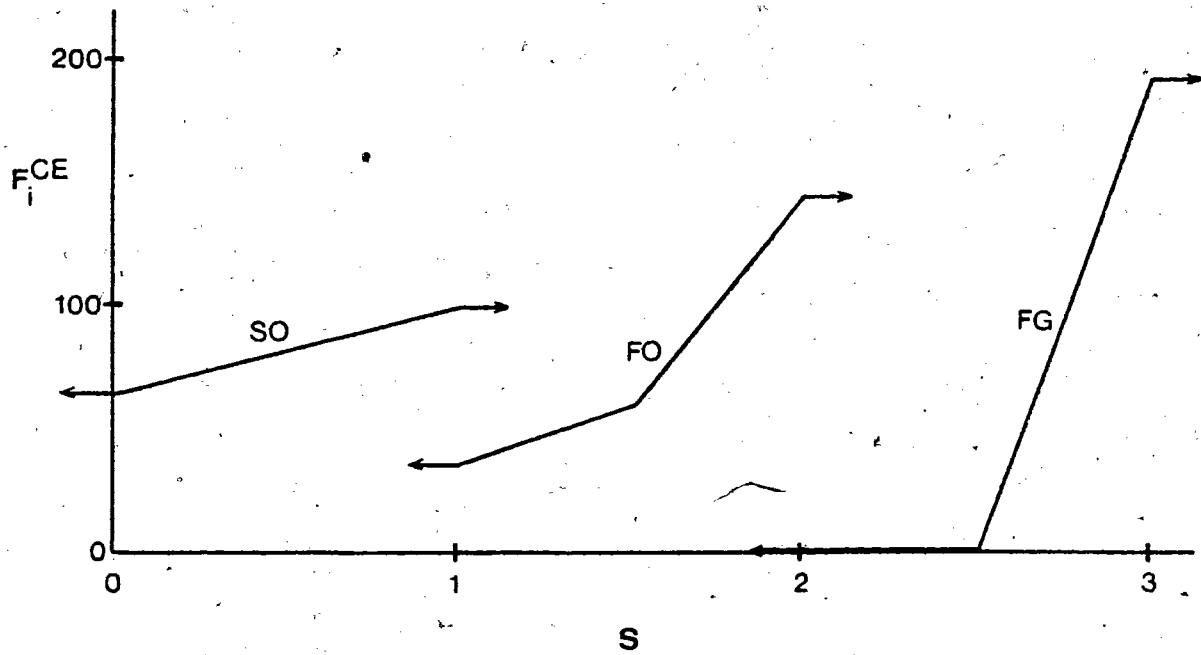
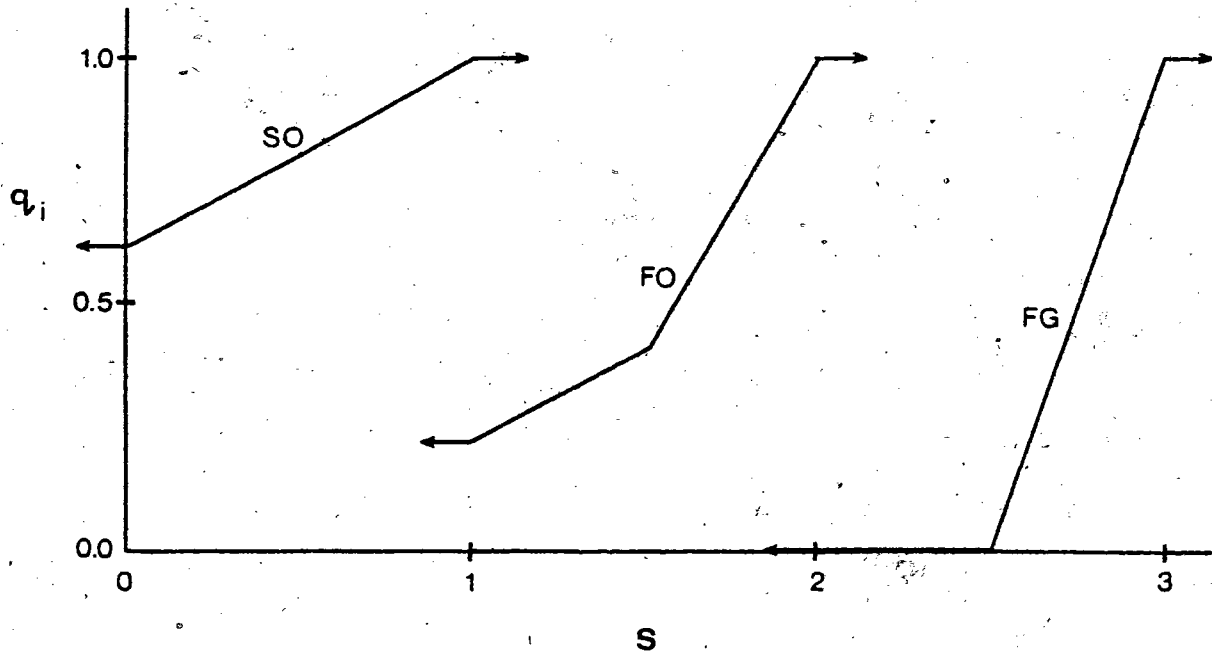


Figure 12 A simplified Stimulation (S)-Activation ( $q$ )-Force ( $F_i^{CE}$ ) relationship of a hypothetical muscle.

### The Role of the Ligaments

The line of action of a ligament generally generates a moment about all three axes at a joint, albeit small about those axes for which large range of movement exist. Similarly, muscles generate moments about all axes but generally of a lesser magnitude about those axes for which movement is constrained. This suggests that forces must be assigned to the muscles and ligaments simultaneously to balance the joint moments. Since the technique used in this thesis to distribute force amongst the muscles only considers the major degrees of freedom of the lower limb the ligaments were not considered. This was based on the assumption that the ligaments generate small moments about the major degrees of freedom due to their smaller moment arms and force when compared to the muscles (Morrison, 1967).

### Analysis

In this section the method used to estimate the muscle forces in the lower limb is developed. A simple example leading to the final solution is presented.

A sagittal plane view of the knee and ankle, with five muscles crossing these joints is shown in Figure 13. It is assumed that all muscles lie in the sagittal plane and +6 and -30 Nm of net muscle moment are required at the knee and ankle, respectively. To make the example simple each muscle was assumed to be composed of one fibre type (SO) and the activation constraints are  $\dot{q} = 0.0$  and  $\hat{q} = 1.0$ . The force exerted by each muscle at full activation ( $\hat{F}^m$ ), and the moment arms of the muscles, at each joint, are given in Table 9. Mathematically, a negative moment arm indicates that the muscle generates a counter-clockwise moment on the segment below that joint. If a muscle does not cross a joint, its moment arm was set to zero.

Two pattern generators are required, one at the knee, the other at the ankle. These in turn facilitate or inhibit a muscle (with signal SM) depending upon that muscle's ability to contribute to the required net muscle moments. If the sign of

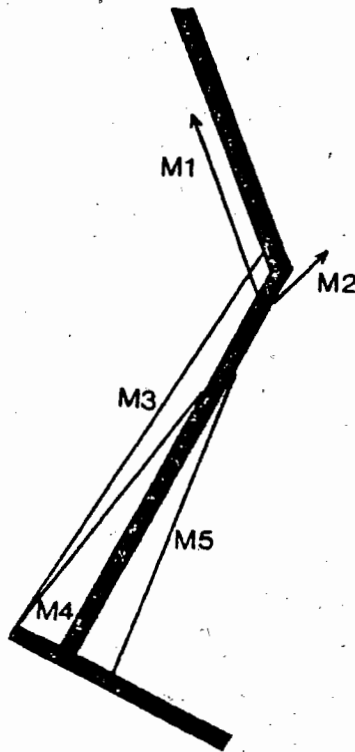


Figure 13 A simplified sagittal plane view of the knee and ankle joints. Five major muscles are shown.

the moment arm of a muscle, at a given joint, is opposite to that of the required net muscle moment, that muscle is inhibited (-SM). If the signs match, it is facilitated (+SM). A muscle with a moment arm of zero is ignored. In the present example muscles 1 and 3 were inhibited and 2 facilitated with signal  $SM_1$ , at the knee and muscles 3 and 4 were facilitated and 5 inhibited by  $SM_2$  at the ankle.

Table 9 Hypothetical Moment Arms (m) and Maximum Force of Five Knee and Ankle Muscles (see text).

| Muscle      | 1     | 2     | 3     | 4     | 5     |
|-------------|-------|-------|-------|-------|-------|
| Moment Arms |       |       |       |       |       |
| Knee        | -0.05 | +0.02 | -0.04 | 0.00  | 0.00  |
| Ankle       | 0.00  | 0.00  | -0.06 | -0.05 | +0.02 |
| F           | 1000  | 2000  | 1250  | 500   | 250   |

A given muscle's force output is a non-linear function of its stimulation. In the present simple example these relationships were linearized to three regions:

$$\begin{aligned}
 SM \leq 0.0, & \quad F^M = \check{F}^M = 0.0 \\
 0.0 < SM \leq 1.0, & \quad F^M = \check{F}^M + SM * (\hat{F}^M - \check{F}^M) \\
 SM > 1.0, & \quad F^M = \hat{F}^M
 \end{aligned} \tag{16}$$

Note that these equations apply to this problem only; the model incorporates all stimulation-muscle force non-linearities (see the Stimulation-activation-muscle force relationship).

A muscle's stimulation is the sum of the inputs from the pattern generators. By solving for the signals from the pattern generators ( $SM_1$  and  $SM_2$ ), the force in each muscle can be determined. Multiplying by the moment arm at a given joint, and summing across muscles, this must equal the required net muscle moment at that joint. We therefore needed to solve two simultaneous non-linear equations for  $SM_1$  and  $SM_2$ . In this example  $SM_1$  and  $SM_2$  were 0.4 and 0.6, respectively. The muscle forces were then determined to be 0, 800, 250, 300 and 0 N. These correspond to an activation of 0.0, 0.4, 0.2, 0.6 and 0.0 for the five muscles concerned.

Expanding the above simple problem to the human locomotor system was straightforward. Knowing the stimulation-

activation-muscle force relationship and the moment arms of the 47 locomotor muscles, signals from 6 pattern generators (three at the hip, two at the ankle and one at the knee) were determined by solving 6 simultaneous non-linear equations to generate the corresponding net muscle moments (IMSL routine ZSCNT, 1980). The form of the equations were as follows:

$$M_{jk} = \sum_m^{47} (MA_{mjk} * F_m^M) \quad (18)$$

where  $M_{jk}$  - jth joint net muscle moment about the kth axis,  
 $MA_{mjk}$  - mth muscle's moment arm at the jth joint about the kth axis,  
 and  $F_m^M$  - force in the mth muscle (function of the stimulation from the pattern generators, its mechanical properties and past history).

Knowing the signals from the six pattern generators the force in each muscle are determined.

To solve for the muscle forces initially the muscle model cannot be executed since the previous muscle forces are not known. Either an estimate of the muscle forces at the previous frame must be made or the activation constraints removed (the author's choice). Whichever method is used, the muscle velocities must also be estimated. This suggests that the computed muscle forces for the first few frames will be in error and that the initial output should be discarded.

#### SUMMARY

It would be naïve to suggest that the model developed in this chapter accurately describes the complex processes for the recruitment of the locomotor muscles. However, it is an attempt to incorporate physiological and neurological data in the solution of force distribution. The model includes the exponential rise and fall of activation which can lead to antagonistic muscular activity, and assumes smooth distribution of forces amongst synergistic muscles, as predicted by EMG.

The method of predicting the muscle forces shares many of the limitations of previous workers. The variety of anatomical data incorporated within the model was at best carefully estimated. These include the geometry and fibre compositions of the muscle and their temporal and dynamic properties. The definition of the joint centre locations and the estimation of the muscle moment arms also had to be rigorously defined.

One criticism of the model is the inclusion of numerous, only partially supported assumptions. These include the ability to accurately estimate the location, lengths and velocities of the muscles from external measurements, the prediction of the muscle force-stimulation relationship from geometrical properties and structure kinematics, and the concept of pattern generators. For these assumptions the author makes no apologies. The model is meant to be a prototype to determine the feasibility of the technique. As improved data becomes available these must be included to improve the model's predictive ability.

## CHAPTER IV

METHODS AND PROCEDURES

To test the model developed in the last chapter a variety of data were required. These include the transformations mapping the skeleton to a subject whilst in the anatomical position and at each instant of time during the movement cycle for which muscle forces are desired. In addition, an estimation of the net muscle moments calculated from the limb kinematics and the ground reaction forces were required. The experimental procedures, equipment and analyses used to determine the input data are discussed in this chapter. Specifics regarding the model implementation are also covered.

EXPERIMENTAL DESIGN

One healthy athletic male Caucasian volunteer was selected for the experiment (age 27 years, height 1.78m, mass 70.8kg) based on availability and the absence of any pathological or neurological disorder which could affect his walking pattern. This subject was required to undergo a lengthy anthropometric session so that a standard lower limb could be scaled to him. A series of trials involving normal gait were then performed. From these trials a representative walking trial was selected. Only one walking trial was used as it was an attempt to test the feasibility of using a new technique to estimate the muscle forces.

MUSCLE FORCE DETERMINATION

To estimate the muscle forces during human activity the model required: 1) the definition of each muscle as scaled to the subject, 2) the instantaneous lengths and velocities of the muscles at those points during the movement cycle for which forces were desired to be calculated, 3) the moment arms of the muscles about the SRS and 4) the net muscle moments calculated relative to the SRS. The procedures used to estimate these model inputs are discussed below.

### Defining the Subject's Lower Limb

In Chapter III an anthropometric model was defined for the human right lower limb in the anatomical position. It was therefore necessary to transform the skeleton data to the subject whilst in the same position. A subsequent transformation of this data to the subject during activity enabled the calculation of the length, velocity and moment arms of the muscles at each instant during movement. In addition, the displacement of each segment's centre of mass and the mass moments of inertia were available.

Anatomical Position To calculate the total length of the muscles the transformation technique was used. Composed of two steps the first necessitated defining a minimum of four points on each segment, locatable on both the skeletal bone and the subject. For the segments of interest several bony landmarks are palpable and are listed in Table 10. Since the location of the muscles and the orientation of the skeletal reference systems (SRS) was the goal of this analysis the X, Y, and Z coordinates of the skeleton palpable points were measured relative to the same reference system  $Q_s$ .

The second step required the collection of the X, Y and Z coordinates of these points outlined in Table 10 on the subject. The subject lay supine upon a table in the anatomical position, whilst these measurements were taken relative to the reference system R. The three-dimensional anthropometer was used to collect these values (see Figure 2). Knowing the coordinates of the palpable points on both the skeleton and subject, transformation matrices were calculated (see Appendix A) which scale, translate and rotate the skeletal material to 'fit' that of the subject. The coordinates defining the muscles, ligaments, reference axes and the location of the centres of mass were then transformed from the skeleton to the subject. For example, the coordinates of a point defining the location of a muscle were multiplied by the corresponding transformation matrix  $[T_s]$  to locate this point in the reference system R. The lengths of the



Table 10 The Location of the Palpable Points on the Skeleton and Subject.

|        |   |
|--------|---|
| Pelvis |   |
| 1      | Pubic crest   |
| 2      | Anterior superior iliac spine (left)  |
| 3      | Anterior superior iliac spine (right)                                       |
| 4      | Posterior superior iliac spine (left)                                       |
| 5      | Posterior superior iliac spine (right)                                      |
| 6      | tip of the coccyx   |
| Thigh  |   |
| 1      | Anterior superior point on greater trochanter                               |
| 2      | most anterior point on lateral condyle                                      |
| 3      | most medial part of medial condyle  |
| 4      | distal part of the lateral condyle just superior to the intercondylar notch |
| 5      | distal part of the medial condyle just superior to the intercondylar notch  |
| Shank  |   |
| 1      | most medial point of medial condyle   |
| 2      | lateral top part of tibial tubercosity                                      |
| 3      | fibular head  |
| 4      | tip of lateral malleolus  |
| 5      | tip of medial malleolus   |
| Foot   |   |
| 1      | medial to insertion of Achilles tendon                                      |
| 2      | lateral to insertion of Achilles tendon                                     |
| 3      | proximal end of 5th metatarsal  |
| 4      | proximal end of 1st metatarsal  |
| 5      | distal end of 3rd metatarsal  |
| 6      | distal end of 5th metatarsal  |
| 7      | medial anterior upper border of talus                                       |

muscles were determined and using the geometrical data in Table 7 the fibre and tendon lengths were calculated.

Knowing the location of the points defining the line of action of the muscles and ligaments the moment arms of these structures were determined (see Appendix C). As noted in Chapter III, however, this technique does not take into account the influence of one muscle overlying another thereby underestimating the muscle's moment arms. To circumvent this problem the location of the muscles as they pass through transverse planes centered at the hip, knee and ankle were defined (see Table 5). It was therefore necessary to scale these values to the subject whilst in the anatomical position. Knowing the X and Z scaling factors

for the subject's thigh, shank and foot (derived from the transformations between the skeleton and the subject (see Appendix A)) the data in Table 5 were appropriately scaled. These points were then used, along with the direction cosines of the muscles calculated from the line of action points, to define the muscle's moment arms.

To scale the 'standard' muscle geometrical data to the subject six anthropometric measurements were required -- two lengths, skin folds and girths. The length of the thigh segment ( $L_T$ ) was defined as being the distance from the most laterally projecting part of the greater trochanter to the average centre of the knee joint. For the shank, the distance from the knee joint centre to the ankle joint was defined as its length ( $L_S$ ). Midway along these two lengths girth ( $C_T, C_S$ ) and skinfold ( $SK_T, SK_S$ ) measurements were taken. The skinfolds were used to adjust the girths because of different subcutaneous fat deposits. By approximating the girth to be the circumference of a circle, the lean girth ( $G$ ) of a segment was estimated by subtracting  $\pi * SK$  from  $C$ .

The two lean girths and lengths were used to scale the 'standard' muscles to the subject. The four scaling factors were defined as follows:

$$S_{LT} = L_T / 39.5 \quad (\text{cm/cm}) \quad (18)$$

$$S_{LS} = L_S / 45.5 \quad (\text{cm/cm}) \quad (19)$$

$$S_{AT} = G_T^2 / 1693 \quad (\text{cm}^2/\text{cm}^2) \quad (20)$$

$$S_{AS} = G_S^2 / 494 \quad (\text{cm}^2/\text{cm}^2) \quad (21)$$

where  $S_{LT}, S_{LS}$  - length scaling factors, and  $S_{AT}, S_{AS}$  - area scaling factors for the thigh and shank, respectively. The numerical values were derived from the 'standard' data base. Those muscles generally contained within the pelvis or thigh segments (indices 1-33) used equations (18) and (20) and all

others (indices 34-47), equations (19) and (21). The cross-sectional area of the tendons ( $A^T$ ) were multiplied by the area scaling factors. The length geometries ( $\%L^F, \%L^T$ ) were not multiplied by scaling factors since these data were given as percentages of muscle length. Total muscle lengths were calculated from the muscle line of action as described previously. Therefore the lengths of the muscles were tailored to a individual subject by the use of the transformations. The angle of pennation was not scaled and the mass of a muscle was multiplied by the length and area scaling factors. The physiological cross-sectional area ( $A^M$ ) of the muscle was:

$$A^M = m_p / (p \cdot \bar{L}_p^F) \cdot E \quad (22)$$

where  $m$  - mass (g),  $p$  - density of muscle ( $1.05 \text{ g cm}^{-3}$ ),  $\bar{L}^F$  - anatomical fibre length (cm), and  $E$  the muscle shape factor. Note the subscript  $p$  denoting muscle geometries previously scaled to the subject.

The maximum in vivo lengths of the muscles were required to implement the model as defined in Chapter III. These were estimated by mathematically moving the joints of the lower limb through their full range of motion about the skeletal reference system axes. The range of motion of the joints are given in Table 11. These are the maximum values as reported by Kapandji (1970). Moving the joints to each possible combination of maximum joint angles (128 positions), and calculating the muscle lengths, the maximum and minimum values were estimated.

During activity The movement pattern of the limbs were required for two purposes: 1) to calculate the net muscle moments and 2) to determine the instantaneous muscle moment arms, lengths and velocities. To track the segments in three-dimensional space a cinematographic system was used.

The subject walked along a prescribed path upon which two Locam cine cameras viewed the subject from the front and right.

Table 11 Range of Motion of the Joints of the Lower Limb.

| Joint      | Range of Motion (degrees) |    |    |    |     |     |
|------------|---------------------------|----|----|----|-----|-----|
|            | +X                        | -X | +Y | -Y | +Z  | -Z  |
| Hip        | 30                        | 65 | 30 | 60 | 140 | 30  |
| Knee       |                           |    |    |    | 0   | 160 |
| Tibiotalar |                           |    |    |    | 25  | 40  |
| Subtalar   | 50                        | 25 |    |    |     |     |
| MTP        |                           |    |    |    | 90  | 50  |

These are the seven major degrees of freedom of the lower limb about the SRS. Note that the MTP is included.

sides, respectively. The two cameras were accurately set at 40 and 160 frames per second using shutter pulse correlators so that every fourth frame of the second camera was synchronized within 1/4 frame ( $\pm 3.13$ ms) of the first. Midway along the walk path two grid boards (1.2 x 2.4m) were placed, joined at right angles, upon which a precision 0.1m control grid was placed. Suspended from the top of the grid boards four damped plumb lines were placed to facilitate the alignment of the reference system (control grids) in space. Along these lines 28 control points (15 mm diameter) were established with respect to the fixed grid origin (GRS). These points were used to create two 4x4 matrices, one for each view, that defined the transformation between the projected films image plane and three dimensional space. The theory and implementation of this technique is described in detail in Appendix D. In the floor beneath this calibrated space a Kistler force plate was mounted. Details regarding the force plate are found in a later section.

The Locam cameras were situated approximately 8m from the grid boards, positioned by referring to the image visible through the Locam viewfinders. A suitable location for a camera was defined as being that location in which the full extent of the control grids could be clearly seen. The focal length of the lens was

then adjusted so the two control grids filled 80 percent of the frame.

Since the technique used to define a point in three dimensional space employed two fixed cameras, once the control points and grid boards were filmed they were removed, permitting subsequent filming of the experimental situation. However, it was important to make sure that subsequent frames of interest did not change scale, translate nor rotate with respect to the frame containing the control points. The incorporation of four points visible in the corners of all the frames, when digitized, allowed for frame registration.

The control grids were not used to correct for mirror, lens and film distortions. Previous work by the author (Pierrynowski, 1980) demonstrated that the control grids were not necessary to increase the accuracy of locating a point in space with the particular setup used. Preliminary work also indicated that the technique and analysis regimen could position a point within 2mm. The control grids were only used to align the reference system in space and fix the 28 control points with respect to it.

At least three markers are necessary to define a rigid body in space. The transformation technique employed in this thesis required 4 markers per segment because scaling in the X, Y and Z directions was initially included. Subsequent processing of the transformation removed the scaling terms. Details are found in Appendix A. Various constraints had to be adhered to when locating these points and included that they were visible in each view, at all times, and that they did not move relative to the underlying bony framework. If many points were located per segment, and skin movement assumed to be random, this error could be minimized. Since the subject was filmed from approximately the front and right sides, markers were located on the subject as indicated in Table 12.

---

Table 12      The Location of the Markers on the Subject.

|        |  |
|--------|--|
| Pelvis |  |
| 1      | 3 o'clock position on the lateral side       |
| 2      | 6 o'clock position on the lateral side       |
| 3      | 9 o'clock position on the lateral side       |
| 4      | 12 o'clock position on the lateral side      |
| 5      | midway between the naval and the pubic crest |
| Thigh  |  |
| 1      | anterior aspect, proximal                    |
| 2      | anterior aspect, proximal middle             |
| 3      | anterior aspect, middle                      |
| 4      | anterior aspect, distal middle               |
| 5      | anterior aspect, distal                      |
| 6      | lateral aspect, proximal                     |
| 7      | lateral aspect, proximal middle              |
| 8      | lateral aspect, middle                       |
| 9      | lateral aspect, distal middle                |
| 10     | lateral aspect, distal                       |
| Shank  |  |
| 1      | anterior aspect, proximal                    |
| 2      | anterior aspect, proximal middle             |
| 3      | anterior aspect, middle                      |
| 4      | anterior aspect, distal middle               |
| 5      | anterior aspect, distal                      |
| 6      | lateral aspect, proximal                     |
| 7      | lateral aspect, proximal middle              |
| 8      | lateral aspect, middle                       |
| 9      | lateral aspect, distal middle                |
| 10     | lateral aspect, distal                       |
| Foot   |  |
| 1      | distal end of the 1st metatarsal             |
| 2      | proximal end of the 1st metatarsal           |
| 3      | distal end of the 4th metatarsal             |
| 4      | proximal end of 4th metatarsal               |
| 5      | distal end of the 5th metatarsal             |

---

From a knowledge of the location of the above markers on the subject in both the anatomical position (reference system R) and in space (GRS), the location of the pelvis, thigh, shank and foot were determined using the transformation method for each frame of cine data. In the present work the talus and toes segment were included with the foot. Future refinements to the data collection techniques should incorporate separate talus and toe movements during movement. These transformations locating the segments in space were then used to estimate the location of the line of action of the muscles, the centre of mass of the segments and the location of the skeletal reference systems.

In Chapter III it was shown that an iterative recursive procedure was used to estimate the muscle forces. It was therefore deemed advantageous to generate any number of samples per movement cycle for any number of cycles. Since the movement patterns were periodic and have all the properties of well behaved functions, the Fourier series representation of each element of the transformation matrices was used. Since the validity of calculating derivatives from displacement data, known to contain noise, depends upon initial noise reduction (Pezzack et al., 1977), the deletion of the higher harmonics from the Fourier series was employed (Cappozzo et al., 1975). A normalized power (the sum of the powers across harmonics equals 100 percent) at each harmonic number, for the 48 transformation elements (four segments times twelve unique elements per transformation), is shown in Figure 14. In this thesis the first four harmonics were included in the reconstructed signals, corresponding to 78 percent power returned. Details regarding the Fourier transformation are found in Appendix E.

#### Net Muscle Moments

To determine the net muscle moments during activity the masses and the three principal moments of inertia for each segment were required. The values used are found in Table 8. The displacements and accelerations of the leg segments and the ground reaction forces were also required through the complete movement cycle.

Segment Kinematics How the displacements and the mass moments of inertia of the segments were measured is alluded to above. It should be noted that the mass moments of inertia were given about three orthogonal axes (SRS) imbedded at each segment's centre of mass. Since the joint moments were initially calculated relative to the global reference system (GRS), imbedded at the joint centres, the mass moments of inertia for each segment were transformed to conform to the GRS.

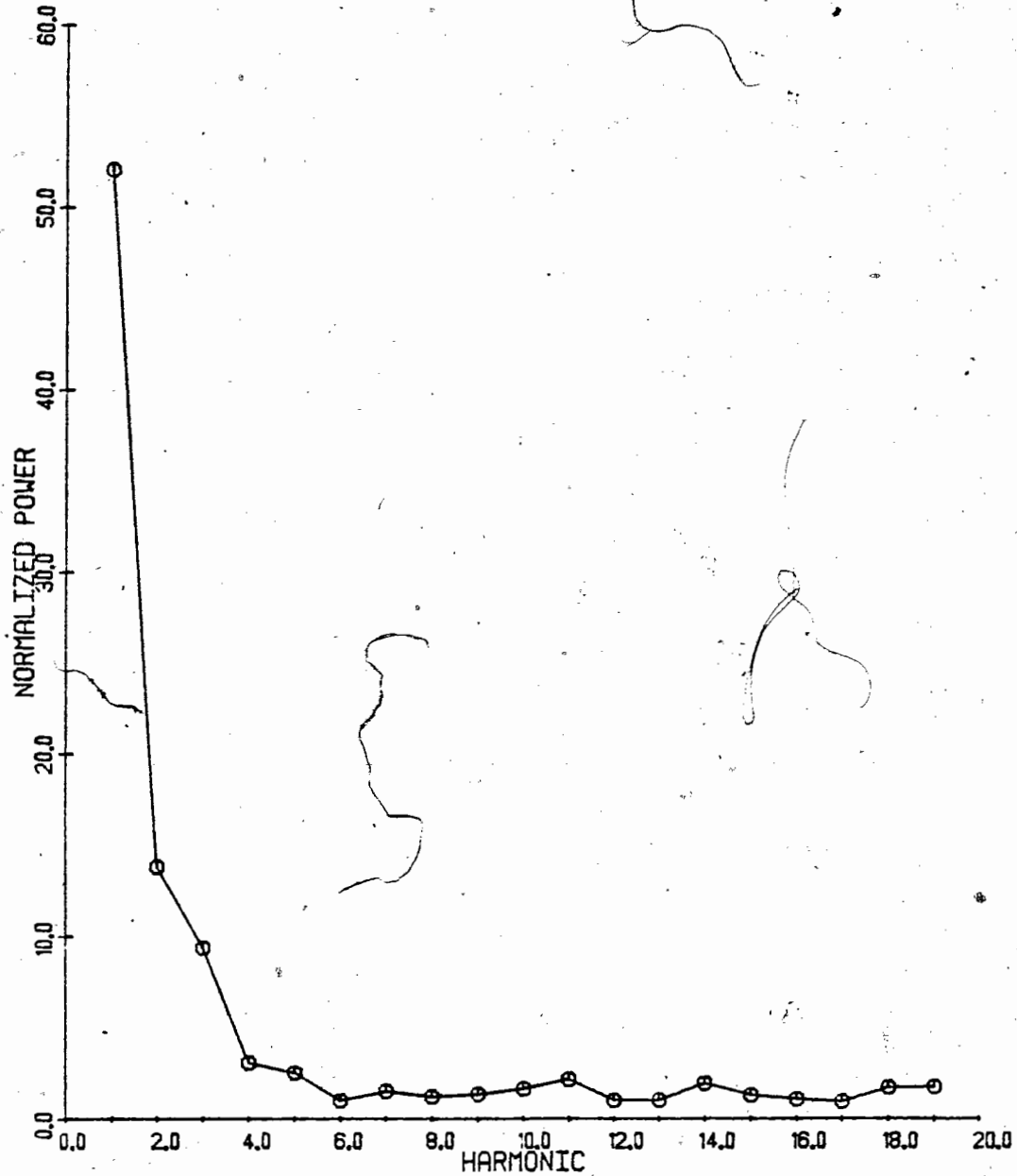


Figure 14 The normalized power (sum of the powers across harmonics equals 100 %) at each harmonic number for the 48 transformation elements (4 segments times 12 unique elements per transformation).



Given the three principal moments of inertia of the  $l$ th segment  $(\bar{I}_{1x}, \bar{I}_{1y}, \bar{I}_{1z})$  through its centre of mass and the direction cosines  $(l, m, n)$  of one of the GRS axes relative to the corresponding SRS axis the moment of inertia was calculated using:

$$I = \bar{I}_{1x} l^2 + \bar{I}_{1y} m^2 + \bar{I}_{1z} n^2 \quad (23)$$

The linear accelerations of the centre of mass of each segment were obtained by differentiating their displacements with respect to time. Since the raw displacement data were suitably smoothed by Fourier series truncation, a finite difference method was used (Dainty, 1979; Winter, 1979). To calculate accelerations from displacement data the following equation was applied:

$$\ddot{x}_t = (x_{t+2\Delta t} + x_{t-2\Delta t} - 2x_t) / 4\Delta t^2 \quad (24)$$

where  $\ddot{x}_t$  is the acceleration at time  $t$ ,  $x_t$  the displacement at time  $t$  and  $\Delta t$  the time between adjacent samples.

The angular accelerations of each segment were obtained in a similar manner from the segment angles. The segment angles were calculated from the points defining the SRS.

Ground Reaction Forces A force measuring device (Kistler 9261A) was mounted in the floor of the walk path to measure the reaction forces on the foot. The force plate determined the location of the centre of pressure, the free moment positioned at the centre of pressure, and the three components of the ground reaction relative to a reference system imbedded within the plate itself (PRS). These data were appropriately amplified, calibrated, synchronized to the cinefilm frames and manipulated to conform to the GRS (see Appendix F).

Analysis A free body diagram of the right leg during the stance phase of walking is shown in Figure 15. The GRS, the three components of the ground reaction force ( $F_{Px}$ ,  $F_{Py}$ ,  $F_{Pz}$ ), and the three reaction forces ( $F_{Hx}$ ,  $F_{Hy}$ ,  $F_{Hz}$ ) and net muscle moments ( $M_{Hx}$ ,  $M_{Hy}$ ,  $M_{Hz}$ ) at the hip are indicated. To define the position of a particular point in the leg appropriate subscripts were used. These are the H-hip, K-knee, A-tibiotalar, and B-subtalar joints, the T-thigh, S-shank, and F-foot centres of mass and O-the centre of pressure on the foot.

Two external forces act on the body segments during walking. The first, gravitational force, was considered to act at the centres of mass for each segment. These were denoted by  $W$  with an appropriate subscript. The second external force was the ground reaction force which was considered to be applied to the foot at the centre of pressure.

By considering a freebody diagram of the leg, cut at any joint, the equations of motion for the remaining 'limb' may be stated in terms of forces and moments. D'Alembert's principles of motion were then used to equate the internal forces and moments with the gravitational, reaction and inertial forces. Table 13 shows the formulas used to calculate the joint reaction forces and the net muscle moments. These forces were resolved into components parallel to the GRS and are denoted with the subscripts X, Y and Z. The sign convention for the joint forces and net muscle moments, with respect to that part of the leg below the joint, is shown in Figure 15. The net muscle moments acting at each joint were then expressed in terms of the appropriate SRS (see Appendix F).

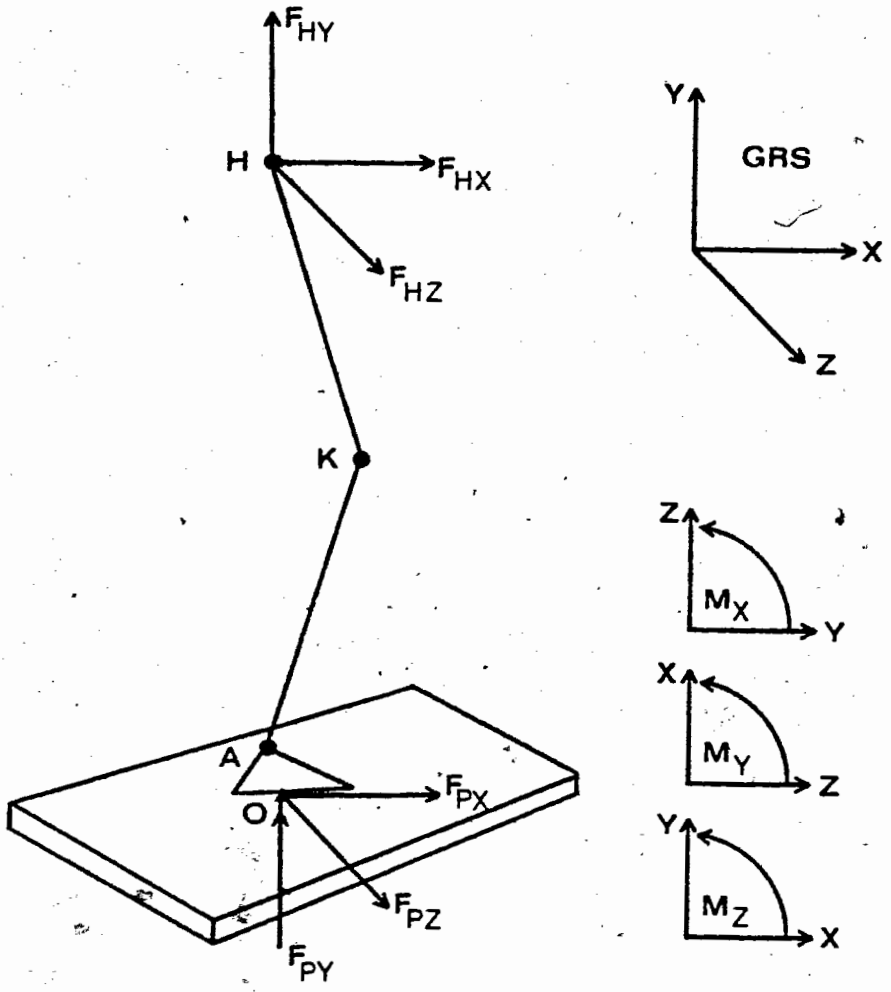


Figure 15 A free-body diagram of the right leg during activity.

Table 13 Formulas Used to Calculate the Joint Reaction Forces and the Net Muscle Moments.

$$F_{jx} = 0 + F_{px} + \sum_{l=j}^6 M_l \ddot{X}_l$$

$$F_{jy} = \sum_{l=j}^6 M_l g + F_{py} + \sum_{l=j}^6 M_l \ddot{Y}_l$$

$$F_{jz} = 0 + F_{pz} + \sum_{l=j}^6 M_l \ddot{Z}_l$$

$$M_{jx} = \sum_{l=j}^6 -M_l g (Z_l - Z_j) + F_{pz} (Y_p - Y_j) - F_{py} (Z_p - Z_j) - \sum_{l=j}^6 (M_l \ddot{Y}_l (Z_l - Z_j) - M_l \ddot{Z}_l (Y_l - Y_j) - I_{lx} \alpha_{lx})$$

$$M_{jy} = M_{py} + F_{px} (Z_p - Z_j) - F_{pz} (X_p - X_j) - \sum_{l=j}^6 (M_l \ddot{Z}_l (X_l - X_j) - M_l \ddot{X}_l (Z_l - Z_j) - I_{ly} \alpha_{ly})$$

$$M_{jz} = \sum_{l=j}^6 M_l g (X_l - X_j) + F_{py} (X_p - X_j) - F_{px} (Y_p - Y_j) - \sum_{l=j}^6 (M_l \ddot{X}_l (Y_l - Y_j) - M_l \ddot{Y}_l (X_l - X_j) - I_{lz} \alpha_{lz})$$

See the nomenclature for the symbol definitions.

### Model Implementation

The calculations required to estimate the forces in the individual muscles were extremely laborious hence a series of six computer programmes were developed. A brief summary of each is found below.

Programme 1: Transformed the skeleton and the 'standard' data bases to define the subject in the anatomical position. The muscle lengths, geometries and moment arms, the ligament moment arms, and the location of the SRS and centres of mass were defined.

Programme 2: Defined the location of the two cine cameras in space using the 28 control points. Estimated the three dimensional location of the segment markers during the walking cycle. Calculated transformations, using the subject markers, to locate the subject's segments in space. Fourier series truncation was used to smooth the data and to define any number of frames per walking cycle (cinefilm taken at 40 fps, analyses at 200 fps).

Programme 3: Transformed the force plate data from an internal reference system (PRS) to the global reference system (GRS).

Programme 4: Calculated the instantaneous lengths, velocities and moment arms of the muscles, and the location of the SRS and centres of mass during the movement cycle.

Programme 5: Calculated the net muscle moments relative to both the GRS and the SRS.

Programme 6: Calculated the output from each pattern generator which in turn specified the forces in the muscles. It should be noted that the data provided three walking cycles after performing the Fourier series reconstruction. The third cycle was used for all data presentation purposes. This was necessary since a recursive procedure was used to estimate the muscle forces (see Chapter III).

These six programmes required five input data files. These contained the following information:

File A: The anthropometric measurements obtained from the subject.

File B: The skelton and 'standard' data bases.

File C: The digitized coordinates of the control points, frame registration points and the segment markers as seen by each cine camera.

File D: A control file defining the number of samples per cycle, cycles, muscles, segments and various user defined options.

File E: The force plate data.

A block diagram of the computer programmes is shown in Figure 16. The computer programmes, written in FORTRAN, were implemented on a IBM System/370 Model 148 computer. The programmes were memory efficient (<256K each) to allow for their eventual implementation on a small in-house mini computer system (Hewlett Packard Series 9800 System 35A).

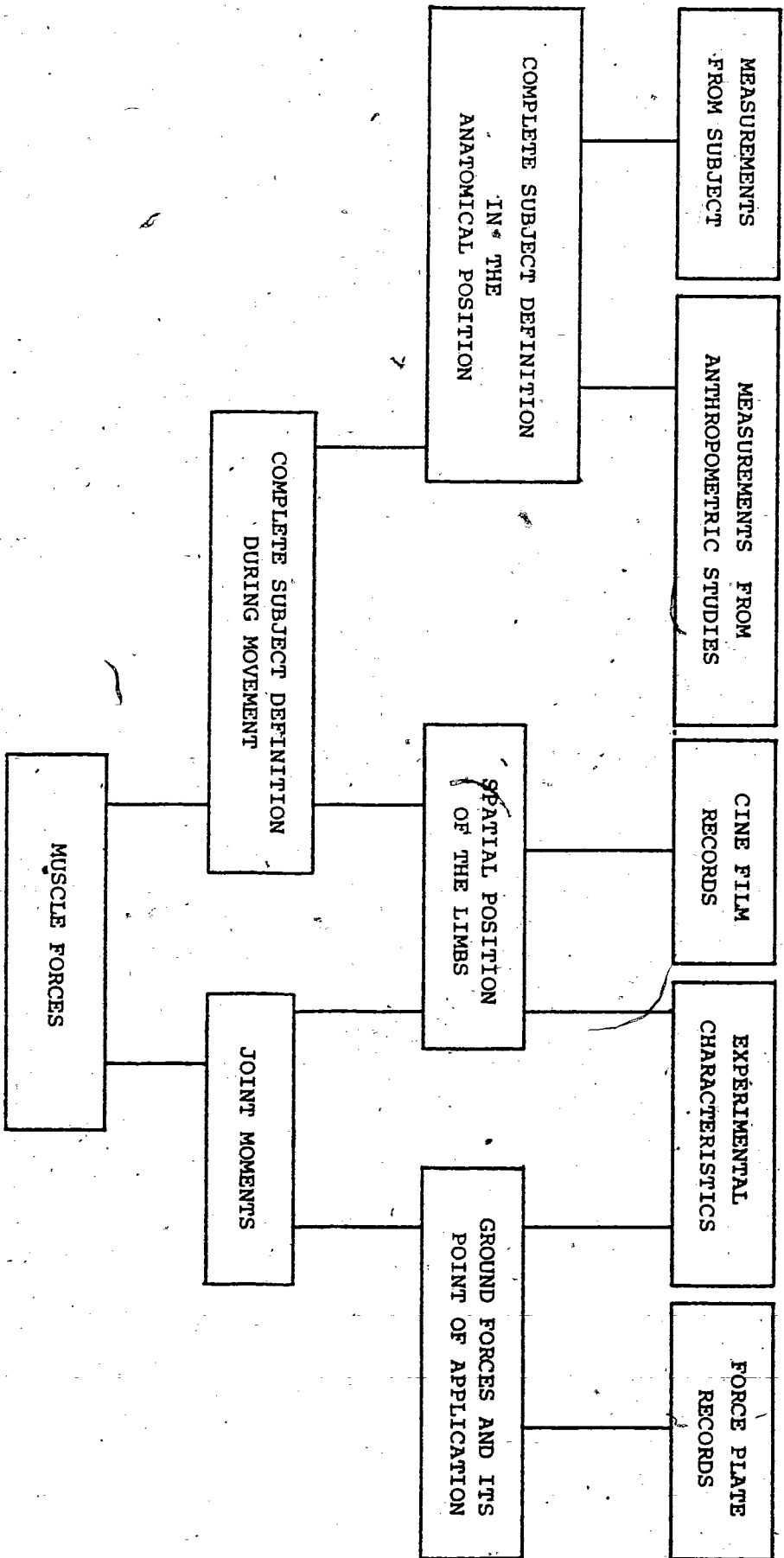


Figure 16 Block diagram of the five input data files (top line) and the six computer programmes.

## CHAPTER V

RESULTS AND DISCUSSION

This chapter presents and discusses the results of the model implementation under the following headings: 1) the definition of the subject's lower limb which includes the muscle and ligament lines of action and moment arms, muscle geometries and the location of the imbedded reference systems and centres of mass, 2) the muscle lengths and velocities during a normal walk, 3) the three-dimensional reaction force and net muscle moments at the joints during gait and 4) the model's prediction of the muscle forces and the pattern generator outputs.

THE SUBJECT'S LOWER LIMBAnatomical Position

A mechanical model of the human right lower limb was defined in Chapter III. These data were scaled to the subject using the techniques outlined in Chapter IV. A definition of the subject's lower limb is presented below.

To transform the lines of action of the muscles and ligaments, the imbedded reference systems and the location of each segment's centre of mass, a homogeneous deformation of the skeleton segments into those of the subject's were performed using  $4 \times 4$  transformation matrices, one for each segment. Each matrix was calculated from the coordinates of the palpable points measured on each skeleton segment and on the subject whilst in the anatomical position. These data and the transformations are found in Table 14. Knowing these transformations the coordinates defining the skeleton SRS and centres of mass (Table 3) were mapped into the subject (Table 15). Similarly, the points defining the skeleton lines of action of the muscles (Table 4) and ligaments (Table 6) were transformed to lie within the subject (Tables 16 and 17). Note that the data presented in Tables 14 to 17 are for the subject in the anatomical position.



Table 14 The Segment Transformations Between the Skeleton and the Subject's Palpable Points. All values in metres.

| Segment | Skeleton Points |       |       | Subject Points |       |       | Transformation |          |          |          |       |       |       |
|---------|-----------------|-------|-------|----------------|-------|-------|----------------|----------|----------|----------|-------|-------|-------|
|         | X               | Y     | Z     | X              | Y     | Z     | X              |          | Y        |          | Z     |       |       |
| Pelvis  | 1               | 0.268 | 0.246 | 0.241          | 0.176 | 1.011 | 0.572          | 1.38627  | -0.33541 | -0.07449 | 0.000 | 0.000 | 0.000 |
|         | 2               | 0.273 | 0.312 | 0.132          | 0.174 | 1.064 | 0.450          | -0.08956 | 1.00311  | -0.01169 | 0.000 | 0.000 | 0.000 |
|         | 3               | 0.276 | 0.318 | 0.346          | 0.177 | 1.076 | 0.699          | -0.03238 | 0.04304  | 1.18591  | 0.000 | 0.000 | 0.000 |
|         | 4               | 0.231 | 0.340 | 0.122          | 0.122 | 1.110 | 0.432          | -0.16763 | 0.83956  | 0.31241  | 1.000 | 0.000 | 0.000 |
|         | 5               | 0.240 | 0.341 | 0.356          | 0.121 | 1.120 | 0.713          |          |          |          |       |       |       |
|         | 6               | 0.154 | 0.227 | 0.238          | 0.017 | 1.024 | 0.582          |          |          |          |       |       |       |
| Thigh   | 1               | 0.141 | 0.562 | 0.159          | 0.112 | 1.024 | 0.728          | 1.14687  | 0.30306  | 0.32424  | 0.000 | 0.000 | 0.000 |
|         | 2               | 0.149 | 0.168 | 0.162          | 0.160 | 0.558 | 0.714          | -0.09799 | 1.16679  | 0.05052  | 0.000 | 0.000 | 0.000 |
|         | 3               | 0.117 | 0.183 | 0.101          | 0.117 | 0.548 | 0.632          | -0.07907 | -0.03505 | 1.18549  | 0.000 | 0.000 | 0.000 |
|         | 4               | 0.132 | 0.153 | 0.162          | 0.142 | 0.536 | 0.708          | -0.00721 | 0.31977  | 0.46531  | 1.000 | 0.000 | 0.000 |
|         | 5               | 0.129 | 0.150 | 0.113          | 0.135 | 0.534 | 0.649          |          |          |          |       |       |       |
| Shank   | 1               | 0.167 | 0.619 | 0.114          | 0.110 | 0.519 | 0.639          | 1.12095  | 0.33120  | 0.23118  | 0.000 | 0.000 | 0.000 |
|         | 2               | 0.214 | 0.586 | 0.153          | 0.158 | 0.500 | 0.695          | -0.12849 | 1.11393  | -0.00574 | 0.000 | 0.000 | 0.000 |
|         | 3               | 0.174 | 0.605 | 0.143          | 0.111 | 0.510 | 0.722          | -0.00770 | 0.05589  | 1.15088  | 0.000 | 0.000 | 0.000 |
|         | 4               | 0.182 | 0.249 | 0.173          | 0.080 | 0.115 | 0.712          | -0.15744 | -0.23206 | 0.47341  | 1.000 | 0.000 | 0.000 |
|         | 5               | 0.198 | 0.259 | 0.120          | 0.094 | 0.129 | 0.657          |          |          |          |       |       |       |
| Foot    | 1               | 0.143 | 0.238 | 0.133          | 0.056 | 0.108 | 0.671          | 1.13239  | -0.15706 | -0.12509 | 0.000 | 0.000 | 0.000 |
|         | 2               | 0.143 | 0.237 | 0.154          | 0.048 | 0.103 | 0.701          | -0.99810 | 1.29542  | 0.16895  | 0.000 | 0.000 | 0.000 |
|         | 3               | 0.218 | 0.209 | 0.140          | 0.139 | 0.060 | 0.716          | -0.65521 | -0.05084 | 1.32146  | 0.000 | 0.000 | 0.000 |
|         | 4               | 0.306 | 0.230 | 0.143          | 0.245 | 0.070 | 0.695          | 0.21956  | -0.17039 | 0.47300  | 1.000 | 0.000 | 0.000 |
|         | 5               | 0.296 | 0.222 | 0.174          | 0.223 | 0.060 | 0.700          |          |          |          |       |       |       |
|         | 6               | 0.278 | 0.213 | 0.187          | 0.195 | 0.053 | 0.725          |          |          |          |       |       |       |
|         | 7               | 0.218 | 0.250 | 0.131          | 0.127 | 0.117 | 0.659          |          |          |          |       |       |       |

Table 15 The Points Defining the Primary and Secondary Skeletal Reference Systems (SRS) and the Centres of Mass Within the Subject (Anatomical Position). All values in mm.

| Reference System | Seg/ <sup>1</sup> <sub>2</sub> <sub>3</sub> | Origin                                     | +X  | +Y       | +Z                        |
|------------------|---|--|-----|----------|---------------------------|
| Pelvis           | /PC<br>/H<br>/CM                            | 172 1004 576<br>110 1024 666               | 222 | 999 575  | 177 1054 575 173 1006 626 |
| Thigh            | /H<br>/K<br>/CM                             | 110 1024 666<br>117 550 675<br>115 822 668 | 159 | 1028 671 | 105 1074 664 104 1025 716 |
| Shank            | /K<br>/TT<br>/CM                            | 117 550 675<br>088 123 681<br>106 376 677  | 167 | 556 680  | 111 600 673 112 551 724   |
| Talus            | /TT<br>/ST<br>/CM                           | 088 123 681<br>087 111 682<br>087 111 682  | 130 | 133 705  | 070 168 693 068 104 723   |
| Foot             | /ST<br>/MTP<br>/CM                          | 087 111 682<br>219 062 703<br>163 079 671  | 117 | 151 681  | 047 142 685 090 110 732   |
| Toes             | /MTP  | 226 057 697                                | 270 | 071 715  | 208 103 707 212 042 743   |

1 location of the primary reference system  
 2 location of the secondary reference system  
 3 location of the centre of mass

Lew and Lewis (1977) remark that the transformational scaling technique is a more accurate method for accounting for individual geometrical differences if sufficient accuracy is used to locate the palpable points. However, if more than 4 points are used to define a transformation the importance of any given point is reduced, a fact not emphasized by Lew and Lewis. In fact they suggest in a recent paper (Lewis *et al.*, 1980) that if more than 4 points are available a non-homogeneous scaling technique, based on finite element principles, be used. Although this technique is accurate it relies on knowing the definite coordinates of the



Table 17 The Points Defining the Line of Action of the Ligaments Within the Subject (Anatomical Position). All values in mm.

| ligament | on segment number | point |      |      |      |      |      |
|----------|-------------------|-------|------|------|------|------|------|
|          |                   | 1     |      |      | 2    |      |      |
| 1        | 1                 | 0141  | 1041 | 0659 | 0119 | 1002 | 0715 |
| 2        | 1                 | 0141  | 1041 | 0659 | 0120 | 0974 | 0702 |
| 3        | 1                 | 0151  | 1016 | 0627 | 0111 | 0968 | 0685 |
| 4        | 1                 | 0064  | 1028 | 0656 | 0095 | 1010 | 0703 |
| 5        | 2                 | 0115  | 0548 | 0633 | 0121 | 0446 | 0665 |
| 6        | 2                 | 0129  | 0522 | 0718 | 0122 | 0503 | 0723 |
| 7        | 2                 | 0105  | 0562 | 0653 | 0087 | 0499 | 0656 |
| 8        | 2                 | 0102  | 0562 | 0678 | 0097 | 0504 | 0683 |
| 9        | 2                 | 0108  | 0567 | 0704 | 0105 | 0509 | 0704 |
| 10       | 2                 | 0103  | 0548 | 0685 | 0127 | 0535 | 0673 |
| 11       | 2                 | 0121  | 0539 | 0667 | 0097 | 0506 | 0681 |
| 12       | 2                 | 0104  | 0562 | 0656 | 0090 | 0498 | 0653 |
| 13       | 3                 | 0091  | 0130 | 0712 | 0084 | 0122 | 0699 |
| 14       | 3                 | 0078  | 0135 | 0694 | 0060 | 0129 | 0691 |
| 15       | 3                 | 0102  | 0144 | 0658 | 0123 | 0119 | 0658 |
| 16       | 3                 | 0083  | 0129 | 0653 | 0076 | 0131 | 0665 |
| 17       | 3                 | 0074  | 0115 | 0712 | 0067 | 0102 | 0706 |
| 18       | 3                 | 0106  | 0152 | 0665 | 0135 | 0114 | 0659 |
| 19       | 3                 | 0102  | 0145 | 0658 | 0127 | 0114 | 0654 |
| 20       | 3                 | 0097  | 0138 | 0659 | 0118 | 0118 | 0650 |
| 21       | 4                 | 0119  | 0116 | 0675 | 0125 | 0118 | 0672 |
| 22       | 4                 | 0106  | 0117 | 0683 | 0100 | 0114 | 0690 |
| 23       | 4                 | 0099  | 0107 | 0689 | 0098 | 0114 | 0690 |
| 24       | 4                 | 0086  | 0105 | 0702 | 0078 | 0090 | 0706 |
| 25       | 5                 | 0059  | 0123 | 0685 | 0058 | 0112 | 0689 |

palpable points to fit the skeleton to these points exactly. It is likely that some error exists in the measurement of the palpable points and a mean square best fit should be employed.

A test of the transformational technique's accuracy can be deduced in two ways from the data presented. First, if one multiplies a skeleton palpable point by the appropriate transformation, the corresponding subject palpable point should be forthcoming. This was done and the maximum absolute coordinate error was 5 mm and the unsigned mean error 2 mm. Second, if one compares the coordinates of the primary and secondary SRS, as given in Table 15, the joint centres should align. For example the primary SRS for the shank (knee) and the secondary SRS for

the thigh (also the knee) are within 2 mm. These results suggest that: 1) geometrical differences between the bones of the human lower limb are largely homogeneous deformations, and 2) the use of a redundant set of points to define a transformation is beneficial. It should be noted, however, that these results were obtained from only one subject which suggests but does not prove the suitability of the scaling technique.

Knowing the coordinates defining the SRS and the lines of action of the muscles and ligaments the moment arms of these structures, relative to the SRS, were calculated. These are presented in Tables 18 and 19. These values were compared to both books of anatomy (Beetham *et al.*, 1965; Crouch, 1972; Grant, 1972; Inman, 1976; Kapanji, 1970; Kendal *et al.*, 1971; Rouviere, 1974; Steindler, 1955; Warfel, 1974) to determine qualitative correctness, and to various published sources (Smidt, 1973; Sutherland, 1966) for quantitative verification.

In most cases the sign and magnitude of the moment arms matched the anatomical atlases and references. Those that did not could be attributed to two references contradicting one another or specialized modelling (one muscle split into various subunits with different actions). These results were partially achieved by the specialized modelling of the muscle's moment arms (see Chapter III) in the neighbourhood of the joint centres. However, it is strongly suggested that a three-dimensional reconstruction of the course of the muscles near the joint centres using X-ray photogrammetry and imbedded wires within the muscle tendons (see An *et al.*, 1979) must be undertaken to better estimate the muscle's moment arms.

To scale the 'standard' muscle geometries from Table 7 the the anatomical length of each muscle ( $L^m$ ) and the length, girth and skin fold thickness of the thigh and shank were required. The segment measurements were 39.8 cm, 50.0 cm and 4.1 mm for the thigh and 44.8 cm, 32.8 cm and 4.6 mm for the shank, respectively. The results of the geometrical scaling are found in

Table 18 The Muscle Moment Arms (SWS) of the Subject (Anatomical Position).  
 All values in mm.

|    | X   | Y   | Z   | X    | Y    | Z   | X    | Y    | Z    | X    | Y    | Z    | X    | Y    | Z   |
|----|-----|-----|-----|------|------|-----|------|------|------|------|------|------|------|------|-----|
| 1  | 006 | 006 | 019 | -039 | 001  | 005 | -023 | -004 | -056 | 001  | 000  | -036 | -002 | -002 | 005 |
| 2  | 024 | 013 | 005 | -032 | 001  | 050 | -021 | -004 | -026 | 001  | 002  | -036 | 001  | 000  | 007 |
| 3  | 011 | 032 | 007 | 010  | -001 | 061 | 023  | 021  | 036  | 000  | -000 | -035 | 000  | -001 | 026 |
| 4  | 005 | 007 | 000 | 007  | -010 | 050 | 008  | 016  | 030  | -027 | 001  | 017  | -027 | 001  | 013 |
| 5  | 027 | 019 | 000 | 035  | -008 | 040 | 004  | 016  | 009  | -035 | -002 | -010 | 011  | 010  | 023 |
| 6  | 013 | 023 | 000 | 003  | -008 | 040 | 004  | 009  | 009  | -009 | 010  | 019  | -009 | 006  | 013 |
| 7  | 012 | 023 | 000 | 003  | -008 | 040 | 004  | 009  | 009  | -009 | 010  | 019  | -009 | 006  | 013 |
| 8  | 012 | 023 | 000 | 003  | -008 | 040 | 004  | 009  | 009  | -009 | 010  | 019  | -009 | 006  | 013 |
| 9  | 012 | 023 | 000 | 003  | -008 | 040 | 004  | 009  | 009  | -009 | 010  | 019  | -009 | 006  | 013 |
| 10 | 012 | 023 | 000 | 003  | -008 | 040 | 004  | 009  | 009  | -009 | 010  | 019  | -009 | 006  | 013 |
| 11 | 012 | 023 | 000 | 003  | -008 | 040 | 004  | 009  | 009  | -009 | 010  | 019  | -009 | 006  | 013 |
| 12 | 012 | 023 | 000 | 003  | -008 | 040 | 004  | 009  | 009  | -009 | 010  | 019  | -009 | 006  | 013 |
| 13 | 012 | 023 | 000 | 003  | -008 | 040 | 004  | 009  | 009  | -009 | 010  | 019  | -009 | 006  | 013 |
| 14 | 012 | 023 | 000 | 003  | -008 | 040 | 004  | 009  | 009  | -009 | 010  | 019  | -009 | 006  | 013 |
| 15 | 012 | 023 | 000 | 003  | -008 | 040 | 004  | 009  | 009  | -009 | 010  | 019  | -009 | 006  | 013 |
| 16 | 012 | 023 | 000 | 003  | -008 | 040 | 004  | 009  | 009  | -009 | 010  | 019  | -009 | 006  | 013 |
| 17 | 012 | 023 | 000 | 003  | -008 | 040 | 004  | 009  | 009  | -009 | 010  | 019  | -009 | 006  | 013 |
| 18 | 012 | 023 | 000 | 003  | -008 | 040 | 004  | 009  | 009  | -009 | 010  | 019  | -009 | 006  | 013 |
| 19 | 012 | 023 | 000 | 003  | -008 | 040 | 004  | 009  | 009  | -009 | 010  | 019  | -009 | 006  | 013 |
| 20 | 012 | 023 | 000 | 003  | -008 | 040 | 004  | 009  | 009  | -009 | 010  | 019  | -009 | 006  | 013 |
| 21 | 012 | 023 | 000 | 003  | -008 | 040 | 004  | 009  | 009  | -009 | 010  | 019  | -009 | 006  | 013 |
| 22 | 012 | 023 | 000 | 003  | -008 | 040 | 004  | 009  | 009  | -009 | 010  | 019  | -009 | 006  | 013 |
| 23 | 012 | 023 | 000 | 003  | -008 | 040 | 004  | 009  | 009  | -009 | 010  | 019  | -009 | 006  | 013 |
| 24 | 012 | 023 | 000 | 003  | -008 | 040 | 004  | 009  | 009  | -009 | 010  | 019  | -009 | 006  | 013 |
| 25 | 012 | 023 | 000 | 003  | -008 | 040 | 004  | 009  | 009  | -009 | 010  | 019  | -009 | 006  | 013 |
| 26 | 012 | 023 | 000 | 003  | -008 | 040 | 004  | 009  | 009  | -009 | 010  | 019  | -009 | 006  | 013 |
| 27 | 012 | 023 | 000 | 003  | -008 | 040 | 004  | 009  | 009  | -009 | 010  | 019  | -009 | 006  | 013 |
| 28 | 012 | 023 | 000 | 003  | -008 | 040 | 004  | 009  | 009  | -009 | 010  | 019  | -009 | 006  | 013 |
| 29 | 012 | 023 | 000 | 003  | -008 | 040 | 004  | 009  | 009  | -009 | 010  | 019  | -009 | 006  | 013 |
| 30 | 012 | 023 | 000 | 003  | -008 | 040 | 004  | 009  | 009  | -009 | 010  | 019  | -009 | 006  | 013 |
| 31 | 012 | 023 | 000 | 003  | -008 | 040 | 004  | 009  | 009  | -009 | 010  | 019  | -009 | 006  | 013 |
| 32 | 012 | 023 | 000 | 003  | -008 | 040 | 004  | 009  | 009  | -009 | 010  | 019  | -009 | 006  | 013 |
| 33 | 012 | 023 | 000 | 003  | -008 | 040 | 004  | 009  | 009  | -009 | 010  | 019  | -009 | 006  | 013 |
| 34 | 012 | 023 | 000 | 003  | -008 | 040 | 004  | 009  | 009  | -009 | 010  | 019  | -009 | 006  | 013 |
| 35 | 012 | 023 | 000 | 003  | -008 | 040 | 004  | 009  | 009  | -009 | 010  | 019  | -009 | 006  | 013 |
| 36 | 012 | 023 | 000 | 003  | -008 | 040 | 004  | 009  | 009  | -009 | 010  | 019  | -009 | 006  | 013 |
| 37 | 012 | 023 | 000 | 003  | -008 | 040 | 004  | 009  | 009  | -009 | 010  | 019  | -009 | 006  | 013 |
| 38 | 012 | 023 | 000 | 003  | -008 | 040 | 004  | 009  | 009  | -009 | 010  | 019  | -009 | 006  | 013 |
| 39 | 012 | 023 | 000 | 003  | -008 | 040 | 004  | 009  | 009  | -009 | 010  | 019  | -009 | 006  | 013 |
| 40 | 012 | 023 | 000 | 003  | -008 | 040 | 004  | 009  | 009  | -009 | 010  | 019  | -009 | 006  | 013 |
| 41 | 012 | 023 | 000 | 003  | -008 | 040 | 004  | 009  | 009  | -009 | 010  | 019  | -009 | 006  | 013 |
| 42 | 012 | 023 | 000 | 003  | -008 | 040 | 004  | 009  | 009  | -009 | 010  | 019  | -009 | 006  | 013 |
| 43 | 012 | 023 | 000 | 003  | -008 | 040 | 004  | 009  | 009  | -009 | 010  | 019  | -009 | 006  | 013 |
| 44 | 012 | 023 | 000 | 003  | -008 | 040 | 004  | 009  | 009  | -009 | 010  | 019  | -009 | 006  | 013 |
| 45 | 012 | 023 | 000 | 003  | -008 | 040 | 004  | 009  | 009  | -009 | 010  | 019  | -009 | 006  | 013 |
| 46 | 012 | 023 | 000 | 003  | -008 | 040 | 004  | 009  | 009  | -009 | 010  | 019  | -009 | 006  | 013 |
| 47 | 012 | 023 | 000 | 003  | -008 | 040 | 004  | 009  | 009  | -009 | 010  | 019  | -009 | 006  | 013 |

Table 19 The Ligament Moment Arms (SRS) of the Subject (Anatomical Position).  
 All values in mm.

|    | HIP  |      |      | KNEE |      |      | TT   |      |      | ST   |      |      | HTP |   |   |
|----|------|------|------|------|------|------|------|------|------|------|------|------|-----|---|---|
|    | X    | Y    | Z    | X    | Y    | Z    | X    | Y    | Z    | X    | Y    | Z    | X   | Y | Z |
| 1  | -006 | 023  | 013  | 032  | -002 | -003 | -006 | 012  | -002 | 001  | 028  | -014 |     |   |   |
| 2  | 000  | 014  | 022  | -045 | 004  | 011  | -005 | 010  | -016 | 017  | -006 | 041  |     |   |   |
| 3  | 032  | 006  | 025  | 016  | -008 | -023 | 030  | 013  | 009  | 023  | -007 | 034  |     |   |   |
| 4  | -004 | -031 | -013 | -029 | 005  | -007 | -013 | -014 | 008  | 008  | -009 | 027  |     |   |   |
| 5  |      |      |      | 008  | -004 | 014  | -023 | 025  | -002 | 017  | -006 | 041  |     |   |   |
| 6  |      |      |      | -000 | -003 | -005 | 031  | 009  | 018  | 023  | -007 | 034  |     |   |   |
| 7  |      |      |      | 018  | -005 | -022 | 032  | 010  | 009  | 024  | -009 | 027  |     |   |   |
| 8  |      |      |      |      |      |      | 028  | 009  | 002  | 006  | -006 | -003 |     |   |   |
| 9  |      |      |      |      |      |      |      |      |      | 008  | 012  | 002  |     |   |   |
| 10 |      |      |      |      |      |      |      |      |      | 007  | -005 | -011 |     |   |   |
| 11 |      |      |      |      |      |      |      |      |      | -002 | 018  | 001  |     |   |   |
| 12 |      |      |      |      |      |      |      |      |      | -010 | -001 | -027 |     |   |   |
| 13 |      |      |      |      |      |      |      |      |      |      |      |      |     |   |   |
| 14 |      |      |      |      |      |      |      |      |      |      |      |      |     |   |   |
| 15 |      |      |      |      |      |      |      |      |      |      |      |      |     |   |   |
| 16 |      |      |      |      |      |      |      |      |      |      |      |      |     |   |   |
| 17 |      |      |      |      |      |      |      |      |      |      |      |      |     |   |   |
| 18 |      |      |      |      |      |      |      |      |      |      |      |      |     |   |   |
| 19 |      |      |      |      |      |      |      |      |      |      |      |      |     |   |   |
| 20 |      |      |      |      |      |      |      |      |      |      |      |      |     |   |   |
| 21 |      |      |      |      |      |      |      |      |      |      |      |      |     |   |   |
| 22 |      |      |      |      |      |      |      |      |      |      |      |      |     |   |   |
| 23 |      |      |      |      |      |      |      |      |      |      |      |      |     |   |   |
| 24 |      |      |      |      |      |      |      |      |      |      |      |      |     |   |   |
| 25 |      |      |      |      |      |      |      |      |      |      |      |      |     |   |   |

Table 20. Included are the muscle's maximum, anatomical and minimum lengths ( $\hat{L}^m$ ,  $\bar{L}^m$ ,  $\check{L}^m$ ), mass (m), and the anatomical length of the muscle fibres ( $\bar{L}^m$ ). The tendon's length ( $L^T$ ) and cross-sectional area ( $A^T$ ) are also included. The areas ( $A_i^c$ ) and the maximum isometric contractile element force values, parallel to its fibres ( $P_i^c$ ) are located in Table 21. To complete the definition of the subject's lower limb a sagittal and frontal plane view of the lines of action of the 47 muscles, scaled to the subject, are shown in Figure 17.

The anatomical data base is a composite of the results reported by many individuals (see Chapter III) coalesced into Table 7. This author's contribution has been to define a method of scaling these data to a particular individual. As such the values reported herein compare favourably with those previously reported.

Fortunately the author was able to obtain the total leg muscle mass values of ten male Belgium cadavers (Cadaver Analysis Study, 1980). The anthropometric measurements needed by the model to estimate the muscle masses were also available. Therefore, an attempt to validate the anatomical model's estimation of the total muscle mass was performed. The results of this validation is found in Table 22.

The model could only account for 67 percent of the directly measured muscle mass. Even considering the 10 percent measured mass due to nerve, circulation and miscellaneous tissue (Martin and Drinkwater, 1981) the model underestimates reality by 20 percent. This suggests that further study must be initiated to scale the 'standard' data base to a particular individual using additional anthropometric measurements. In the context of this thesis this discrepancy was minimized by increasing each predicted muscle mass by 25 percent when the individual muscle forces were calculated. This leads to a similar increase in the cross-sectional area of each muscle with a concomitant increase in its maximum isometric force.



Table 20 The Subject's Muscle Geometrical Data. Part I.

|    | max<br>length<br>muscle<br>(mm) | anat<br>length<br>muscle<br>(mm) | min<br>length<br>muscle<br>(mm) | anat<br>length<br>fibre<br>(mm) | anat<br>length<br>tendon<br>(mm) | area<br>tendon<br>(mm*mm) | mass<br>(g) |
|----|---------------------------------|----------------------------------|---------------------------------|---------------------------------|----------------------------------|---------------------------|-------------|
| 1  | 303                             | 298                              | 241                             | 239                             | 60                               | 56.1                      | 178.9       |
| 2  | 247                             | 238                              | 162                             | 238                             | 0                                | 0.0                       | 199.8       |
| 3  | 108                             | 89                               | 43                              | 81                              | 9                                | 26.6                      | 7.0         |
| 4  | 107                             | 83                               | 34                              | 75                              | 8                                | 26.6                      | 11.2        |
| 5  | 114                             | 99                               | 71                              | 65                              | 35                               | 26.6                      | 64.3        |
| 6  | 95                              | 84                               | 57                              | 34                              | 51                               | 26.6                      | 47.5        |
| 7  | 174                             | 151                              | 75                              | 113                             | 38                               | 26.6                      | 40.5        |
| 8  | 103                             | 55                               | 29                              | 55                              | 0                                | 0.0                       | 41.9        |
| 9  | 163                             | 131                              | 70                              | 131                             | 0                                | 0.0                       | 54.5        |
| 10 | 346                             | 253                              | 234                             | 253                             | 0                                | 0.0                       | 188.2       |
| 11 | 183                             | 123                              | 88                              | 123                             | 0                                | 0.0                       | 339.1       |
| 12 | 321                             | 246                              | 220                             | 246                             | 0                                | 0.0                       | 1339.7      |
| 13 | 476                             | 393                              | 363                             | 295                             | 98                               | 26.6                      | 433.2       |
| 14 | 248                             | 164                              | 139                             | 164                             | 0                                | 0.0                       | 999.2       |
| 15 | 126                             | 94                               | 41                              | 75                              | 19                               | 33.6                      | 99.3        |
| 16 | 149                             | 121                              | 29                              | 97                              | 24                               | 33.6                      | 229.3       |
| 17 | 144                             | 124                              | 47                              | 99                              | 25                               | 33.6                      | 229.3       |
| 18 | 133                             | 101                              | 38                              | 86                              | 15                               | 22.4                      | 229.3       |
| 19 | 183                             | 144                              | 93                              | 122                             | 22                               | 22.4                      | 882.4       |
| 20 | 175                             | 131                              | 62                              | 111                             | 20                               | 22.4                      | 882.4       |
| 21 | 256                             | 256                              | 163                             | 231                             | 26                               | 22.4                      | 882.4       |
| 22 | 699                             | 655                              | 544                             | 199                             | 465                              | 46.0                      | 1555.1      |
| 23 | 607                             | 666                              | 450                             | 85                              | 481                              | 46.0                      | 462.5       |
| 24 | 585                             | 533                              | 383                             | 49                              | 180                              | 46.0                      | 301.8       |
| 25 | 652                             | 567                              | 402                             | 340                             | 227                              | 21.0                      | 178.9       |
| 26 | 646                             | 535                              | 337                             | 321                             | 214                              | 11.2                      | 103.4       |
| 27 | 609                             | 588                              | 438                             | 470                             | 118                              | 42.0                      | 157.9       |
| 28 | 629                             | 537                              | 487                             | 55                              | 215                              | 42.0                      | 183.0       |
| 29 | 711                             | 520                              | 390                             | 76                              | 234                              | 35.0                      | 201.2       |
| 30 | 85                              | 85                               | 202                             | 128                             | 157                              | 15.4                      | 136.9       |
| 31 | 577                             | 463                              | 463                             | 87                              | 93                               | 15.4                      | 711.2       |
| 32 | 573                             | 459                              | 459                             | 81                              | 115                              | 9.8                       | 441.5       |
| 33 | 574                             | 461                              | 461                             | 91                              | 92                               | 5.6                       | 243.1       |
| 34 | 145                             | 121                              | 119                             | 96                              | 24                               | 5.9                       | 29.4        |
| 35 | 516                             | 467                              | 406                             | 61                              | 303                              | 29.9                      | 122.3       |
| 36 | 543                             | 468                              | 375                             | 57                              | 304                              | 49.8                      | 221.4       |
| 37 | 514                             | 465                              | 404                             | 93                              | 72                               | 10.0                      | 115.7       |
| 38 | 444                             | 366                              | 303                             | 38                              | 293                              | 41.8                      | 389.9       |
| 39 | 439                             | 399                              | 339                             | 82                              | 16                               | 49.8                      | 154.8       |
| 40 | 448                             | 392                              | 429                             | 39                              | 295                              | 41.8                      | 103.8       |
| 41 | 577                             | 332                              | 487                             | 46                              | 269                              | 51.7                      | 882.2       |
| 42 | 338                             | 299                              | 260                             | 63                              | 269                              | 27.9                      | 499.0       |
| 43 | 734                             | 539                              | 182                             | 46                              | 126                              | 10.0                      | 225.3       |
| 44 | 334                             | 474                              | 474                             | 65                              | 432                              | 31.8                      | 84.5        |
| 45 | 587                             | 424                              | 404                             | 51                              | 360                              | 31.8                      | 225.3       |
| 46 | 559                             | 510                              | 472                             | 43                              | 332                              | 29.8                      | 225.3       |
| 47 | 715                             | 535                              | 535                             | 48                              | 347                              | 29.8                      | 74.5        |

Table 21 The Subject's Muscle Geometrical Data. Part II.

|    | area<br>muscle<br>(CM*CM) | area<br>SO<br>(CM*CM) | area<br>FO<br>(CM*CM) | area<br>FG<br>(CM*CM) | Porce<br>muscle<br>(N) | Porce<br>SO<br>(N) | Porce<br>FO<br>(N) | Porce<br>FG<br>(N) |
|----|---------------------------|-----------------------|-----------------------|-----------------------|------------------------|--------------------|--------------------|--------------------|
| 1  | 14.27                     | 7.14                  | 2.85                  | 4.28                  | 570.9                  | 285.5              | 114.2              | 171.3              |
| 2  | 18.36                     | 9.18                  | 3.67                  | 5.51                  | 734.6                  | 367.3              | 146.9              | 220.4              |
| 3  | 11.24                     | 0.62                  | 0.25                  | 0.37                  | 49.6                   | 24.8               | 9.9                | 14.9               |
| 4  | 2.14                      | 1.07                  | 0.43                  | 0.64                  | 85.5                   | 42.7               | 17.1               | 25.6               |
| 5  | 18.96                     | 9.48                  | 3.79                  | 5.69                  | 758.6                  | 379.3              | 151.7              | 227.6              |
| 6  | 16.12                     | 8.06                  | 3.22                  | 4.84                  | 644.9                  | 322.5              | 129.9              | 193.5              |
| 7  | 5.12                      | 2.56                  | 1.02                  | 1.54                  | 204.7                  | 102.3              | 40.9               | 61.4               |
| 8  | 8.79                      | 4.39                  | 1.76                  | 2.64                  | 351.5                  | 175.8              | 70.3               | 105.5              |
| 9  | 7.11                      | 3.20                  | 1.07                  | 1.64                  | 284.5                  | 128.0              | 42.7               | 113.8              |
| 10 | 18.30                     | 9.90                  | 2.75                  | 3.66                  | 732.2                  | 366.1              | 109.8              | 146.4              |
| 11 | 4.24                      | 2.33                  | 0.64                  | 0.77                  | 169.9                  | 84.9               | 25.4               | 30.9               |
| 12 | 11.35                     | 6.66                  | 1.70                  | 2.40                  | 453.9                  | 226.9              | 68.1               | 90.2               |
| 13 | 29.36                     | 16.66                 | 4.40                  | 5.81                  | 1174.4                 | 587.2              | 176.2              | 232.3              |
| 14 | 7.47                      | 3.36                  | 1.12                  | 1.33                  | 298.7                  | 134.4              | 44.8               | 119.5              |
| 15 | 5.09                      | 3.55                  | 1.42                  | 1.33                  | 228.3                  | 114.1              | 56.7               | 85.1               |
| 16 | 7.50                      | 2.55                  | 1.10                  | 1.65                  | 283.0                  | 110.0              | 44.0               | 66.0               |
| 17 | 5.35                      | 2.68                  | 1.07                  | 1.61                  | 214.0                  | 107.0              | 42.8               | 64.2               |
| 18 | 16.48                     | 8.24                  | 3.30                  | 4.94                  | 659.3                  | 329.7              | 131.9              | 197.8              |
| 19 | 11.55                     | 5.78                  | 2.31                  | 3.47                  | 462.1                  | 231.0              | 92.4               | 138.6              |
| 20 | 12.70                     | 6.35                  | 2.54                  | 3.81                  | 507.8                  | 253.9              | 101.6              | 152.3              |
| 21 | 10.25                     | 5.13                  | 2.05                  | 3.08                  | 410.1                  | 205.1              | 82.0               | 123.0              |
| 22 | 35.33                     | 17.67                 | 7.07                  | 10.60                 | 1413.3                 | 706.6              | 282.7              | 424.0              |
| 23 | 7.73                      | 5.41                  | 0.77                  | 1.55                  | 309.0                  | 166.3              | 30.9               | 61.8               |
| 24 | 93.38                     | 46.69                 | 14.01                 | 32.68                 | 3735.4                 | 1867.7             | 560.3              | 1307.4             |
| 25 | 9.52                      | 4.76                  | 1.43                  | 3.33                  | 380.6                  | 190.3              | 57.1               | 133.2              |
| 26 | 4.30                      | 2.36                  | 0.64                  | 1.29                  | 171.9                  | 94.5               | 25.8               | 51.6               |
| 27 | 4.80                      | 2.40                  | 0.96                  | 1.44                  | 191.9                  | 95.9               | 38.4               | 57.6               |
| 28 | 54.07                     | 24.33                 | 8.11                  | 21.63                 | 2162.8                 | 973.3              | 324.4              | 865.1              |
| 29 | 47.99                     | 31.20                 | 4.80                  | 12.00                 | 1919.7                 | 1247.8             | 192.0              | 479.9              |
| 30 | 19.35                     | 12.57                 | 1.93                  | 4.84                  | 773.8                  | 503.0              | 77.4               | 193.5              |
| 31 | 147.75                    | 66.49                 | 29.55                 | 51.71                 | 5910.1                 | 2659.6             | 1182.0             | 2068.6             |
| 32 | 87.91                     | 43.96                 | 13.19                 | 30.77                 | 3516.5                 | 1758.2             | 527.5              | 1230.8             |
| 33 | 45.65                     | 22.83                 | 6.85                  | 15.98                 | 1826.1                 | 913.0              | 273.9              | 639.1              |
| 34 | 5.51                      | 2.76                  | 0.83                  | 1.93                  | 220.6                  | 110.3              | 33.1               | 77.2               |
| 35 | 34.50                     | 18.97                 | 5.17                  | 10.35                 | 1379.9                 | 758.9              | 207.0              | 414.0              |
| 36 | 63.36                     | 34.85                 | 9.50                  | 19.01                 | 2534.3                 | 1393.9             | 380.1              | 760.3              |
| 37 | 3.21                      | 1.44                  | 0.48                  | 1.28                  | 128.3                  | 57.7               | 19.2               | 51.3               |
| 38 | 187.15                    | 140.36                | 28.07                 | 18.72                 | 7486.1                 | 5614.6             | 1122.9             | 748.6              |
| 39 | 39.53                     | 27.67                 | 3.95                  | 7.91                  | 1581.1                 | 1106.8             | 158.1              | 316.2              |
| 40 | 50.85                     | 27.97                 | 12.71                 | 10.17                 | 2034.2                 | 1118.8             | 508.5              | 406.8              |
| 41 | 39.85                     | 23.95                 | 3.99                  | 11.98                 | 1596.7                 | 958.0              | 159.7              | 479.0              |
| 42 | 20.08                     | 9.04                  | 3.01                  | 8.03                  | 803.4                  | 361.5              | 120.5              | 321.3              |
| 43 | 5.31                      | 1.86                  | 1.06                  | 2.39                  | 212.3                  | 74.3               | 42.5               | 95.5               |
| 44 | 23.55                     | 9.42                  | 3.53                  | 1.60                  | 942.2                  | 376.9              | 141.3              | 424.0              |
| 45 | 11.93                     | 5.66                  | 2.39                  | 3.58                  | 477.1                  | 238.6              | 95.4               | 143.1              |
| 46 | 12.91                     | 5.16                  | 2.58                  | 5.16                  | 516.5                  | 206.6              | 103.3              | 206.6              |
| 47 | 26.53                     | 13.27                 | 3.98                  | 9.29                  | 1061.3                 | 530.7              | 159.2              | 371.5              |

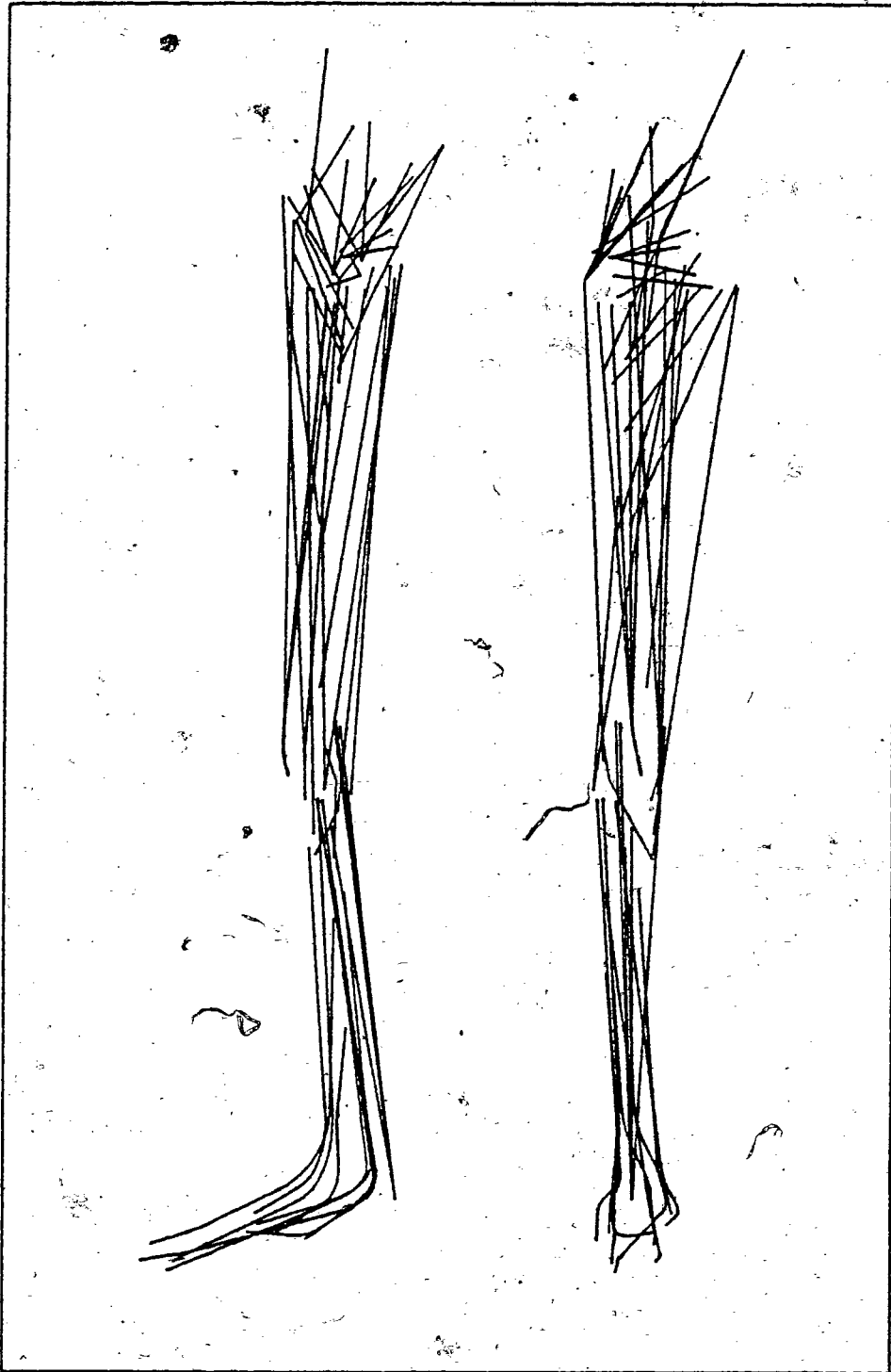


Figure 17 A medial and frontal view of the muscle lines of action as modelled within the subject.

Table 22 Validation of the Model's Estimation of the Total Muscle Mass.

| Cadaver | Muscle Mass (g) |           |
|---------|-----------------|-----------|
|         | Measured        | Predicted |
| 1       | 4574            | 3398      |
| 2       | 6024            | 4183      |
| 3       | 4153            | 2413      |
| 4       | 2901            | 1782      |
| 5       | 5877            | 3656      |
| 6       | 5357            | 3542      |
| 7       | 7923            | 5131      |
| 8       | 4888            | 3411      |
| 9       | 7896            | 5306      |
| 10      | 5489            | 3926      |
|         | mean            | 3675      |
|         | SD              | 1077      |

### During Activity

The movement pattern of the subject's right lower limb was analysed for one complete walking cycle at 200 frames per second. Transformation matrices were used to define the location of each segment relative to the anatomical position for 195 instants during this cycle. The points defining the lines of action of the muscles, the SRS and the centres of mass were therefore defined. The muscle lengths, velocities and moment arms were then calculated from these points. A stick figure representation of the subject's right lower limb during the walk is shown in Figure 18.

The stride time and length, calculated from right heel contact to right heel contact, were 0.975 s and 1.473 m, respectively, and right toe off occurred at 62 percent of the stride cycle.

# KINEMATICS OF THE WALK

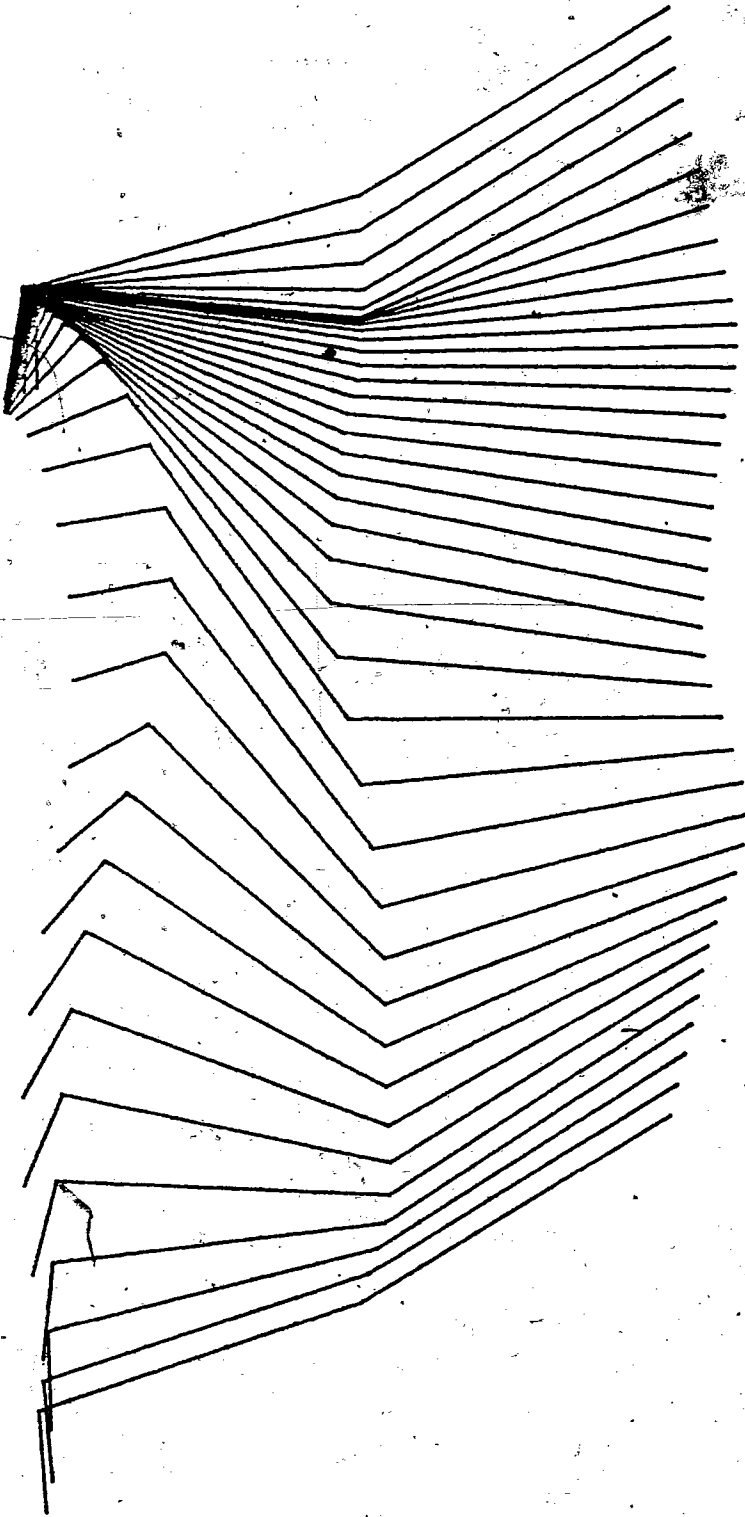


Figure 18 The kinematics of the walk, right heel contact to right heel contact.

## MUSCLE KINEMATICS

As demonstrated in Chapter III, the length and velocity of a muscle has a profound effect on the amount of force that can be generated by it. Therefore, it is of interest to examine the length and velocity changes of the muscles during the gait cycle. These values are presented in Figures 19 and 20. All curves begin and end at right heel contact.

Frigo and Pedotti (1977) report the sagittal plane length changes of 11 major locomotor muscles during level walking. Their results compare quite well with those of Figure 19 both in magnitude and pattern even though they did not consider the muscle length changes in the coronal or transverse planes. This was not surprising since the greatest angular changes at the joints occur in the sagittal plane. The results of the present investigation also compare well to those reported by Grieve *et al.* (1978) who examined the length changes in gastrocnemius during level walking.

It is interesting to compare the muscle velocities (Figure 20) with the maximum fibre lengths ( $\hat{L}^F$  given in Table 20) since in Chapter III it was shown that the maximum rate of fibre shortening is proportional to the fibre length. For the parallel fibred muscles the mean (standard deviation) maximum concentric and eccentric fibre velocities were 0.43 (0.17) and 0.46 (0.18)  $\hat{L}^F \text{ s}^{-1}$ , respectively. These results substantiate those reported by Hardt (1978). Therefore, it seems likely that during normal walking the slow twitch fibres rarely exceed their maximum rate of intrinsic shortening ( $V_0$ , which equals  $1.0 \hat{L}^F \text{ s}^{-1}$ ) during concentric contractions. For the pennate muscles the velocities were 1.17 (0.55) and 1.07 (0.50)  $\hat{L}^F \text{ s}^{-1}$ , respectively. This suggests that if these muscles were recruited during the phases of maximal concentric velocities the slow twitch fibres would exert no force. However, muscles tend to be inactive during these conditions (Morrison, 1970).

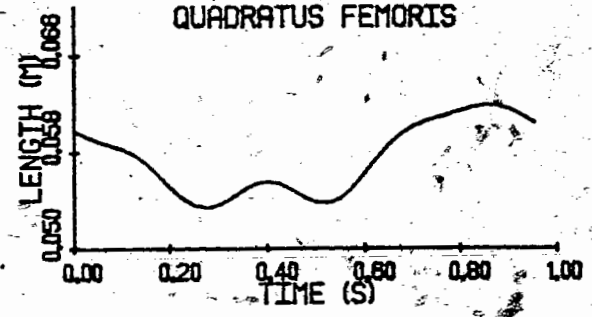
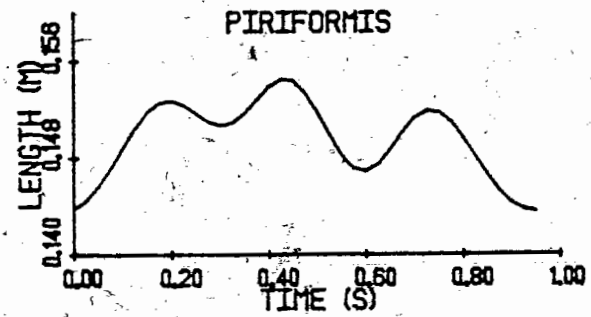
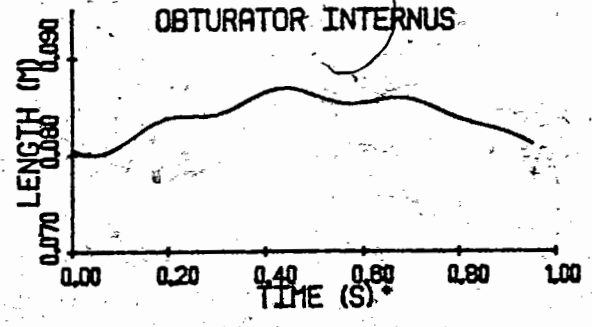
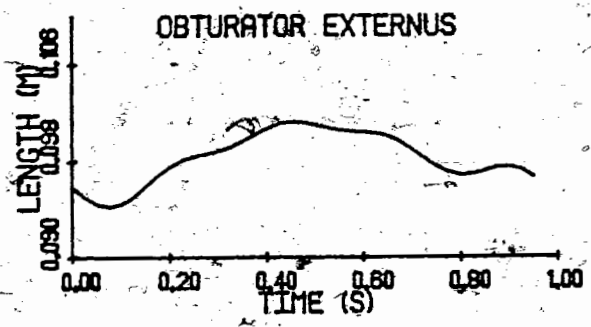
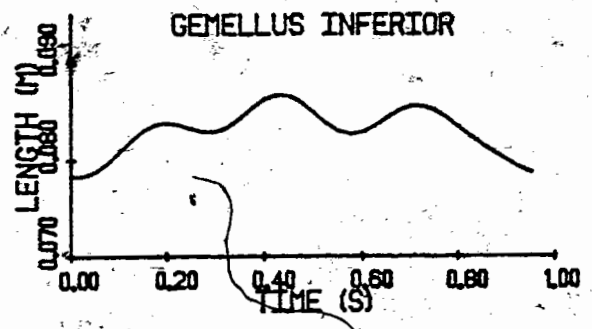
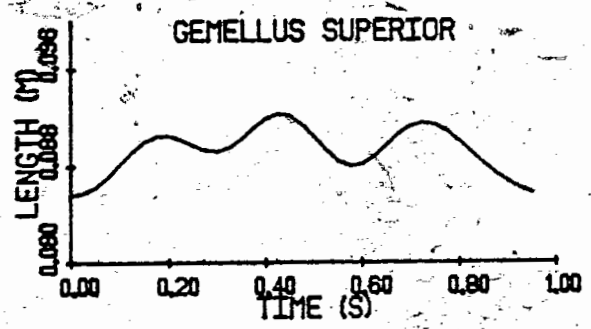
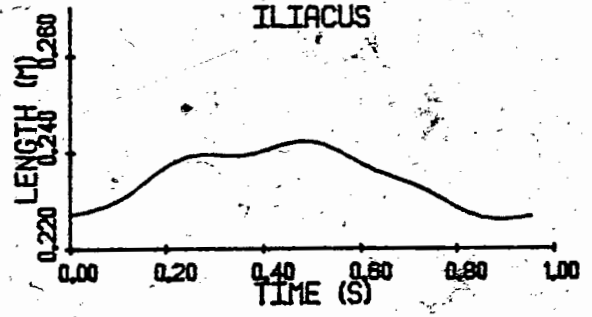
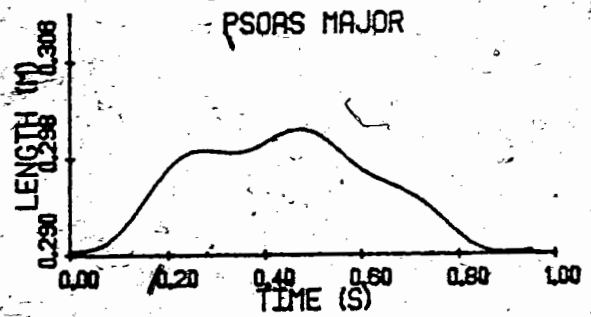


Figure 19 The muscle lengths during the walking cycle.

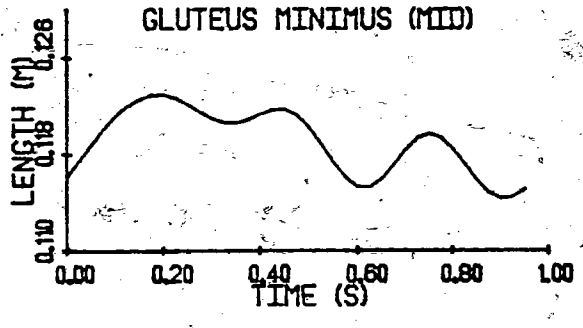
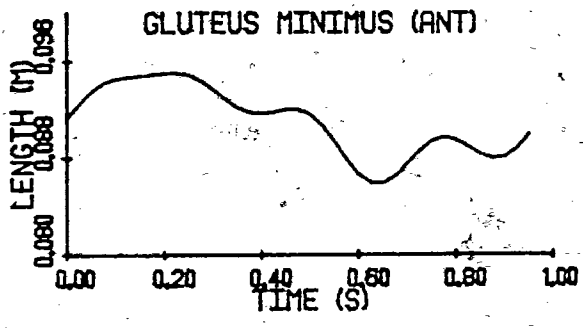
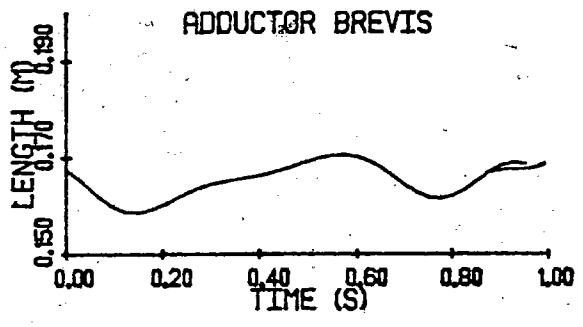
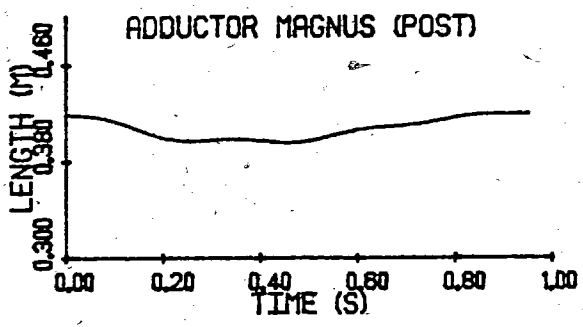
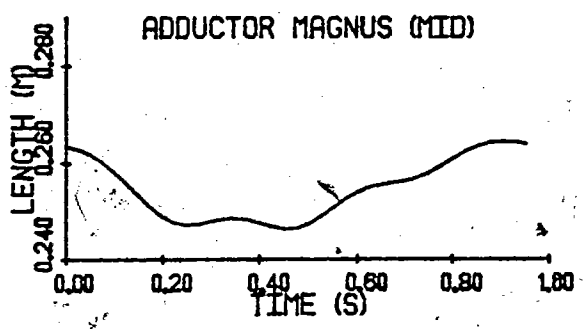
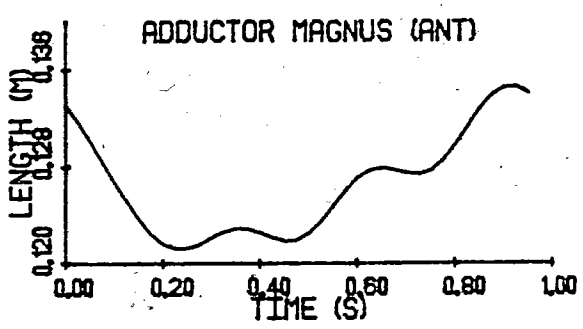
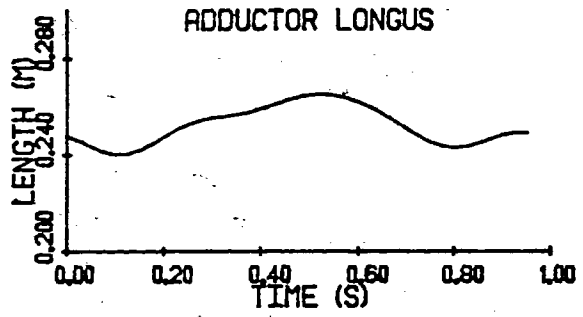
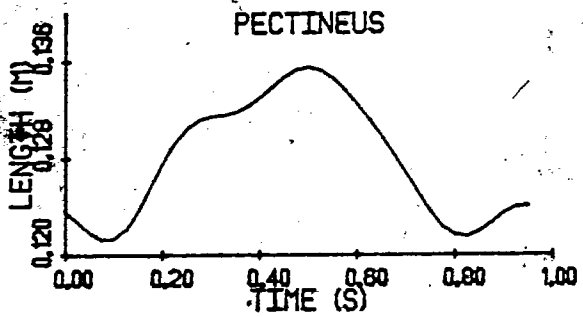


Figure 19 Continued.



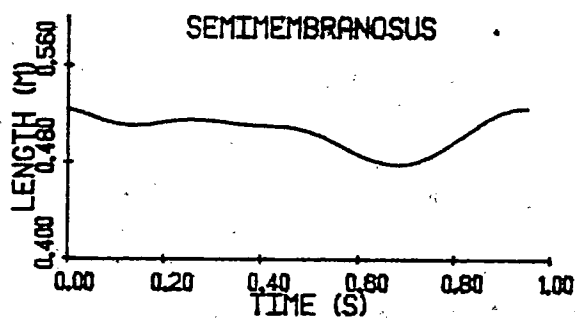
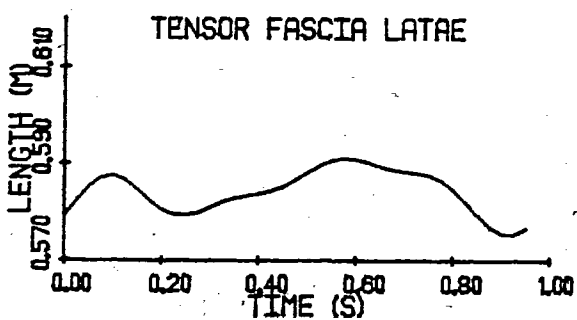
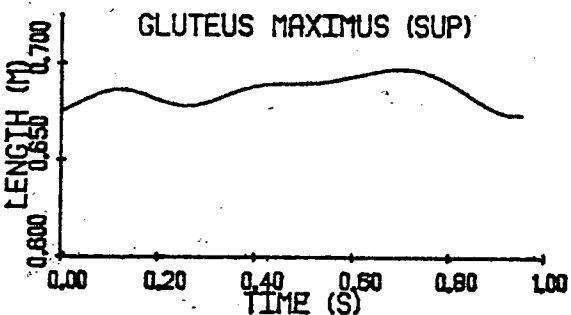
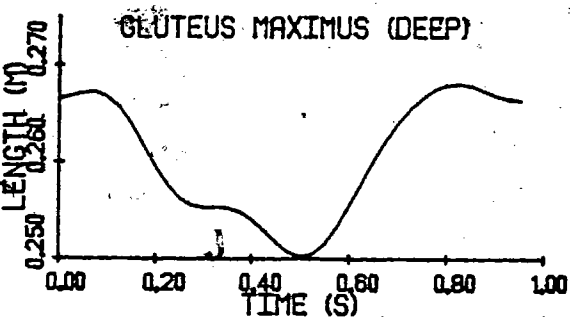
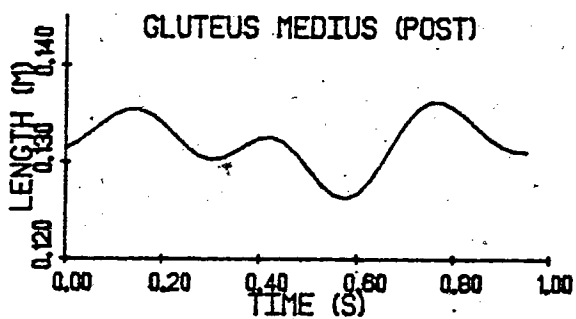
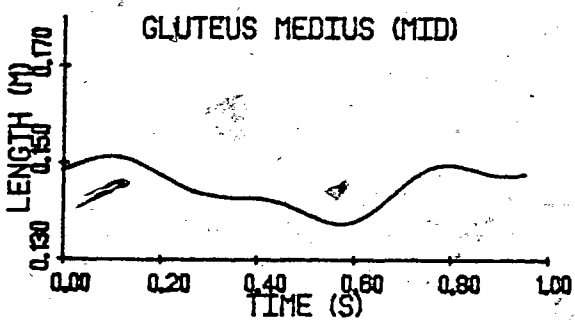
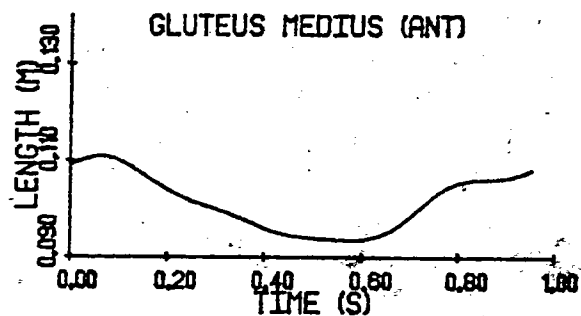
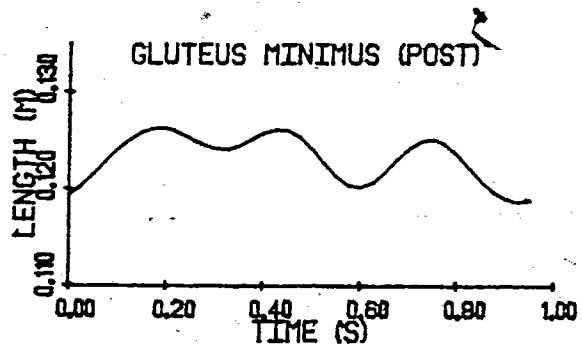


Figure 19 Continued.

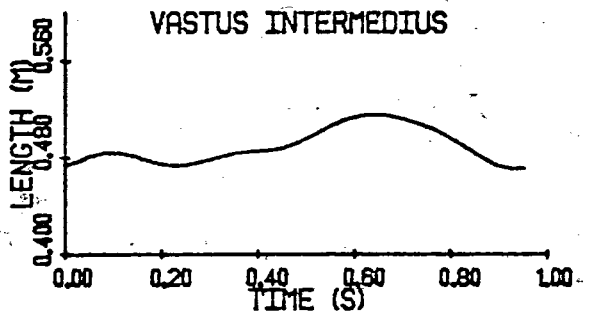
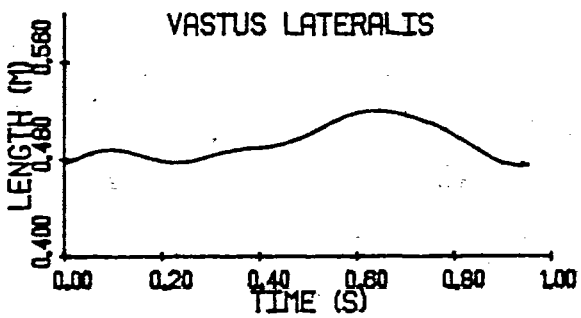
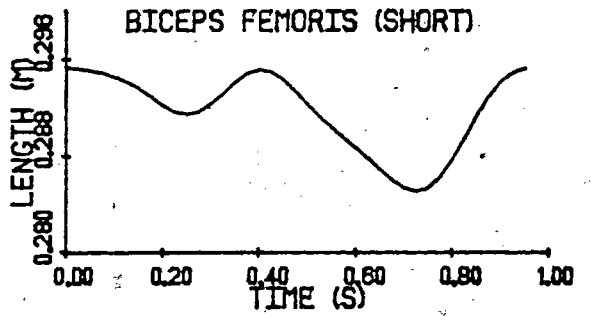
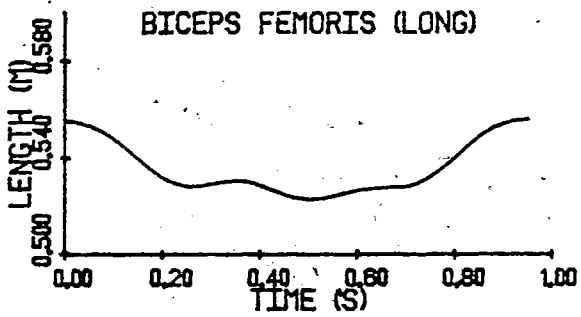
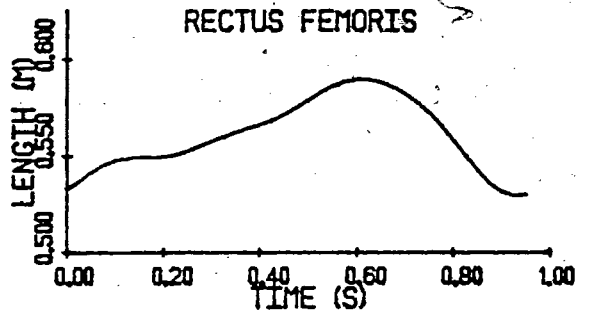
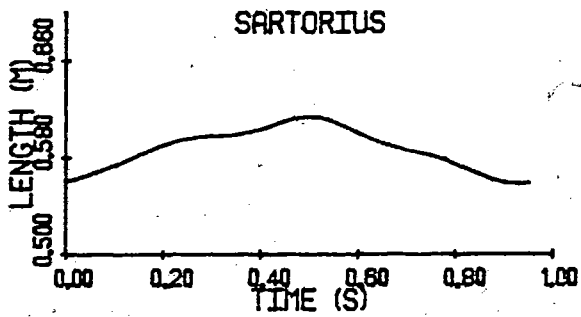
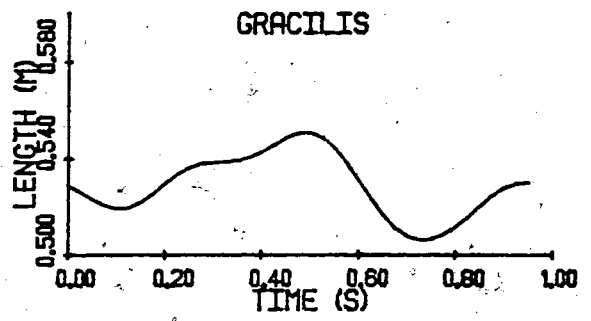
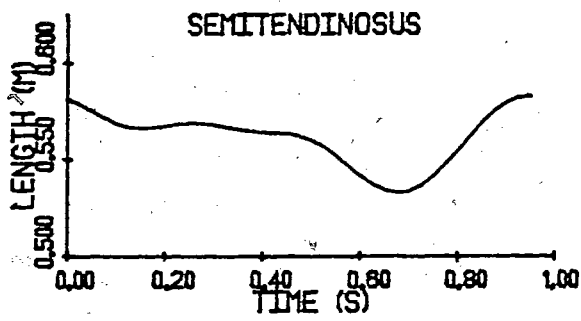


Figure 19

Continued.

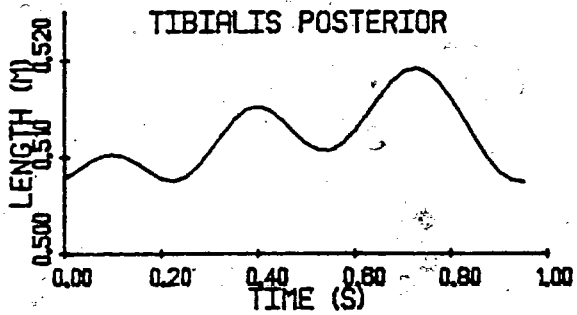
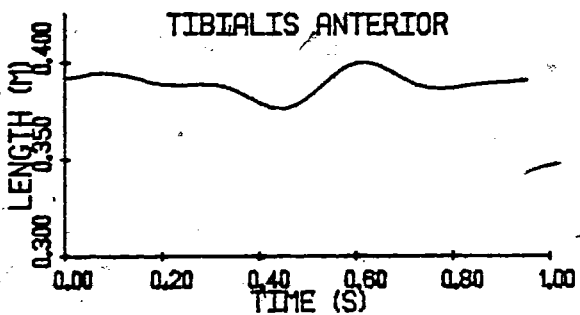
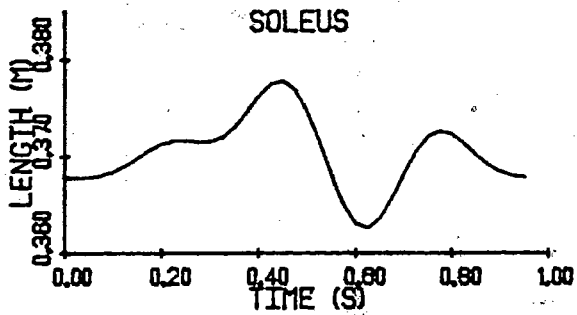
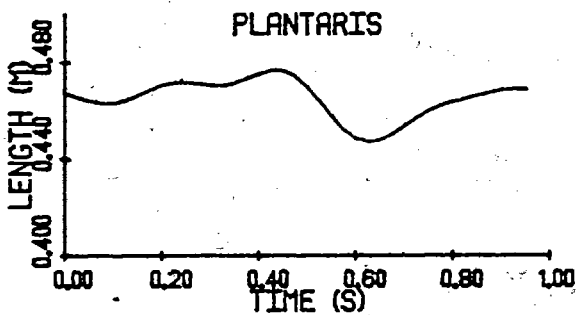
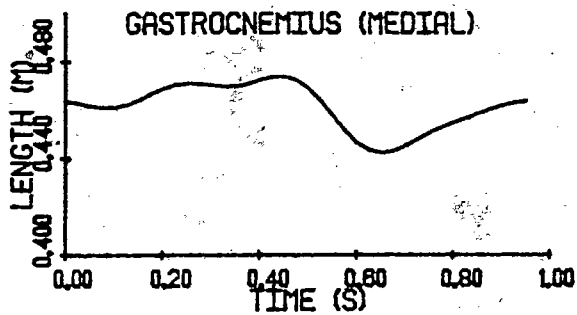
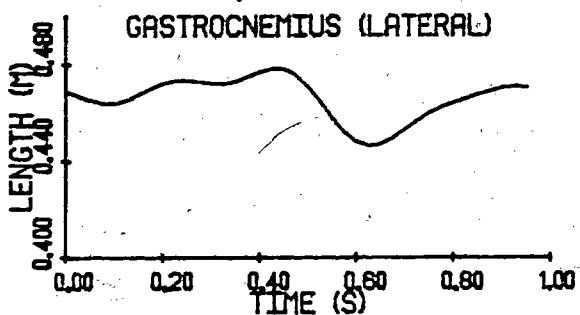
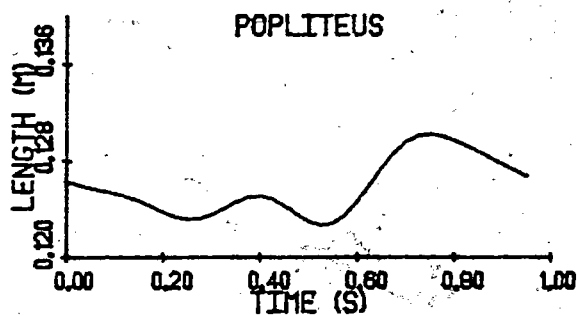
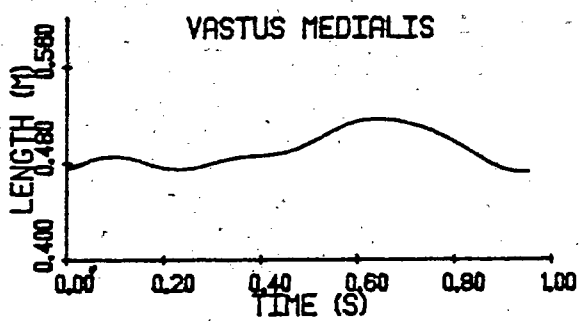


Figure 19

Continued.

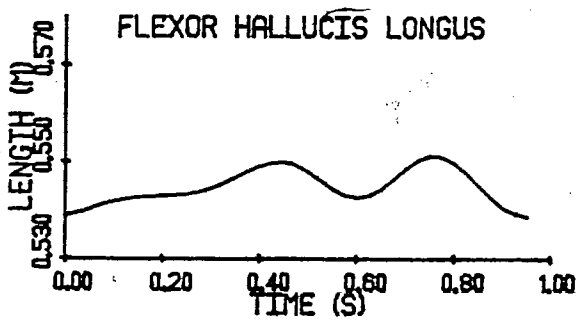
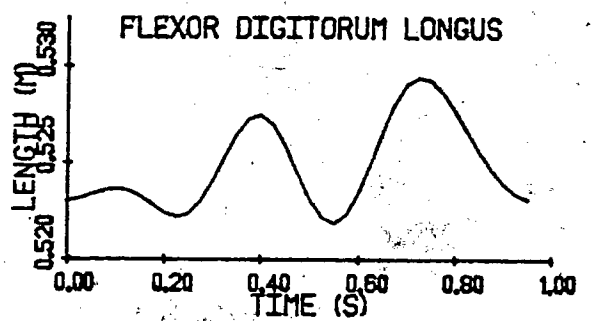
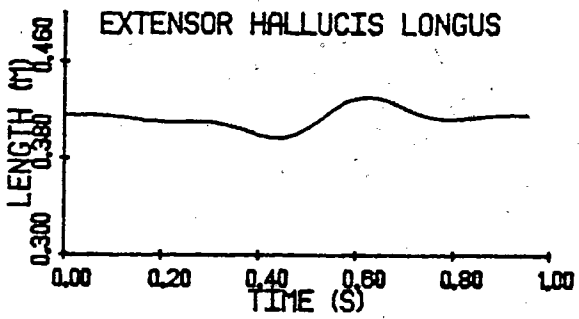
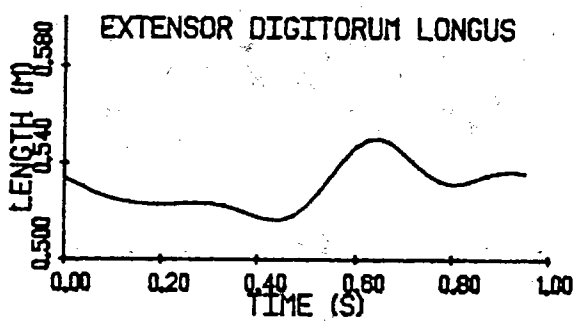
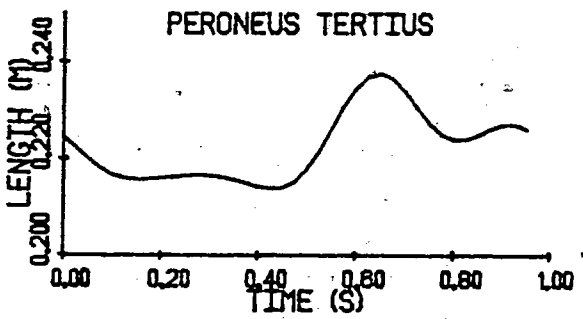
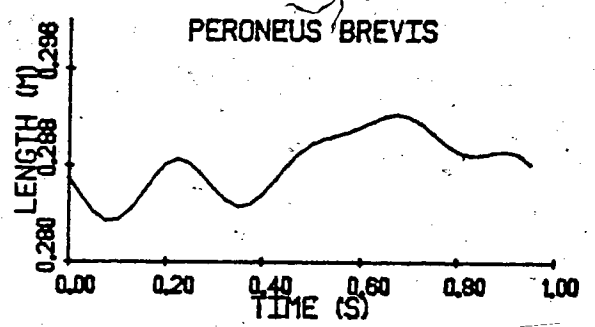
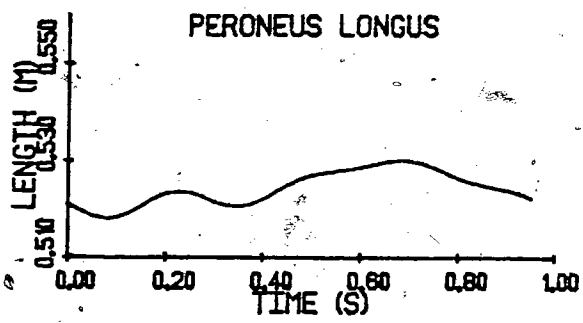


Figure 19 Continued.

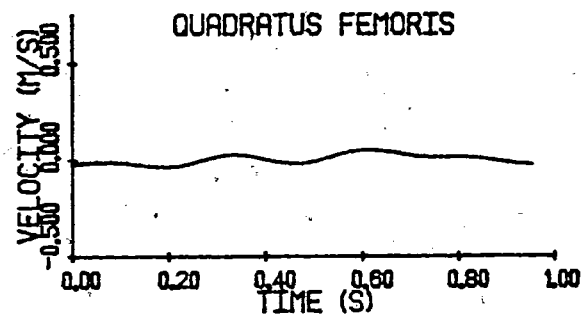
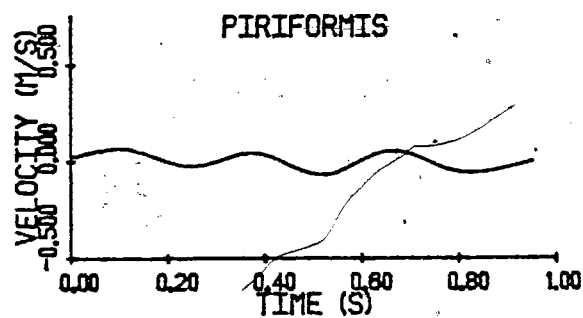
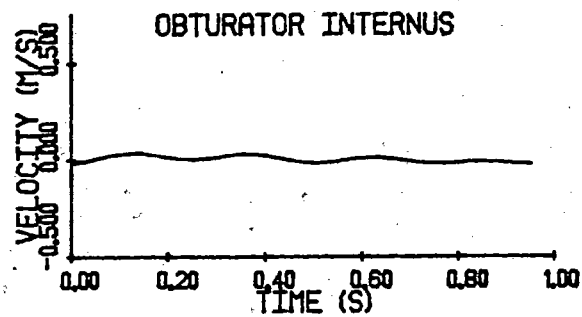
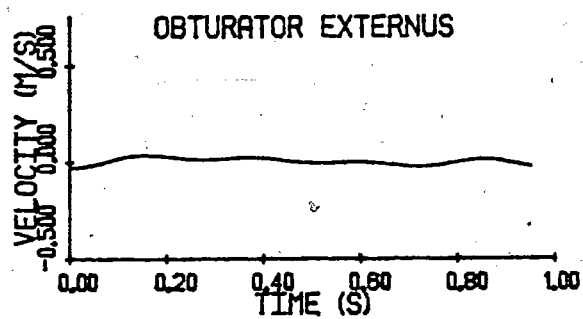
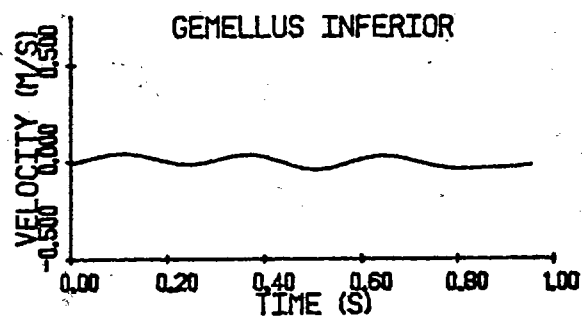
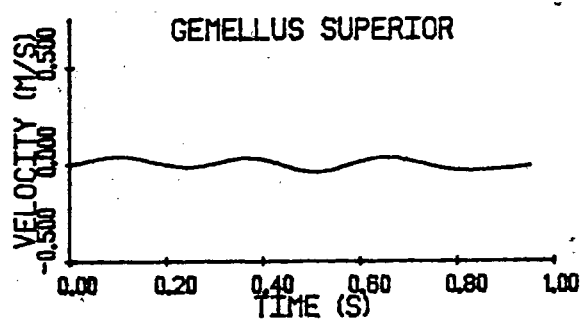
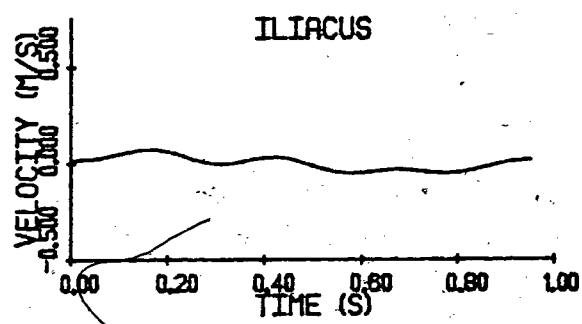
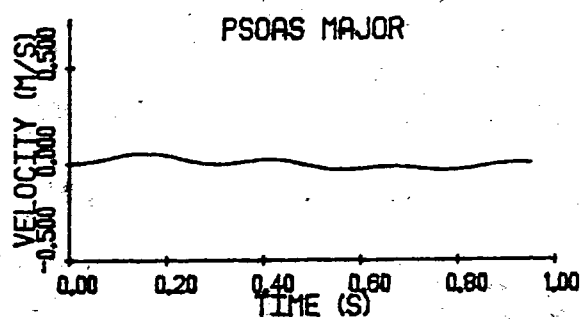


Figure 20 The muscle velocities during the walking cycle.

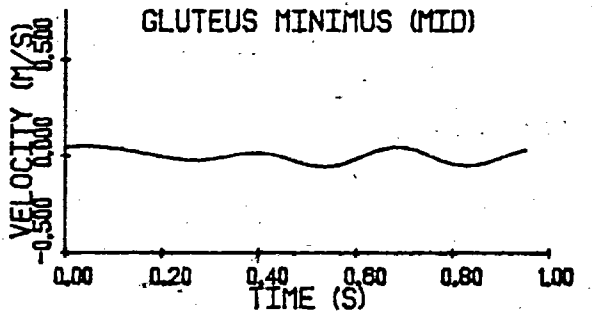
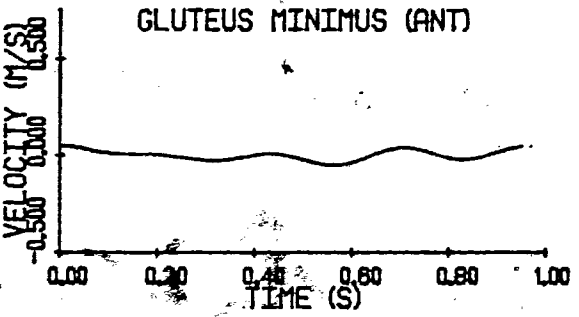
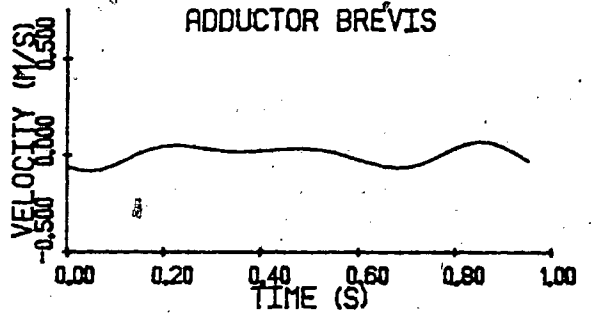
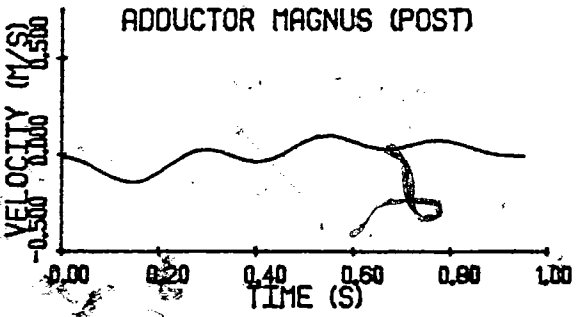
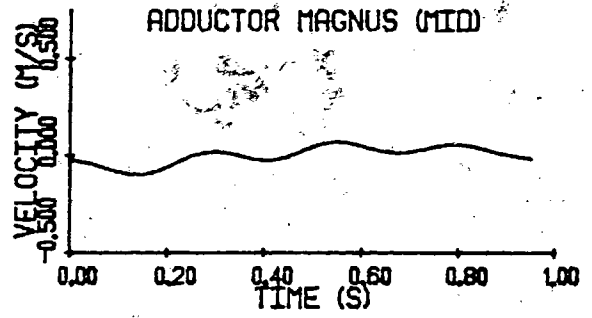
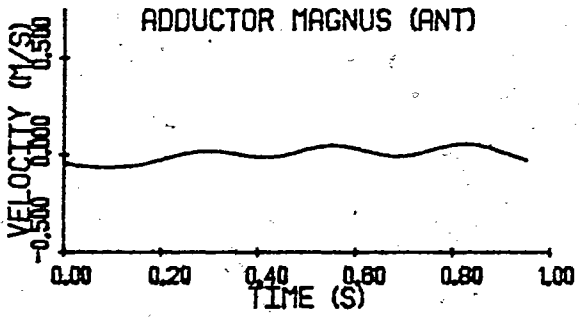
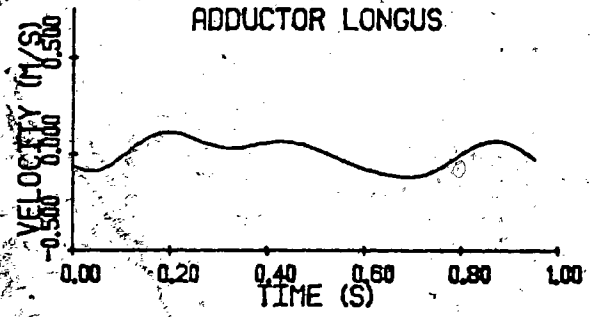
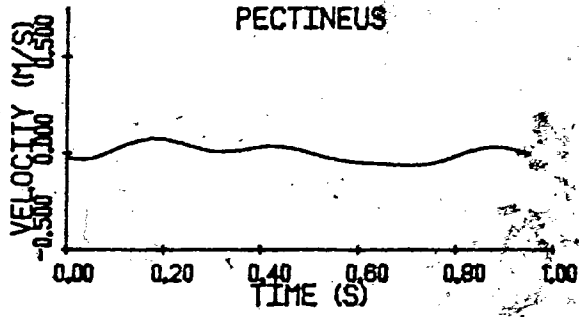


Figure 20

Continued.

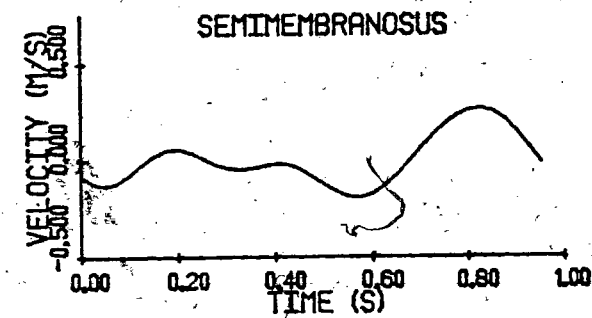
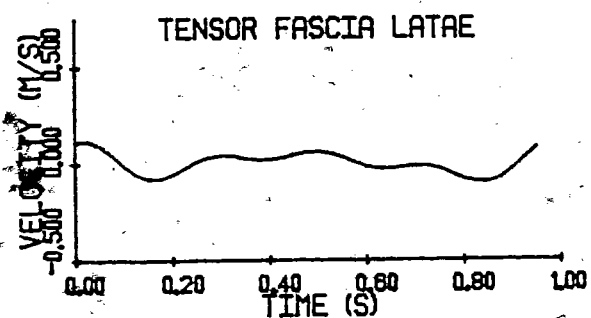
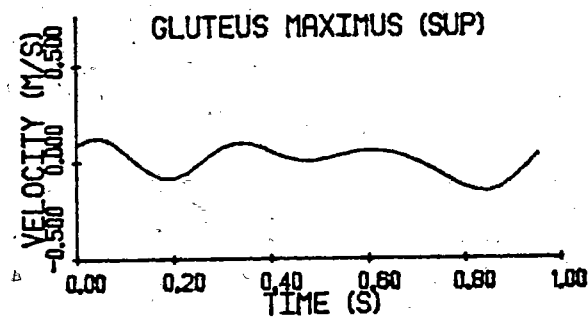
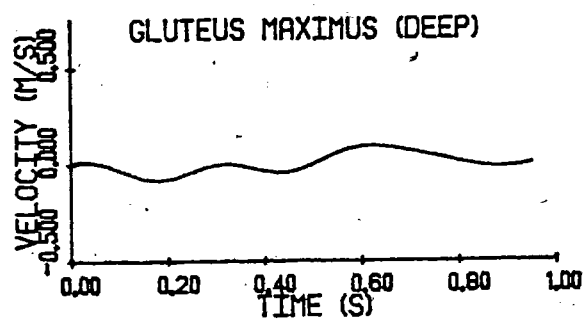
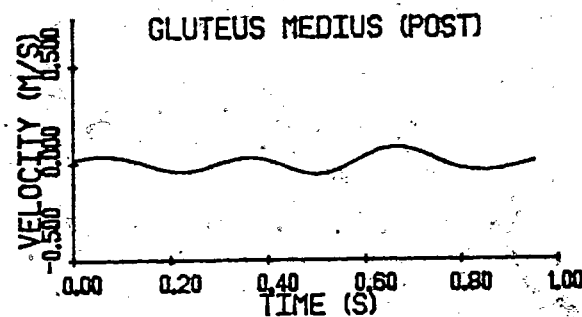
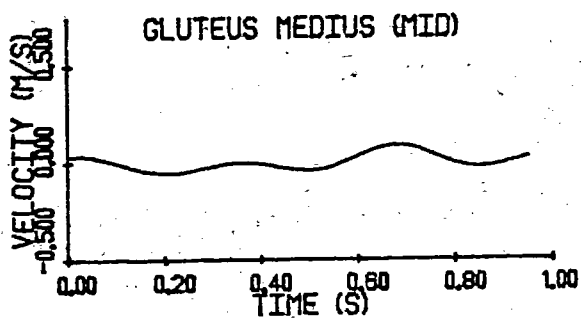
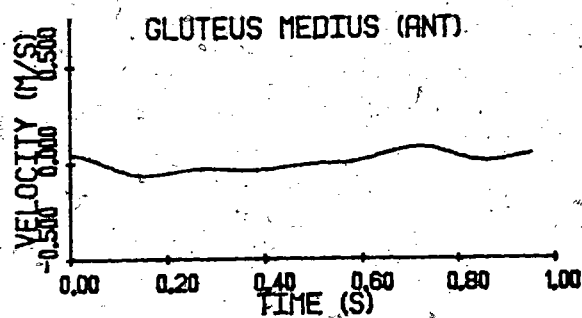
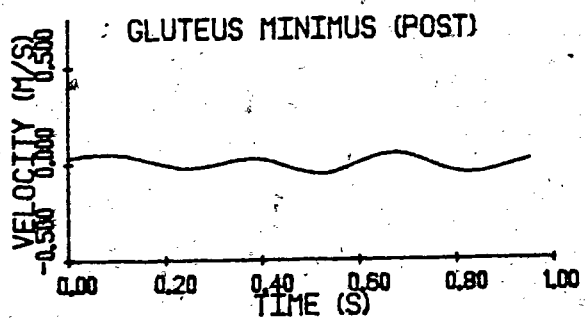


Figure 20 Continued.

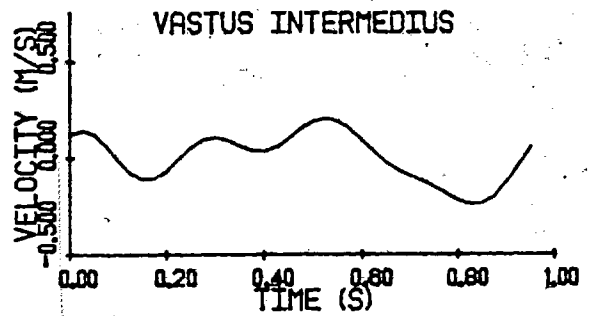
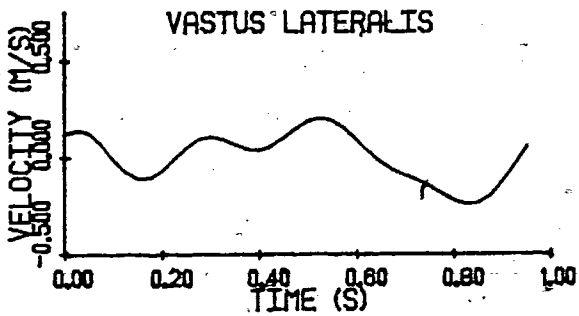
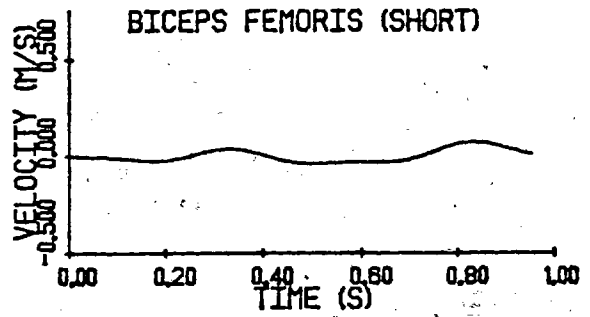
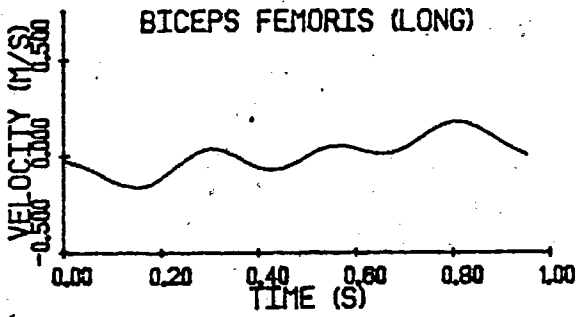
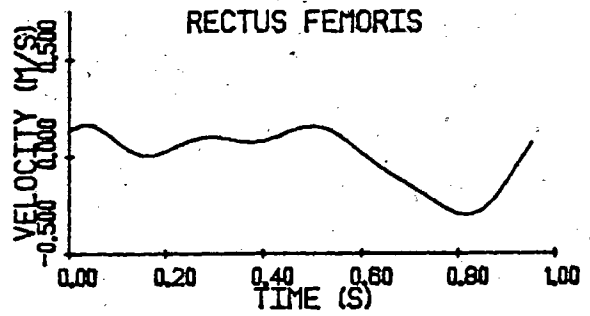
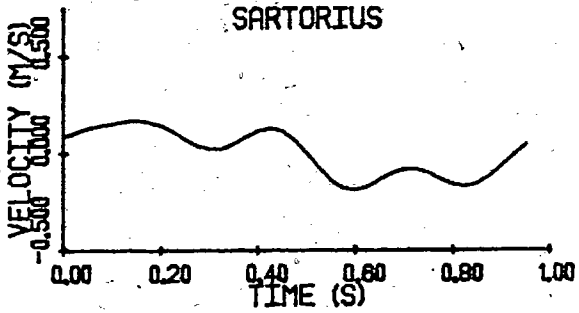
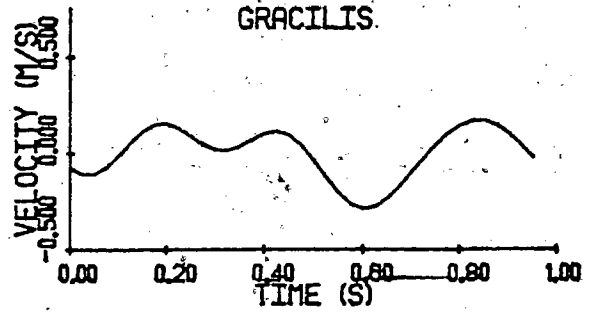
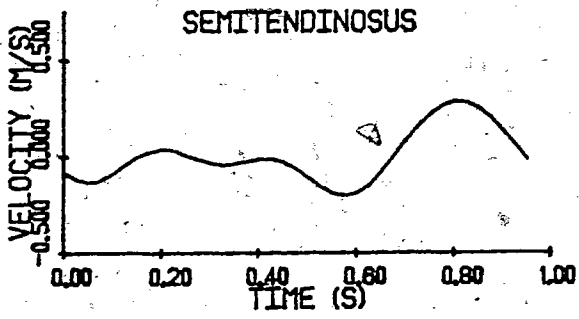


Figure 20 Continued.



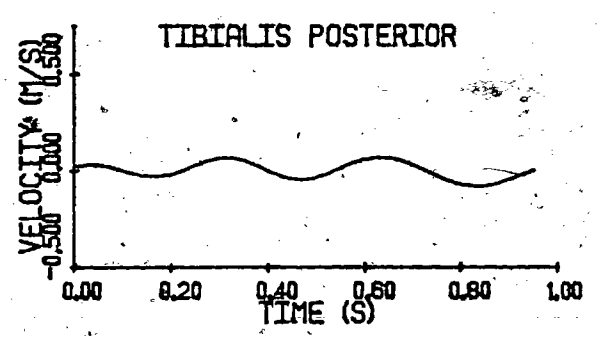
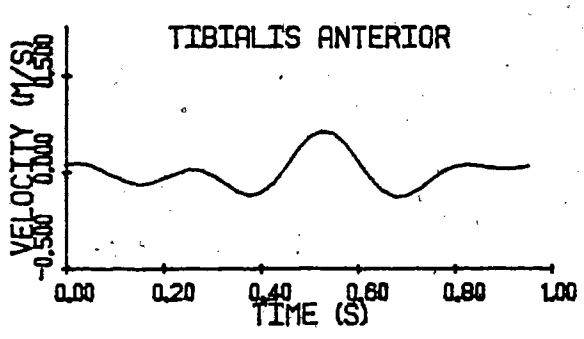
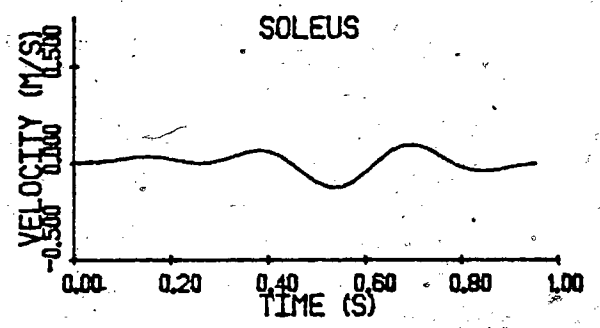
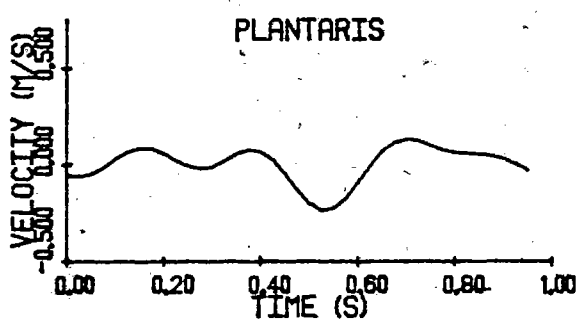
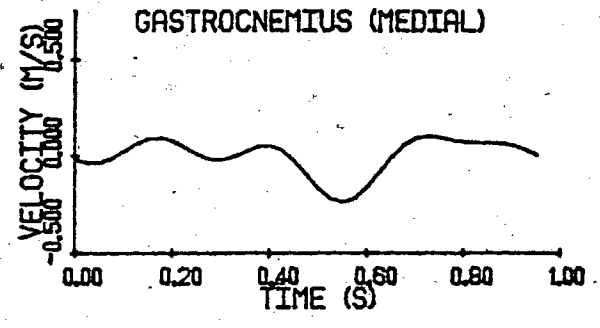
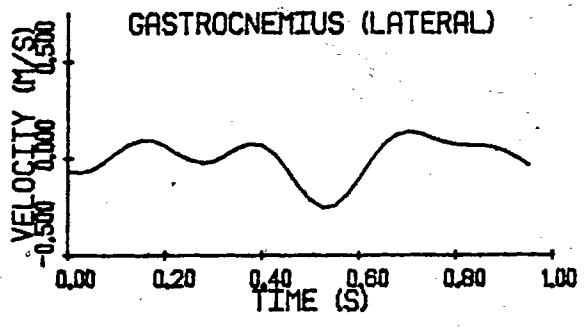
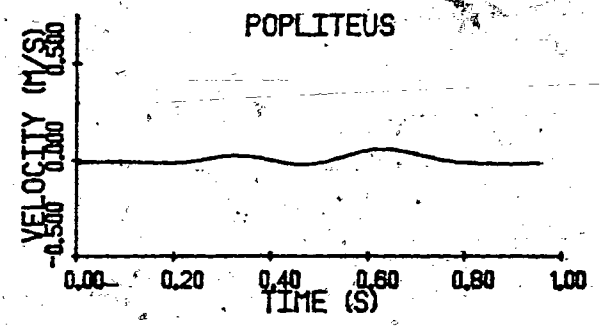
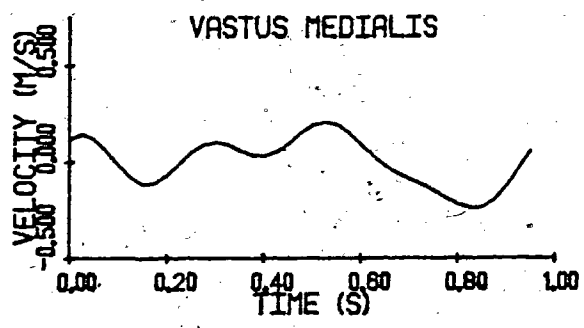


Figure 20 Continued.

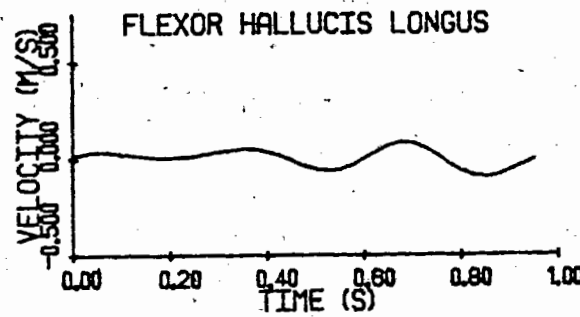
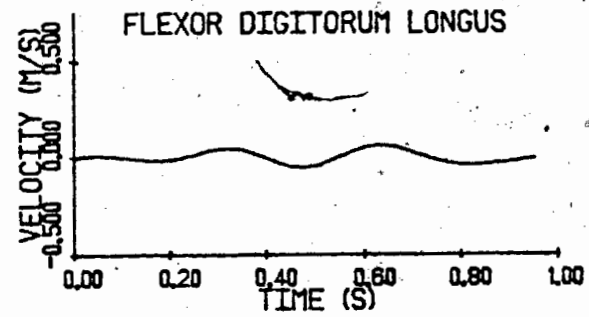
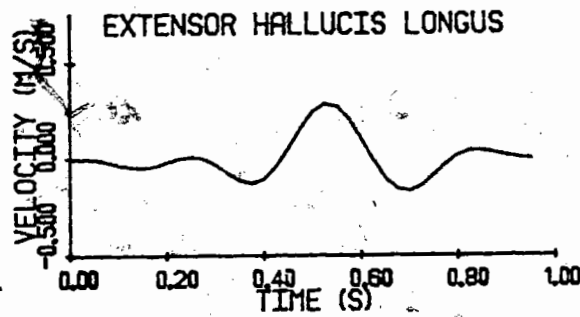
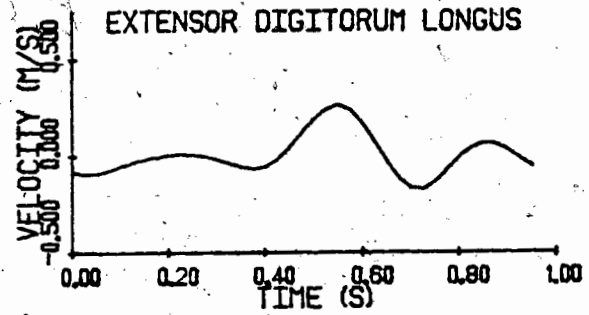
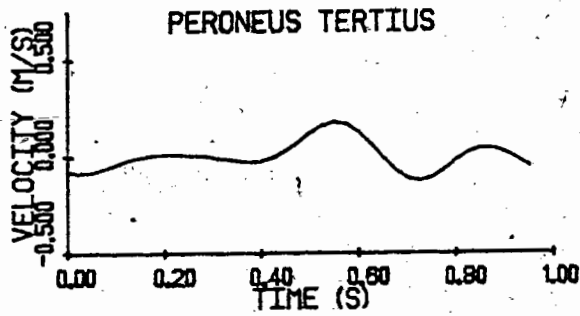
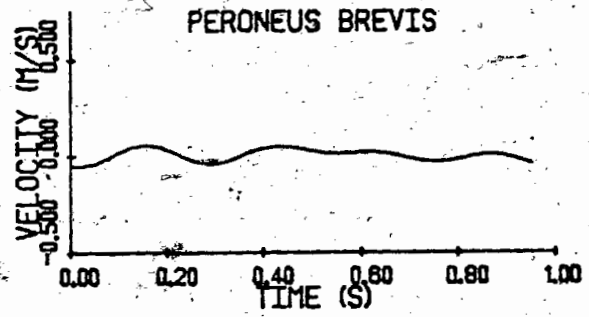
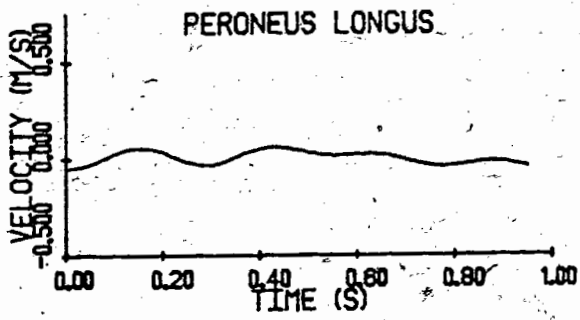


Figure 20 Continued.

### NET MUSCLE MOMENTS

The joint reaction forces and the net muscle moments relative to the GRS are plotted in Figures 21 and 22. These were compared to the works of Bresler and Frankel (1950) and Paul (1974) who determined similar values. Since the present analyses include the inertial contribution towards the moment about the long axis of the leg, a constituent not included in the above works, differences were noted but were of small magnitude. Note that each curve begins and ends at right heel contact and that the stride time was 0.975 s of which the latter 38 percent was the swing phase.

The X-components of moment at the hip, knee and ankle joints demonstrate the effect of man's bipedal form of locomotion. Abductive muscle moments are required during single support to prevent the subject from falling towards the unsupported side. As pointed out by Bresler and Frankel (1950) the large abduction moment at the hip is overlooked when sagittal plane analyses are performed.

The Y-components of moment are of small magnitude and indicate the twisting moments (torques) at the joints. The hip demonstrates the largest moment due to the added influence of the thigh. At heel contact a medial rotary moment followed by a lateral rotary component during foot flat was evident at all the joints. This is due to the rotation of the trunk relative to the leg during gait (Eberhart et al., 1954).

The Z-components of moment are of the largest magnitude since they are responsible for man's progression. At the hip a large extensor moment exists at heel contact. This is to retard the motion of the lower limb to make ready foot contact. This is followed by a flexor moment, peaking just before right toe off, to accelerate the limb for the swing phase.

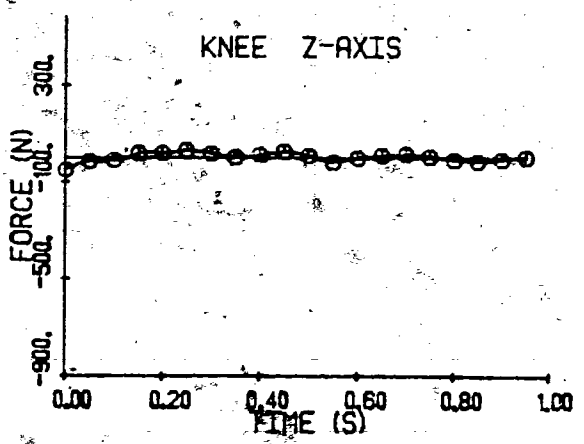
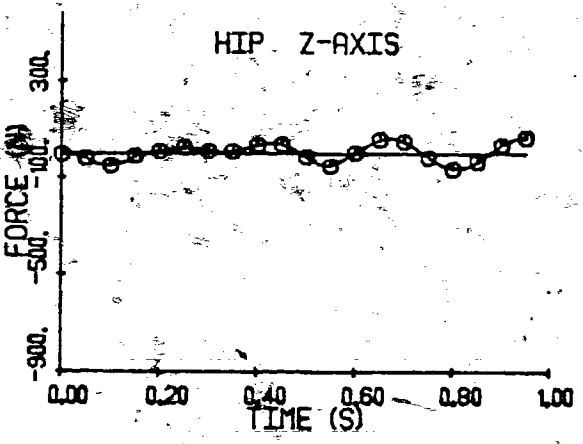
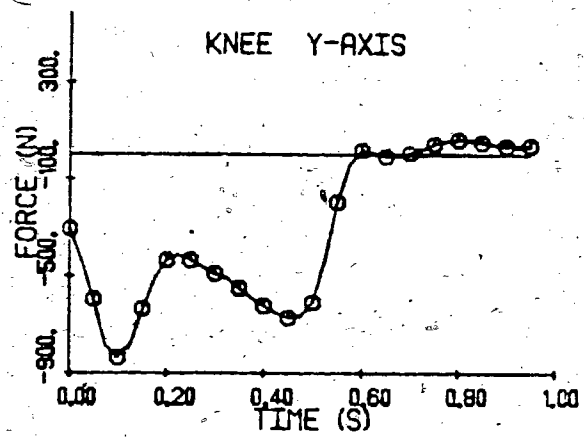
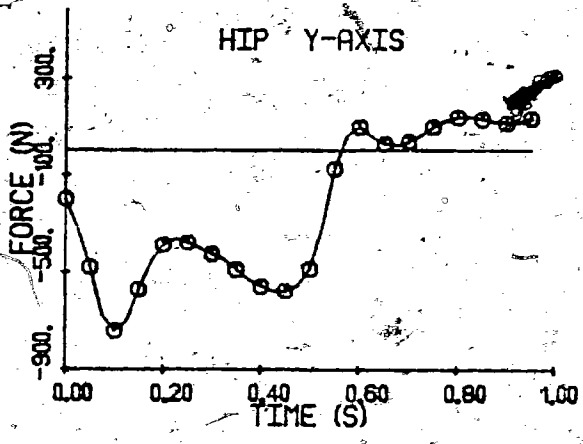
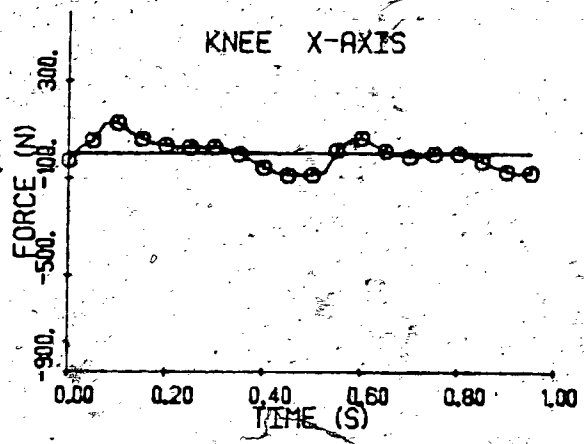
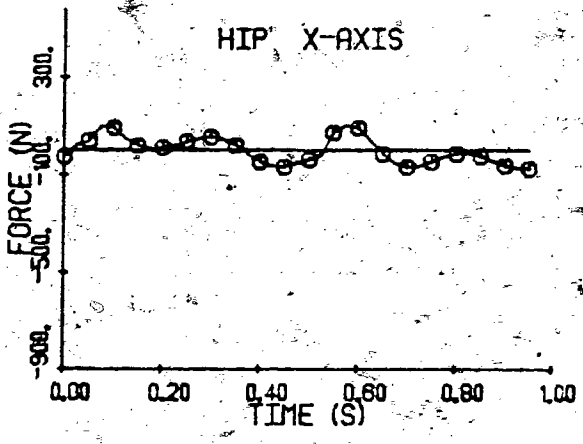


Figure 21 - The joint forces in the global reference system.

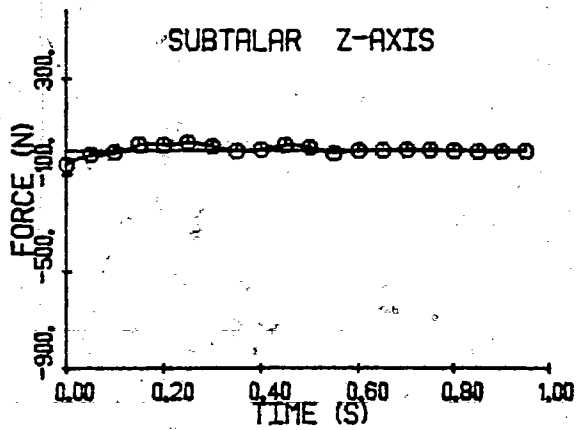
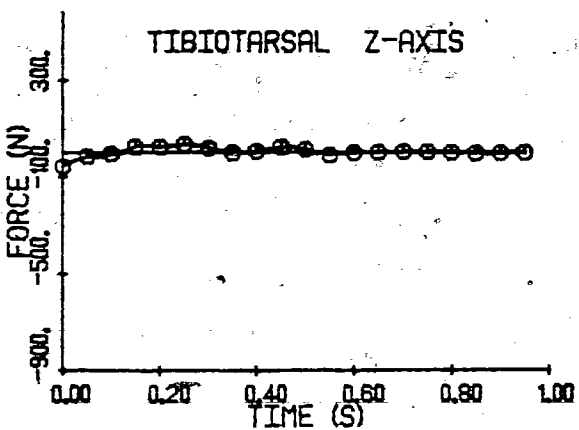
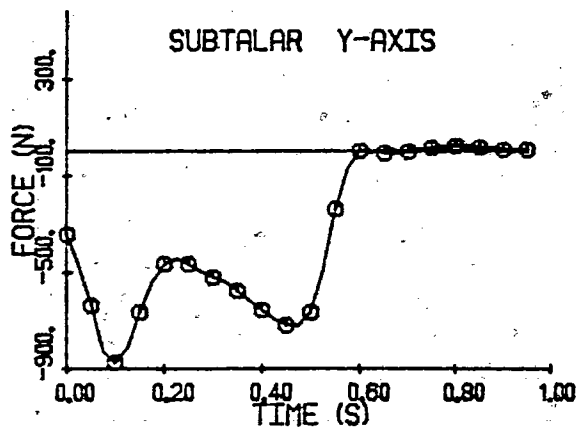
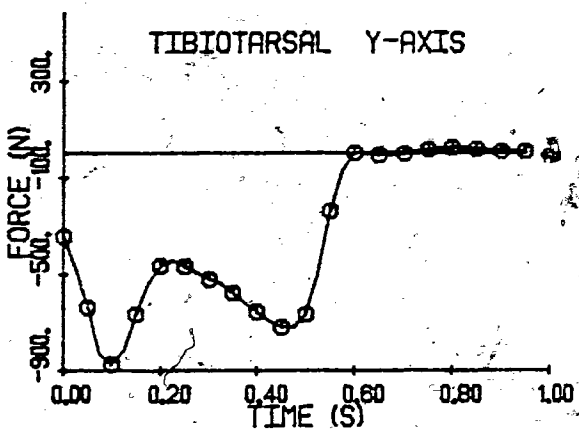
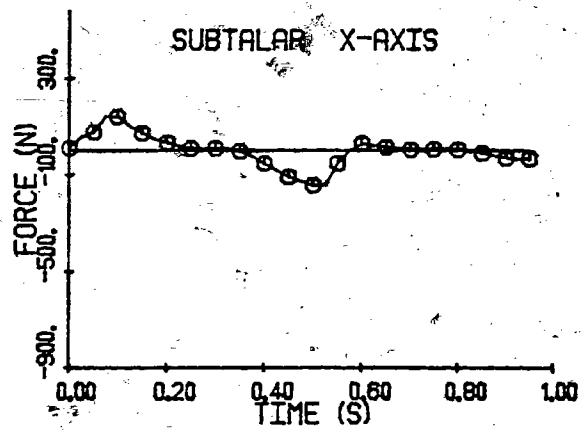
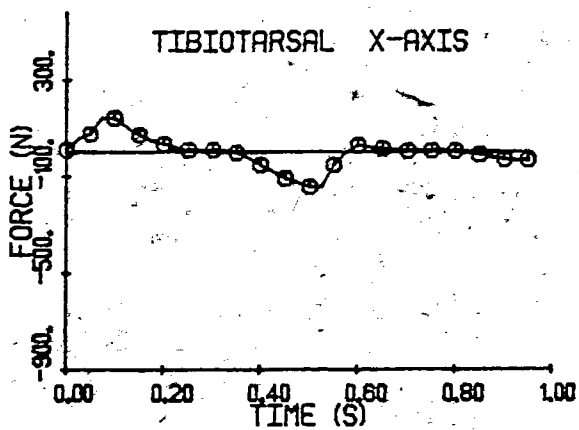


Figure 21 Continued.

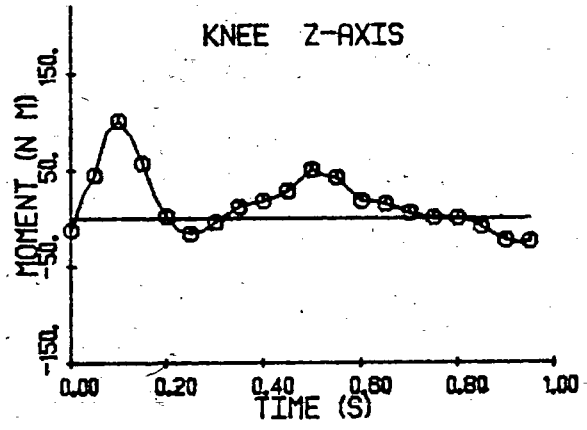
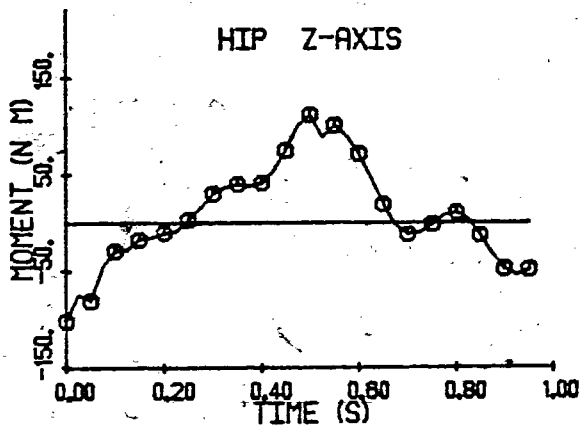
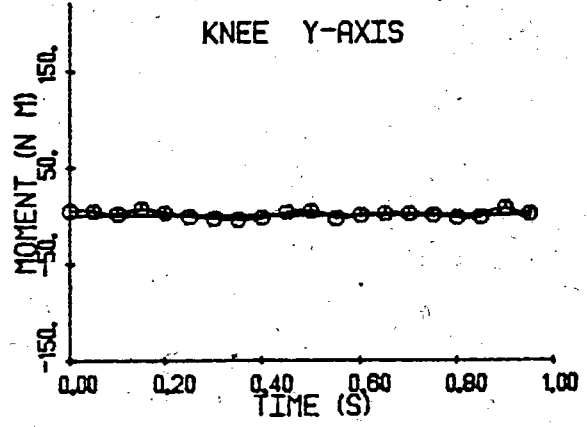
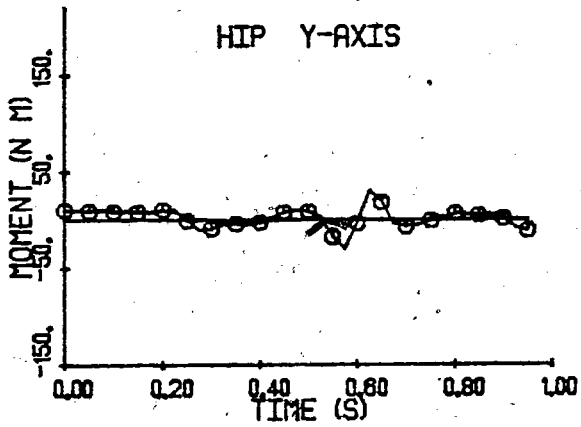
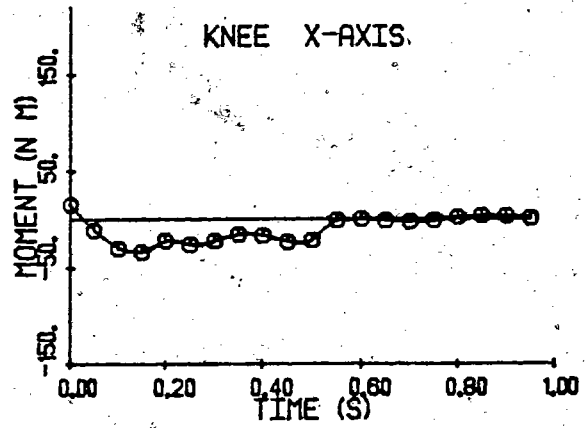
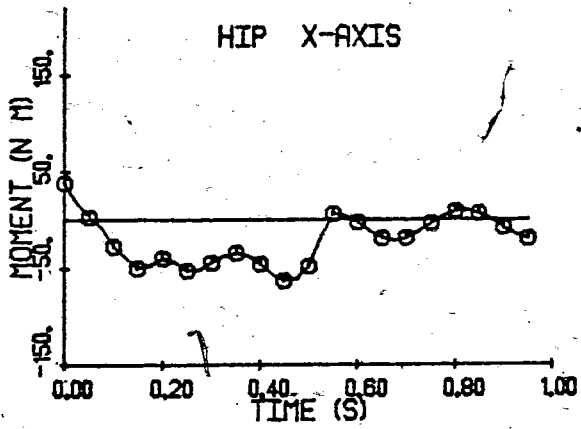


Figure 22 The net muscle moments in the global reference system.

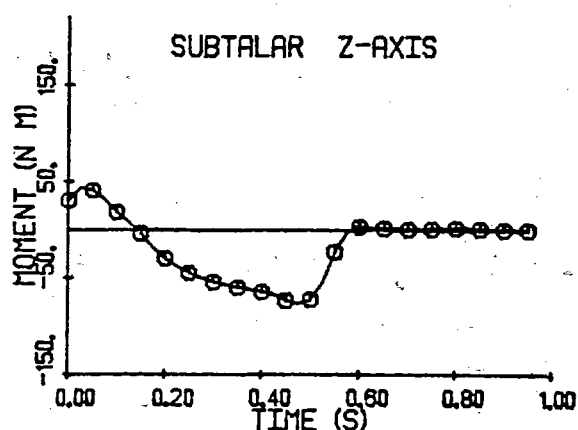
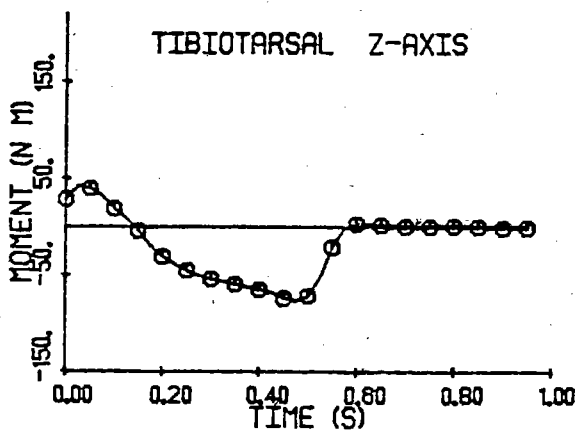
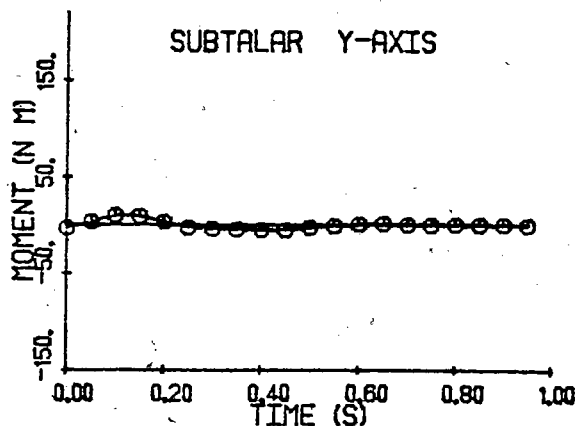
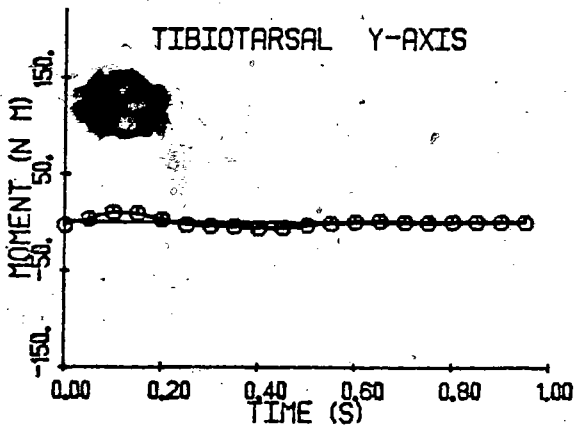
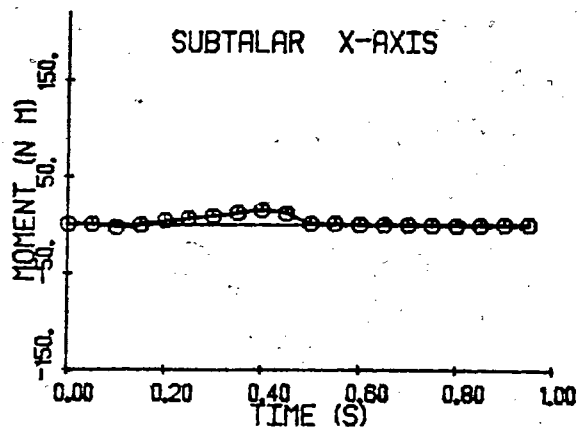
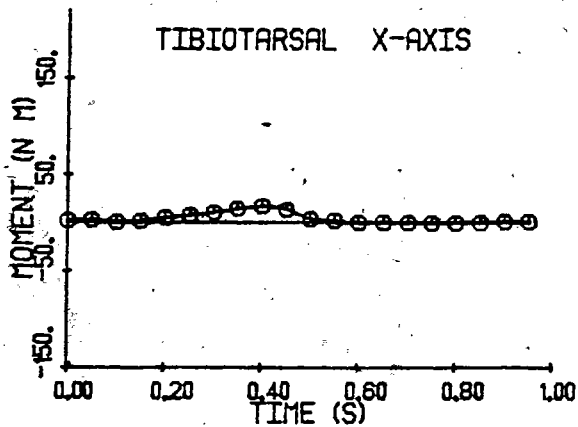


Figure 22 Continued.

A review of the knee moment curves in the literature by Winter (1980) demonstrated inconsistent results. However, nothing abnormal about the gait patterns of the subject's examined were reported. A few generalities about the form of the curves can be made to which the present values conform. Following heel contact and prior to toe off a moment tending to extend the knee exists. This is not surprising since the knee must be stabilized to support the weight of the body. Only during foot flat and part of the swing phase, is the knee unlocked (flexed). Bresler and Frankel (1980) remark that these actions permit the subject to move forward with a minimal raising of his/her centre of mass. This leads to the beneficial result of decreased energy expenditure.

At the ankle the flexion-extension moment is consistent to that reported by previous investigators. A positive moment is required just after heel contact to prevent the foot from slapping the ground. The latter part of the stance phase is extensive -- the triceps surae are active to lift and propel the body forward.

The results of the computation of the net muscle moments relative to the SRS are given in Figure 23. These values were used to calculate the muscle forces. As expected these net muscle moment curves are similar to those calculated about the GRS but take into account the spatial position of the segments.

#### MODEL RESULTS

In this section the major results of the thesis are presented. The muscle forces during a normal walk and an estimation of the actual neural input to each muscle are given. In addition, the response of selected muscles to maximal stimulation are plotted.



### Response of Some Muscles to Maximal Stimulation

Figure 24 shows the normalized force profile of eight muscles maximally stimulated from 10 to 70 ms. These muscles were chosen since they represent a variety of geometries - parallel and pennate, long and short tendons, and a variety of fibre type distributions.

Examining the response of the individual fibre types separately these exhibit the well known force outputs for fast and slow mammalian muscles (Bahler et al., 1968; Close, 1964; Hatze, 1977a; Norris, 1961; Wilkie, 1950). This was expected since the model was based on results obtained by these authors. However, the response of the total muscle to a step input of stimulation does not demonstrate the smooth increase in force as shown in the literature. A change in slope is evident when the fast twitch fibres reach near maximal force. The model's failure is due to the fast and slow twitch fibres being synchronously stimulated, each of which has different mechanical properties. Improved model prediction would result if a population of fibres (motor units) were asynchronously stimulated to smooth out the rise in force profile. In the present application, that of predicting muscle forces during normal gait, if one assumes that the fast twitch fibres are infrequently recruited the predicted and actual force deviation would be small.

### Muscle Forces During the Walk

The total muscle force and the force estimated to be generated by each of the modelled fibres using the physiological model are plotted in Figure 25. All curves begin and end at right heel contact which defines one walking stride. The 'boxes' on some plots represent those phases in the gait cycle for which EMG activity has been shown to be present (University of California, 1953).

The force profiles obtained for most muscles compare well to the EMG activity when one considers that the EMG activity precedes the muscle tension by approximately 80 ms (University of

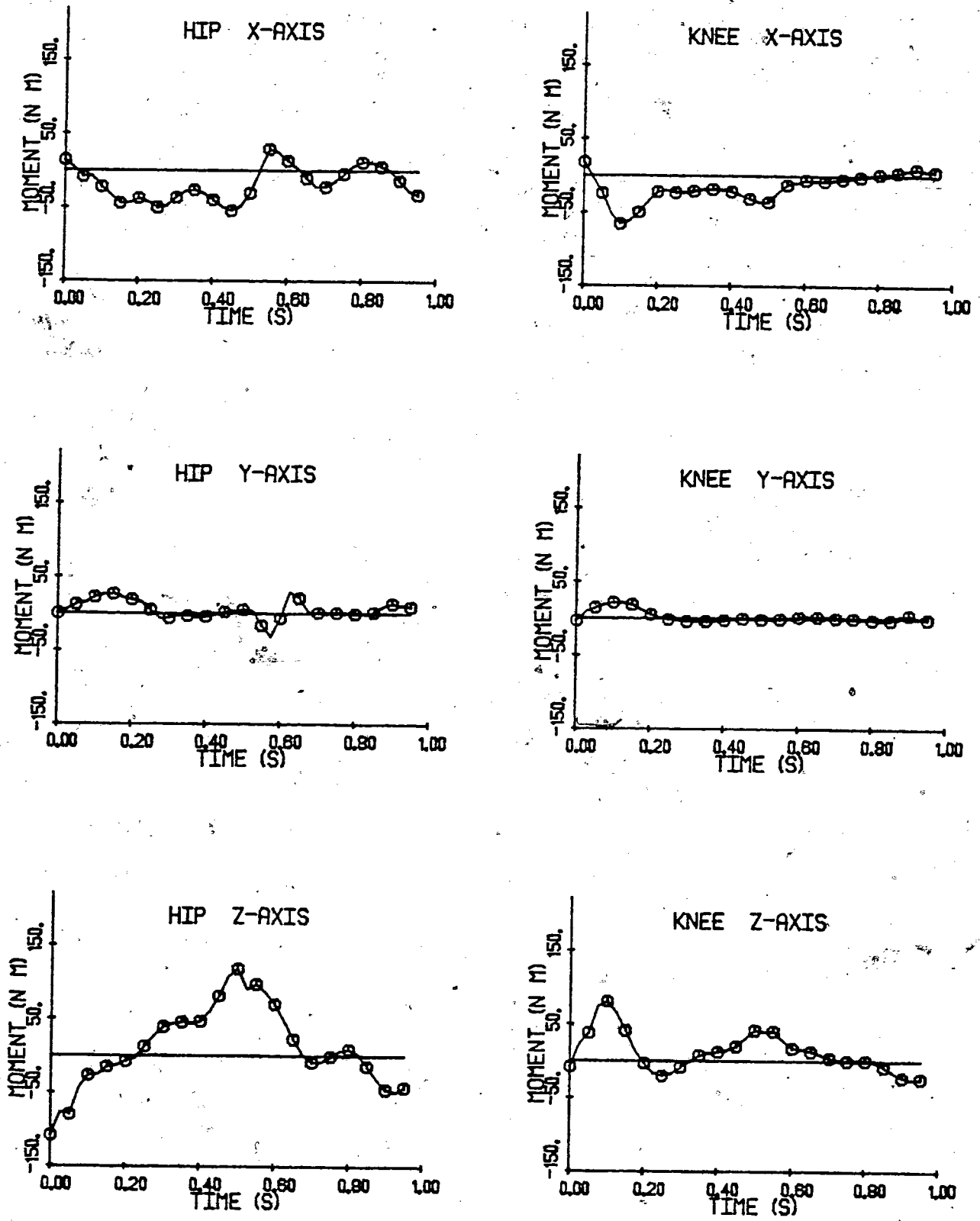


Figure 23 The net muscle moments in the skeletal reference system.

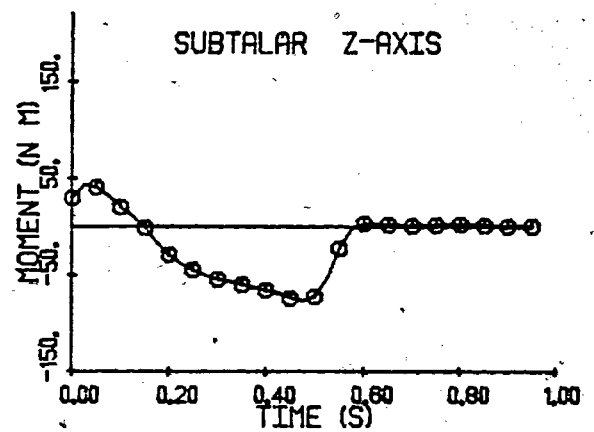
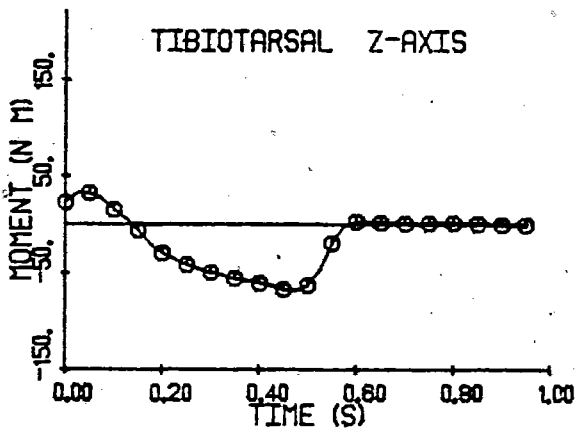
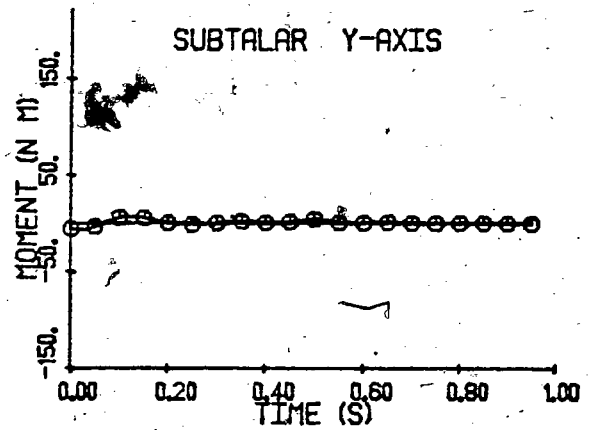
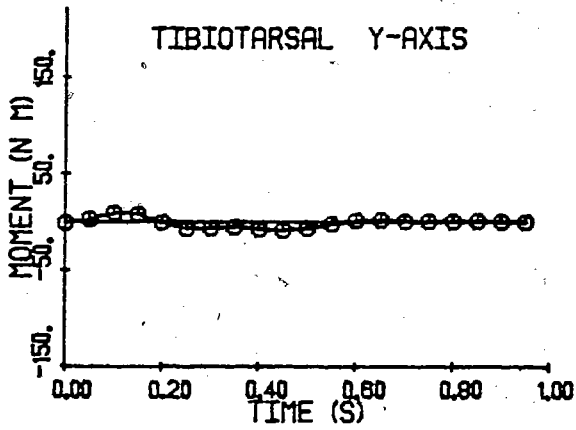
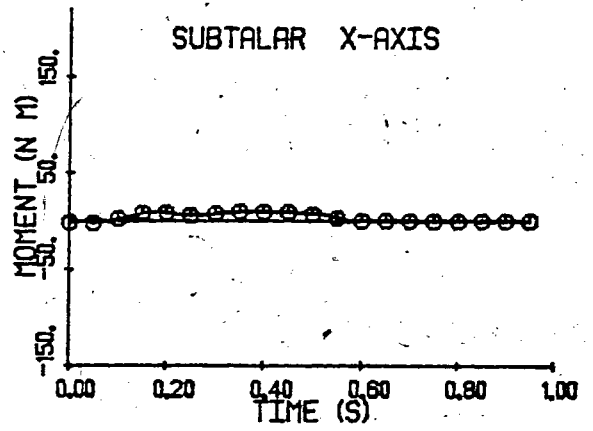
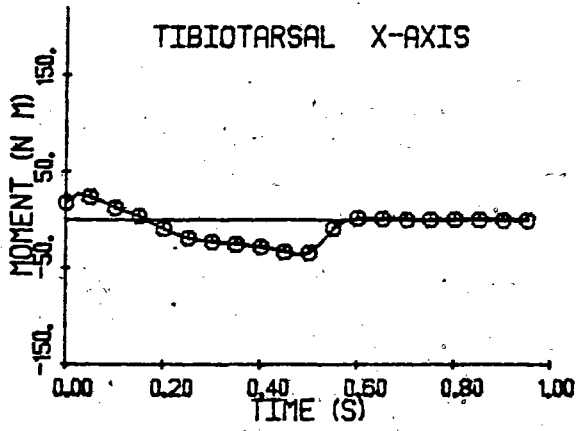


Figure 23 Continued.

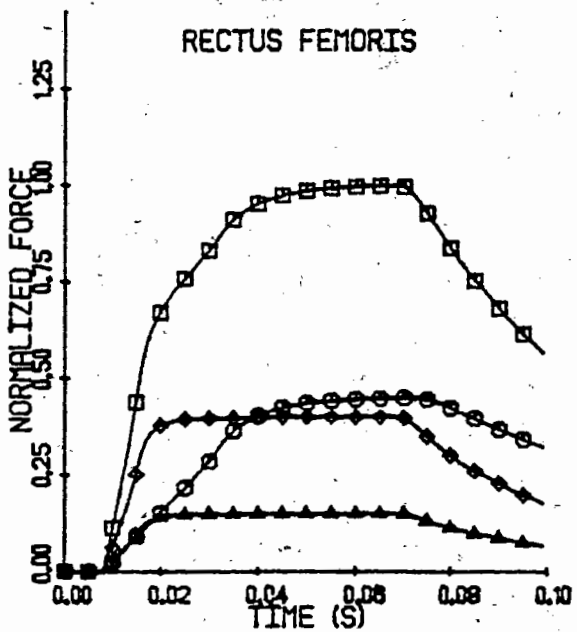
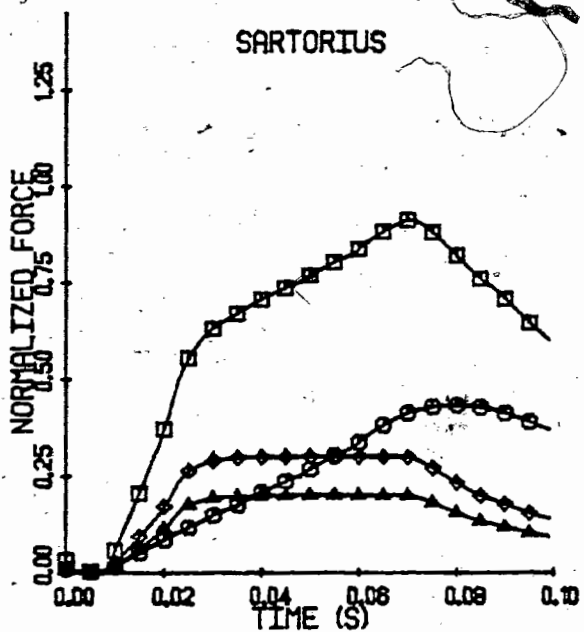
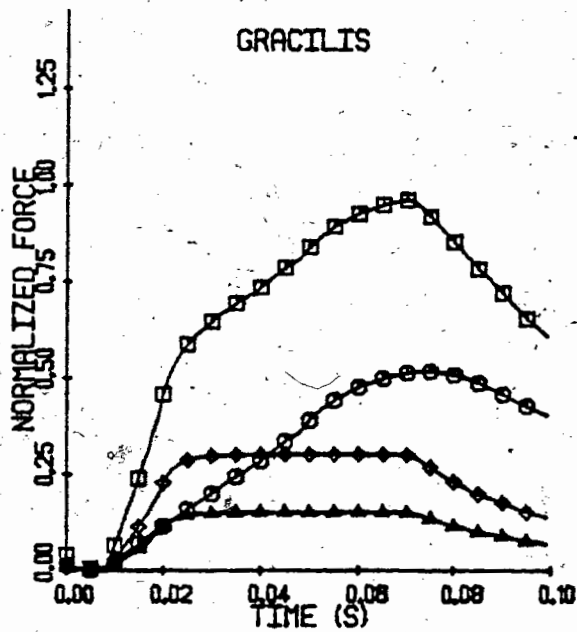
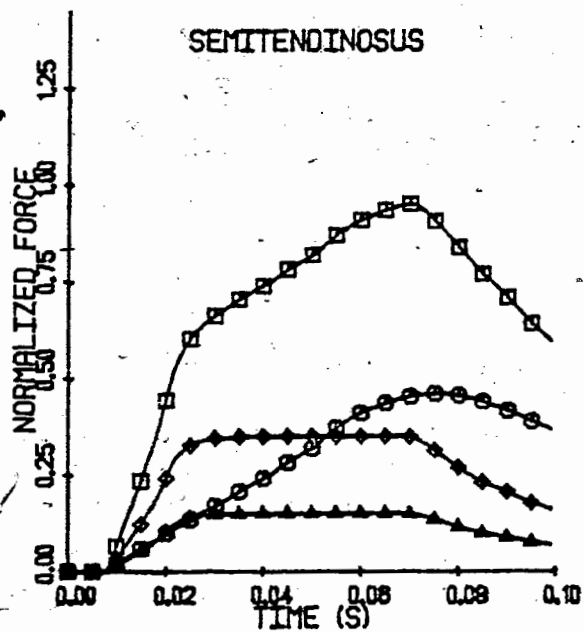


Figure 24

Response of some muscles to maximal stimulation from 10 to 70 ms. All muscles at their rest length and isometric. The total muscle (square), and the slow oxidative (circle), fast oxidative (triangle), and fast glycolytic (diamond) fibre force profiles are shown. All results normalized to the total muscle's maximum isometric force.

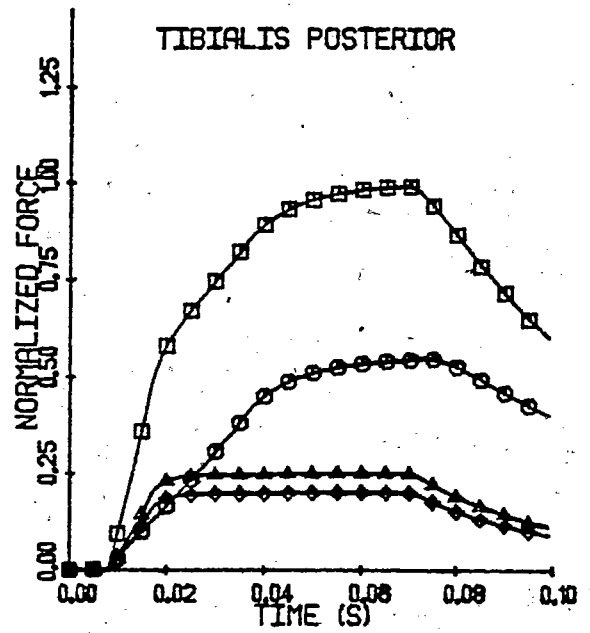
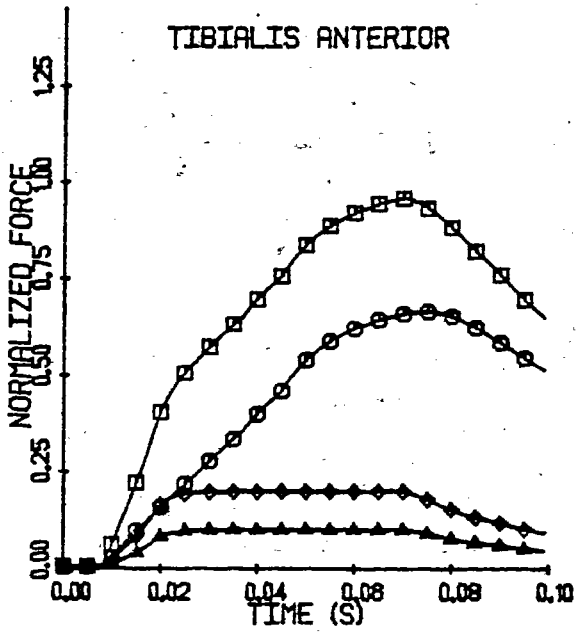
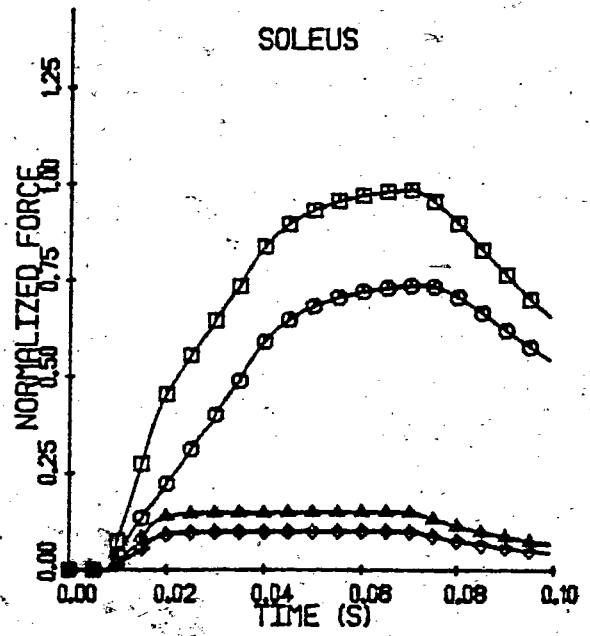
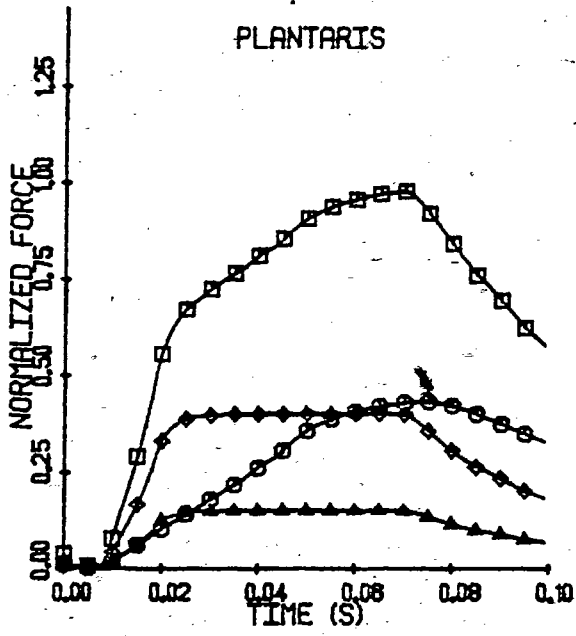


Figure 24 Continued.

California, 1953). One also expects differences in the EMG pattern between subjects and trials (Eberhart et al., 1954) so that the published EMG data may be viewed as a guide not as an absolute indication of the temporal activation of the locomotor muscles. The model does predict the smooth distribution of force amongst synergists (eg. the hip adductors and flexors, the vasti and the triceps surae) and a physiological time course for each muscle's force profile.

The model was able to assign individual muscle forces well within the imposed physiological constraints to generate the required joint moments. These constraints included their moment arms, force per unit cross sectional area, the force-length and force-velocity relationships, activation, elastic and geometrical considerations. This is contrast to the work of Patriarco et al. (1981) who included physiological constraints in the context of an optimization model only if they did not significantly increase the total muscle force levels. It is also interesting to note that they used a value of  $150 \text{ N cm}^{-2}$  for the maximum force per unit cross-sectional area of the muscle; this is nearly four times the value suggested in the literature (see Chapter III).

In this thesis the mean peak muscle force, normalized to isometric was  $0.21 \pm 0.14 \text{ SD}$  which suggests that only the slow twitch fibres were recruited during the normal walk. This is verified in Figure 25 which shows that the fast twitch fibres were infrequently recruited. It is interesting to note that the four muscles which showed fast fibre activity (obturator internus, adductor longus and brevis, and sartorius) are all hip lateral rotators and flexors. Comparing the mean level of muscle recruitment (mean normalized muscle force) at the lower limb joints, the hip shows the greatest activity. This could be explained by the models requirement to generate the net muscle moments about all three hip axes. Although the present state of technology can not give a definitive answer on the true level of muscular activity in vivo, if the mean muscular recruitment at

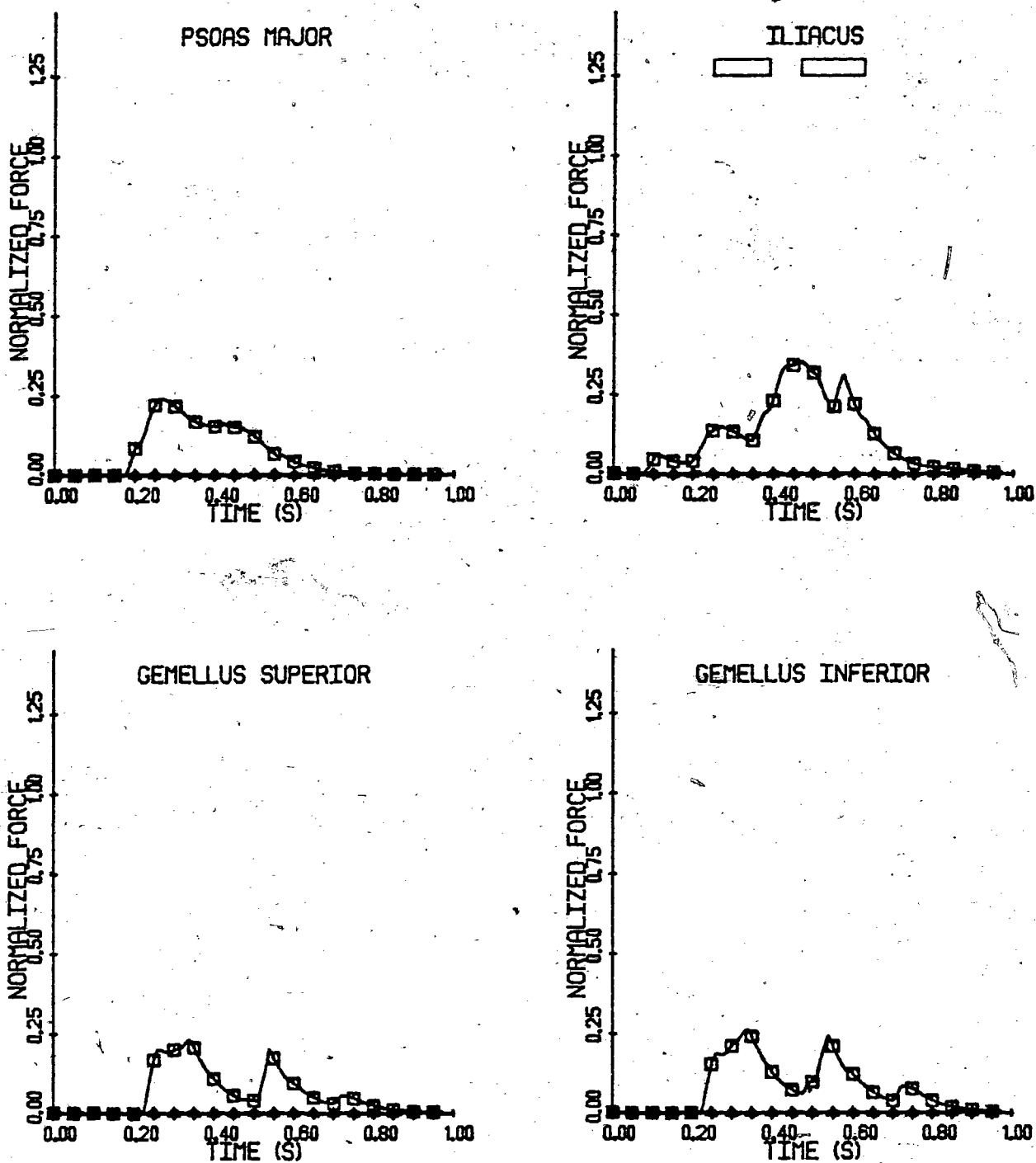


Figure 25

The muscle forces during the walk. The total muscle (square), and the slow oxidative (circle), fast oxidative (triangle), and fast glycolytic (diamond) fibre force profiles are shown. All results normalized to the total muscle's maximum isometric force. The 'boxes' represent published EMG activity.

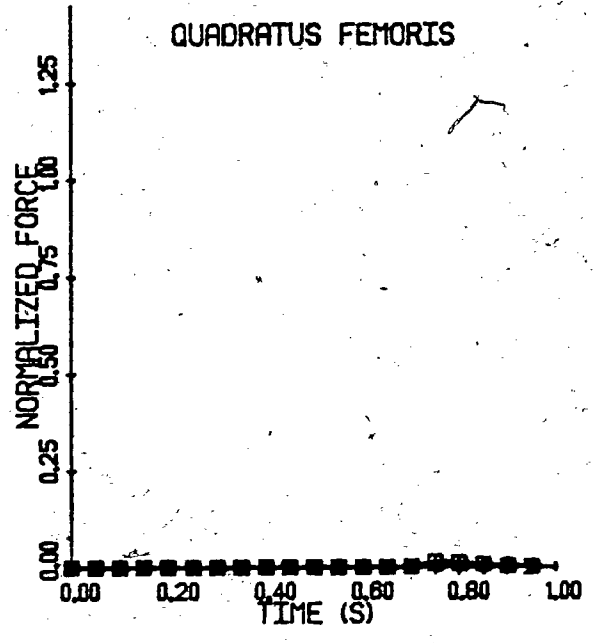
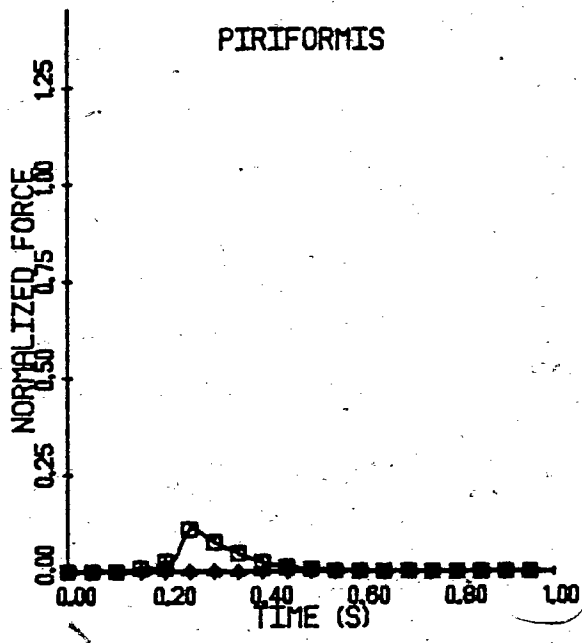
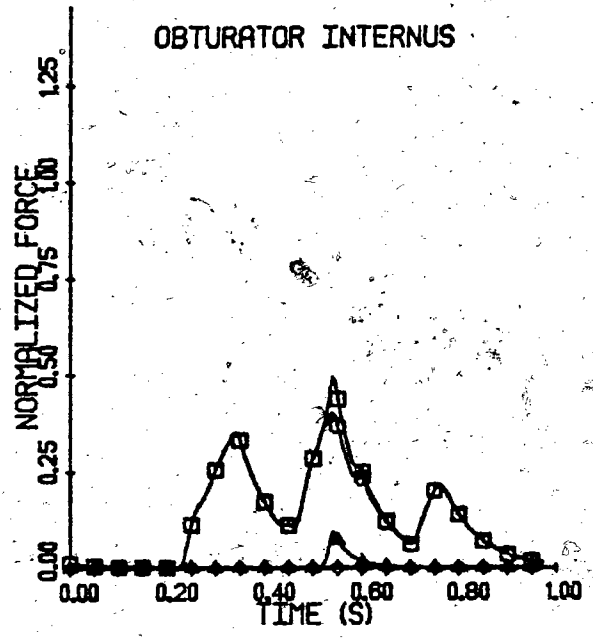
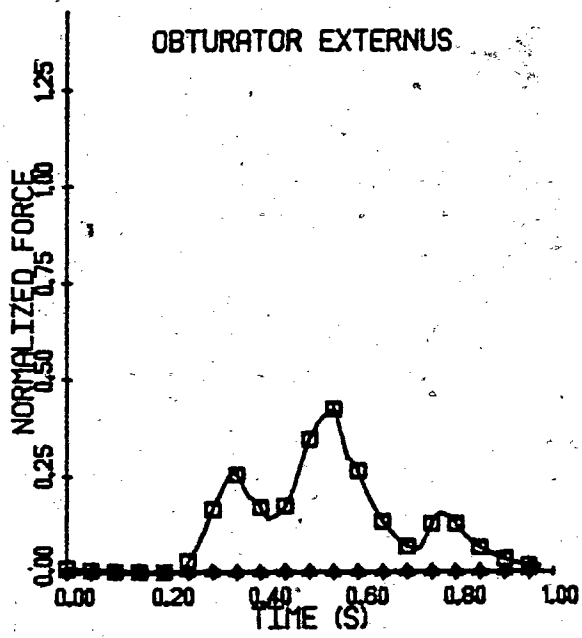


Figure 25 Continued.



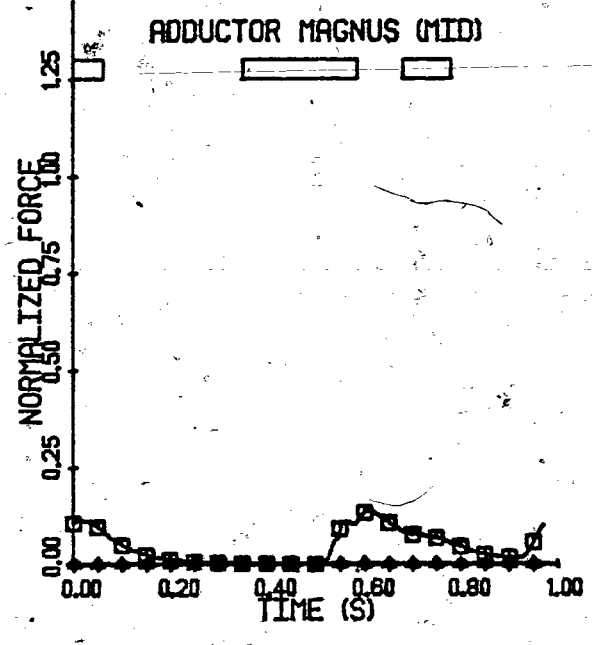
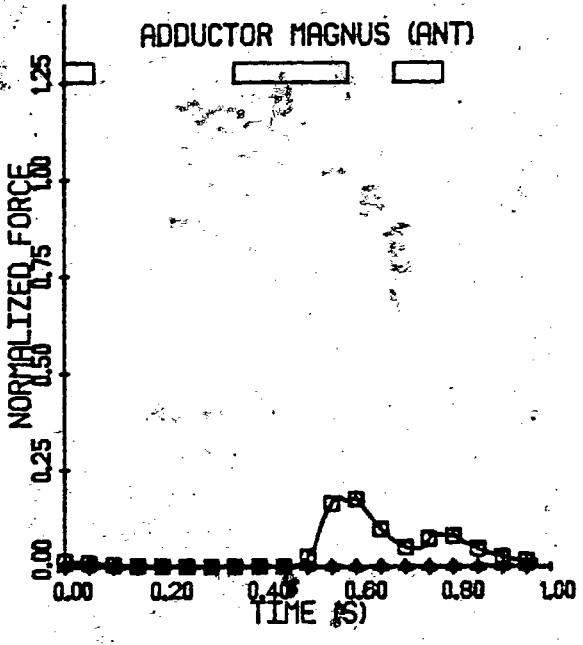
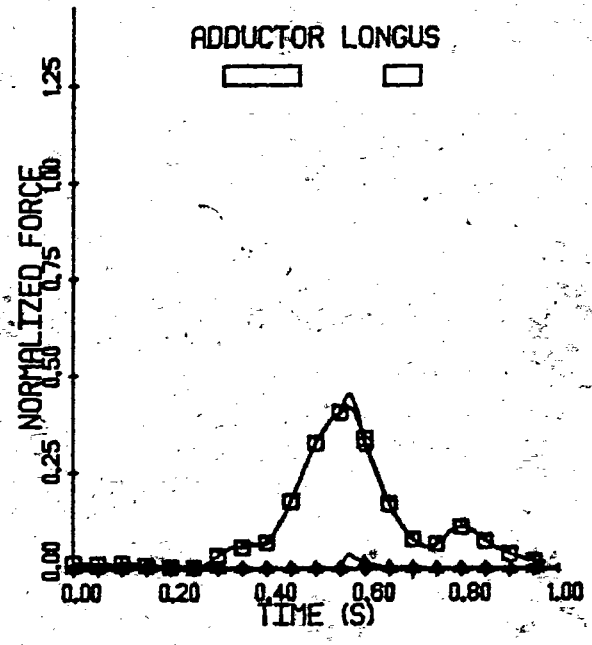
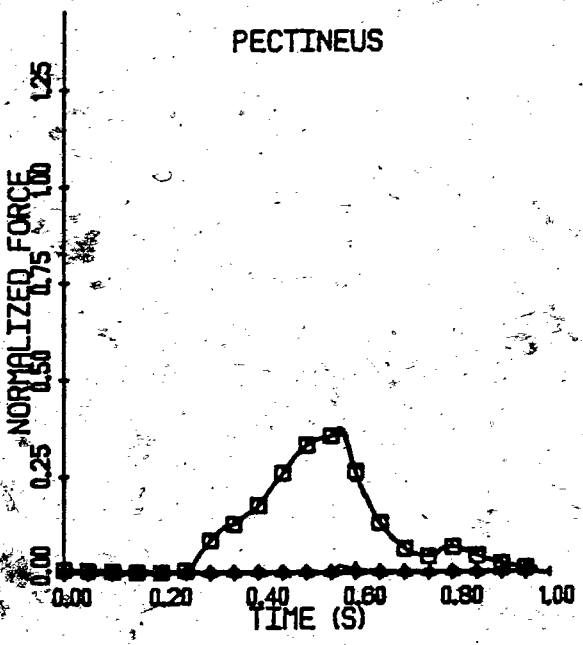


Figure 25 Continued.

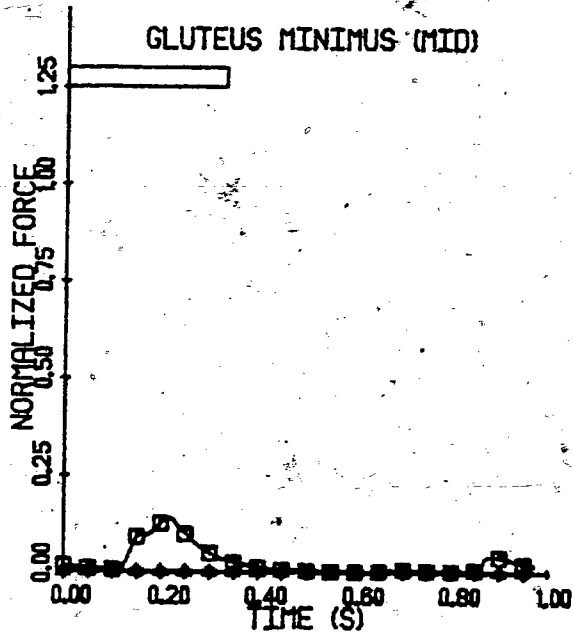
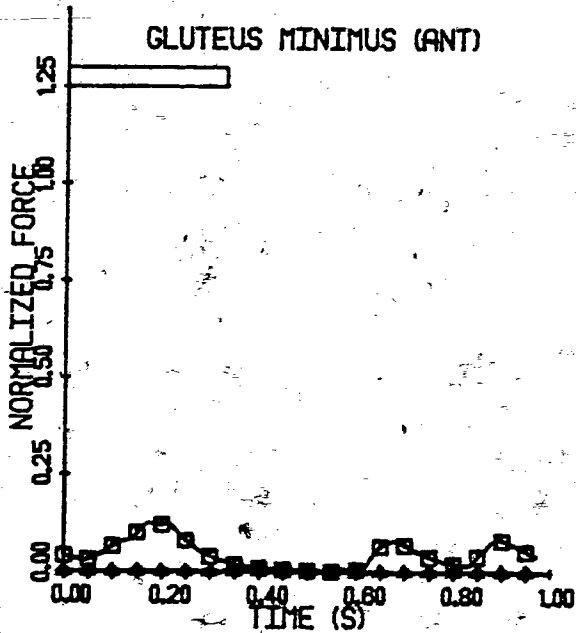
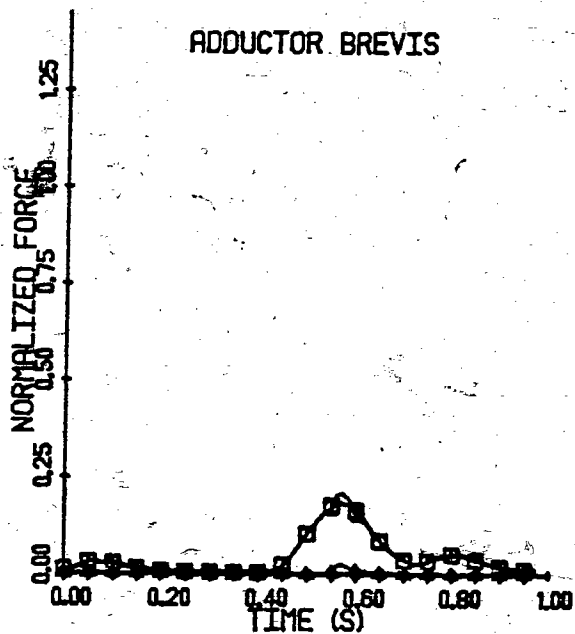
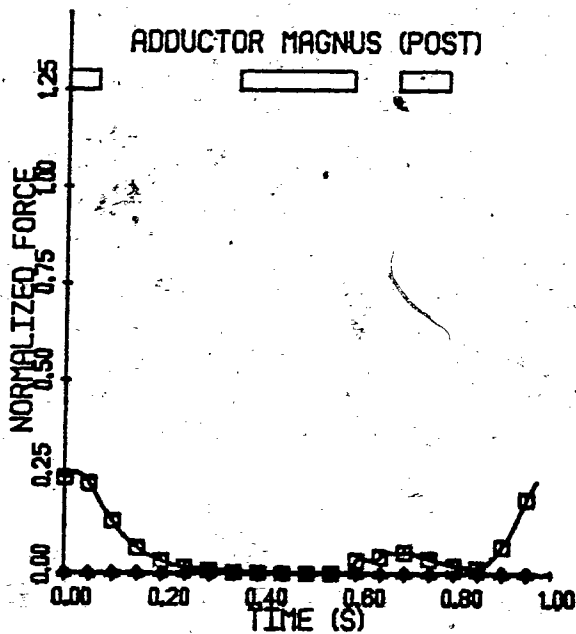


Figure 25 Continued.

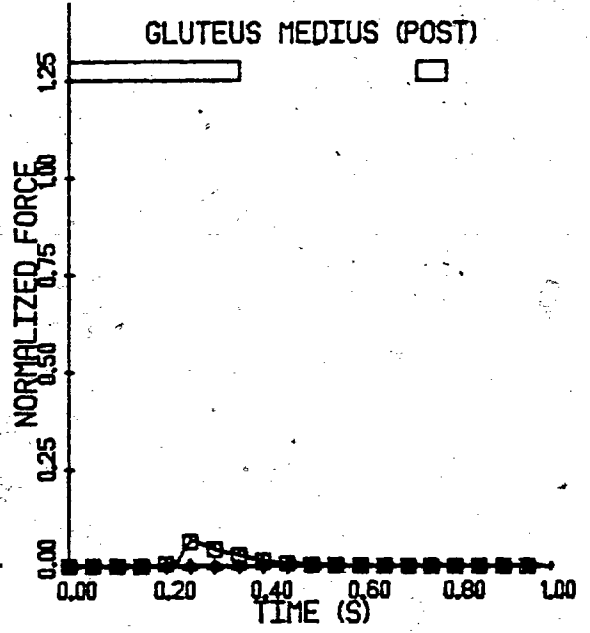
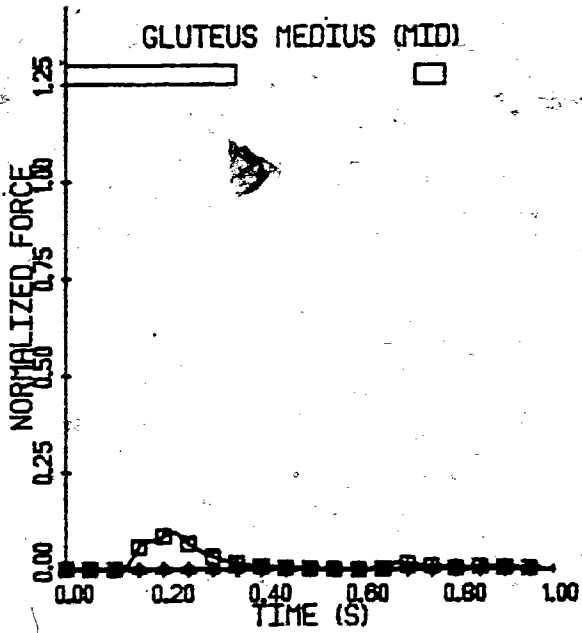
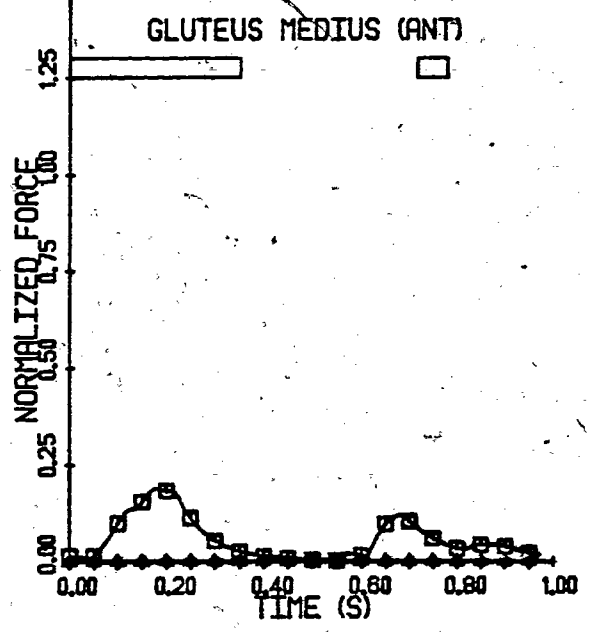
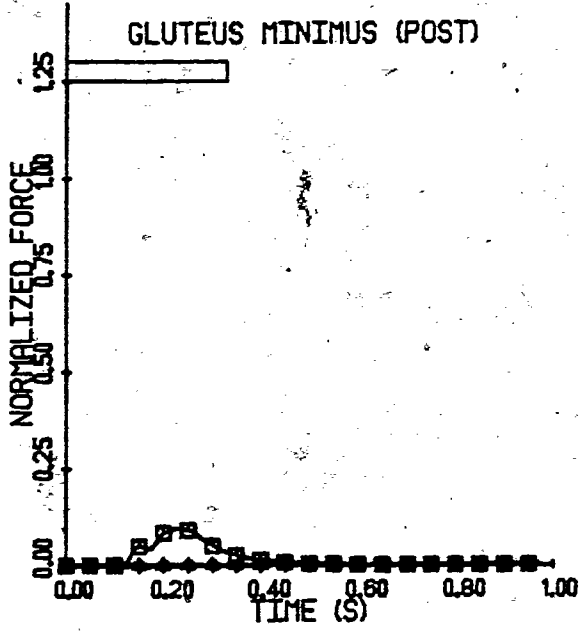


Figure 25 Continued.

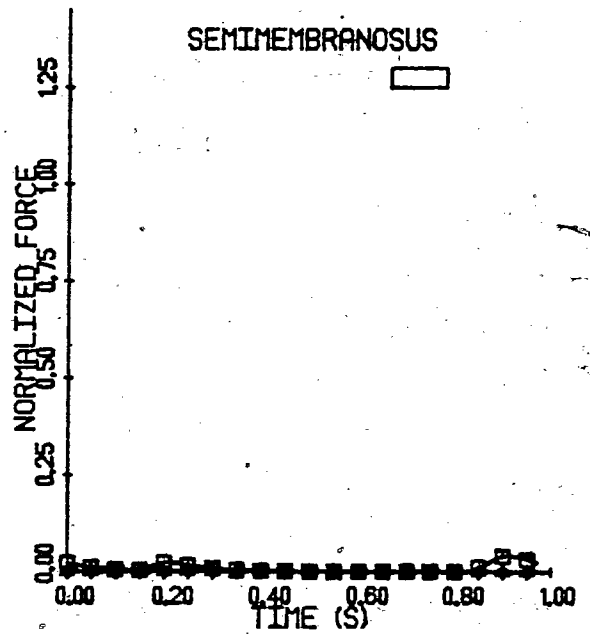
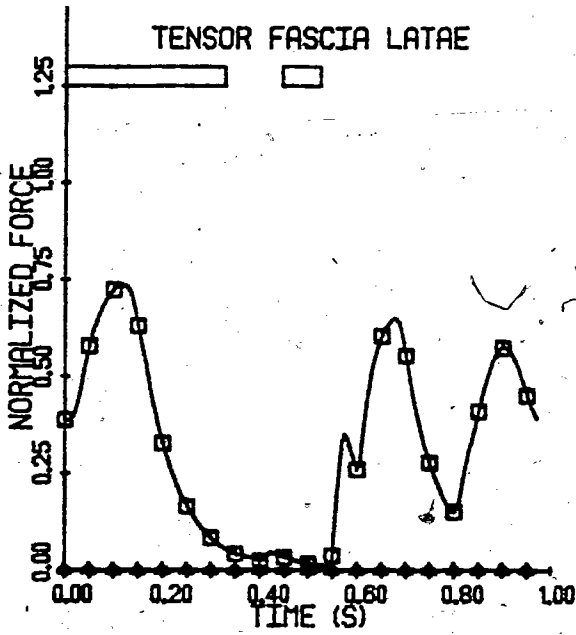
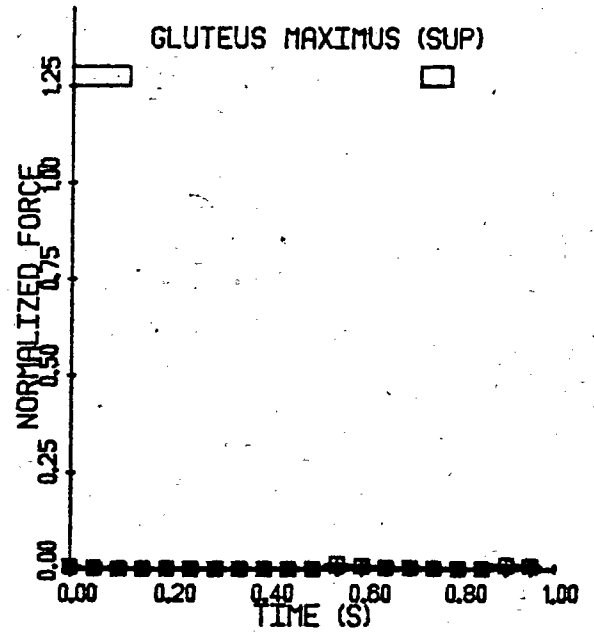
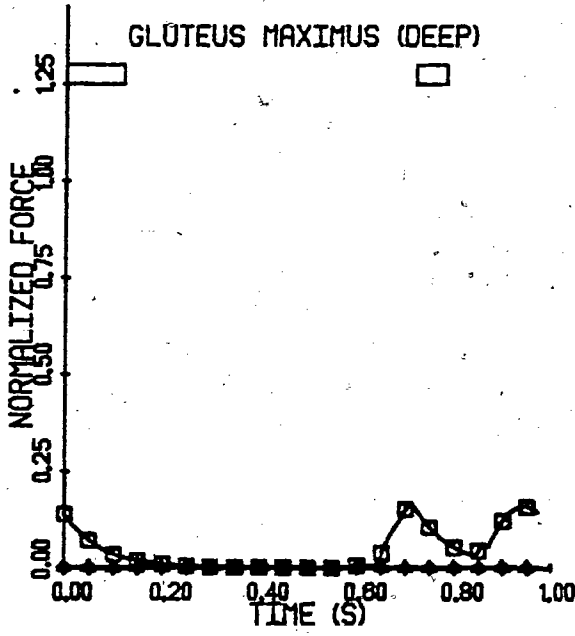


Figure 25 Continued.

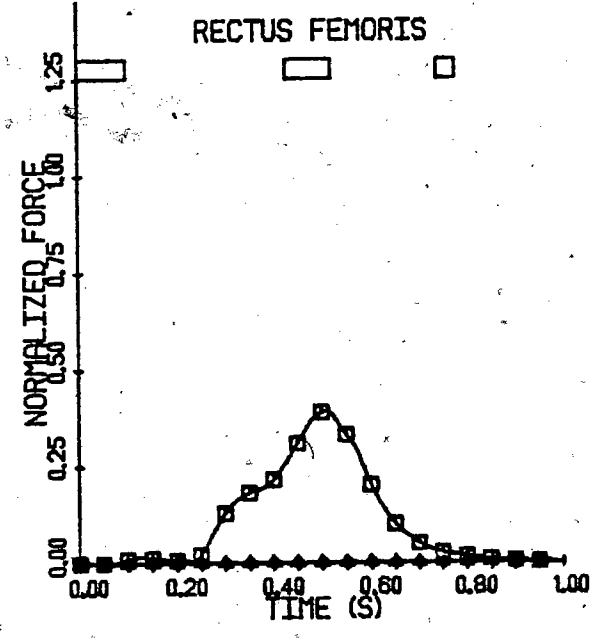
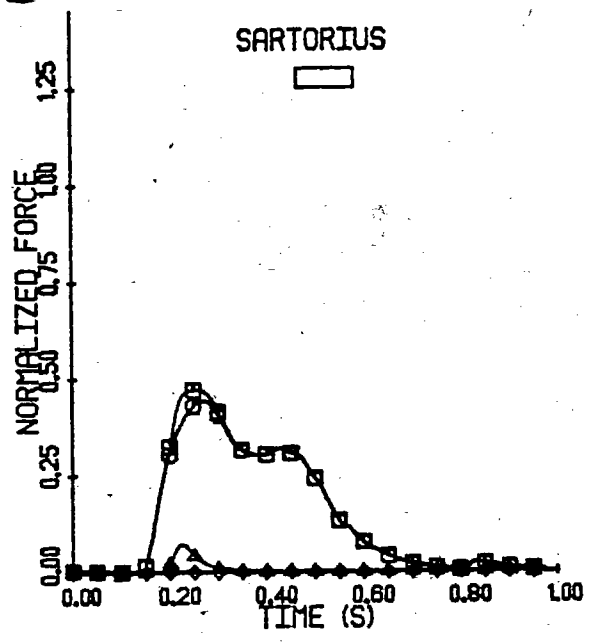
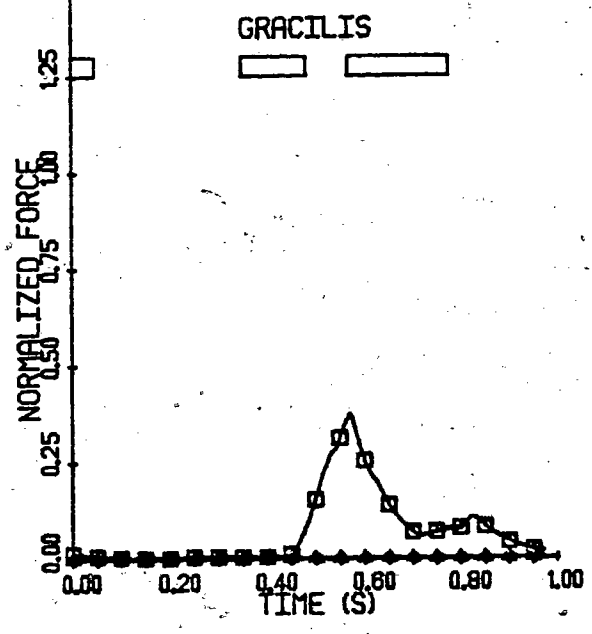
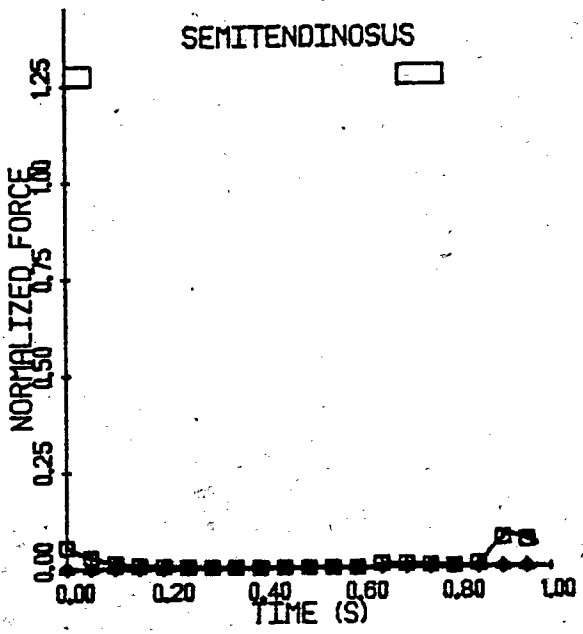


Figure 25 Continued.

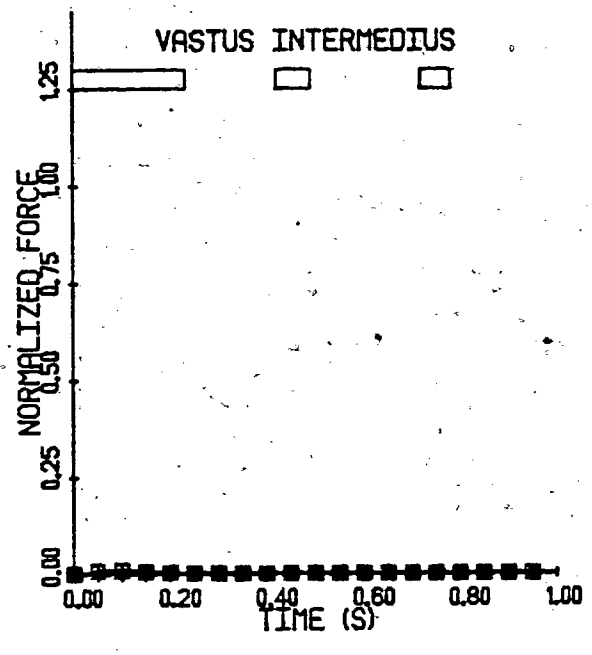
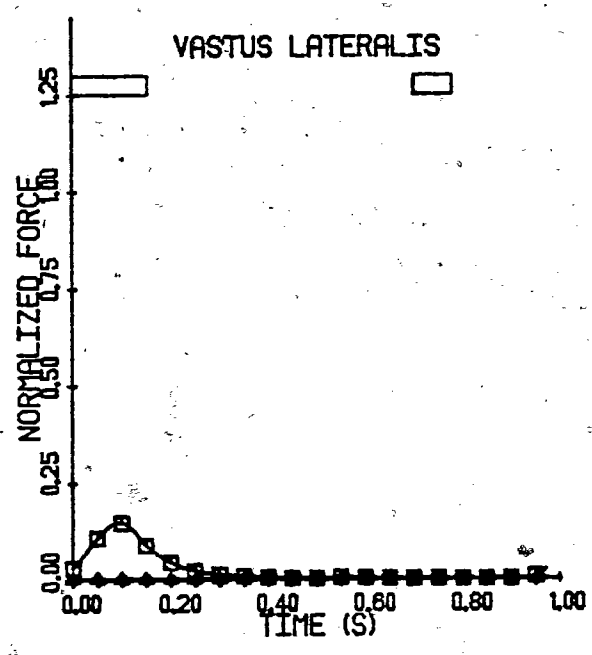
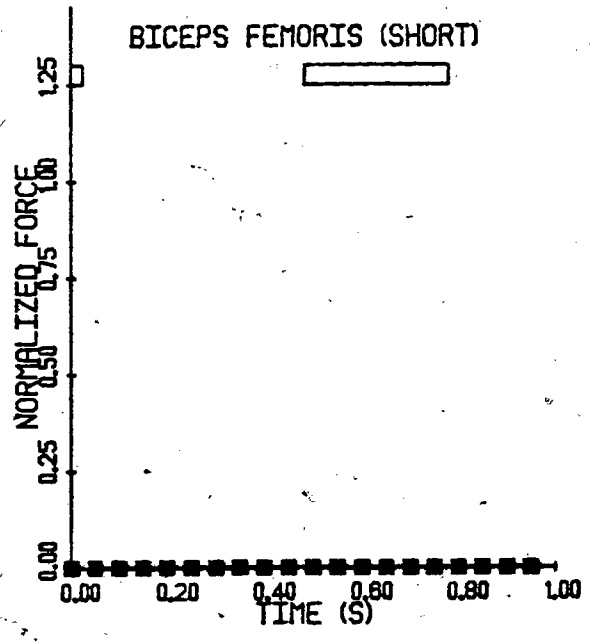
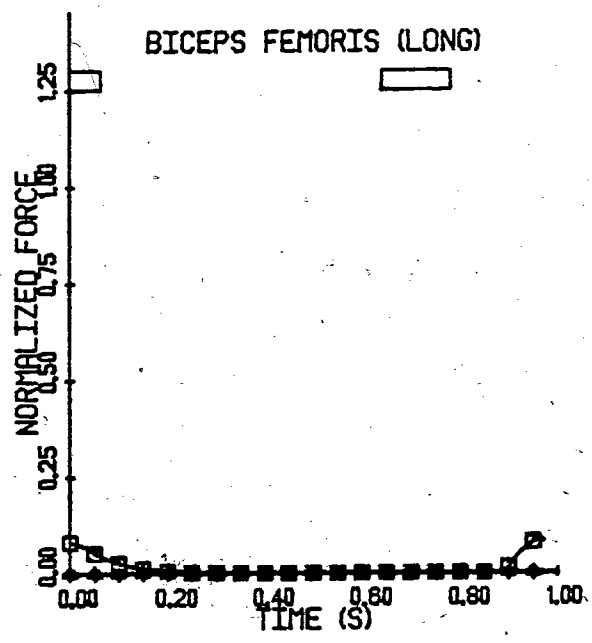


Figure 25 Continued.

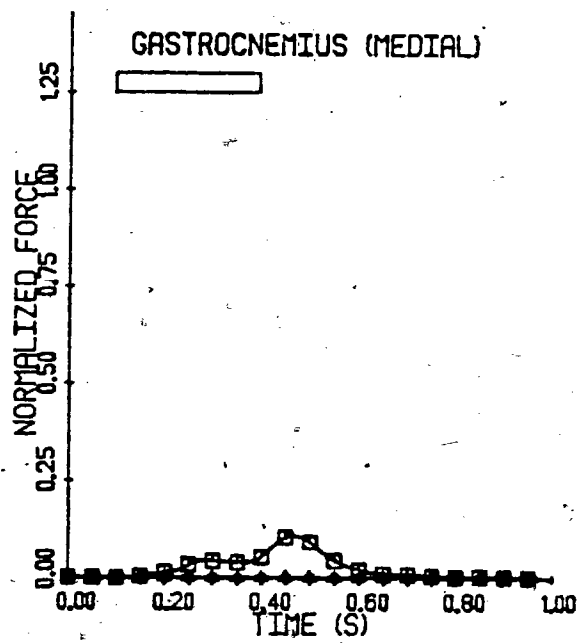
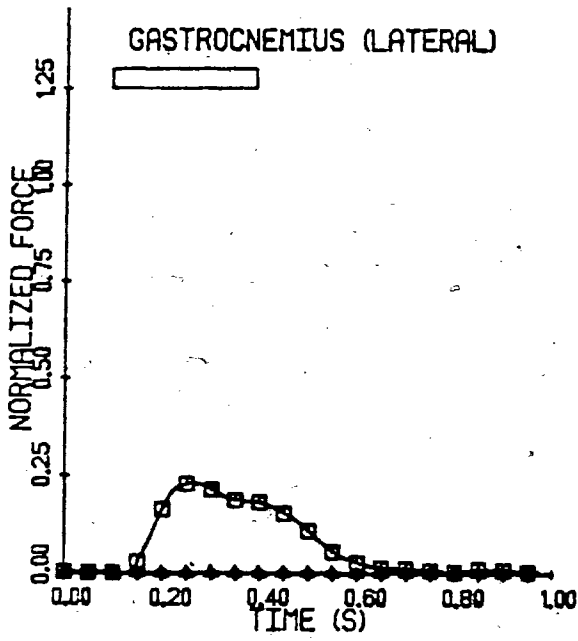
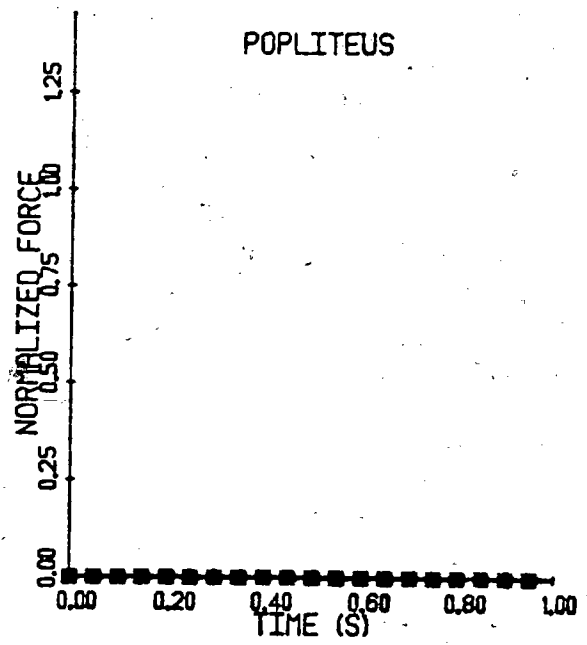
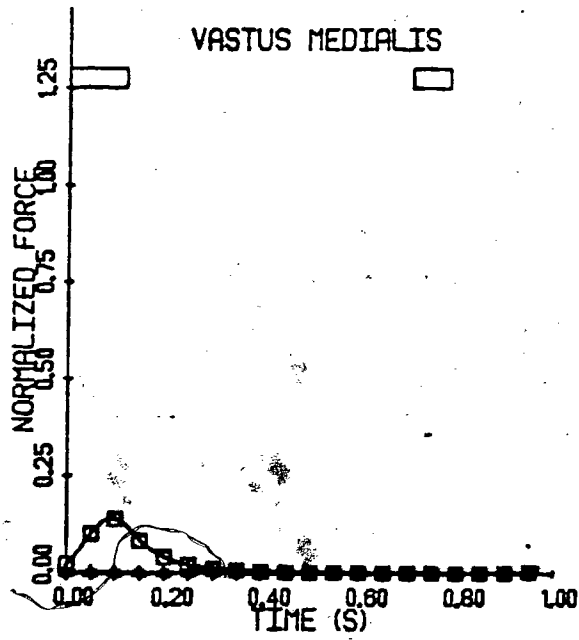


Figure 25 Continued.

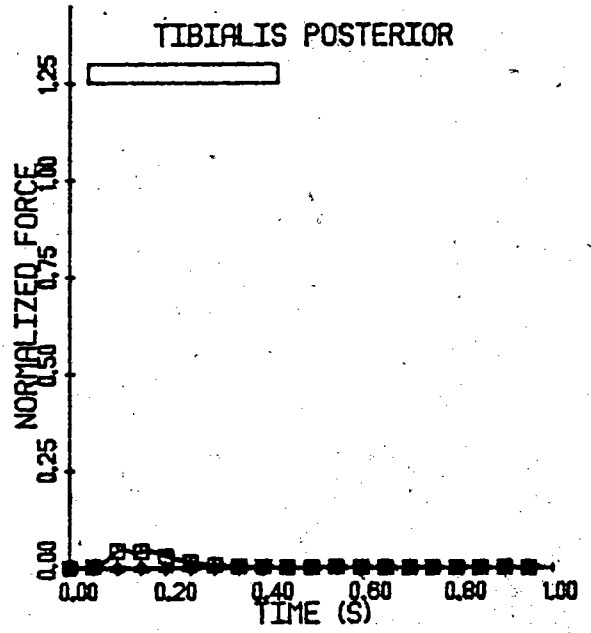
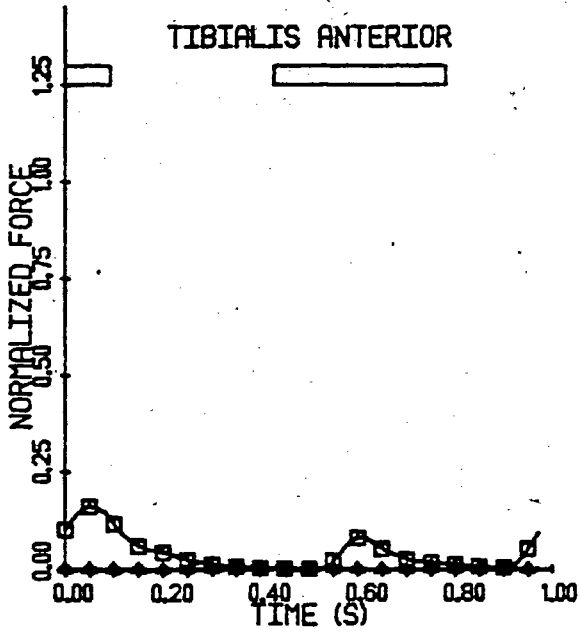
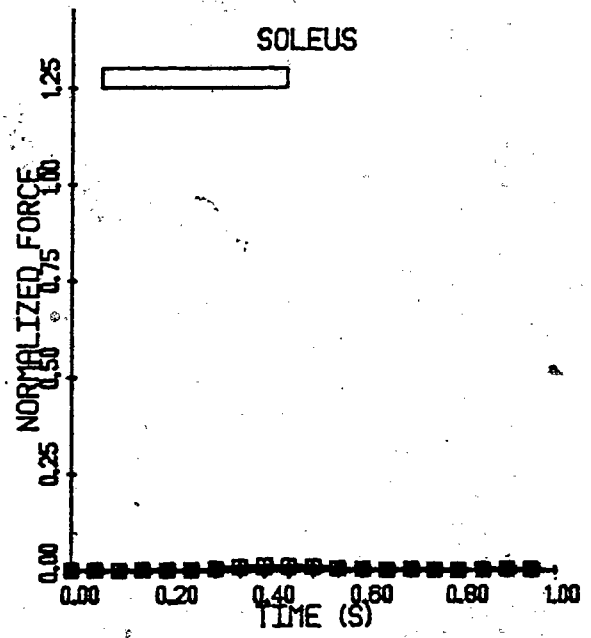
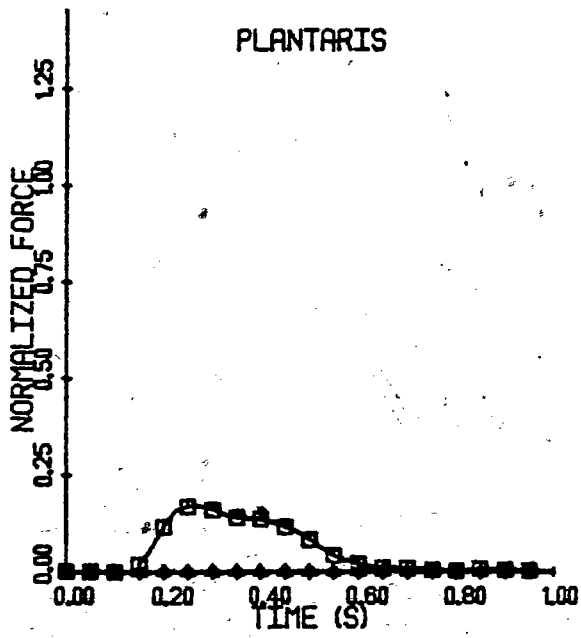


Figure 25 Continued.



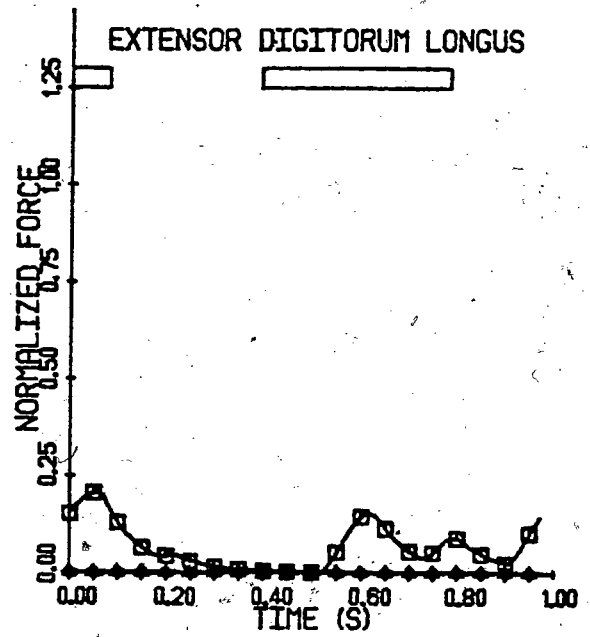
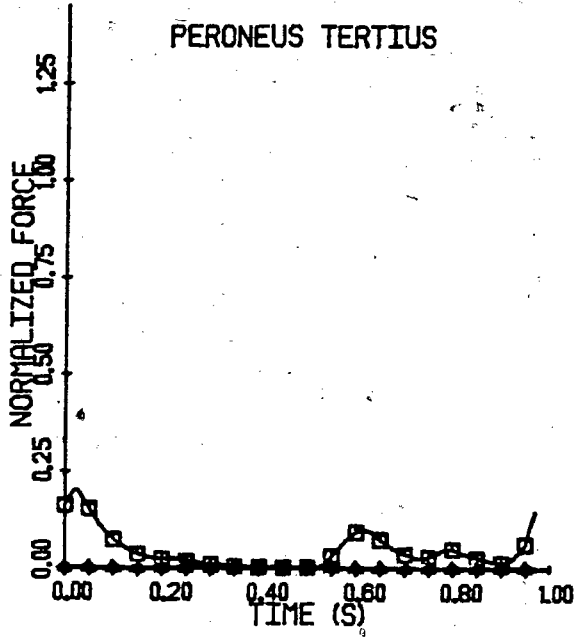
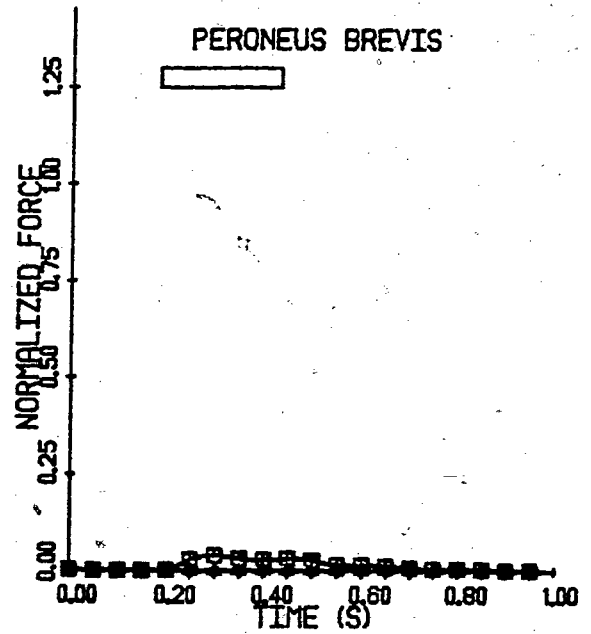
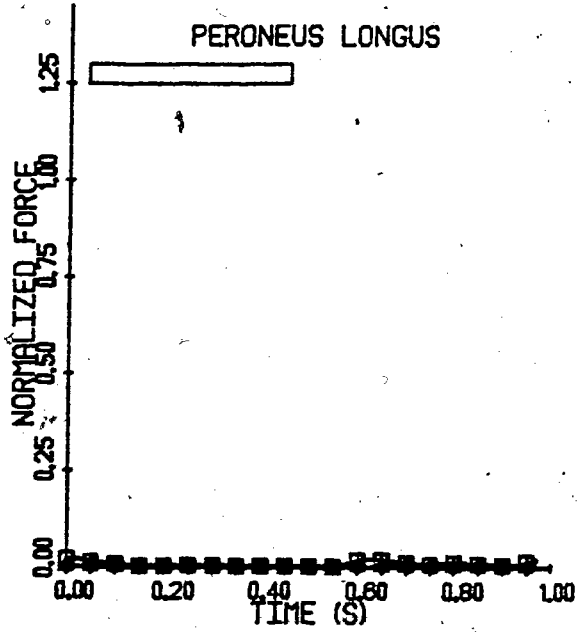


Figure 25 Continued.

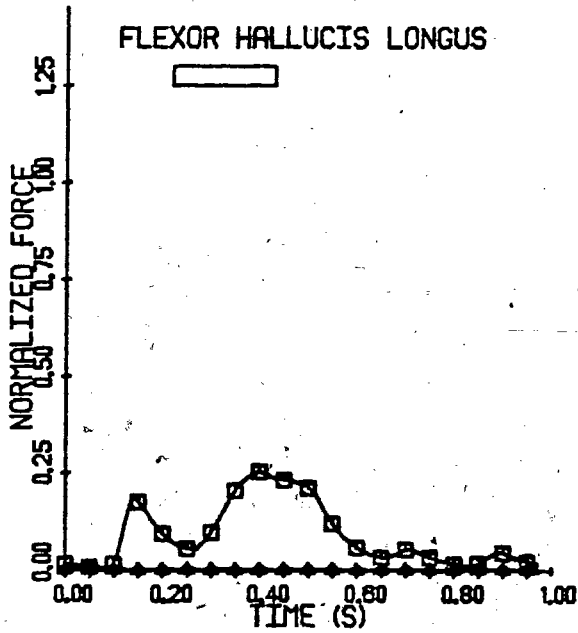
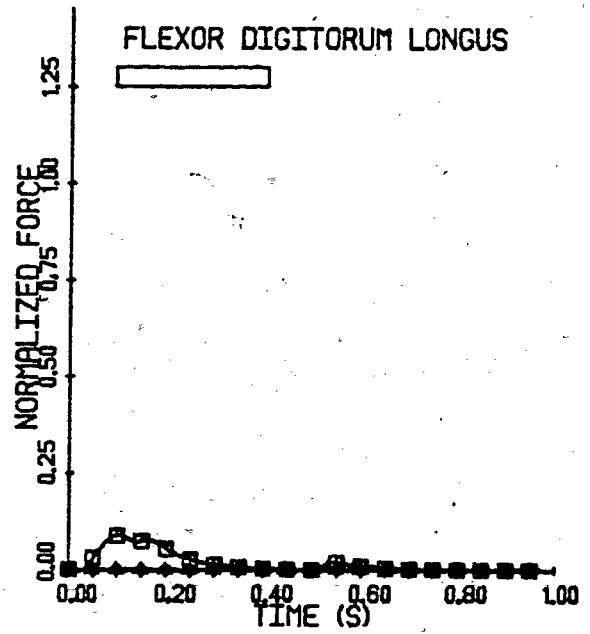
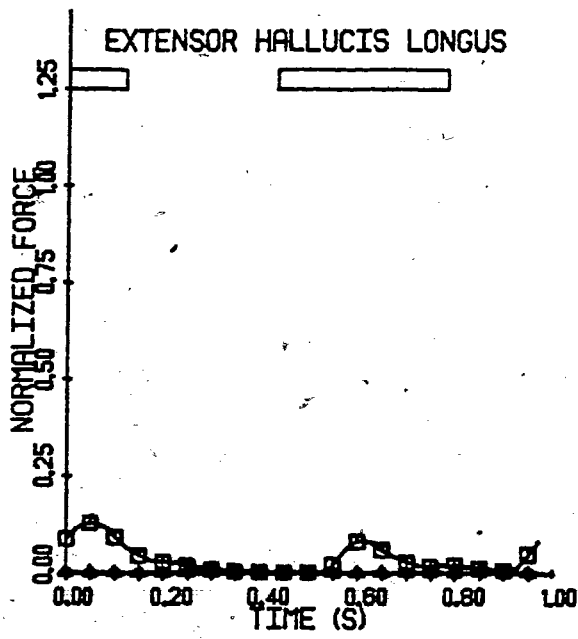


Figure 25 Continued.

the hip is not greater than that of the knee or ankle, this suggests either imprecise moment arm estimations or an improper choice of the number of pattern generators controlling the hip movements. Only with directly validated muscle force predictions, through muscle force transducers or quantitative EMG techniques, will this be proven.

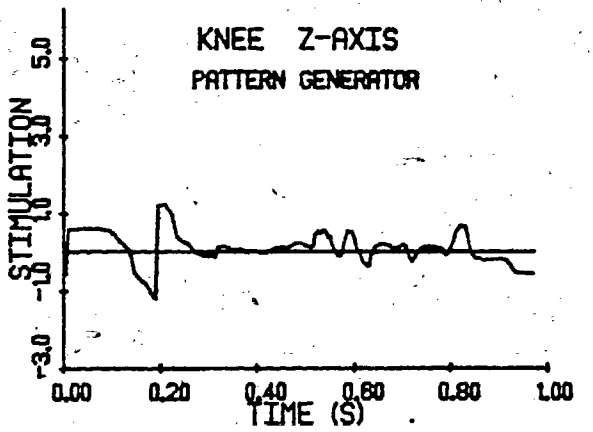
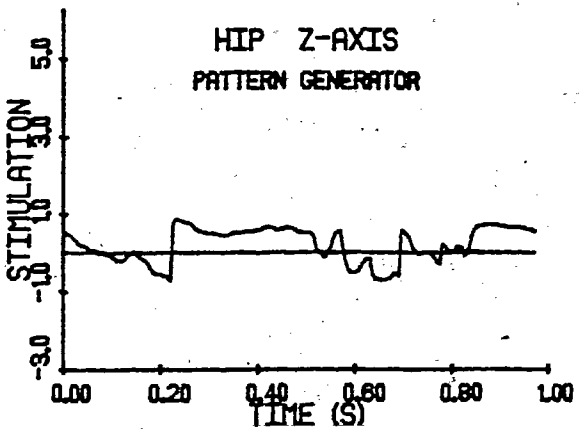
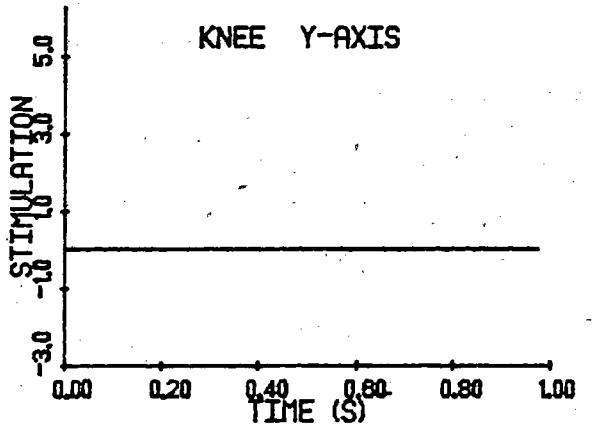
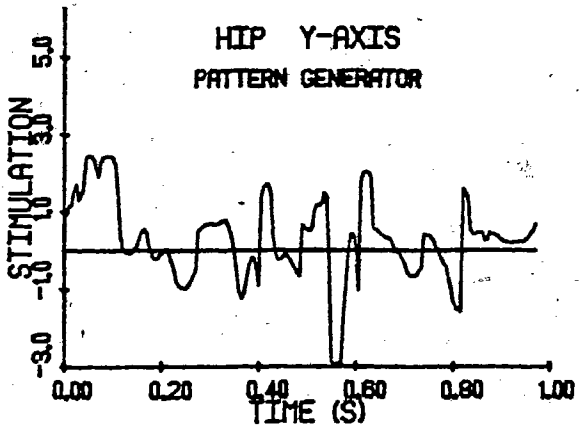
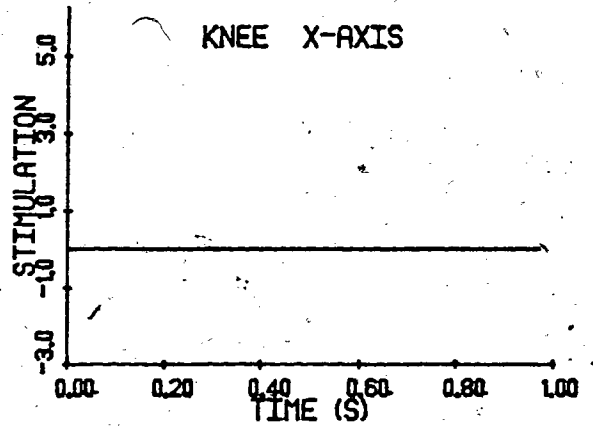
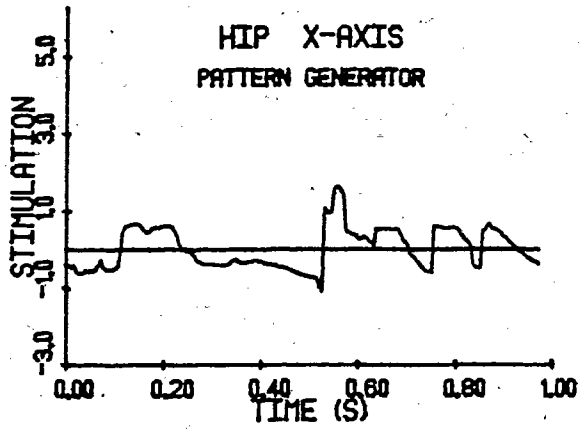
Antagonistic activity was predicted for normal walking, demonstrated by the vasti and the hamstrings being active just after heel contact. The model allows such activity due to a physiological time course for the decline in muscle tension and the need to satisfy a number of joint moments simultaneously.

The results of the physiological model's estimation of the individual muscle forces during normal walking, when compared to the University of California's EMG data, was generally excellent suggesting that it could be used as a muscle force predictor. Better anatomical data and a rigorous validation of the model must be undertaken however, before it can be used in research or clinical settings (see Panjabi, 1979).

#### Pattern Generator Outputs

The temporal profile of the outputs from the six pattern generators are presented in Figure 26. Six generators were hypothesized, one for each major degree of freedom in the lower limb, which interact to define the neural input to the locomotor muscles.

A pattern generator stimulates those muscles which can generate a required net muscle moment (see the control model section of Chapter III). Why is it then that at certain phases in the gait cycle the wrong muscles are recruited? This is evident whenever a generator outputs a negative stimulus. For example, during most of the stance phase a positive (inversion) moment is required at the subtalar joint, yet the foot everters (peronei, extensor digitorum longus) are recruited. One reason is that the foot inverters could not be deactivated quickly enough,



7  
Figure 26 The pattern generator outputs.

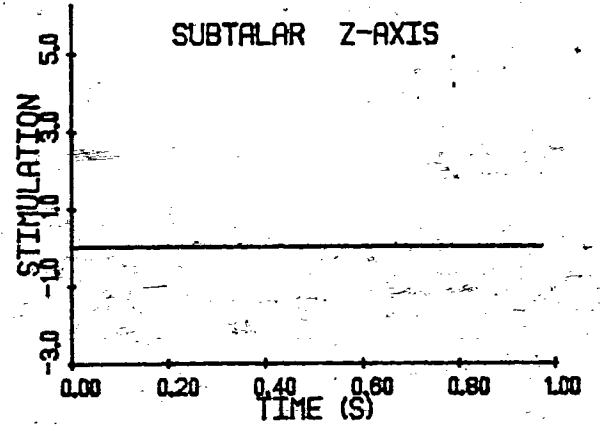
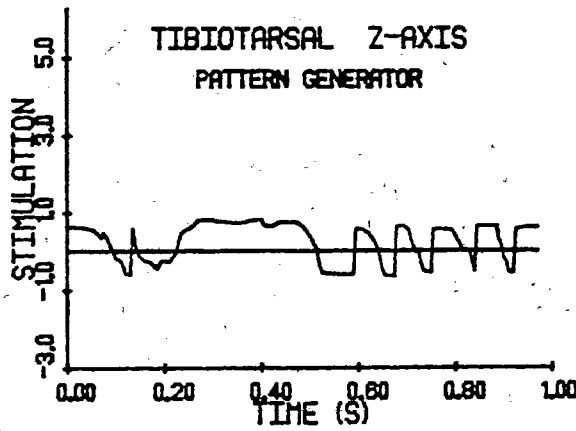
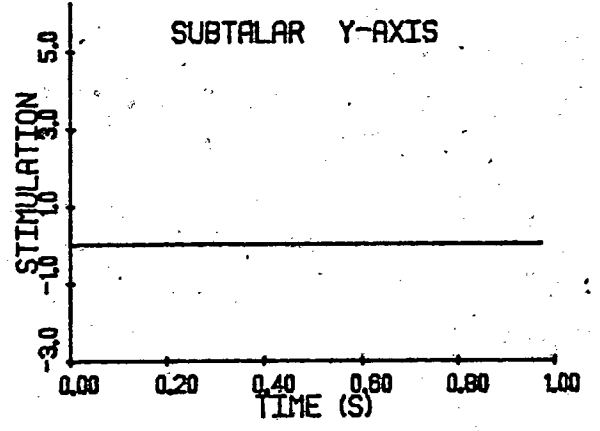
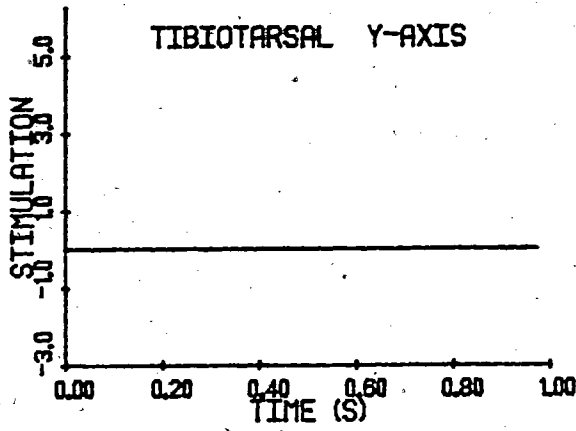
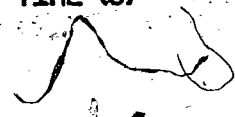
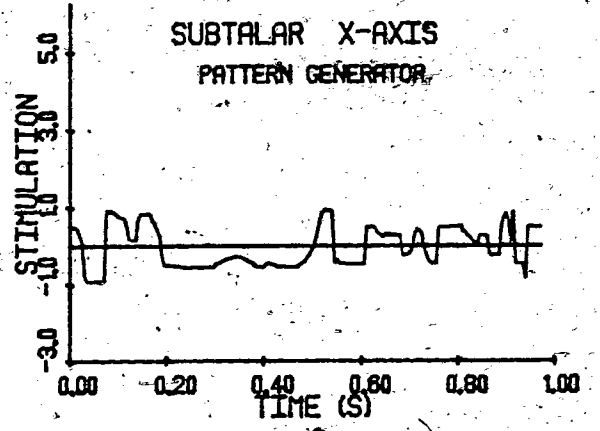
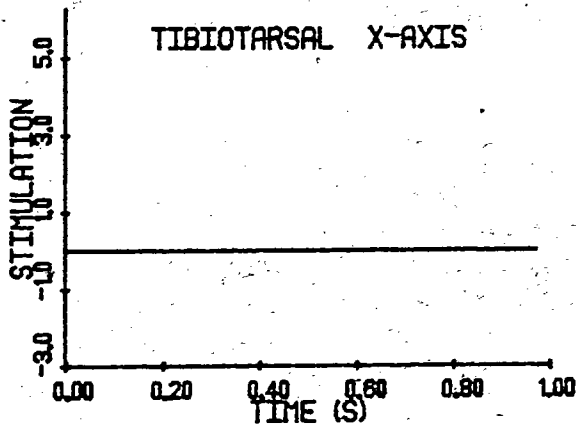


Figure 26 Continued.

necessitating that the everters be recruited to produce the net muscle moment as externally measured. A second reason is that a given muscle might have to be considered by more than one pattern generator. If a muscle satisfies the moment at one joint but oversatisfies the moment at another, the latter moment must be balanced by antagonistic activity. At the ankle a large extensor moment is required, which when satisfied causes an inversion moment due to the joint anatomy. This unwanted moment must be balanced by antagonistic activity. An interesting outcome of this is that whenever a pattern generator outputs a negative stimulus, antagonistic muscle activity occurs at that degree of freedom in the model. This should not be interpreted as that only when a pattern generator outputs a negative stimuli antagonistic activity occurs. Co-contraction can occur due to the time it takes for a muscle to abolish tension even in the absence of stimulation.

The output from the pattern generators interact to form the neural input to each of the 47 modelled muscles (see Figure 27). Again the 'boxes' on some plots represent those phases in the gait cycle for which EMG activity has been shown to be present (University of California, 1953). If a muscle received a net negative stimulation its input was set to 0.0 and a net stimulation greater than 3.0 was reset to 3.0. Note that since stimuli greater than 0.5, 1.5 and 2.5 recruit the SO, FO and FG fibres, respectively, these curves reinforce the model's prediction that the fast twitch fibres are infrequently needed during normal walking.

Poor temporal correspondence exists between the model's prediction of the neural input to the muscles and that shown by EMG data. This suggests that the control model is deficient in one or more areas. A possible source of error is in omitting the rich feedback the spinal cord receives from the muscles. These signals, reporting the length, velocity and tension states of the muscle (Lundberg, 1969), can modify the magnitude of the neural

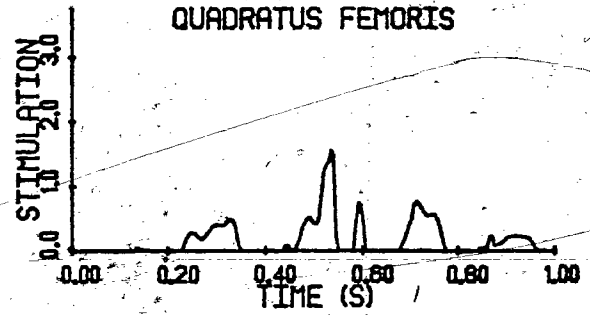
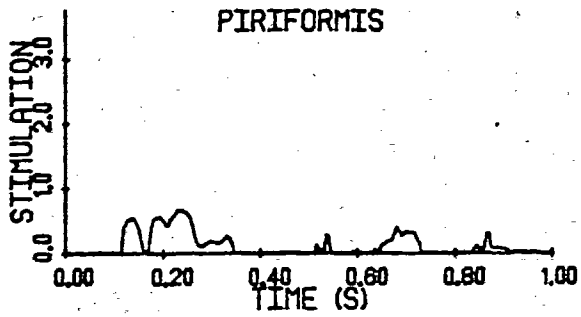
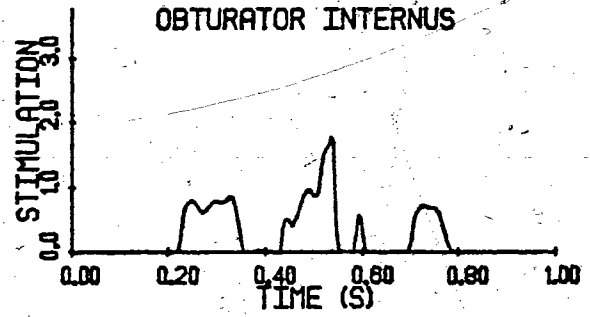
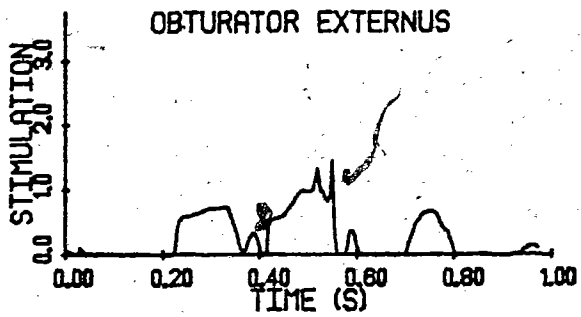
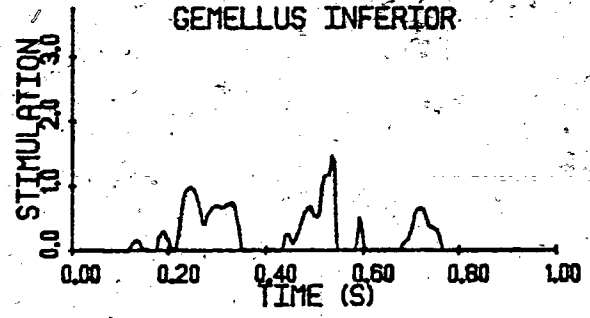
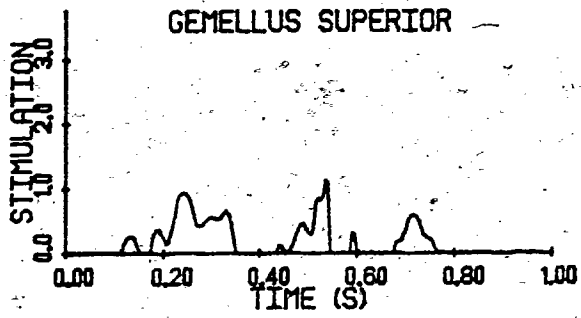
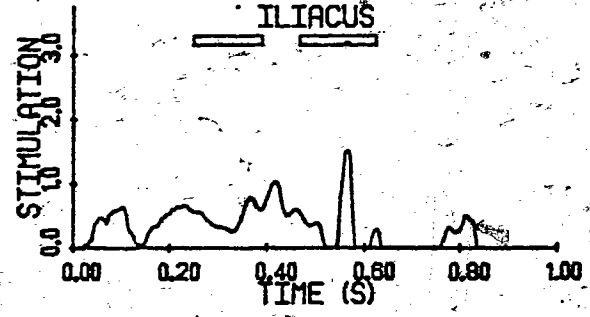
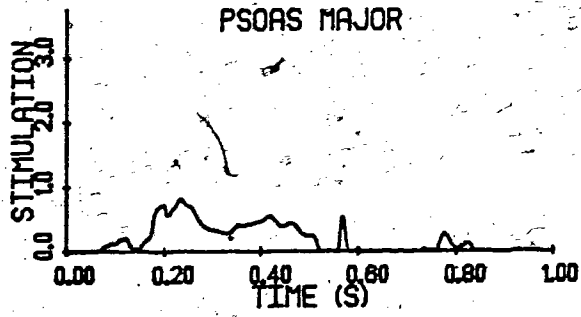


Figure 27 Stimuli to the muscles from the pattern generators. The 'boxes' represent published EMG data.

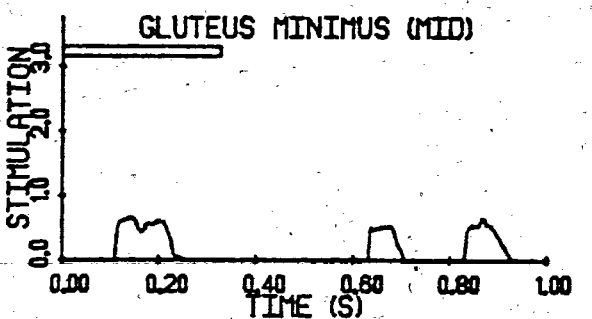
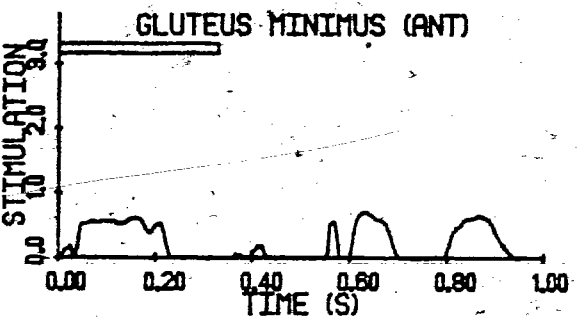
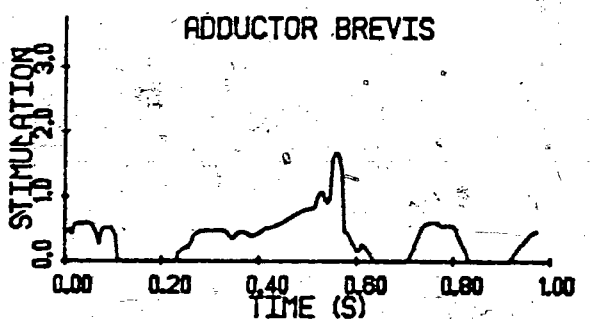
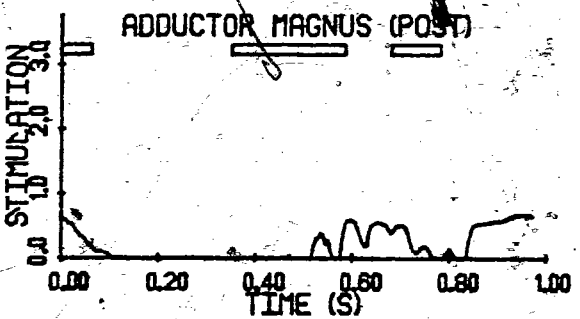
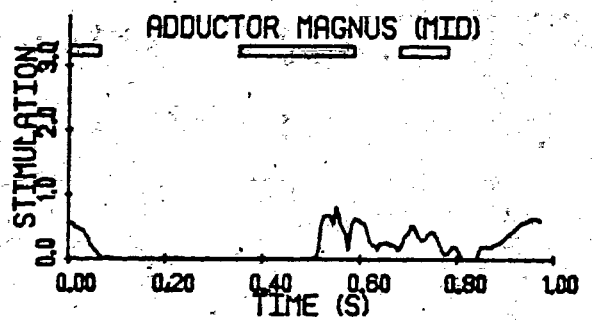
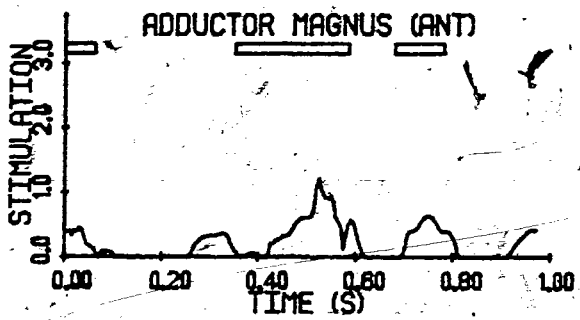
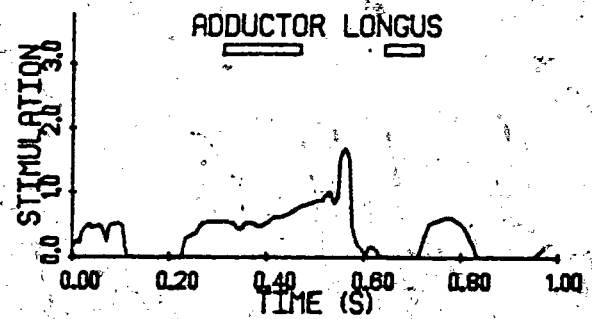
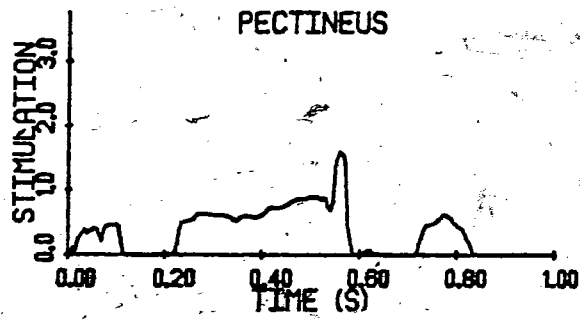


Figure 27 Continued.



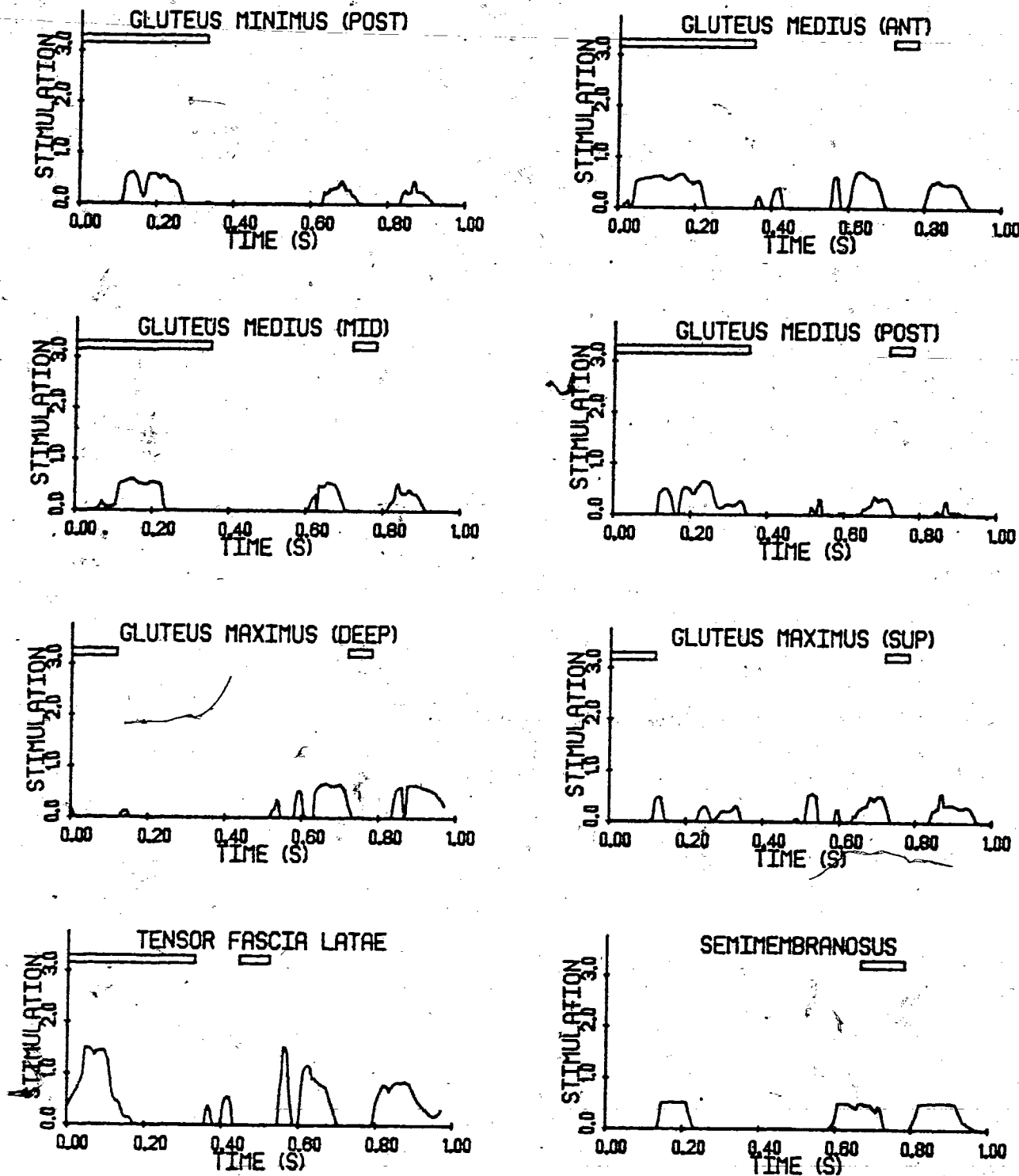


Figure 27

Continued.

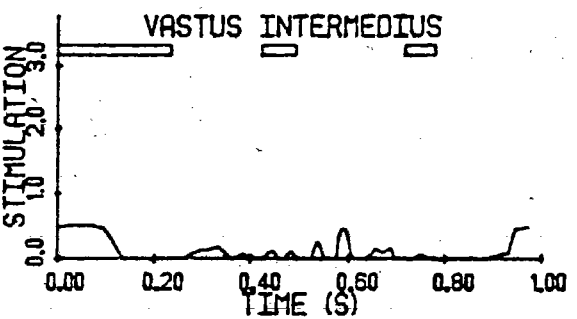
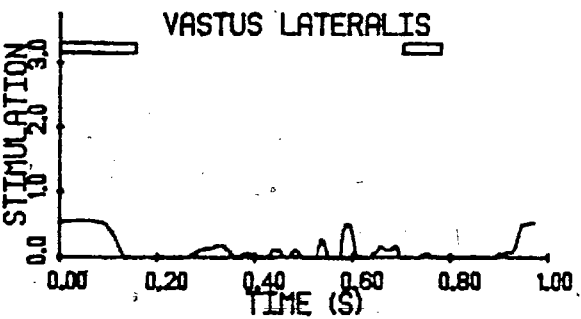
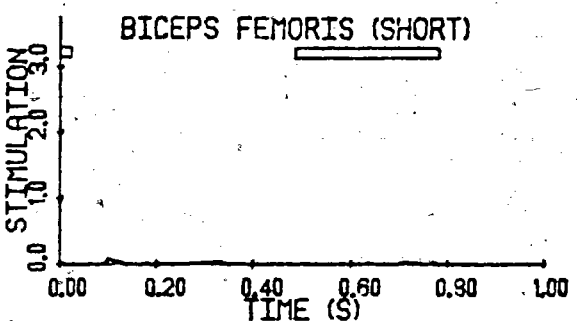
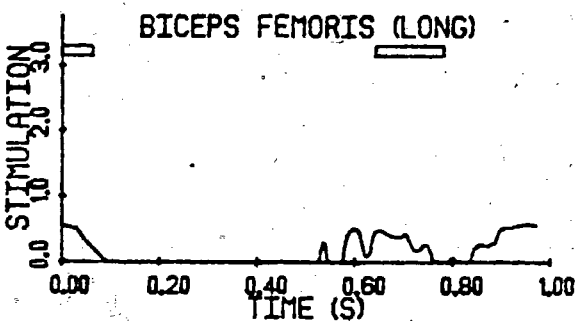
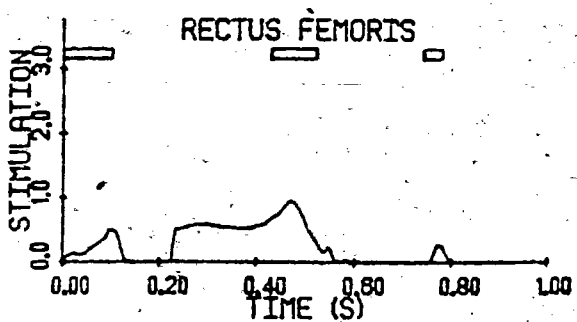
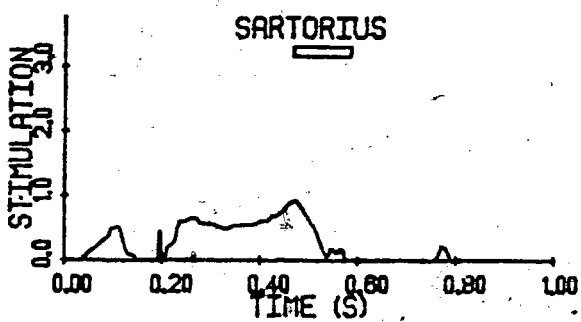
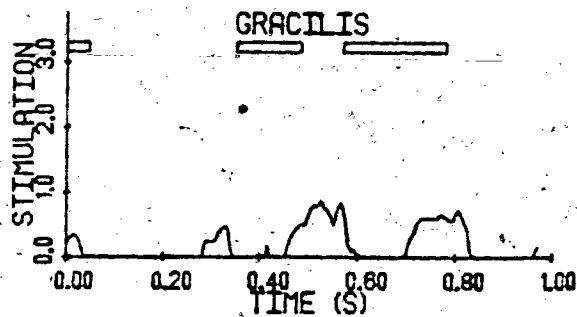
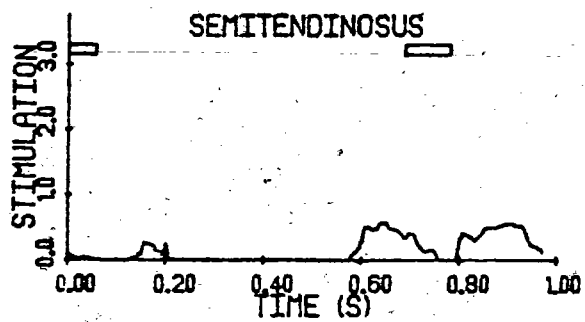


Figure 27

Continued.

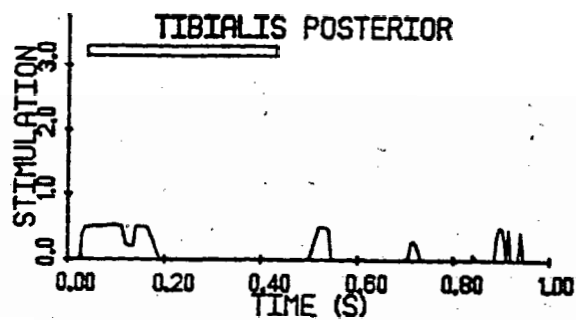
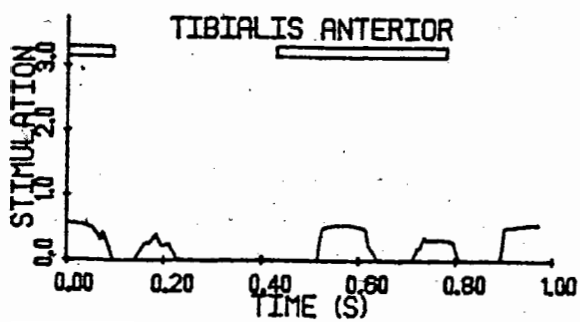
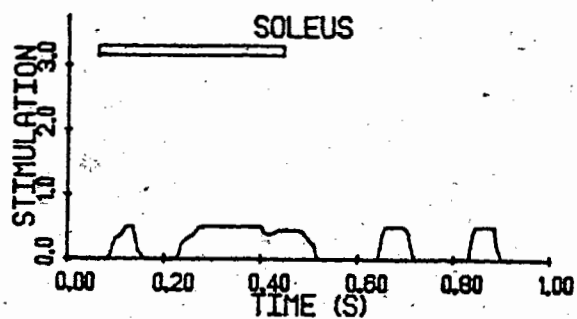
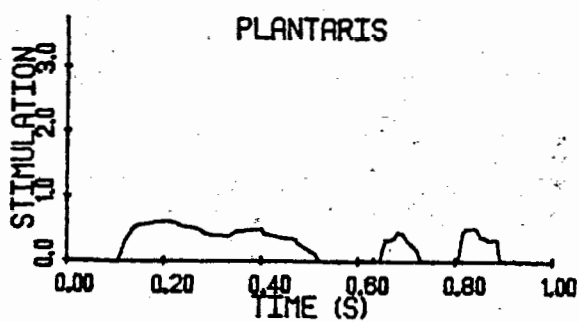
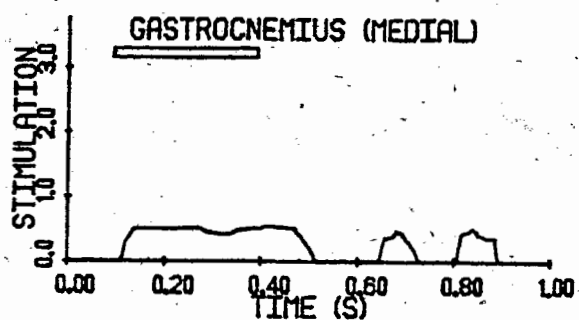
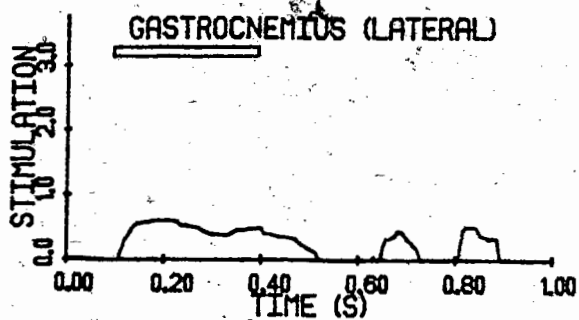
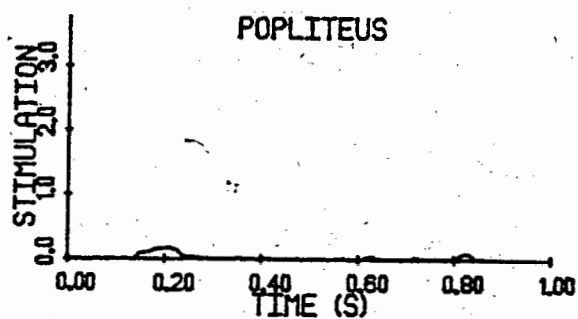
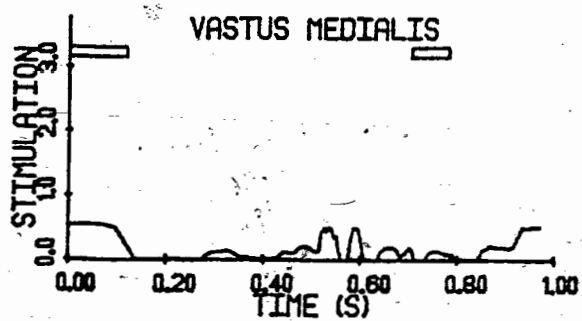


Figure 27.

Continued.

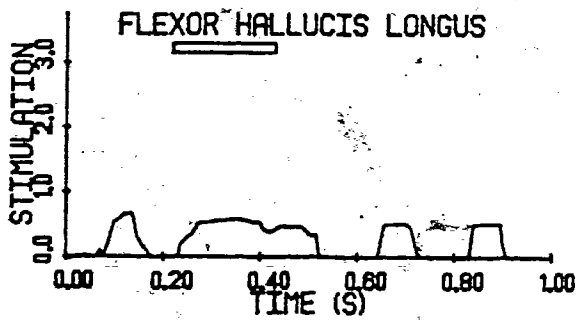
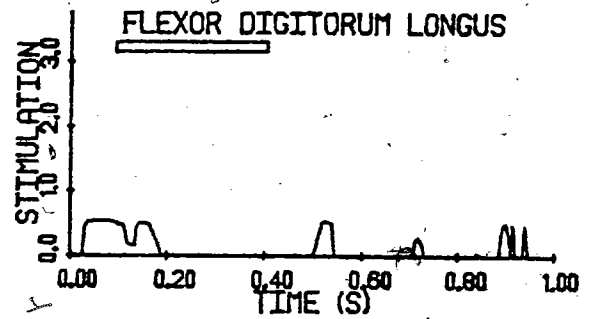
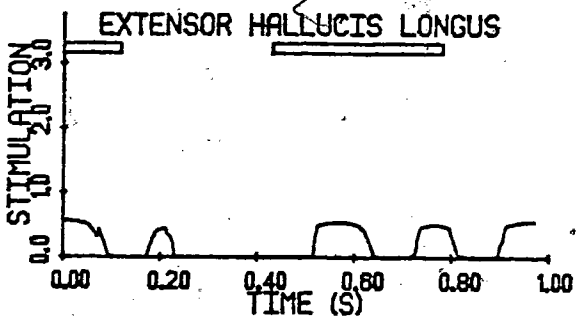
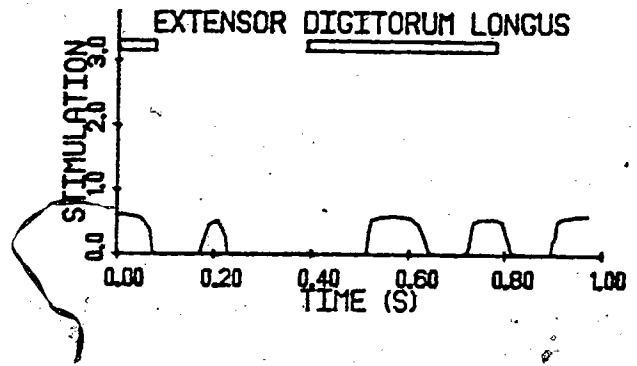
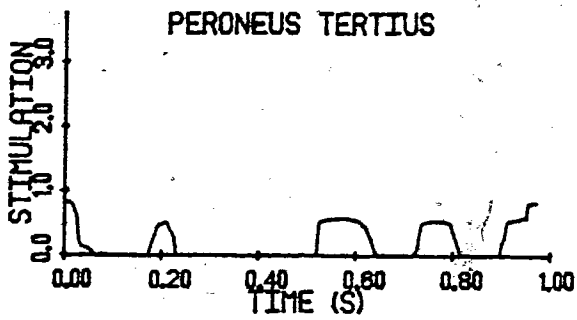
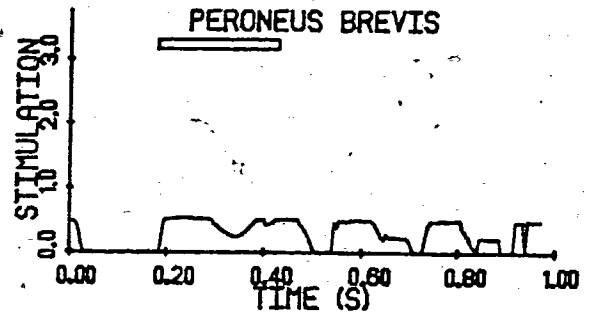
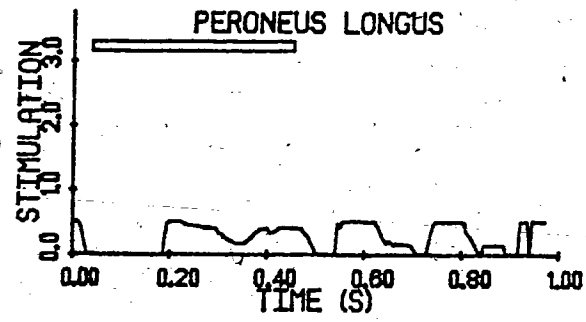


Figure 27 Continued.

stimulation to a specific muscle (Grillner, 1975). The incorporation of the modulating effect of the muscle spindles and golgi tendon organs into future versions of the model may be warranted.

A second source of error may reside within the specific analysis performed. The gait cycle was broken into 195 equal time intervals ( $\Delta t = 0.005$ ) for analysis. This means that the muscles could only receive a finite number of different stimulation levels. The rapid on-off stimulation patterns received by some muscles, which are reflected in their jerky force-time profiles, may be minimized if the analysis was performed with a smaller  $\Delta t$ . It is interesting to note that Hatze's model (1975a) requires a  $\Delta t$  ten times smaller than that used in this thesis. In the context of this thesis a smaller  $\Delta t$  was not used because of limited computer resources. It should be noted that the model was run at 40 frames per second giving muscle force patterns not vastly different from those presented in the body of this thesis. Since the force-velocity relationship tends to damp out the rapid changes in the activation profile, very fast sampling and analysis rates may not be required. It is recommended, however, that the sensitivity of the model to different interval times be explored.

One of the intents of this thesis was to use the results of the physiological model to examine the hypothesis that the outputs from the pattern generators were simple oscillating signals (Patla, 1981; Perret and Cabelguen, 1980). These interact, stimulate the muscles, and form the movement we call walking (Grillner, 1975; Shik and Orlovsky, 1976). When one examines Figure 26 however, no such statement can be made. The pattern generators, as defined in this thesis, output rather complex waveforms which suggest a mathematical rather than a physiological foundation.

Further work on the analysis of the pattern generator signals seems warranted to describe them in terms of neurophysiological

constructs. Insufficient experimental evidence is available to do this at the present time. A second version of the model could then be constructed to activate the muscles via the pattern generator model to predict the resulting segment kinematics.

#### Discussion and Implications of the Findings

The scientific literature suggests two distinct approaches to predict muscle forces. The first, the 'reduction' method (Paul, 1965; Morrison, 1968), makes a series of anatomical and functional simplifications to reduce the number of force-carrying structures crossing a joint to make the problem mathematically solvable. This method is useful when joint force rather than muscle forces are required.

The second procedure, which solves for individual muscle forces, is the 'optimization' approach. This method, developed since the early seventies (Seireg and Arvikar, 1973, 1974; Penrod, 1974), is based on the assumption that the body selects muscles for a given activity according to some objective such as the minimization of muscle force. This technique has been widely used with varying degrees of success. In general, muscle force solutions have improved with the introduction of physiologically based constraints such as minimizing muscle stress (Crowninshield, 1978; Pedotti *et al.*, Patriarco *et al.*, 1981), power (Hardt, 1978), or endurance (Crowninshield and Brand, 1981).

In this thesis a simple neurophysiological control model is developed to select individual muscles for a given activity. Mathematical analogues of the locomotor muscles, incorporating force-length-velocity-activation properties derived from geometrical and published data, are stimulated to generate the segment movements as externally recorded. Since individual muscle control is founded upon physiological constructs, mathematically based optimization techniques are not required. This is not to say that the execution of movement does not follow some objective such as the minimization of energy cost or maximizing endurance.

The control model assumes that if some objective is followed it is 'hard-wired' into the neurological control system through evolution.

A comparison of the model's estimation of the individual muscle force profiles with published EMG data shows good results. This enthusiasm is not mirrored when the EMG patterns are compared to the model's estimation of the actual neural input to the muscles. The incorporation of afferent input and the inclusion of more precise internal model parameters seems warranted. However, the results partially demonstrate that it is feasible to construct a physiological model to evaluate individual muscle forces from limb kinematics. In addition, such a model gives quantitatively better results than reduction or optimization techniques.

The model is founded upon the ability to accurately estimate the lengths and velocities of the muscles from external measurements and the prediction of the muscle force-stimulation relationship from geometrical properties and structure kinematics. These data were acquired from the literature to test the model's premise that individual muscle forces could be calculated.

One possible criticism of this thesis is that many assumptions were made to develop and implement the model. A brief critique of the model's assumptions is found at the end of Chapter III. It could be argued then that having built a highly speculative model it might have been better to choose a small part of the total project and validate it. It was the authors intention, however, to develop and implement the framework of the model within the context of a specific goal, that being it's use in either clinical or sport applications. It's validation, employing several neural, physiological, and mechanical measures, would be a much larger study taking many years.

One validation method would be a comparison of the maximum net muscle moment generated by a subject (i.e. using the CYBEX isokinetic dynamometer) to that estimated by the computer model. Specific experimental protocols could also be designed to examine the intrinsic strength, moment arm estimations and the force-length-velocity-activation properties of specific muscle groups (see Hatze, 1980b).

A second and better validity check of the model would be to perform a cat experiment simultaneously measuring the limb and joint kinematics (Manter, 1938), the electromyographic activity of the locomotor muscles (Engberg and Lundberg, 1969), and recording the afferent and efferent nerve potentials (Perret and Cabelguen, 1980). Direct muscle force (Walmsley *et al*, 1978) and length measurements (Prochazka *et al*, 1974) would also be used. Upon completing this experimental phase the cat would be anesthetized and the mechanical properties of the locomotor muscles determined (Burke *et al*, 1973; Joyce *et al*, 1969). The final experimental phase would see the geometrical properties of the sacrificed cat acquired. Only through a set of experiments such as these could the model within this thesis, or any technique that attempts to solve for individual muscle forces, be validated. Such an experiment must be the thrust of a major research effort in the near future.

The model within this thesis could also be used as a research tool in which systematic alteration of the muscle properties would allow their true values to be estimated. For instance, one shortcoming of this thesis is that the fast twitch fibers were not recruited during the walk. By studying some maximal human movement (eg. maximum one-legged vertical jump) several muscles should generate near maximal forces. This test could justify or specify some of the model's internal assumptions, in particular the maximum intrinsic strength of the muscles. Similar experiments could be constructed to test the sensitivity of the modelled solutions to variations in these internal parameters.



Fundamental changes to the model, such as the number of pattern generators and how they control the individual muscles, could also be suggested by appropriate model manipulations.

A complete kinetic description of human gait has many applications including the improvement of athletic performance and the clinical study of pathological gait arising from muscle activation abnormalities, tendon transplants or amputation. The usefulness of the present implementation of the physiological model for these purposes is limited in that it is very time consuming which may not be tolerated by the coach or physician. The kinematic description of the moving subject was acquired from cinematography which requires time for both processing and data extraction. Ideally an on-line kinematic data acquisition system (SELSPOT, electrogoniometry) married to a computer capable of simultaneously calculating the muscle forces would see wide application. Since the present implementation takes approximately 30 minutes to analyze one second of human activity individual muscle force analyzes may never find wide use in sport or clinical settings.

## CHAPTER VI

SUMMARY, CONCLUSIONS AND RECOMENDATIONSSUMMARY

The aim of this thesis is to formulate and implement a model capable of predicting the individual muscle forces in the right lower limb of a walking man. The approach developed is a physiological hierarchical model the lowest level of which concerns itself with the data necessary to define the musculo-skeletal system. These include the muscle's moment arms, lengths and velocities. Data describing the muscle anatomy and bone structure are also included.

The middle section, the muscle model, defines the force-length-velocity-activation relationship of a single muscle unit. These data, with those from the anatomical model, are used to estimate the maximum and minimum force a muscle can exert given its previous force history, current kinematics and previous stimulation. The stimulation needed to generate any intermediate force is also defined.

At the top of the hierarchy the control model provides a singular solution of the muscle forces, within the constraints defined in the muscle and anatomical models, by stimulating the muscles. The control model selects the muscle stimuli, based on a simple neurophysiological model of pattern generators, to satisfy the measured net muscle moments about those axes for which large range of movement exist. It is assumed that one pattern generator exists for each major degree of freedom in the leg.

Estimating the muscle forces during human activity required a variety of information. One male volunteer was selected and underwent a lengthy anthropometric session so that a standard

lower limb, defined in the anatomical model, could be scaled to him using homogeneous transformations and anthropometric measurements. This scaling defined the geometrical definition of the muscles required in the analysis.

A walking trial involving normal gait was performed. Both three-dimensional cinematographic and force plate records were collected to define the kinematics of the leg segments and the ground reaction forces. From these data the instantaneous lengths, velocities and moment arms of the muscles and the net muscle moments were calculated. These data were then used to estimate the output from the pattern generators which in turn specified the neural input to and the force in each muscle.

### CONCLUSIONS

Based on the findings of this study, which examined one subject, the following conclusions seem warranted:

1. the use of transformations to scale a skeleton to a subject suggests that a) geometrical differences between the bones of the lower limb are largely homogeneous deformations and b) the use of a redundant set of points to define the transformation is beneficial;
2. the anthropometric scaling technique used to define the geometrical properties of the muscles accounted for 80 percent of the total muscle mass of the lower limb when compared to Cadaver data. This suggests that either the scaling technique or the geometrical data base were incorrect;
3. the techniques used to track the subject's segments in space (three-dimensional cinematography) and to synchronize the force plate and film data gave good results when the magnitude and pattern of the joint moments and forces were compared to those in the literature;

4. the combination of accurate modelling of the line of action of the muscles and good segmental kinematics allowed good estimations of the in vivo length changes of the muscles during activity;
5. the muscle model does not adequately predict the force response of a total muscle to a step input of stimulation due to the slow and fast twitch fibres being synchronously recruited; and
6. individual muscle forces were predicted using the physiological model developed in this thesis. Muscle recruitment was confined almost entirely to the slow twitch fibres and both the synergistic and antagonistic actions of muscle were demonstrated during normal gait.

#### RECOMMENDATIONS

On the basis of the data obtained and the problems encountered in this study the following recommendations into the use of a physiological model to solve for individual muscle forces seem warranted:

1. that the accurate modelling of the musculo-skeletal system be explored both as a separate intensive investigation and as a series of revisions to the present anatomical model,
2. that the anthropometric scaling technique be improved to better predict the mass and cross-sectional properties of the locomotor muscles,
3. that the muscle model be modified to include the asynchronous recruitment of motor units,
4. that the data collection and analysis protocol be replicated with the inclusion of EMG data so that the predicted muscle force profiles may be compared to the EMG data,

5. that the sensitivity of the model solutions to varying data collection rates be explored,
6. that further work be done on the modelling of the pattern generators, and
7. that a rigorous validation of the model be undertaken to define limits on the acceptability of its predictions.

APPENDIX A

Homogeneous transformation from one three-dimensional space to another.

If  $[x \ y \ z \ 1]$  is some point in three-dimensional space, we can transform it to some other space  $[x' \ y' \ z' \ 1]$  using:

$$[x \ y \ z \ 1] * [T'] = [x' \ y' \ z' \ 1] \quad (A1)$$

where

$$[T'] = \begin{bmatrix} T_{11} & T_{12} & T_{13} & 0 \\ T_{21} & T_{22} & T_{23} & 0 \\ T_{31} & T_{32} & T_{33} & 0 \\ T_{41} & T_{42} & T_{43} & 1 \end{bmatrix} \quad (A2)$$

This 4x4 transformation can be partitioned into four separate sections:

$$\left[ \begin{array}{ccc|c} 3 \times 3 & & & 3 \\ \hline 1 \times 3 & & & 1 \end{array} \right] \quad (A3)$$

The 3x3 matrix creates a linear transformation in the form of scaling, shearing and rotation. The 1x3 row matrix produces translation and the 3x1 column matrix perspective transformations. The final single element provides for overall scaling. It should be noted that the first three columns of  $[T']$  act exclusively on the X, Y and Z coordinates, respectively, whilst the fourth column acts on all values. Since we are not interested in a perspective transformation, and wish to scale the X, Y and Z coordinates independently, the fourth column in equation A2 has been set to zeros and one.

Expanding equation (A1) and simplifying:

$$\begin{aligned} T_{11} x + T_{21} y + T_{31} z + T_{41} &= x' \\ T_{12} x + T_{22} y + T_{32} z + T_{42} &= y' \\ T_{13} x + T_{23} y + T_{33} z + T_{43} &= z' \end{aligned} \quad (A4)$$

Assuming that  $x, y, z$  and  $x', y'$  and  $z'$  are known, Equation (A4) represents three equations in the 12 unknown transformation elements. Applying these equations to  $n$  ( $n \geq 4$ ) non-coplanar known points, in two reference systems, yields a system of  $3n$  equations in 12 unknowns. The transformation can then be determined. If  $n > 4$  the problem is overspecified and can only be solved by some mean or best fit technique. The use of more than four points increases the accuracy of the technique and should be used whenever possible.

It is also possible to decompose the transformation matrix into three matrices: the first ( $T_s$ ) includes scaling terms ( $S_x, S_y, S_z$ ), another ( $T_R$ ) rotations ( $R_x, R_y, R_z$ ) and the third ( $T_T$ ) translations ( $T_x, T_y, T_z$ ). These matrices are written:

$$[T_s] = \begin{bmatrix} S_x & 0 & 0 & 0 \\ 0 & S_y & 0 & 0 \\ 0 & 0 & S_z & 0 \\ 0 & 0 & 0 & 1 \end{bmatrix} \quad (A5)$$

$$[T_T] = \begin{bmatrix} 1 & 0 & 0 & 0 \\ 0 & 1 & 0 & 0 \\ 0 & 0 & 1 & 0 \\ T_x & T_y & T_z & 1 \end{bmatrix} \quad (A6)$$

$$[T_R] = \begin{bmatrix} CR_x*CR_y & SR_x*CR_y & -SR_y & 0 \\ -SR_x*CR_z + CR_x*SR_y*SR_z & CR_x*CR_z + SR_x*SR_y*SR_z & CR_y*SR_z & 0 \\ SR_x*SR_z + CR_x*SR_y*CR_z & -CR_x*SR_z + SR_x*SR_y*CR_z & CR_y*CR_z & 0 \\ 0 & 0 & 1 & 0 \end{bmatrix} \quad (A7)$$

where  $c$  and  $s$  are the cosine and sine of the rotation angles respectively.

Concatenation of these three matrices:

$$T_c = T_R * T_s * T_T \quad (A8)$$

gives a matrix whose elements approximate those calculated via equation (A4). We can therefore define 12 nonlinear equations with 9 unknowns. This can be solved using a nonlinear least square algorithm (eg. IMSL - ZXSSQ, 1980). It is then possible to reconstruct a transformation matrix which includes only those constituents the user desires (eg. rotations and translations).



APPENDIX BDefining the muscle curvilinear sections.

Let a pair of points through which the curve must pass be the vectors  $P_1$  and  $P_2$ . Corresponding tangent vectors at these points are  $\dot{P}_1$  and  $\dot{P}_2$ . In the model these are determined from the direction cosines of the two straight line segments surrounding the curvilinear section. This allows a smooth transition between the straight and curved muscle sections.

A parametric cubic polynomial was used to fit the curved section. Within the cubic section the parameter  $t$  varies between the two end points  $t_1$  and  $t_2$ . To simplify calculations we can assign  $t_1 = 0$ . A parametric cubic polynomial may be written as:

$$P(t) = A + Et + Ct^2 + Dt^3 \quad (B1)$$

where  $P(t) = [x(t) \ y(t) \ z(t)]$  is the position vector of any point on the curve. Since  $P_1$ ,  $P_2$ ,  $\dot{P}_1$ , and  $\dot{P}_2$  are defined as above the four coefficients in equation (B1) are calculated as follows:

$$\begin{aligned} A &= P_1 \\ B &= \dot{P}_1 \\ C &= 3(P_2 - P_1)/t_2^2 - (2\dot{P}_1 + \dot{P}_2)/t_2 \\ D &= 2(P_2 - P_1)/t_2^3 + (\dot{P}_1 + \dot{P}_2)/t_2^2 \end{aligned} \quad (B2)$$

Any point and the length between the limits  $t_1$  and  $t_2$  can then be calculated.

APPENDIX CDefining the muscle and ligament moment arms.

The muscle and ligament moment arms (MA), relative to the GRS imbedded at each joint centre, were calculated from the line of action of these structures in the neighbourhood of the joint centers (JC). Given two points defining the direction and line of action of a muscle or ligament ( $EP_{1k}$  to  $EP_{2k}$ , where k represents the X, Y and Z coordinate), the direction cosines (D) of this structure were calculated.

$$D_k = (EP_{2k} - EP_{1k}) / \left( \sum_{k=1}^3 (EP_{2k} - EP_{1k})^2 \right)^{0.5} \quad (C1)$$

The coordinates of  $EP_{1k}$  relative to the joint centre were determined using:

$$P_k = EP_{1k} - JC_k \quad (C2)$$

The moment arms were then calculated.

$$\begin{aligned} MA_1 &= P_2 * D_3 - P_3 * D_2 \\ MA_2 &= P_3 * D_1 - P_1 * D_3 \\ MA_3 &= P_1 * D_2 - P_2 * D_1 \end{aligned} \quad (C3)$$

Equations (C1) to (C3) calculate the moment arms of a structure relative to the GRS. To transform these moment arms to the SRS the method discussed in Appendix F was used.

APPENDIX DThree-dimensional filming using the direct linear transformation.

For those unfamiliar with the homogeneous coordinate representation a brief introduction is given. In this notation, a point is represented in three dimensions whose real coordinates are in X, Y, and Z, either as the four part row vector  $[X \ Y \ Z \ 1]$  where 1 is the scale factor or the homogeneous term, or as any multiple of that vector where w is arbitrary, e.g.  $[wX, wY, wZ, w]$ . This vector can be represented in lower case notation  $[x, y, z, w]$  because X, Y, and Z can always be determined by dividing out w.

We can now define a generalized 4x4 transformation matrix for three-dimensional homogeneous coordinates. Thus, if  $[x \ y \ z \ w]$  is some point in three-dimensional space, we can transform it into some other space  $[x' \ y' \ z' \ w']$  using:

$$[x \ y \ z \ 1] * [T'] = [x' \ y' \ z' \ 1] \quad (D1)$$

where  $[T']$  is discussed in Appendix A. A more complete examination of the various transformations incorporated within this matrix is found in Newman and Spruell (1979).

It is important to note that the transformation projects one three-dimensional space into another three-dimensional space. These results can then be projected onto a two-dimensional plane, say  $Z = 0$  by using:

$$[T''] = \begin{bmatrix} 1 & 0 & 0 & 0 \\ 0 & 1 & 0 & 0 \\ 0 & 0 & 0 & 0 \\ 0 & 0 & 0 & 1 \end{bmatrix}$$

(D2)

Concatenation of the two matrices yields:

$$[T] = [T''] [T'] = \begin{bmatrix} F_{11} & F_{12} & 0 & F_{14} \\ F_{21} & F_{22} & 0 & F_{24} \\ F_{31} & F_{32} & 0 & F_{34} \\ F_{41} & F_{42} & 0 & F_{44} \end{bmatrix} \quad (D3)$$

It is now useful to write the transformation as:

$$[X \ Y \ Z \ 1] * [T] = w' [x^* \ y^* \ 0 \ 1] \quad (D4)$$

Note that  $x^*$  and  $y^*$  are the coordinates in the perspective projection onto the  $Z = 0$  plane. A similar procedure can be followed using projections onto the  $X = 0$  or  $Y = 0$  planes.

In a two dimensional view, produced by a camera, the depth coordinate is no longer available. Hence we can rewrite the projection as:

$$[X \ Y \ Z \ 1] * \begin{bmatrix} T_{11} & F_{12} & F_{13} \\ T_{21} & F_{22} & F_{23} \\ T_{31} & F_{32} & F_{33} \\ T_{41} & F_{42} & F_{43} \end{bmatrix} = w' [x^* \ y^* \ 1] \quad (D5)$$

Writing out equations (D5) we get:

$$\begin{aligned} T_{11} X + T_{21} Y + T_{31} Z + T_{41} &= w' x^* \\ T_{12} X + T_{22} Y + T_{32} Z + T_{42} &= w' y^* \\ T_{13} X + T_{23} Y + T_{33} Z + T_{43} &= w' \end{aligned} \quad (D6)$$

Substituting  $w'$  from the third equation into the first two and regrouping yields:

$$\begin{aligned} (T_{11} - T_{13} x^*) X + (T_{21} - T_{23} x^*) Y + (T_{31} - T_{33} x^*) Z + (T_{41} - T_{43} x^*) &= 0 \\ (T_{12} - T_{13} y^*) X + (T_{22} - T_{23} y^*) Y + (T_{32} - T_{33} y^*) Z + (T_{42} - T_{43} y^*) &= 0 \end{aligned} \quad (D7)$$

As suggested by Sutherland (1974) equation (D7) can be considered in three different ways.

- 1) Assume  $[T]$  and  $X, Y,$  and  $Z$  are known. We then have two equations with unknowns  $x^*$  and  $y^*$ . They may be used to solve directly for the coordinates of the perspective projection. This technique is often used in computer graphics (Sutherland, 1974; Newman and Sproull, 1979) to generate perspective views of objects.
- 2) If we know the transformation  $[T]$  and the positions of a point  $(x^*, y^*)$  in a picture, using equation (D7) yields two equations with the three unknowns  $X, Y,$  and  $Z$ . The location of a point in three-dimensional space can not be solved with this information. However, if two views are available, then equation (D7) can be written for both projections. Denoting the superscripts 1 and 2 to distinguish the same point in two views, we can define the following equations:

$$[A] * [X] = [B]$$

$$\text{where } [A] = \begin{bmatrix} T_{11}^1 & -T_{13}^1 & x^1 & T_{11}^1 & -T_{13}^1 & x^1 & T_{11}^1 & -T_{13}^1 & x^1 \\ T_{12}^1 & -T_{13}^1 & y^1 & T_{12}^1 & -T_{13}^1 & y^1 & T_{12}^1 & -T_{13}^1 & y^1 \\ T_{21}^2 & -T_{23}^2 & x^2 & T_{21}^2 & -T_{23}^2 & x^2 & T_{21}^2 & -T_{23}^2 & x^2 \\ T_{22}^2 & -T_{23}^2 & y^2 & T_{22}^2 & -T_{23}^2 & y^2 & T_{22}^2 & -T_{23}^2 & y^2 \end{bmatrix}$$

$$[X]^T = [X \ Y \ Z]$$

$$\text{and } [B]^T = [T_{43}^1 x^1 - T_{41}^1 \ T_{43}^1 y^1 - T_{42}^1 \ T_{43}^2 x^2 - T_{41}^2 \ T_{43}^2 y^2 - T_{42}^2]$$

(D8)

Equation (D8) represents four equations with the three unknowns X, Y, and Z. The problem is thus overspecified and can only be solved by some mean or best-fit technique. This can be accomplished by solving:

$$[A]^T[A][X] = [A]^T[B] \quad (D9)$$

where  $[A]^T$  is the transpose of  $[A]$ . If no solution is possible, the conditions imposed are redundant and no unique solution exists.

- 3) If the location of several points which appear in the perspective projection are known in three-dimensional space and in image space, then it is possible to determine the elements which make up the transformation matrix. These transformation elements can subsequently be used to determine the location of unknown points using the technique described above. Expanding equation (D7):

$$\begin{aligned} T_{11} X + T_{21} Y + T_{31} Z + T_{41} - T_{13} Xx^* - T_{23} Yx^* - T_{33} Zx^* - T_{43} x^* &= 0 \\ T_{12} X + T_{22} Y + T_{32} Z + T_{42} - T_{13} Xy^* - T_{23} Yy^* - T_{33} Zy^* - T_{43} y^* &= 0 \end{aligned} \quad (D10)$$

Assuming that  $x, y$  and  $X, Y$ , and  $Z$  are known, Equation (D10) represents two equations in the 12 unknown transformation elements. Applying these equations to  $n$  ( $n \geq 6$ ) non-coplanar known locations (control points) in both three-dimensional space and in the image plane (digitized coordinates) yields a system of  $2n$  equations in 12 unknowns. One can then determine the transformation. If  $n > 6$ , a least squares fit must be computed to solve for the unknowns. Cavanagh (1979) has reported that the use of 20 control points can, under certain circumstances, improve the accuracy of the DIT by an order of magnitude.

Equation (D10) has 12 unknowns but they are not linearly independent since it contains an arbitrary scale factor. Hence  $T_{43}$  may be defined as unity and the resulting transformation normalized. This reduces the requirement to 11 equations or  $5\frac{1}{2}$  points.

It should be noted that no prior knowledge of the transformation is required in the ELT method. Knowing the locations of several control points situated throughout the two photographic fields, and solving for the transformation, determines the location and the orientation of the cameras. These transformation elements can then be used to solve for the three-dimensional location of unknown points visible in both images.

APPENDIX EData smoothing using the Fourier transform.

A methodological problem long known in biomechanics research has been the validity of calculating derivatives from displacement data known to contain noise. It is known that the operation of differentiation increases the amplitude components linearly as a function of frequency; double differentiation results in an increase proportional to the square of the frequency. Since the noise is of a higher frequency than the signal of interest, unless some attempt at noise attenuation is made the calculation of velocity and acceleration from displacement is meaningless.

Two techniques have been applied to biomechanical data, digital filtering and Fourier series truncation as used by Pezzack et al. (1977) and Cappozzo et al. (1975), respectively. Digital filtering, since it is a recursive procedure, is limited in that a number of 'leading-in' data points must be available to initialize the filter. It is unclear, however, how many points are necessary; estimates range from 4 (Winter, 1979) to 15 (Dainty, 1979). A second prerequisite to use the digital filter is a knowledge of the frequency composition of the signal to be processed. This is generally made available from the second smoothing technique, Fourier series truncation.

Any signal as a function of time [F(t)] can be represented by a summation of harmonics:

$$F(t) = a_0 + \sum_{j=1}^N (a_j \sin w_j t + b_j \cos w_j t) \quad (E1)$$

- where ,  $a_0$  - mean value (DC component) of the signal  
 $j$  - harmonic number  
 $a_j, b_j$  - the amplitude of the  $j$ th harmonic  
 $w_j$  - the frequency of the  $j$ th harmonic  
 $N$  - the total number of harmonics in the data



The smoothing process consists of deleting the higher harmonics from the Fourier series. The choice of the number of harmonics to include in the reconstructed signal is done by inspecting the power at each harmonic (Cappozzo et al., 1975). The power at the  $j$ th harmonic is given by:

$$P_j = a_j^2 + b_j^2 \quad (E2)$$

When the power at a lower harmonic approaches that of the higher harmonics, or when the sum of the first  $j$  powers equals a predetermined value (eg. 90 percent) this is the harmonic selected for truncation.

APPENDIX FChanging reference systems.

On several occasions it was necessary to transform a set of data from one reference system ( $R_1$ ) to another ( $R_2$ ). Given the origin and three points equidistant along the X, Y and Z axes for  $R_1$  and  $R_2$  a transformation was calculated (see Appendix A) which translates and rotates  $R_1$  to  $R_2$ . Scaling was not included as equidistant points were used.

REFERENCES

- Abbott B.C., B. Bigland and J.M. Ritchie, The physical cost of negative work, J. Physiol. 117:380-390 (1952).
- Abbott B.C., and D.R. Wilkie, The relation between velocity of shortening and the tension-length curve of skeletal muscle, J. Physiol. 120:214-223 (1953).
- Alexander R.McN., and G. Goldspink, Mechanics and Energetics of Animal Locomotion Chapman and Hall, Ltd., London, 1977.
- Alexander R. McN., and A. Vernon, The dimensions of knee and ankle muscles and the forces they exert, J. Human Movement Studies 1:115-123 (1975).
- Allum J.H.J and I.R. Young, The relaxed oscillation technique for the determination of the moment of inertia of the limb segments, J. Biomechanics 9:21-25 (1976).
- An K.N., E.Y. Chao, W.P. Cooney and R.L. Linscheid, Normative model of human hand for biomechanical analysis, J. Biomechanics 12:775-788 (1979).
- An K.N., F.C. Hui, B.F. Morrey, R.L. Linscheid and E.Y. Chao, Muscles across the elbow joint: a biomechanical analysis, J. Biomechanics 14:659-670 (1981).
- Anderson P., Capillary density in skeletal muscle of man, Acta Physiol. Scand. 95:203-205 (1975).
- Anticsson E.K., Automatic 3-D gait analysis using a selfport based system, Proc. International Society of Electrophysiological Kinesiology, Boston, Mass., (1979).
- Arcan M., M. Brull and A. Voloshin, A new development in locomotion analysis: The integrated gait laboratory. Proc. Biomechanics Sport Games and Sport Activities, Wingate Inst. Phys. Ed. and Sport, Israel, pg.19-29 (1979).
- Ariano M.A., R.B. Armstrong and V.R. Edgerton, Hindlimb muscle fibre populations of five mammals, J. Histochem. Cytochem. 21:51-55 (1973).
- Arnold V.G. and W. Worthmann, Zur Querschnittsmessung von Sehnen Unter biomechanischen Gesichtspunkten, Anat. Anz. 135:288-294 (1974).
- Arvikar R.J., A mathematical model for the musculoskeletal system for the lower extremities. M.Sc. Thesis in Engineering, The University of Wisconsin, 1971.
- Awan M.Z. and G. Goldspink, Energetics of the development and maintenance of isometric tension by mammalian fast and slow muscles, J. Mechanochemistry Cell Motility 1:97-108 (1972).

Bahler A.S., Series elastic component of mammalian skeletal muscle, Amer. J. Physiol. 213:1560-1564 (1967).

Bahler A.S., Modeling of mammalian skeletal muscle, IEEE Trans. Biomed. Engr. 15:249-256 (1968).

Bahler A.S., J.T. Fales and K.L. Zierler, The active state of mammalian skeletal muscle, J. Gen. Physiol. 50:2239-2253 (1967).

Bahler A.S., J.T. Fales and K.L. Zierler, The dynamic properties of mammalian skeletal muscle, J. Gen. Physiol. 51:369-384 (1968).

Barbenel J.C., The biomechanics of the temporomandibular joint: A theoretical study, J. Biomechanics 5:251-256 (1972).

Barret B. The length and mode of termination of individual muscle fibres in the human sartorius and posterior femoral muscles, Acta Anat. 48:242-257 (1962).

Bartholomew S.H., Determination of knee moments during swing phase of walking and physical constraints of the human shank, Biomechanics Lab Report, UCAL Berkeley, Series II, Issue 19 (1952).

Beetham W.P., H.F. Polley, C.H. Slocumb and W.F. Weaver, Physical examination of the joints. W.B. Saunders Company, Philadelphia, 1965.

Benedict J.V., I.B. Walker and E.H. Harris, Stress-strain characteristics and tensile strength of unembalmed human tendon, J. Biomechanics 1:53-63 (1968).

Benninghoff A. and H. Rollhauser, Zur inneren Mechanik des gefiederten Muskels, Pflugers Arch. 254:527-548 (1952).

Bigland B. and O.C.J. Lippold, The relation between force, velocity and integrated electrical activity in human muscles, J. Physiol. 123:214-224 (1954).

Binder M.D., W.E. Cameron and D.G. Stuart, Speed-force relations in the motor units of the cat tibialis posterior muscle, Amer. J. Phys. Med. 57:57-65 (1978).

Blacharski P.A., J.M. Scmerset and D.G. Murray, A three-dimensional study of the kinematics of the human knee, J. Biomechanics 8:375-384 (1975).

Blanton P.L., and N.L. Biggs, Ultimate tensile strength of fetal and adult human tendons, J. Biomechanics 3:181-189 (1970).

Bornhorst W.J., and J.E. Minardi, A phenomenological theory of muscular contraction, II. Generalized length variations, Biophysical Journal 10:155-172 (1970).

Braune W. and C. Fisher, Über den Schwerpunkt des menschlichen Körpers, mit Rücksicht auf die Ausrüstung des deutschen Infanteristen. Abh. d. math.-phys. cl. d. K. Sachs. Gesellsch. der Wiss., Bd. 26, S. 561-672 (1889).

Bresler B., and J.P. Frankel, The forces and moments in the leg during level walking, Amer. Soc. Mech. Engr. 48-A-62:27-35 (1950).

Bub D., Morphologische und funktionelle Analyse des Musculus adductor magnus und Musculus gracilis. Doctoral Thesis. University of Rostock, 1963.

Buchthal F. and H. Schmalbruch, Contraction times and fiber types in intact human muscle, Acta Physiol. Scand. 79:435-452 (1970).

Burke R.E., A comment on the existence of motor unit "types", in The Nervous System Volume 1: The Basic Neurosciences, D.B. Tower, ed., Raven Press: New York, 1975, pp. 611-619.

Burke R.E., and V.R. Edgerton, Motor unit properties and selective involvement in movement, Movement, Exercise and Sport Science Reviews 3:31-81 (1975).

Burke R.E., D.N. Levine, P. Tsairis and R.E. Zajac, Physiological types and histochemical profiles in motor units of the cat gastrocnemius, J. Physiol. 234:723-748 (1973).

Burke R.E., and P. Tsairis, Anatomy and innervation ratios in motor units of cat gastrocnemius, J. Physiol. 234:749-765 (1973).

Cadaver Analysis Study, Instituut voor Morfologie, Vrije Universiteit Brussel, J.P. Clarys, A.D. Martin and D.T. Drinkwater, 1980.

Calow D.R. and R. McN. Alexander, A mechanical analysis of the hind limb of a frog (Rana temporaria), J. Zool. 171:293-321 (1973).

Cappozzo A., T. Leo and A. Pedotti, A general computing method for the analysis of human locomotion, J. Biomechanics 8:307-320 (1975).

Carlson F.D. and D.R. Wilkie, Muscle Physiology. Prentice-Hall, Inc., Englewood Cliffs, 1974.

Cavanagh P.R., Instrumentation and methodology in biomechanical studies of sport games, Proc. Biomechanics Sport Games and Sport Activities, Wingate Inst. Phys. Ed. and Sport, Israel, pp. 12-18 (1979).

Cavanagh P.R. and M.A. LaFortune, Ground reaction forces in distance running, J. Biomechanics 13:397-406 (1980).

- Cavanagh P.R. and R.J. Gregor, Knee joint torque during the swing phase of normal treadmill walking, J. Biomechanics 8:337-344 (1975).
- Chaffin D.B., A computerized biomechanical model - Development of and use in studying gross body actions, J. Biomechanics 2:429-441 (1969).
- Chao E.Y. and K. Rim, Application of optimization principles in determining the applied moments in the human leg joints during gait, J. Biomechanics 6:497-510 (1973).
- Chapman A.E., The investigation of mechanical models of muscle based upon direct observations of voluntary dynamic human muscular contraction. Ph.D. Thesis. University of London, 1975.
- Chhibber S.R. and I. Singh, Asymmetry in muscle weight and one-sided dominance in the human lower limbs, J. Anat. 106:553-556 (1970).
- Chow C.K. and D.H. Jacobson, Studies of human locomotion via optimal programming, Math. Biosc. 10:239-306 (1971).
- Clauser E.C., J.T. McConville and J.W. Young, Weight, volume, and center of mass of segments of the human body, Aerospace Medical Research Laboratory, Wright-Patterson Air Force Base, Ohio, Report AMRL-TR-69-70 (1969).
- Close R.I., Dynamic properties of fast and slow skeletal muscles during development, J. Physiol. 173:74-95 (1964).
- Close R.I., Dynamic properties of mammalian skeletal muscle, Physiol. Reviews 52:129-199 (1972).
- Costill D.L., W.J. Fink and M.L. Pollock, Muscle fiber composition and enzyme activities of elite distance runners, Med. Sci. Sport 8:96-100 (1976).
- Cronkite A.E., The tensile strength of human tendons, Anat. Rec. 64:173-186 (1936).
- Crouch J.E., Functional Human Anatomy, second edition, Lea and Febiger, Philadelphia, 1972.
- Crowninshield R.D., Use of optimization techniques to predict muscle forces, J. Biomechanical Engrg. 100:88-92 (1978).
- Crowninshield R.D. and P.A. Brand, A physiologically based criterion of muscle force prediction in locomotion, J. Biomechanics 14:793-802 (1981).
- Crowninshield R.D., R.C. Johnson, J.G. Andrews and R.A. Brand, A biomechanical investigation of the human hip, J. Biomechanics 11:75-85 (1978).

Dainty D.A., Validation of a technique for determining ground reaction forces in three dimensions. Ph.D. Thesis. Department of Physical Education, The Pennsylvania State University, 1979.

Dempster W.T., Space requirements of the seated operator. Geometrical, kinematic, and mechanical aspects of the body with special reference to the limbs. WADC Technical Report 55-159, Wright Air Development Centre, Air Research and Development Command, United States Air Force, Wright-Patterson Air Force Base, Ohio (1955).

Desmedt J.E. and E. Godaux, Ballistic contractions in man: Characteristic recruitment pattern of single motor units of the tibialis anterior muscle, J. Physiol. 264:673-693 (1977a).

Desmedt J.E. and E. Godaux, Fast motor units are not preferentially activated in rapid voluntary contractions in man, Nature 267:717-719 (1977b).

Dostal W.F. and J.G. Andrews, A three-dimensional biomechanical model of hip musculature, J. Biomechanics 14:803-812 (1981).

Drillis R. and R. Contini, Body segment parameters, Technical Report Number 1166.03, School of Engineering and Science, New York University, New York, 1966.

Esbashi S. and E. Endo, Calcium and muscle contraction, Prog. Biophys. 18:123-183 (1968).

Eberhart H.D., V.T. Inman and E. Bresler, The principal elements in human locomotion, in Human Limbs and Their Substitutes, P.E. Klopsteg and P.D. Wilson, eds., Harner Publishing Company, New York, 1954.

Eberstein A. and J. Goodgold, Slow and fast twitch fibers in human skeletal muscle, Amer. J. Physiol. 215:535-547 (1968).

Edgerton V.R., J.L. Smith and D.R. Simpson, Muscle fibre type populations of human leg muscles, Histochem. J 7:259-266 (1975).

Edman K.A.P., G. Elzinga and M.I.M. Noble, Enhancement of mechanical performance by stretch during tetanic contractions of vertebrate skeletal muscle fibres, J. Physiol. 281:139-155 (1978).

Edman K.A.P., and A. Kiessling, The time course of the active state in relation to sarcomere length and movement studied in single skeletal muscle fibres of the frog, Acta Physiol. Scand. 81:182-196 (1971).

Elder G.C.B., The heterogeneity of fibre type populations in human muscle, Med. Science Sport 9:64 (1977).

Elder G.C.B., Personal communication, McMaster University, Canada, 1980.

- Elftman H., Forces and energy changes in the leg during walking, Amer. J. Physiol. 125:339-356 (1938).
- Elftman H., The function of the muscles in locomotion, Amer. J. Physiol. 125:357-366 (1939).
- Engberg G.I. and A. Lundberg, An electromyographic analysis of stepping in the cat, Experientia 18:174-187 (1962).
- Engin A.E., Passive resistive torques about the long bone axes of major human joints, Aviat., Space and Enviro. Med. 50:1052-1057 (1979).
- Essen B., and T. Haggmark, Lactate concentration in type I and type II muscle fibres during muscular contractions in man, Acta Physiol. Scand. 95:344-346 (1975).
- Essen B., and J. Henriksson, Glycogen content of individual muscle fibers in man, Acta Physiol. Scand. 90:645-647 (1974).
- Eycleshymer A.C., and D.M. Schoemaker, A Cross-Section Anatomy, Appleton-Century-Crofts, New York, 1970.
- Felkel E.O., Determination of acceleration from displacement time data, Prosthetic Devices Research Project, UCAL Berkeley, Series, II, Issue 16 (1951).
- Fenn W.O. and E.O. Marsh, Muscular force at different speed of shortening, J. Physiol. 85:277-297 (1935).
- Finlay F.R. and P.V. Karpovich, Electrogoniometric analysis of normal and pathological gaits, Res. Quart. 35:379-384 (1964).
- Fisher O., Theoretical fundamentals for a mechanics of living bodies, (1906) in Human Mechanics - Four Monographs Abridged. W.M. Krogman and F.E. Johnston, eds., University of Pennsylvania, Philadelphia, 1963.
- FitzHugh R., A model of optimal voluntary muscular control, J. Math. Biol. 4:203-236 (1977).
- Frigo C. and A. Pedotti, Determination of muscle length during locomotion, in Biomechanics VI, E. Asmussen and K. Jorgensen, eds., University Park Press, Baltimore, 1977, pp. 355-360.
- Garnett R.A.F., M.J. O'Donovan, J.A. Stephens and A. Taylor, Motor unit organization of medial gastrocnemius, J. Physiol. 287:33-43 (1978).
- Gibbs C.L. and W.R. Gibson, Energy production of rat soleus muscle, Amer. J. Physiol. 223:864-871 (1972).



- Gollnick P.D., R.E. Armstrong, C.W. Saubert, K. Piehl and B. Saltin, Enzyme activity and fibre composition in skeletal muscle of untrained and trained men, J. Appl. Physiol. 33:312-319 (1972).
- Gollnick P.D., J. Karlsson, K. Piehl and B. Saltin, Selective glycogen depletion in skeletal muscle fibres of man following sustained contractions, J. Physiol. 241:59-67 (1974).
- Gordon A.M., A.F. Huxley and F.J. Julian, The variation in isometric tension with sarcomere length in vertebrate muscle fibres, J. Physiol. 184:170-192 (1966).
- Goslow G.E., W.E. Cameron and D.G. Stuart, The fast twitch motor units of cat ankle flexors. I. Tripartite classification on basis of fatigability, Brain Research 134:35-46 (1977a).
- Goslow G.E., W.E. Cameron and D.G. Stuart, The fast twitch motor units of cat ankle flexors. II. Speed-force relations and recruitment order, Brain Research 134:47-57 (1977b).
- Graham Brown T., Die Reflexfunktionen der Zentralnerven mit besonderer Berücksichtigung der rhythmischen Fachigkeiten beim sargeiter, Ergebn. Physiol. 15:480-790 (1916).
- Grant J.C.B., An Atlas of Anatomy. The Williams and Wilkins Co., 5th Edition, Baltimore, 1972.
- Gratz C.M., Tensile strength and elasticity tests on human fascia latae, J. Bone Jt. Surg. 13:173-186 (1931).
- Green H., Personal Communication, University of Waterloo, Canada, 1979.
- Grieve D.W. and R.V. Gear, The relationship between length of stride, step frequency, time of swing and speed of walking for children and adults, Ergonomics 9:379-399 (1966).
- Grieve D.W., S. Pheasant and P.P. Cavanagh, Prediction of gastrocnemius length from knee and ankle joint posture, in Biomechanics VI-A, E. Asmussen and K. Jorgensen, eds., pp. 405-411 (1978).
- Grillner S., Locomotion in the spinal cat, in Control of Posture and Locomotion, F.B. Stein, K.G. Pearson, R.S. Smith, and J.B. Redford, eds., Plenum, New York, 1973, pp. 515-535.
- Grillner S., Locomotion in vertebrates: Central mechanisms and reflex interaction, Physiol. Reviews 55:247-304 (1975).
- Grillner S. and P. Zangger, Locomotor movements generated by the deafferented spinal cord, Acta Physiol. Scand. 91:38A-39A (1974).
- Haggmark T., E. Jansson and B. Svane, Cross-sectional area of the thigh muscle in man measured by computed tomography, Scand. J. Clin. Invest. 38:355-360 (1978).

- Hanavan E.P., A mathematical model of the human body, AMRL-TR-64-102, Aerospace Medical Research Laboratories Wright-Patterson Air Force Base, Ohio, 1964.
- Hannah R.E., Interpretation of clinical gait analysis data, Proc. Special Conference of the Can. Soc. Biomechanics, - Human Locomotion, London, pp80-87 (1980).
- Hanson J. and H.F. Huxley, Structural basis of the cross-striations in muscle, Nature 172:530-532(1953).
- Hardt D.E., Determining muscle forces in the leg during normal human walking - An application and evaluation of optimization methods, J. Biomechanical Engr. 100:72-78(1978).
- Hardt D.E. and R.W. Mann, Muscle forces during walking: A minimum energy approach, Proc. International Society of Electrophysiological Kinesiologists, Boston, Mass., (1979).
- Hardt D.E. and R.W. Mann, A five body - three dimensional dynamic analysis of walking, J. Biomechanics 13:455-457(1980).
- Harris E.H., B.R. Bass and I.B. Walker, Tensile strength and stress-strain relationships in cadaveric human tendons, Anat. Rec. 148:289(1964).
- Hatze H., A control model of skeletal muscle and its application to a time-optimal bic-motion. Ph.D. Thesis. University of South Africa, 1975a.
- Hatze H., A new method for the simultaneous measurement of the moment of inertia, the damping coefficient and the location of the centre of mass of a body segment in situ, Eur. J. Appl. Physiol. 34:217-226(1975b)
- Hatze H., The complete optimization of a human motion, Math. Biosc. 28:99-135(1976).
- Hatze H., A myocybernetic control model of skeletal muscle, us Biol. Cybernetics 25:103-119(1977a).
- Hatze H., A complete set of control equations for the human musculic-skeletal system, J. Biomechanics 10:799-805(1977b).
- Hatze H., Critique of Pedotti's et al., Optimization of Muscle Force Sequencing in Human Locomotion, in Mathematical Biosciences, 38:57-76(1978), Applied Mechanics Reviews 32:1353-1354(1979).
- Hatze H., A model for the computational determination of parameter values of anthropometric segments, J. Biomechanics 13:833-843(1980a).
- Hatze H., Myocybernetic Control Models of Skeletal Muscle - Characteristics and Applications. University of South Africa Press, 1980b.

- Hatze H., The use of optimally regularized Fourier series for estimating higher-order derivative of noisy biomechanical data, J. Biomechanics 14:13-18 (1981).
- Hatze H. and J.D. Buys, Energy-optimal controls in the mammalian neuromuscular system, Biol. Cybernetics 27:9-20 (1977).
- Haxton H.A., Absolute muscle force in the ankle flexors of man, J. Physiol. 103:267-273 (1944).
- Hellander E. and C.-A. Thulin, Isometric tension and myofilament cross-sectional area in striated muscle, Amer. J. Physiol. 202:824-826 (1962).
- Henneman E. and C.B. Olson, Relations between structure and function in the design of skeletal muscle, J. Neurological Sciences 28:581-598 (1965).
- Henneman E., G. Somjen and D.O. Carpenter, Functional significance of cell size in spinal motoneurons, J. Neurophysiol. 28:560-580 (1965).
- Herman R., H. Schumberg and S. Reiner, A rotational joint apparatus: A device for study of tension-length relations of human muscle, Med. Res. Engn. 6:18-20 (1966).
- Hill A.V., The maximum work and mechanical efficiency of human muscles, and their most economical speed, J. Physiol. 56:19-41 (1922).
- Hill A.V., The heat of shortening and the dynamic constants of muscle, Proc. Royal Soc. Lond. 126:136-195 (1938).
- Huxley A.F. and R.M. Simmons, Mechanical properties of the cross-bridges of frog striated muscle, J. Physiol. 218:59P-60P (1971).
- Ikai M. and T. Fukunaga, A study on training effect on strength per unit cross-sectional area by means of ultrasonic measurement, Int. Z. angew. Physiol. 28:173-180 (1970).
- IMSL, International Mathematical and Statistical Library, Inc., Programmes ZSCNT, ZXMIN and ZXSSQ, Edition 8, Houston, Texas, 1979.
- Inman V.T., The Joints of the Body. The Williams and Wilkins Company, Baltimore, 1976.
- Jensen R.F., A model for body segment parameters, Unpublished Report, Laurentian University, Ontario, 1975.
- Jensen R.H. and D.T. Davy, An investigation of muscle lines of action about the hip: A centroid line approach vs the straight line approach, J. Biomechanics 8:103-110 (1975).

- Jensen R.H. and W.T. Metcalf, A systematic approach to the quantitative description of musculo-skeletal geometry, J. Anat. 119:209-221 (1975).
- Jewell B.R. and D.R. Wilkie, An analysis of the mechanical components in frog's striated muscle, J. Physiol. 143:515-540 (1958).
- Johnson, M.A., J. Polgar, D. Weightman and D. Appleton, Data on the distribution of fibre types in thirty-six human muscles. An autopsy study, J. Neurol. Sciences 18:111-129 (1973).
- Joyce G.C., P.M.H. Rack and D.R. Westbury, The mechanical properties of cat soleus muscle during controlled lengthening and shortening movements, J. Physiol. 204:461-474 (1969).
- Kann von F., Uber Dicke und Zahl Der Muskelfaser auf verschiedenen Querschnittshoehen des Musculus Sartorius Beim Menschen, Acta Anat. 30:351-357 (1957).
- Kapandji I.A., The Physiology of the Joints. Volume Two. Lower Limb. Churchill Livingstone, London, 1970.
- Katz B., The relation between force and speed in muscular contraction, J. Physiol. 96:45-64 (1939).
- Kendall H.O., F.P. Kendall and G.E. Gladsworth, Muscles: Testing and Function, second edition, The Williams and Wilkins Company, Baltimore, 1971.
- Kettlekamp D.B., R.J. Johnston, G.L. Smidt, E.Y. Chao and M. Walker, An electrogoniometric study of knee motion in normal gait, J. Bone Jt. Surg 52A:775-790 (1970).
- Khan M.A. and N. Khan, Statistical analysis of muscle fibre types from four human skeletal muscles, Anat. Anz. 144:246-256 (1976).
- Kolb H., Morphologische und Funktionelle Analyse des M. Tibialis Anterior, Z. fur Anat. Entwickl. 106:770-781 (1937).
- Komi P.V., J.H.I. Viitaslo, M. Havu, A. Thorstensson, B. Sjodin and J. Karlsson, Skeletal muscle fibres and muscle enzyme activities in monozygous and dizygous twins of both sexes, Acta Physiol. Scand. 100:385-392 (1977).
- Kuo S.S., Numerical Methods and Computers. Addison-Wesley, Reading, Mass., 1965.
- Ladrick I., Morphologische und funktionelle Analyse des M. adductor longus et brevis und des M. pectineus. Doctoral Thesis. University of Rostock, 1963.
- Lamoreux L.W., Kinematic measurements of walking, Amer. Soc. Mech. Engrs. 30:2-11 (1972).

- Levens A.S., C.E. Berkeley, V.T. Inman and J.A. Blosser, Transverse rotation of the segments of the lower extremity in locomotion, J. Bone Jt. Surg. 30A:859-872(1948).
- Levin A. and J. Wyman, The viscous elastic properties of muscles, Proc. Royal Soc. Lond. 101:218-243(1927).
- Lew W.D. and J.L. Lewis, An anthropometric scaling method with application to the knee joint, J. Biomechanics 10:171-181(1977).
- Lewis J.L., W.D. Lew and J.R. Zimmerman, A nonhomogeneous anthropometric scaling method based on finite element principles, J. Biomechanics 13:815-824(1980).
- Lundberg A., Reflex control of stepping, The Nansen Memorial Lecture V. Oslo: Universitetsforlaget, 1-42(1969).
- Mann R. and P. Sprague, A kinetic analysis of the ground leg during sprint running, Res. Quarterly 51:334-348(1980)
- Manter J.T., The dynamics of quadrupedal walking, J. Exptl. Biol. 15:522-540(1938).
- Marey E.J., Terrestrial locomotion of bipeds and quadrupeds, J. de l'Anat. et de la Physiol 9:42-80(1873).
- Margaria R., Biomechanics and Energetics of Muscular Exercise. Clarendon Press, Oxford, 1976.
- Marks M. and G. Hirschberg, Analysis of hemiplegic gait, Annals, New York Acad. Sci. 74:59-72(1958)
- Martin A.D. and D.T. Drinkwater, Personal Communication, Simon Fraser University, Canada, 1981.
- Matsumoto Y., Validity of the force-length relation for muscle contraction in the length region,  $l \leq l_0$ , J. Gen. Physiol. 50:1125-1137(1967).
- McCrorey H.I., H.H. Gale and N.R. Alpert, Mechanical properties of cat tenuissimus muscle, Amer. J. Physiol. 210:114-120(1966).
- McGhee R.B., S.H. Koozekanni, S. Gupta and T.S. Cheng, Automatic estimation of joint forces and moments in human locomotion from television data, Proc. of IV IFAX Symp. on Identification and Parameter Estimation, USSR (1976).
- Miller D.I., Body segment contributions to sport skill performances: Two contrasting approaches, Research Quarterly 51:219-233(1980).
- Milner-Brown H.S., R.B. Stein and R. Yemm, The orderly recruitment of human motor units during voluntary isometric contractions, J. Physiol. 230:359-370(1973).

- Miyashita M., H. Matsui, M. Miura, T. Hoshikawa and S. Toyoshima, Electricmyographic study on positive and negative works. III. Relationship between force, velocity and integrated electrical activity in positive and negative works, Res. J. phys. Educ. (Japan) 14:98-101(1969).
- Morrison J.B., The forces transmitted by the human knee joint during activity. Ph.D. Thesis in Engineering. University of Strathclyde, 1967.
- Morrison J.B., Bioengineering analysis of force actions transmitted by the knee joint, Biomed. Engn. 3:164-170(1968).
- Morrison J.B., The mechanics of muscle function in locomotion, J. Biomechanics 3:431-451(1970).
- Muller G., Ueber Struktur und Funktion der Glutealmuskeln sowie des M. tensor fascia latae. Doctoral Thesis. University of Rostock, 1966.
- Muller K., Ueber Struktur und Funktion der inneren Huftmuskeln. Doctoral Thesis. University of Rostock, 1967.
- Murray M.P., A.B. Drought and R.C. Kory, Walking patterns of normal men, J. Bone Jt. Surg. 46A:335-360(1964).
- Muybridge E., The human figure in motion. Dover Publication Inc., New York, 1955.
- Neumann K., Struktur- und Funktionsanalyse des Musculus quadriceps femoris. Doctoral Thesis. University of Rostock, 1963.
- Newmann W.M. and R.F. Sproule, Principles of Interactive Graphics. McGraw-Hill, New York, Second Edition, 1979.
- Norman R.W. and D.A. Winter, Biomechanics: A review of literature with recommendation for research, University of Waterloo Research Institute, Project No. 603-07(1976).
- Norris F.H., Isometric relaxation of striated muscle, Amer. J. Physiol. 201:403-407(1961).
- Nubar Y. and R. Contini, A minimal principle in biomechanics, Bull. Math. Biophysics 23:377-390(1961).
- Oberg K., Mathematical modelling of human gait: an application of the SELSPOT system, in Biomechanics IV, R.C. Nelson and C.A. Morehouse, eds., pp. 78-84(1974).
- O'Connell A.L., An estimation of tension exerted by hip extensors during two different balance poses on the right lower extremity, in Biomechanics III, S. Cerquiglini, A. Venerando and J. Wartenweiler, eds., pp. 172-174(1973).
- O'Malley C.D. and J.B. Saunders, Leonardo da Vinci on the human body. H. Schuman, Inc., New York, 1952.

- Otahal S., A method of measuring some kinetic properties of voluntary muscle activity, in Biomechanics II, J. Vredenburg and J. Wartenweiler, eds., pp. 181-184 (1971).
- Page R.L., Moments of inertia of the human body about a vertical axis, Research in Physical Education 4:221-223 (1969).
- Page R.L., Manikin method of finding the centre of gravity, Research in Physical Education 1:14-23 (1969).
- Page R.L., Moments of inertia of the human body - 1. British J. Physical Education 1:33-40 (1970).
- Page R.L., Moments of inertia of the human body - 2. British J. Physical Education 1:61-63 (1970).
- Panjabi M., Validation of mathematical models, J. Biomechanics 12:238 (1979).
- Parmley W.W., L.A. Yeatman and E.H. Scnenblick, Differences between isotonic and isometric force-velocity relations in cardiac and skeletal muscle, Amer. J. Physiol. 219:546-550 (1970).
- Patla A., On pattern generators for locomotion in mammals, Ph.D. Thesis, Simon Fraser University, 1981.
- Patriarco A.G., R.W. Mann, S.R. Simons and J.M. Mansour, An evaluation of the Approaches of Optimization Models in the prediction of muscles forces during human gait, J. Biomechanics 14:513-525 (1981).
- Paul J.P., Bio-engineering studies of the forces transmitted by joints. (II) Engineering analysis, in Biomechanics and Related Bio-Engineering Topics, Pergamon Press, Oxford, 1965, pp. 369-380.
- Paul J.P., Comparison of EMG signals from leg muscles with the corresponding force actions calculated from walkpath measurements, in Human Locomotor Engineering, The Institution of Mechanical Engineers, London, 1974.
- Pedotti A., Modelling biological systems by optimization methods, in Advances in Cybernetics and Systems, J. Rose, ed., Gordon and Breach, New York, 3:1307-1318 (1974).
- Pedotti A., V.V. Krishnan and L. Stark, Optimization of muscle-force sequencing in human locomotion, Math. Biosc. 38:57-76 (1978).
- Penrod D.D., D.T. Davy and D.F. Singh, An optimization approach to tendon force analysis, J. Biomechanics 7:123-129 (1974).
- Perret C. and J.-M. Cabelguen, Main characteristics of the hindlimb locomotor cycle in the decorticate cat with special reference to bifunctional muscles, Brain Research 187:333-352 (1980).

- Pezzack J.C., R.W. Norman and D.A. Winter, An assessment of derivative determining techniques used for motion analysis, J. Biomechanics 10:377-382 (1977).
- Pierrynowski M.R., Three-dimensional filming using the direct linear transformation, Unpublished work, 1980.
- Plagenhoef S., Computer programs for obtaining kinetic data of human movement, J. Biomechanics 1:221-234 (1968).
- Plagenhoef S., Patterns of Human Motion - A Cinematographic Analysis Prentice-Hall, Englewood Cliffs (1971).
- Plaja J., F. Maldonado and J.-R. Goig, Accelerometric and goniometric patterns of normal and pathological gaits, in Biomechanics V-A, P.V. Komi, ed., pp 347-351 (1975).
- Prince F.P., R.S. Hikida and F.C. Hagerman, Human muscle fibre types in weight lifters, distance runners and untrained subjects, Pflugers Arch. 363:19-26 (1976).
- Prince F.P., R.S. Hikida and F.C. Hagerman, Muscle fibre types in human athletes and non-athletes, Pflugers Arch. 371:161-165 (1977).
- Prochazka A., R.A. Westerman and S.P. Ziccone, Remote monitoring of muscle length and EMG in unrestrained cats, Electroencephalog. Clin. Neurophysiol. 37:649-653 (1974).
- Ramsey R.W. and S.F. Street, The isometric length-tension diagram of isolated skeletal muscle fibers of the frog, J. Cell. Comp. Physiol. 15:11-34 (1940).
- Reys J.H.O., Über die Absolute Kraft der Muskeln im Menschlichen Körper, Pflugers Arch. 160:183-204 (1915).
- Robertson D.G.E. and D.A. Winter, Prediction of ground reaction forces from kinematics, Can. J. App. Sport Sciences 4:252 (1979).
- Rohmann E., Struktur- und Funktionsanalysen der oberflächlichen Flexoren des Unterschenkels (M. gastrocnemius, M. plantaris longus und M. soleus). Doctoral Thesis. University of Rostock, 1963.
- Rouviere H., Anatomie Humaine, Descriptive, topographique et fonctionnelle, third edition, Volume III: membres, Systeme nerveux central, Masson et Cie, Paris, 1974.
- Saito M., K. Kobayashi, M. Miyashita and T. Hoshikawa, Temporal pattern in running, in Biomechanics IV, R.C. Nelson and C.A. Morehouse, eds., pp. 106-111 (1974).
- Saunders J., V. Inman and H. Eberhardt, The major determinants in normal and pathological gait, J. Bone Jt. Surg. 35A:543-558 (1953).



Schmalbruch H. and Z. Kamieniecka, Fiber types in the human brachial biceps muscle, Exp. Neurol. 44:313-328 (1974).

Schumacher V.G.H. and F. Wolff, Trockengewicht und physiologischer Querschnitt der menschlichen Skelettmuskulatur. I. Trockengewichte, Anat. Anz. 118:317-330 (1966a).

Schumacher V.G.H. and F. Wolff, Trockengewicht und physiologischer Querschnitt der menschlichen Skelettmuskulatur. II. Physiologische Querschnitte, Anat. Anz. 119:259-269 (1966b).

Schwarzacher H.J., Über die Länge und Anordnung der Muskelfasern im menschlichen Skelettmuskel, Acta Anat. 37:217-231 (1959).

Seireg A. and R.J. Arvikar, A mathematical model for evaluation of forces in lower extremities of the musculo-skeletal system, J. Biomechanics 6:313-326 (1973).

Seireg A. and R.J. Arvikar, The prediction of muscular load sharing and joint forces in the lower extremities during walking, J. Biomechanics 8:89-102 (1975).

Sexton A.W. and J.W. Gerston, Isometric tension differences in fibers of red and white muscles, Science 157:199 (1967).

Shurrager P.S. and F.A. Dykman, Walking spinal carnivores, J. Comp. Physiol. Psychol. 44:252-262 (1951).

Shik M.L. and G.N. Orlovsky, Neurophysiology of locomotor automatism, Physiol. Reviews 56:465-501 (1976).

Smidt G.L., Biomechanical analysis of knee flexion and extension, J. Biomechanics 6:79-92 (1973).

Smith A.J., Photographic analysis of movement, in Techniques for the Analysis of Human Movement, D.W. Grieve, D.I. Miller, D. Mitchelson, J.F. Paul and A.J. Smith, eds., Princeton Book Company, Princeton, New Jersey, pp3-32, 1976.

Soderberg G.L., R. Reiss, R.C. Johnston and R. Gabel, Kinematic and Kinetic Changes during gait as a result of hip disease, in Biomechanics V-A, P.V. Komi, ed., pp.437-443 (1975).

Sokolowska-Pituchowa J., C. Miaskiewicz, A. Skawina and K. Makos, Morphology and some measurements of the peroneus tertius in man, Polia Morphol. 33:91-103 (1974).

Sommerville D.M.V., Analytical Geometry of three dimensions, University Press, Cambridge, 1959.

Stein R.B. and E.Y.M. Wong, Analysis of models for the activation and contraction of muscle, J. Theor. Biol. 46:307-327 (1974).

- Steindler A., Kinesiology of the Human Body under Normal and Pathological Conditions, second edition. Charles C. Thomas, Publishers, Springfield, Illinois, 1955.
- Sugi H., Tension changes during and after stretch in frog muscle fibres, J. Physiol. 225:237-253 (1972).
- Sutherland D.H., An electrogoniometric study of the plantar flexors of the ankle in normal walking on the level, J. Bone Jt. Surg. 48-A:66-71 (1966).
- Sutherland D.H. and J.L. Hagy, Measurement of gait movements from motion picture film, J. Bone Jt. Surg. 54A:787-797 (1972).
- Sutherland I.E., Three-dimensional data input by tablet, Proc. Inst. Electr. Engr. 62:453-461 (1974).
- Tardieu C., P. Colbeau-Justin, M.D. Bret, A. Lespargot, E. Huet de la Tour and G. Tardieu, An apparatus and a method for measuring the relationship of triceps surae torques to tibio-tarsal angles in man, Eur. J. Applied Physiol. 35:11-20 (1976).
- Taub E. and A.J. Berman, Movement and learning in the absence of sensory feedback, in The Neuropsychology of Spatially Oriented Behaviour, S.J. Freedman, ed., Dorsey, Homewood, Ill., 1968, pp. 173-192.
- Thorstensson A., G. Gimby and J. Karlsson, Force velocity relations and fibre composition in human knee extensor muscle, J. Appl. Physiol. 40:12-16 (1976).
- Thurnaur P.G., Kinematics of finite, rigid body displacements, Amer. J. Physiol. 35:1145-1154D (1967).
- Trzenschik K. von and H.H. Loetzke, Strukturanalytische Untersuchungen am M. Soleus des Menschen, Anat. Anz. 124:297-313 (1969).
- University of California, The pattern of muscular activity in the lower extremity during walking, Institute of Engineering Research, Series II, Issue 25, Berkley, 1953.
- van Attevelde H. and A. Crowe, Active tension changes in frog skeletal muscle during and after mechanical extension, J. Biomechanics 13:323-331 (1980).
- van Faassen F., N.H. Molen and W. Bcon, Biomechanics of the normal and the pathological gait, in Biomechanics II, J. Vredenburg and J. Wartenweiler, eds., pp. 260-265 (1969).
- van Gheluwe B., A new three-dimensional filming technique involving simplified alignment and measurement procedures, in Biomechanics IV, R.C. Nelson and C.A. McCreesh, eds., pp. 476-481 (1974).

- Viitasalo J.T. and P.V. Komi, Force-time characteristics and fiber composition in the human leg extensor muscles, Europ. J. Applied Physiol. 40:7-15 (1978).
- Voss H., Tabelle der Muskelgewichte des Mannes, berechnet und zusammengestellt nach den Untersuchungen von W. Theile (1884), Anat. Anz. 103:356-360 (1956).
- Walker L.B., F.H. Harris and J.V. Benedict, Stress-strain relationship in human cadaveric plantaris tendon: a preliminary study, Med. Elect. Biol. Engn. 2:31-38 (1964).
- Walmsley B., J.A. Hodgson and R.E. Furke, Forces produced by medial gastrocnemius and soleus muscles during locomotion in freely moving cats, J. Neurophysiol. 41:1203-1216 (1978).
- Warfel J.H., The Extremities, fourth edition. Henry Kimpton Publishers, London, 1974.
- Wells J.B., Comparison of mechanical properties between slow and fast mammalian muscles, J. Physiol. 178:252-269 (1965).
- Wendt I.R. and C.L. Gibbs, Energy production of rat extensor digitorum longus muscle, Amer. J. Physiol. 224:1081-1086 (1973).
- Wilkie D.R., The relation between force and velocity in human muscle, J. Physiol. 110:249-280 (1950).
- Winter D.A., The locomotion laboratory as a clinical assessment system, Med. Progr. Technol. 4:95-106 (1976).
- Winter D.A., Biomechanics of human movement. John Wiley and Sons, New York, 1979.
- Winter D.A., R.K. Greenlaw and D.A. Hobson, Television-computer analysis of kinematics of human gait, Computers and Biomed. Research 5:498-504 (1972).
- Winter D.A., A.O. Quanbury, D.A. Hobson, H.G. Sidewall, G. Reimer, B.G. Trenholm, T. Steinke and H. Shlosser, Kinematics of normal locomotion - A statistical study based on TV data, J. Biomechanics 7:479-486 (1975).
- Wold S., Spline functions in data analysis, Technometrics 16:1-11 (1974).
- Woltring H.J., Calibration and measurement in 3-dimensional monitoring of human motion by optoelectronic means. I. Preliminaries and Theoretical Aspects, Biotelemetry 2:169-196 (1975).
- Woltring H.J., Calibration and measurement in 3-dimensional monitoring of human motion by optoelectronic means. II. Experimental results and discussion, Biotelemetry 3:65-97 (1976).

Yamada H., Strength of Biological Materials. The Williams and Wilkins Company, Baltimore, 1970.

Yeo B.P., Investigations concerning the principle of minimal total muscular force, J. Biomechanics 9:413-416 (1976).

Zatziorsky V.M. and S.Y. Alexhinsky, Simulation of human locomotion in space, in Biomechanics V-B, P.V. Komi, ed., pp387-394 (1975).

Zerniche R.F., G. Caldwell and E. Roberts, Fitting Biomechanical data with cubic spline functions, Res. Quarterly 47:9-19 (1976).